
University of Leicester

# HUMAN UROTENSIN-II RECEPTOR DESENSITISATION

**Madura Suharshana Batuwangala**

**University Department of Cardiovascular Sciences**

**(Pharmacology and Therapeutics Group)**

**University of Leicester**

**Thesis submitted for the Degree of Doctor of Philosophy**

**In joint collaboration with Università degli studi Ferrara (Italy)**

**July 2009**

**Human Urotensin-II Receptor Desensitisation**

Madura Suharshana Batuwangala

Human Urotensin-II (U-II) is a cyclic undecapeptide that binds to the U-II receptor UT. The desensitisation mechanisms of the UT receptor ($G_{q/11}$ coupled GPCR) are not well defined and hampered by (1) lack of native (*in-vitro*) models; (2) paucity of ligands, especially non-peptides and (3) irreversible binding of U-II. There are some limited studies using rat aorta, where a U-II induced primary contractile response was reduced upon a secondary re-challenge after 5-hours.

Studies were undertaken to characterise cell lines expressing native (SJCRH30) and recombinant human hUT (HEK293 and CHO) for their suitability in binding and functional assays (PI and $Ca^{2+}$). SAR studies were carried out to characterise novel analogues modified at $Tyr^9$ of the U-II(4-11) template. This led to the identification of [3,5-diiodo$Tyr^9$]U-II(4-11) a partial agonist in aorta and $Ca^{2+}$ assays at rat UT. Full agonism was demonstrated at hUT in PI and $Ca^{2+}$ assays. Efforts were made to delineate functional and genomic desensitisation of hUT. There was no functional desensitisation in SJCRH30. In $HEK293_{hUT}$ functional heterologous desensitisation of hUT was observed, this was not so in $CHO_{hUT}$; instead $P_2YR$ was functionally attenuated. In SJCRH30 6-hr U-II treatments led to UT mRNA reduction. Genomic desensitisation was also studied in Peripheral blood mononuclear cells (PBMCs). U-II treatments alone did not affect UT mRNA. Lipolysaccharide treatment of PBMCs led to UT mRNA upregulation which was desensitised with U-II treatments. In recombinant systems UT mRNA was upregulated at 6-hr U-II treatments.

In conclusion modification of the U-II(4-11) template at $Tyr^9$ is useful for reducing efficacy. There is a difference in desensitisation profiles of native and recombinant hUT, where native receptors are not prone to functional desensitisation while receptor mRNA is reduced. In recombinant systems, hUT undergoes desensitisation ($HEK293_{hUT}$ only) while receptor mRNA is increased in both systems.

**Acknowledgements**

My zest for science and cell signaling could not have developed without a very important person: Ali (Mobasheri) for giving me a wonderful opportunity as an undergraduate project student at the University of Westminster.

My PhD has been a wonderful journey filled with a lot of great memories. It could not have been completed without the help and encouragement of a number of people. I would like to thank my supervisors Dave Lambert, Leong Ng, and Giro Calo' for giving me the opportunity to nurture my ideas and gain valuable experience in and out of the laboratory.

My friends in Leicester who are like family to me since my arrival in 2003: Gita (sis), Karl (Thanks for the chats as a colleague and also as a friend since CSMM days!) Eleanor & Vicky (remember those early fun times back in the day?), Vicki (Ginger), Anna and Eleni.

Much of my research work could not have happened if not for the generous help and support of the following people:

Team Leicester: Dave, John, Tim, Ed and Paul (Mazza Blue).

Team Ferrara: "Section of Pharmacology"- Giro (the George Clooney of Pharmacology) Vale, Anna, Raphaella, Nicholas, Stefano, Luca (Rocco) and Marcello (thanks for the entertaining conversations and lewd humour). "Pharmaceutical Chemistry" - Remo, Erika, Miky and Claudio (the Willie Wonka of Chemistry).

The friends who got me through those days when I missed home while in Italy; I'm very grateful for the beautiful times we shared– Milijana (mange tout Rodney), Ajay (the man the legend size does matter), Pawel (sandalman) and Kasia. I love you guys and miss you loads!

Finally and very importantly I would like to thank family: amma, appachi, aiya, Noemi and Anita (my wonderful fiancée) for helping me get through the tough times and being there for me when I needed you the most. Much love always.

The work presented within this thesis has formed a basis of an international collaboration between the University of Leicester, Department of Cardiovascular Sciences (UK) and Università degli studi Ferrara (Italy), Department of Clinical and Experimental Medicine, Section of Pharmacology.

**TABLE OF CONTENTS**

## I. Abbreviations

| | |
|---|---|
| 5-HT | 5-Hydroxytryptamine |
| ATP | Adenosine triphosphate |
| BAPTA | Bis(o-aminophenoxy)ethane-*N,N,N',N'*- tetracetic acid |
| BSA | Bovine Serum Albumin |
| Cch | Carbachol |
| cDNA | Complimentary DNA |
| CHO | Chinese Hamster Ovary |
| CNS | Central Nervous System |
| DAG | Diacylglycerol |
| DIPCDI | Diisopropylcarbodiimide |
| DMSO | Dimethylsulphoxide |
| DNA | Deoxyribonucleic acid |
| dNTP | Deoxyribonucleotide triphosphates |
| DPM | Disintegrations per minute |
| dsDNA | Double stranded DNA |
| dTTP | Deoxythymidine triphosphate |
| dUTP | Deoxyuridine trisphosphate |
| EC50 | Effective concentration producing a half-maximal response |
| EDTA | Ethylenediaminetetraacetic acid |
| EGTA | Ethylene glycol bis(β-aminoethyl ether)- N,N,N',N'- tetraacetic acid |
| ET-1 | Endothelin-1 |
| $Et_3SiH$ | Triethylsilane |
| FFPE | Formalin-fixed paraffin-embedded |
| FLIPR | Fluorescent Imaging Plate Reader |
| Fluo-4 AM | Fluo-4 acetoxymethyl ester |
| Fura-2 AM | Fura-2 acetoxymethyl ester |
| GAPDH | Glyceraldehyde 3-Phosphate Dehydrogenase |
| GPCR | G-protein coupled receptor |
| GRK | G-protein coupled receptor kinase |
| HBSS | Hank's Balanced Salt Solution |
| hCMV | Human Cytomegalovirus |
| HEK293 | Human Embryonic Kidney |
| HEPES | *N*-2-Hydroxyethylpiperazine-*N'*-2-Ethanesulfonic acid |
| HOBt | hydroxybenzotriazole |
| HTS | High Throughput System |
| $IP_3$ | Inositol 1, 4, 5- trisphosphate |
| keV | Kiloelectron volts |
| KHB | Krebs HEPES buffer |
| KO | Knockout |
| LiCl | Lithium Chloride |
| LPS | Lipopolysaccharide |
| miRNA | micro RNA |
| mRNA | Messenger RNA |
| NSB | Non-specific binding |
| NTR | Nontranslated region |

| | |
|---|---|
| PBMC | Peripheral blood mononuclear cells |
| PIP2 | Phosphatidylinositol 4,5-bisphosphate |
| PKA | Protein kinase A |
| PKC | Protein kinase C |
| PLC | Phospholipase C |
| PM | Plasma membrane |
| PMT | Photomultiplier tube |
| RFU | Relative Fluorescence Units |
| RNAi | Ribonucleic acid interference |
| ROS | Reactive Oxygen Species |
| RPM (rpm) | Revolutions per minute |
| RT-PCR | Reverse transcription polymerase chain reaction |
| RT-qPCR | Reverse transcription quantitative polymerase chain reaction |
| SARs | Structure activity relationship studies |
| SJCRH30 | Rhabdomyosarcoma |
| TFA | Trifluoroacetic acid |
| TGFβ-1 | Transforming growth factor beta 1 |
| tIP | Total inositol phosphates |
| TK | Tyrosine kinase |
| U-II | Urotensin-II |
| UNG | Uracil-*N*-glycosylase |
| URP | U-II related peptide |
| UT | Urotensin II receptor |
| VSMCs | Vascular smooth muscle cells |

## II. Glossary

| | |
|---|---|
| Agonist | A drug that binds to and activates a receptor. Agonists can be *full*, *partial* and *inverse* in nature. A *full agonist* produces a full response while binding to a low proportion of receptors. A *partial agonist* exhibits lower efficacy than a full agonist and can only evoke a submaximal response while occupying a population of receptors. An *inverse agonist* evokes responses opposite to an agonist by binding to the same receptor. |
| Antagonist | A drug that is capable of inhibiting the effect of an agonist. Antagonists can be surmountable (*competitive*) or insurmountable (*non-competitive*). A *competitive antagonist* will bind to the same site as an agonist without evoking any biological effect thereby preventing agonist driven activation. A non-competitive antagonist binds to a site close to the agonist site, thereby preventing the activation of the receptor when the agonist binds. Both classes of compound can exist as reversible or irreversible; where the former can be washed off while the latter cannot be displaced by washing or competing ligands. |
| $B_{max}$ | The receptor density in a given preparation, which is determined by saturation binding experiments. Receptor density is measured in the unit mol/g of protein. |
| Cheng and Prusoff Equation | A formula that is used to calculate the inhibition constant ($K_i$) of an antagonist in relation to the $IC_{50}$. The latter value is obtained by carrying out competition binding experiments. |
| Desensitisation | A phenomenon that occurs when a receptor is unable to evoke a response upon secondary challenge by an agonist after an initial primary stimulus. |
| $EC_{50}$ | The molar concentration of an agonist that produces 50% of the maximum possible response for a given agonist. It is also referred to as the $pEC_{50}$, which is the negative logarithm of the $EC_{50}$. |
| Efficacy | A term used to describe the manner in which an agonist response varies according to the number of receptor it occupies. A high efficacy agonist will produced a maximal response while occupying a low proportion of receptors whilst a low efficacy agonist will only evoke a lower response even when occupying a greater receptor population. |
| *Ex-vivo* | Taking place outside of living organisms (e.g. tissue bioassays are ex-vivo). |
| $IC_{50}$ | The molar concentration of an antagonist which causes 50% maximal inhibition or in binding studies defined as the molar concentration of competing ligand which reduces specific binding of a radiolabel by 50%. |
| *In-vitro* | Taking place in an environment outside of living organisms |

| | |
|---|---|
| | (e.g. tests tubes, eppendorf tube, petri-dish, tissue culture flask). |
| *In vivo* | Taking place inside living organisms. |
| $K_B$ | Equilibrium dissociation constant that denotes antagonism of a physiological response by an antagonist. It is the molar concentration antagonist that occupies 50% of a total receptor population at equilibrium. It is also quoted as the $pK_B$ which is the negative logarithm of the $K_B$ value. |
| $K_d$ | Equilibrium dissociation constant that represents the molar concentration of radioligand that occupies 50% of a receptor population. This value is determined by saturation binding experiments. |
| $K_i$ | Similar to the $K_B$ however is a measurement obtained through binding studies. It is the molar concentration of competing ligand that would occupy 50% of receptor population if no radioligand was occupying the receptor population. It is also expressed as $pK_i$. The negative logarithm of the $K_i$ value. |
| Non specific binding (NSB) | Binding of the tracer (radiolabel) to sites/components other than the experimental system. |
| $pA_2$ | The negative logarithm of the molar concentration of antagonist that is capable of shifting an agonist concentration curve by 2-fold. It represents the measurement of potency of the antagonist. |
| Potency | The molar concentration range over which a drug produces a response. It is usually defined as $EC_{50}$ or $pEC_{50}$, where the latter is the negative logarithm of the $EC_{50}$ value. |
| Relative intrinsic activity | The maximal response of an agonist expressed as a fraction of the maximal response to another agonist. |
| Scatchard analysis | A linear transformation method employed to saturation binding data |
| Specific binding | A proportion of radiolabel tracer that can be displaced by ligands specific for a given receptor. |

## III. List of figures

## IV. List of tables

*To the teachers in my life (past and present) who showed me the way and believed in my abilities*

# 1. Introduction

## *1.1. Urotensin and its receptor UT*

Urotensin-II (U-II) is a cyclic dodecapeptide originally isolated from the urophysis of the teleost fish Gillichthys mirabilis in 1969 (Onan *et al.*, 2004a; Onan *et al.*, 2004b). This neurohaemal organ is unique to the goby fish (Ashton, 2006), which shares some structural similarities with the mammalian hypothalamoneurohypophysial axis (Herold *et al.*, 2003). Given that U-II is classed a vasoconstrictor, it would be reasonable to assume that its physiological effects are comparable to that of endothelin-1, which causes constriction of most blood vessels uniformly. This peptide is complex in that its vasoactive effects are dependent on species and type of vascular bed therefore highlighting the necessity to understand the intricacies of this peptide (Zhu *et al.*, 2006).

U-II acts as a very potent constrictor in arterial beds whilst it acts as a relaxant of small pulmonary arteries. Although it was initially isolated from fish, a role for this peptide in humans was not described until 1998 when the existence of prepro U-II was described in the human spinal cord and other surrounding tissues.

The prepro-peptide of U-II exists as two forms in humans; a 124 and 139 amino acid length peptide. Mature U-II can be cleaved from either of these longer peptides (Douglas *et al.*, 2000a).

Although U-II was isolated from the caudal neurosecretory system of fish its expression is not restricted to this organ, for example numerous biochemical and immunohistochemical studies have demonstrated the expression of U-II peptide in whole brain extracts of fish and also the CNS of the frog and tetrapods (Coulouarn *et al.*, 1998) (Coulouarn *et al.*, 1999).

U-II varies structurally from species to species at the N-terminus (Figure. 1.1), however the core cyclic hexapeptide (-CFWKYC-) of the parent molecule is conserved throughout mammalian, amphibian and piscine species (Douglas *et al.*, 2000a).

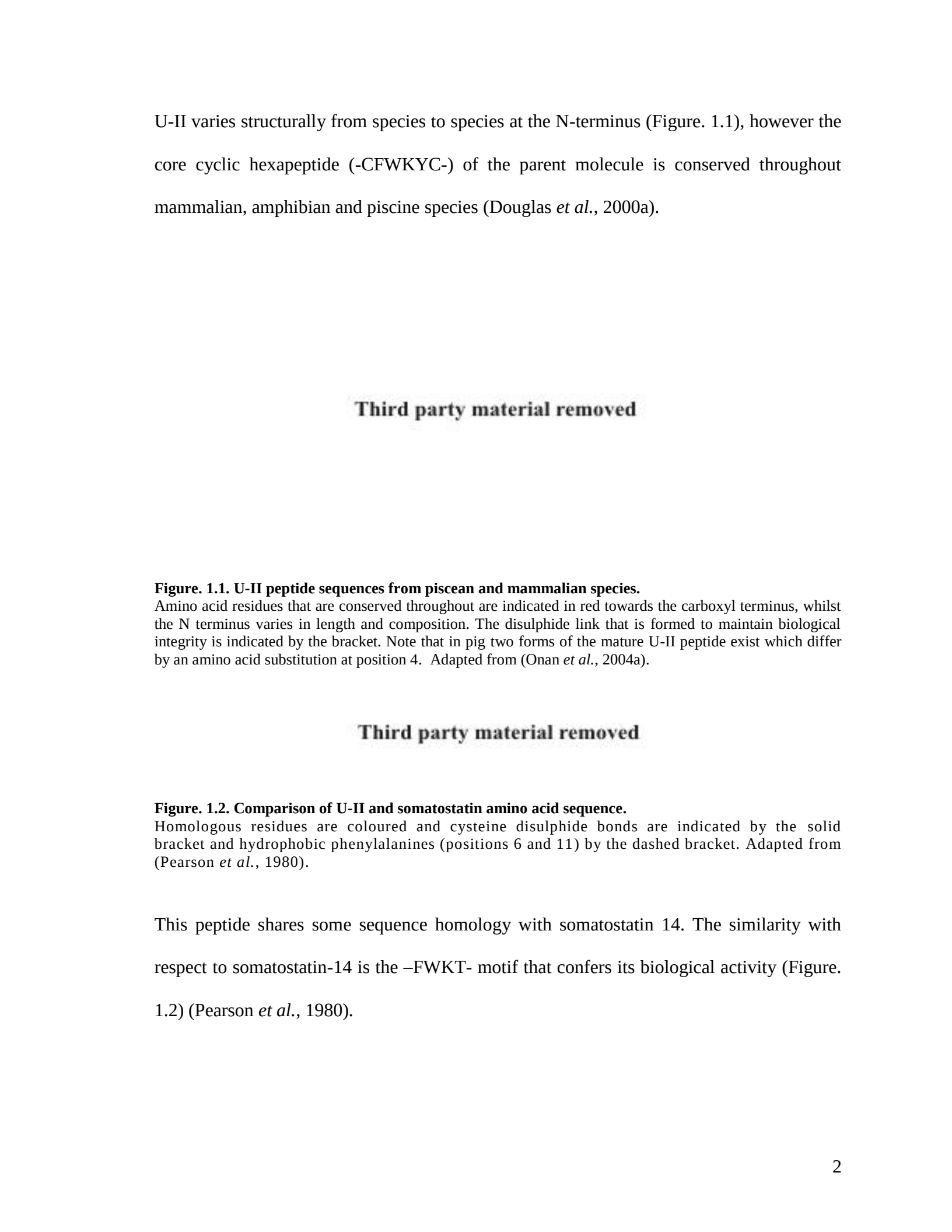


**Figure. 1.1. U-II peptide sequences from piscean and mammalian species.**
Amino acid residues that are conserved throughout are indicated in red towards the carboxyl terminus, whilst the N terminus varies in length and composition. The disulphide link that is formed to maintain biological integrity is indicated by the bracket. Note that in pig two forms of the mature U-II peptide exist which differ by an amino acid substitution at position 4. Adapted from (Onan *et al.*, 2004a).




**Figure. 1.2. Comparison of U-II and somatostatin amino acid sequence.**
Homologous residues are coloured and cysteine disulphide bonds are indicated by the solid bracket and hydrophobic phenylalanines (positions 6 and 11) by the dashed bracket. Adapted from (Pearson *et al.*, 1980).

This peptide shares some sequence homology with somatostatin 14. The similarity with respect to somatostatin-14 is the –FWKT- motif that confers its biological activity (Figure. 1.2) (Pearson *et al.*, 1980).

Goby U-II is a 12 amino acid peptide AGTADCFWKYCV (Kinney *et al.*, 2002), whilst human U-II is an 11mer (ETPECFWKYCV) (Onan *et al.*, 2004a). Truncation of the N terminus of goby U-II, i.e. the first 5 amino acid residue (AGTAD) reduces the potency by 4 fold. Truncating the wildtype sequence from 12 amino acid residues to 6 residues (-CFWKYC) results in a 10 fold reduction in potency (Table 1.1). Additionally introducing non-essential amino acids by means of an alanine scan also contributes to reduction in potency.



**Table. 1.1. Activity of U-II analogues.**
Agonists from wildtype (WT), N terminus truncated and alanine scan mutants as measured by calcium mobilisation assays. * denotes inactive as antagonist at 1000 nM and ‡ percent activation at given concentration. Adapted from (Kinney *et al.*, 2002).

The significance of the conserved amino acid sequence for full activity was assessed by altering the original CFWKYC sequence (see Table 1.1) (Kinney *et al.*, 2002).

In addition to U-II, a paralogue of this ligand was also identified in the spinal cord and brain of mouse, rat and human (Sugo *et al.*, 2003).

## Third party material removed

**Figure. 1.3. Structure of URP in mouse, rat and human.**

The peptide referred to as urotensin related peptide (URP) is characterised by the absence of the first 4 amino acid residues of U-II (Figure. 1.3). While it retains the cyclic pharmacophore of the hU-II peptide it contains an Ala reside at position 4 in place of an Asp residue as seen with the human U-II structure. Studies have shown the affinity of URP for human GPR14 to be slightly higher than hU-II (8.68 vs 8.55 respectively); however in rat thoracic aorta it retains agonist activity with slightly lower potency than hU-II (7.55 vs 8.11). With this in mind it has been suggest that URP is an endogenous ligand of GPR14 in addition to U-II (Chatenet *et al.*, 2004).

The cloning and chromosomal mapping of urotensin II receptor (then referred to as GPR14) was first carried out using rat genomic DNA. Sequence analysis demonstrated that this new gene shared an overall 27% amino acid identity with the somatostatin receptor SSTR4, and 41% identity with its transmembrane domains (TMD). Sequence alignments also confirmed that GPR14 was a candidate GPCR due to the presence of 7 TMDs (Marchese *et al.*, 1995) (Figure. 1.4). Although U-II had already been described, at this point in time its target receptor was not known and although GPR14 was identified as a novel GPCR its cognate ligand was not known, hence GPR14 remained an orphan GPCR with no known ligand.

The demonstration that U-II is the endogenous ligand of rat GPR14 was first described using Chinese hamster ovary (CHO) cells stably expressing rat GPR14 (as a screening tool) and porcine spinal cord derived U-II. In this study porcine U-II isoforms *a* and *b* evoked arachidonic acid metabolite release from transfected cells. Human U-II also evoked a response. Interestingly although somatostatin shares the Phe-Trp-Lys the peptide did not

have any effect on the recombinant model (Mori *et al.*, 1999). Further studies demonstrated the actions of human U-II (hU-II) on rGPR14 transfected into human embryonic kidney (HEK293) cells and COS-7 cells (Liu et al., 1999). Assays using aequorin and fura-2 demonstrated a robust dose dependent increase in intracellular calcium ($[Ca^{2+}]_i$) thus suggesting that GPR14 is a GPCR coupled to $G_{q/11}$ G-proteins. The $EC_{50}$ was recorded at 5, 5.6 and 7.2 nM for fish, frog and human U-II respectively. Somastostatin was also capable of evoking intracellular $Ca^{2+}$ mobilisation however at a much lower efficacy (where the $EC_{50}$ was > 1 μM).

Using the original rGPR14 as a probe, a 389 residue human GPCR sharing 75% homology with rGPR14 was isolated. RT-PCR revealed abundant mRNA expression in the heart and pancreas. Quantitative RT-PCR demonstrated the expression of low levels of mRNA transcript in substansia nigra, thalamus and occipital gyrus. Goby U-II selectively evoked robust calcium mobilisation responses where recorded in HEK293 cells transiently expressing both rat and human GPR14, where the $EC_{50}$ were 0.78± 0.18 and 0.47± 0.14 nM respectively (Ames *et al.*, 1999).

**Figure. 1.4. The Urotensin-II receptor.**
The receptor is characterised by 7 lipophilic transmembrane domains (TMD) a motif shared by all GPCR family members. Extracellular and intracellular loops are indicated (E1-E3 and I1-I3 respectively). Putative phosphorylation sites within the carboxyl (C) terminal are shown in red circles. The sequence on the right of the TMD is the expanded view of the carboxyl terminus for human UT with details of the residues showing putative phosphorylation sites (red boxes) for casein kinase 1 (CK1) and protein kinase A and C (PKC A/C).Adapted from (Onan *et al.*, 2004a).

### *1.2. Signal transduction pathway*

With the cloning of UT in humans and other mammalian species, the suggestion that the UT was a $G_{q/11}$ coupled GPCR (Liu *et al.*, 1999) (Nothacker *et al.*, 1999) required further validation. The signalling pathway of $G_{q/11}$ GPCRs is illustrated in Figure. 1.5. U-II binding to its receptor UT causes the activation of $G_{\alpha q/11}$ G-proteins thereby leading to the activation of Phospholipase C (PLC) causing hydrolysis of phosphatidylinositol 4,5-bisphosphate ($PIP_2$) to inositol 1, 4, 5- trisphosphate ($IP_3$) and formation of diacylglycerol (DAG) which stimulates protein kinase C (PKC). An increase in $Ca^{2+}$ mobilisation occurs and there is evidence for $Ca^{2+}$ influx.

In rabbit aorta hU-II causes a concentration dependent release of total [$^3$H] inositol phosphate ([$^3$H] $IP_x$) where the maximum was recorded at $10^{-7}$ M ($pEC_{50}$ 8.61±0.17). The PLC inhibitor 2-nitro-4-carboxyphenyl-N-N-diphenylcarbamate (NDCC) at $10^{-4}$ M causes a significant depletion of $IP_x$ in the presence of $10^{-6}$ M hU-II (Saetrum Opgaard *et al.*, 2000).

Goby U-II is capable of inducing concentration dependent $Ca^{2+}$ mobilisation in HEK293 cells expressing rat (rUT) and human UT (hUT). Furthermore human U-II alone is also capable of inducing concentration dependent $Ca^{2+}$ mobilisation in $HEK293_{hUT}$ cells (Ames *et al.*, 1999). Exposure of rodent aorta preparations to hU-II causes a transient increase of $[Ca^{2+}]_i$ as does $K^+$, however the U-II induced increase in $[Ca^{2+}]_i$ is significantly smaller in comparison to that induced by $K^+$. The hU-II induced responses can be inhibited completely by a combination of verapamil, $La^{3+}$ and thapsigargin (voltage gated $Ca^{2+}$ channel blocker, non-selective cation channel blocker and sarcoplasmic reticulum pump inhibitor respectively) (Tasaki *et al.*, 2004).

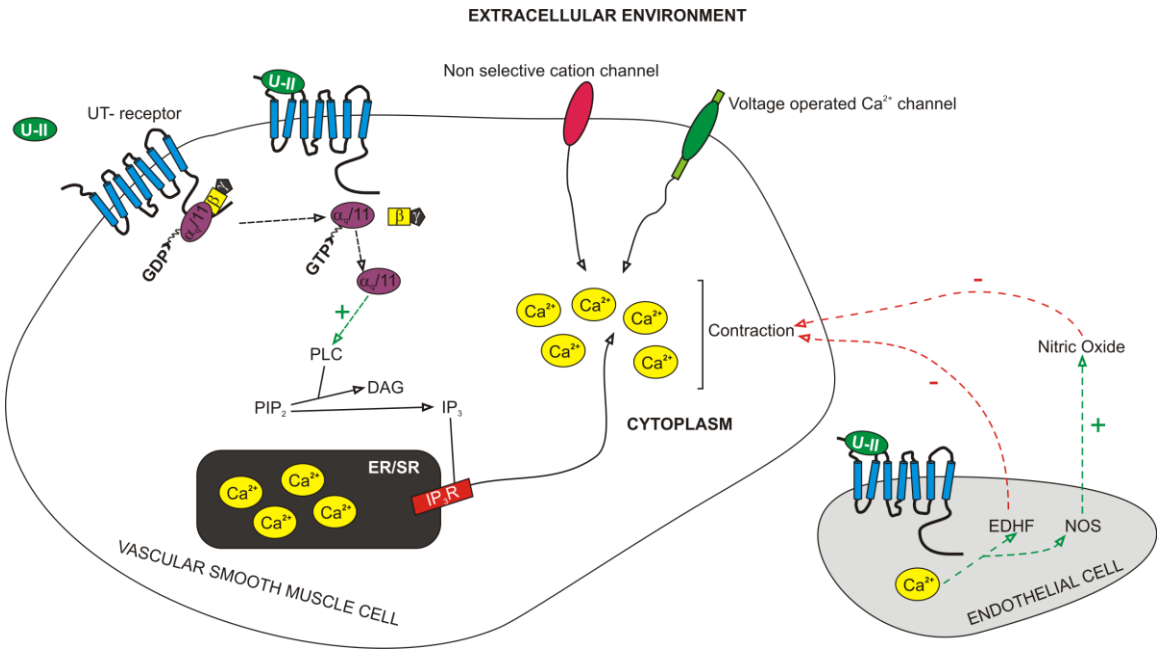


**Figure. 1.5. Proposed signal transduction mechanisms in the U-II/UT system.**
In vascular smooth muscle, U-II peptide binds to its respective receptor UT leading to the dissociation of the G-protein complex $\alpha\beta\gamma$ to yield active $G\alpha_{q/11}$ which in turn causes the hydrolysis of $PIP_2$ (phosphatidylinositol 4, 5,- bisphosphate) to Inositol 1, 4, 5- trisphosphate ( $IP_3$) and diacylglycerol (DAG) by phospholipase C (PLC). $IP_3$ causes intracellular calcium to rise by binding to the $IP_3$ receptor ($IP_3R$) which release $Ca^{2+}$ from the endoplasmic/sarcoplasmic reticulum (ER/SR) thereby leading to contraction. Cytoplasmic $Ca^{2+}$ concentrations are also elevated as a consequence of the opening of channels on the plasma membrane. On the endothelium, UT receptor activation culminates in the synthesis and release of nitric oxide and endothelium derived hyperpolarizing factor, which causes vasodilation. Adapted from (Ong *et al.*, 2005) and (Zhu *et al.*, 2006).

### *1.3. Characterisation of the U-II/UT system*

U-II has been demonstrated as being a potent vasoactive peptide not only in humans but also in non-human primates and rodent models of cardiovascular disease (Ovcharenko *et al.*, 2006). In addition to being studied in relation to the cardiovascular system, it also has been studied in relation to the renal system (Thanassoulis *et al.*, 2004);(Zhu *et al.*, 2006). The distribution of U-II and its receptor UT are outlined in Table 1.2 and 1.3 along with its effects.



**Table. 1.2. Distribution of U-II peptide and its respective receptor UT in various human tissues.**
Adapted from (Yoshimoto *et al.*, 2004).

Third party material removed

**Table. 1.3. Summary of effects of urotensin-II.**
Adapted from (Russell, 2004).

### 1.3.1. *Ex-vivo* studies

*Studies in blood vessel preparations*

The effects of U-II on blood vessel preparations from both animals and humans have been studied extensively. hU-II applied either as a single bolus or cumulatively caused slow onset sustained contraction and elevated tone in rat proximal descending thoracic aorta. Furthermore hU-II was 3, 16, 32, 661 and 708 fold potent in comparison to [$Arg^8$]vasopressin, ET-1, noradrenaline, 5-HT and prostaglandin F2$\alpha$ respectively. Whilst hU-II induced detectable consistent contractile response in thoracic aorta, the peptide induced contractions in three out of four carotid arteries and two out of four distal abdominal aortae. No contractile responses were observed in jugular vein preparations (Douglas *et al.*, 2000b).

Interestingly, in mice the cumulative addition of hU-II (≤ 300 nM) or the addition of a single bolus (1 μM) had no effect on contraction in mouse isolated proximal thoracic, medial and abdominal aorta, however noradrenaline induced robust concentration dependent contractile responses in these tissues (-log[$EC_{50}$] ranging from 8.46±0.05 to 8.57±0.05 and $R_{max}$ ranging from 156±16.8% to 171±13.8% of 60 mM KCl). In blood vessels isolated from the cynomolgus monkey (*Macaca fascicularis*), namely the left anterior descending coronary artery; pulmonary artery; distal abdominal aorta and common carotid artery hU-II acted as a potent and efficacious spasmogen in comparison to endothelin-1 and 5-hydroxytryptamine. hU-II exhibited a broad spectrum of vasoconstrictor activity (-log[$EC_{50}$] ranging from 8.96±0.15 to 9.92±0.13, $R_{max}$ from 43±16 to 527±135% of 60 mM KCl). A rather unique contractile profile was observed in vessels isolated from dogs. Whilst the left circumflex coronary artery and pulmonary vein responded to hU-II in a concentration dependent manner no contractile response was observed in the pulmonary and femoral arteries (Douglas *et al.*, 2000b).

Variations in response to hU-II were also observed in rabbits, pigs and Guinea pigs; where hU-II effects were observed in some (thoracic and pulmonary aorta) arterial and venous (jugular) vessels in rabbit and coronary artery of pig. Interestingly no responses were observed in Guinea pig arterial and venous vessels. The effects of hU-II on vessels of human origin were also variable. hU-II induced contractile responses were observed in umbilical veins and arteries, epigastric veins and facial veins. The maximal effect produced by hU-II was very small in comparison to maximal effects induced by KCl (Camarda *et al.*, 2002b). These studies provide firm evidence that hU-II acts as a very potent spasmogen

in isolated vessels, furthermore these studies demonstrate significant anatomical and species differences with regard to vascular reactivity.

*Studies in muscle and vessels*

Human U-II at maximal dose (20 nM) was capable of causing an increase in contractile force of human right atrial trabeculae and right ventricles and dose dependent positive inotropic effects in right atrial trabeculae. Additionally it was capable of causing arrhythmias characterised by ectopic contractions and also increased tone of the coronary artery (Russell *et al.*, 2001). Although the contractile response of U-II is somewhat restricted to the arterial side of the vasculature there is significant variation in the contractile effects between species, vascular beds and vessels. Furthermore its constrictive effects are induced and sustained at picomolar concentrations hence it is resistant to "wash-out" (Douglas *et al.*, 2004).

The vasoconstrictive properties are to a greater or lesser extent accompanied by its capacity to act also as a vasodilator. Higher concentrations of hU-II (100 and 1000 nM) applied to organ bath preparations of rat left coronary artery exhibit vosodilatory effects. However at lower concentrations (1- 30 nM) hU-II caused vasoconstriction which was enhanced once the tissues were stripped of the endothelium (Bottrill *et al.*, 2000). Interestingly when the tissue was pre-contracted with 5-HT (5-hydroxytryptamine) hU-II (3-300 nM) caused relaxation which was inhibited in the presence of the nitric oxide synthase (NOS) inhibitor L-NAME, thus demonstrating that the vasorelaxant effects of U-II are nitric oxide (NO) mediated (Bottrill *et al.*, 2000). Vasoconstriction was not observed in rat small mesenteric arteries, even after endothelium denudation; however vasodilation was evident in methoxamine pre-contracted intact small mesenteric arteries where sustained relaxation

was achieved at higher concentrations of hU-II. The vasorelaxant effects of hU-II were potentiated in the presence of L-NAME, which were completely abolished in the presence of 25 mM KCl thereby suggesting the activity of an NO independent vasodilatory mechanism mediated by endothelium-derived hyperpolarizing factor (EDHF) that is sensitive to KCl (Bottrill *et al.*, 2000).

### 1.3.2. *In-vivo* studies

A U-II mediated increase in mean arterial pressure (MAP) and heart rate has been demonstrated in normotensive (WKY – Wistar Kyoto) and spontaneously hypertensive (SHR) conscious rats with significant changes in the pressor response are observed in the latter animal model (Lin *et al.*, 2003). Intracerebroventricular (ICV) infusion of U-II has also been studied in conscious sheep, with an increase in systemic haemodynamics was characterised by an increase in MAP, cardiac output, heart rate, mesenteric flow, renal flow and coronary flow (Watson *et al.*, 2004).

Haemodynamic evaluation in anaesthetised monkeys demonstrated dose dependent responses yielding severe myocardial depression and circulatory collapse. Intravenous U-II administration at <30pmol $kg^{-1}$ caused a slight increase in cardiac output and reduction in regional vascular resistance. However there was no alteration in the arterial blood pressure. Increased vascular resistance and downregulation of myocardial function was observed with U-II at ≥30pmol $kg^{-1}$ (Ames *et al.*, 1999).

ICV administration of U-II in rats caused increases in behavioural activity as indicated by upregulation of rearing, grooming and cage transits; furthermore inactivity was also diminished in familiar environments in a dose dependent manner (upto 10 μg). This

increase in activity could also be linked with expression of UT receptor RNA in regions of the brain such as striatum, nucleus accumbens, cortex, amygdala and thalamus; thus implicating the U-II/UT system in contributing towards motor activity. Plasma endocrine markers such as prolactin and thyroid stimulating hormone were also elevated significantly as a consequence of U-II exposure though no significant alteration to corticosterone was observed (Gartlon *et al.*, 2001). In mice, U-II ICV administration causes a dose dependent increase in locomotion and ambulatory movements in familiar environments (Do-Rego *et al.*, 2005). Furthermore increased locomotor activity has been recorded in *Oncorhynchus mykiss* (rainbow trout) (Lancien *et al.*, 2004).

There is also evidence implicating U-II effect on rapid eye movement (REM) sleep in rats as U-II co-localises with choline acetyltransferase in the mesopontine tegmental (MPT), pedunculopontine tegmental (PPT) and lateral dorsal tegmental (LDT) nuclei. Local and ICV administration of low dose U-II increased total REM sleep time which was reversed by administering the U-II antagonist SB-710411. This increase in REM sleep time was shown to be caused by increased cholinergic stimulation (de Lecea *et al.*, 2008).

### 1.3.3. Knockout studies

Deletion of the UT receptor in the UT knockout (KO) mice does not affect the basal haemodynamics in comparison to wildtype (WT) mice. U-II caused a dose dependent vasoconstriction of isolated aortae in wildtype mice. However this was abolished in the KO model. Both WT and KO tissue responded to other spasmogens, namely potassium chloride, phenylephrine and carbachol thus demonstrating that UT receptor deletion selectively abolished U-II induced responses without affecting reactivity to the spasmogens

tested (Behm *et al.*, 2003). Studies in apololipoprotein E (ApoE) knockout ($ApoE^{-/-}$) mice demonstrated increased expression of UT receptor in $ApoE^{-/-}$ mice. In these studies mice of 18, 28 and 38 week ages were examined. Increased UT receptor mRNA was noted in aortae in $ApoE^{-/-}$ mice at all ages compared to wildtype ($ApoE^{+/+}$). Interestingly the 28 week mice showed significantly higher expression compared to 18 and 38 week mice. [$^{125}$I]-U-II ligand binding studies in 18 and 38 week $ApoE^{-/-}$ mice displayed extremely low expression of UT receptor. Studies in the 28 week mice however demonstrated a higher $B_{max}$ (64.2%) in the KO tissue to that of WT tissue (145±18 fmol/mg and 89±16 fmol/mg protein respectively, $p< 0.05$). The $K_d$ was not significantly different between both tissue types (3.86±0.77 nmol/L and 3.98±0.70 nmol/L). Competitive PCR reactions demonstrated a UT receptor expression in all three age groups. However no PCR products for U-II peptide were detected in all age groups except for the U-II peptide positive control (brain) (Wang *et al.*, 2006).

There is growing evidence for the association of U-II and its receptor in the pathogenesis of atherosclerosis. An increase in plasma U-II can be correlated with increasing severity of atherosclerosis in arteries of carotid and coronary origin (Heringlake *et al.*, 2004) (Suguro *et al.*, 2007). U-II also acts as a mitogen by promoting vascular smooth muscle cell proliferation by a synergistic mechanism via serotonin and mildly oxidizing LDL (Watanabe *et al.*, 2001a; Watanabe *et al.*, 2001b); furthermore U-II also promoted reactive oxygen species (ROS) generation through NADPH oxidase (Djordjevic *et al.*, 2005) which potentiated the mitogenic effects of U-II.

Shiraishi and co-workers (Shiraishi *et al.*, 2008) have recently studied the effects of U-II on the accumulation of atherosclerotic lesions and foam cell formation. Measurements regarding the latter were made by assessing oxidizing LDL generation, ROS generation and

expression of proteins such as ACAT-1 (acetyl-Coenzyme A acetyltransferase), CD-36 and scavenger receptor class A. U-II was capable of causing an upregulation of all these molecules compared to control animals (on chow diet); furthermore their expression was reduced significantly in the presence of aminoquinoline (with the exception of ox-LDL).

U-II and its receptor are upregulated in the kidney medulla of rats with streptozotocin induced diabetes (Tian *et al.*, 2008). U-II induced effects were characterised by increased TGF-β1 mRNA expression and increased fibronectin, collagen IV and renal morphological changes. Targeting the UT receptor with RNAi resulted in the downregulation of the TGF-β1 production.

### 1.3.4. Clinical studies

It has now been established that U-II is elevated in many cardiovascular pathologies e.g. hypertension, congestive heart failure (CHF), coronary artery disease (CAD), atherosclerosis, diabetes and renal failure (Thanassoulis *et al.*, 2004); (McDonald *et al.*, 2007).

*Hypertension*

The effects of U-II on the vascular tone of healthy normal subjects and patients with hypertension have been assessed using iontophoresis and laser Doppler velocimetry. In normotensive subjects U-II caused a dose dependent vasodilator response, whilst a dose dependent increase in vasoconstriction was observed in hypertensive subjects (Sondermeijer *et al.*, 2005).

*Heart failure*

Evidence suggesting a role for hU-II in the pathophysiology of heart failure (HF) has been growing (Table 1.4). In a study carried out on patients suffering from heart failure (New York Heart Association - NYHA class IV) compared to healthy individuals, plasma U-II levels were higher in heart failure patients (3.9±1.4pmol/L) than in controls (1.9±0.9pmol/L). The increased levels of plasma U-II also correlated significantly with plasma endothelin-I and adrenomedullin (Richards *et al.*, 2002). Although Plasma U-II is elevated in HF the levels do not change with increasing NYHA grading, whilst levels of the neurohormonal marker BNP (brain natriuretic peptide) increased with increased HF grading (Ng *et al.*, 2002). U-II peptide expression is elevated in the myocardium of patients with end-stage congestive heart failure and ischaemic heart disease. Furthermore UT receptor expression is also upregulated in ischaemic heart disease and dilated cardiac myopathy compared to normal healthy controls (Douglas *et al.*, 2002). Whilst Ng and colleagues found no change in plasma U-II immuno reactivity with NYHA scoring, another group found a correlation between plasma U-II immunoreactivity and NYHA scoring. Additionally immunoreactivity inversely correlated with left ventricular ejection fraction (Lapp *et al.*, 2004). These findings have recently been also corroborated by Gruson and co-workers (Gruson *et al.*, 2006). The effects of U-II on vascular tone in patients with chronic HF have been assessed and compared to normal healthy subjects. The drug was administered by means of iontophoresis. Laser Doppler velocimetry was used to measure changes in skin microvascular tone. In normal subjects U-II caused dose dependent vasodilation whilst in chronic HF patients a dose dependent vasoconstriction was observed (Lim *et al.*, 2004).

| Location | Comment | Reference |
|---|---|---|
| Plasma | Peptide ↑ with increased NYHA class scoring | (Richards *et al.*, 2002) |
| Plasma | Peptide ↑ in HF, but remains unaltered with progression in NYHA class scoring | (Ng *et al.*, 2002) |
| Tissue | Peptide ↑ in myocardium<br>↑ of UT in ischaemic heart diseases and cardiac myopathy | (Douglas *et al.*, 2002) |
| Plasma | ↑ of plasma U-II immunoreactivity correlated with NYHA class scoring | (Gruson *et al.*, 2006; Lapp *et al.*, 2004) |
| Microvasculature | Dose dependent vasodilatation (normal)<br>Dose dependent vasoconstriction (chronic heart failure) | (Lim *et al.*, 2004) |
| Plasma | No observable changes in plasma U-II levels correlated with NYHA scoring<br>No alterations in gene expression | (Kruger *et al.*, 2005)<br>(Dschietzig *et al.*, 2002) |
| Plasma | Congenital ↑ of U-II peptide | (Simpson, 2006) |
| Plasma | Peptide ↑ in acute myocardial infarction | (Khan *et al.*, 2007) |
| Plasma | Plama U-II is ↓ in acute coronary syndromes in comparison to patients of stable coronary artery disease | (Joyal *et al.*, 2006) |
| Plasma | U-II immunoreactivity is ↑ in congestive heart failure sufferers compared to healthy hearts | (Russell *et al.*, 2003) |

**Table. 1.4. Summary of studies relating to hU-II/UT system with reference to heart failure.**

Conversely some studies also suggest no change in plasma U-II in HF patients (NYHA class II to III) who have undergone a standard symptom-limited incremental bicycle ride compared to normal healthy individuals (Kruger *et al.*, 2005). Furthermore no changes in plasma U-II and peptide gene expression in vascular and myocardial tissue have been demonstrated in CHF (Dschietzig *et al.*, 2002).

*Diabetes and renal failure*

Urotensin II peptide upregulation has been associated with diabetes where its gene is located in chromosome 1p36-p32 a region associated with susceptibility to type 2 diabetes mellitus (DM) in Japanese subjects. Two genetic polymorphisms, designated as T21M and S89N have been identified by SNP genotyping. The latter was elevated in type 2 DM

patients in comparison to normal patients, whilst the former remained unchanged in both cohorts (Wenyi *et al.*, 2003).

Recently the association of U-II with the S89N polymorphism has been studied further by looking at plasma U-II levels in relation to the severity of diabetic retinopathy (simple and preproliferative/proliferative). As the type of retinopathy progressed, an increase in plasma U-II was observed (Suguro *et al.*, 2008).

Plasma U-II levels have also been demonstrated to be elevated in patients with renal failure, it was postulated that this increase may be due to decreased excretion of circulating U-II peptide by the kidneys (Totsune *et al.*, 2001). The plasma levels of U-II are also significantly elevated in patients suffering from DM (non proteinuric and proteinuric) in comparison to normal patients; however no significant difference was noted in the two (non proteinuric and proteinuric) diabetic groups (Totsune *et al.*, 2003).

Palosuran is a nonpeptidic U-II antagonist that has been studied in rodent models of acute renal failure and diabetes. In macroalbuminuric diabetic patients, palosuran (125 mg twice daily for 13.5 days) decreased (relative to baseline) the 24-hour urinary albumin excretion rate by 26.2% in patients with normal to mildly impaired renal function and by 22.3% in patients with moderate to severely impaired renal function. This is the first study using U-II receptor antagonists in humans and suggests that palosuran may benefit diabetic patients with renal failure. Further studies with this and the other available UT antagonists are eagerly awaited (Sidharta *et al.*, 2006). Additionally this compound has shown to be beneficial in rodent models of diabetes where it is capable of improving the survival rate of animals by upregulating insulin and reducing glycaemia, glycosylated haemoglobin and serum lipids. Furthermore palosuran was capable delaying the onset of proteinuria and renal damage and also improving renal blood flow (Clozel *et al.*, 2006). Recently caution

has been advised when using palosuran as it appears to evoke its action differentially in intact cells and vascular tissues (Behm *et al.*, 2008).

Under clinical circumstances prolonged exposure of a receptor to a drug results in desensitisation. This process causes attenuation of receptor function. Currently the desensitisation mechanisms of the UT receptor are not well defined; mainly as the peptide binds irreversibly to the receptor. Studies are ongoing to develop reversible U-II agonists which could facilitate the elucidation of desensitisation mechanisms.

### *1.4. Pharmacological desensitisation*

The extracellular signals that activate GPCRs can comprise of stimuli that include; hormones, pheromones, neurotransmitters, light, enzyme, odour and taste. GPCR activation culminates in the dissociation of heterotrimetric G-protein complex $\alpha\beta\gamma$ into $G\alpha$ and $G\beta\gamma$ subunits which are capable of regulating numerous downstream effector mechanisms in a positive or negative manner. The manner in which a GPCR responds to stimuli can be affected by desensitisation in which, upon stimulation by an agonist, the responsiveness of the GPCR wanes over time; in this context time can be in the order of seconds, minutes, hours and days (Ferguson *et al.*, 1998).

The process of receptor desensitisation can occur through homologous or heterologous mechanisms. Generally speaking when an agonist binds to a receptor this results in activation of the receptor signalling cascade; in homologous desensitisation a receptor evokes a primary response due to a primary stimulation, it is unable to evoke a secondary response (to a secondary stimulus) that is commensurate with the original primary response. On the contrary heterologous desensitisation occurs when a receptor loses its capacity to respond as a consequence of the activation of an unrelated GPCR in its vicinity.

Homologous desensitisation processes are thought to be associated with changes that occur to the GPCR itself while heterologous desensitisation is thought be associated changes to the GPCR as a consequence of alterations to the signalling components downstream in the GPCR signalling pathway (Kelly *et al.*, 2008).

### 1.4.1. Homologous desensitisation

Initial research on desensitisation mechanisms were believed to occur as a consequence of second messenger dependent protein kinases such as PKA and PKC exclusively (Benovic *et al.*, 1985), however the seminal research conducted on the $\beta_2$ adrenergic receptor system demonstrated that desensitisation could occur in the absence of PKA. This thereafter led to the identification of alternative mediator "β-adrenoceptor kinase" or β-ARK (Benovic *et al.*, 1986). β-ARK belongs to a family of molecules now collectively referred to as the GRKs (G-protein coupled receptor kinases). It was demonstrated that GRKs alone were not capable of attenuating GPCR responsiveness (Pitcher *et al.*, 1992) and that they required a secondary molecule – called arrestins (Lohse *et al.*, 1990). This led to the development of the classical pathway of homologous desensitisation (Figure. 1.6).

Upon agonist stimulation heterotrimeric G-protein $G_\alpha$ uncoupling occurs leading to the activation of downstream effector mechanisms. The agonist bound receptor is then susceptible to phosphorylation by GRK. Once the phosphorylation event has taken place, arrestin is recruited to the C-terminus of the phosphorylated receptor and targets it to be internalised. Internalisation may lead to receptor downregulation i.e. degradation of the receptor or dephosphorylated and resensitised whereby the receptor is re-sequestered back to the plasma membrane to form a functional receptor.

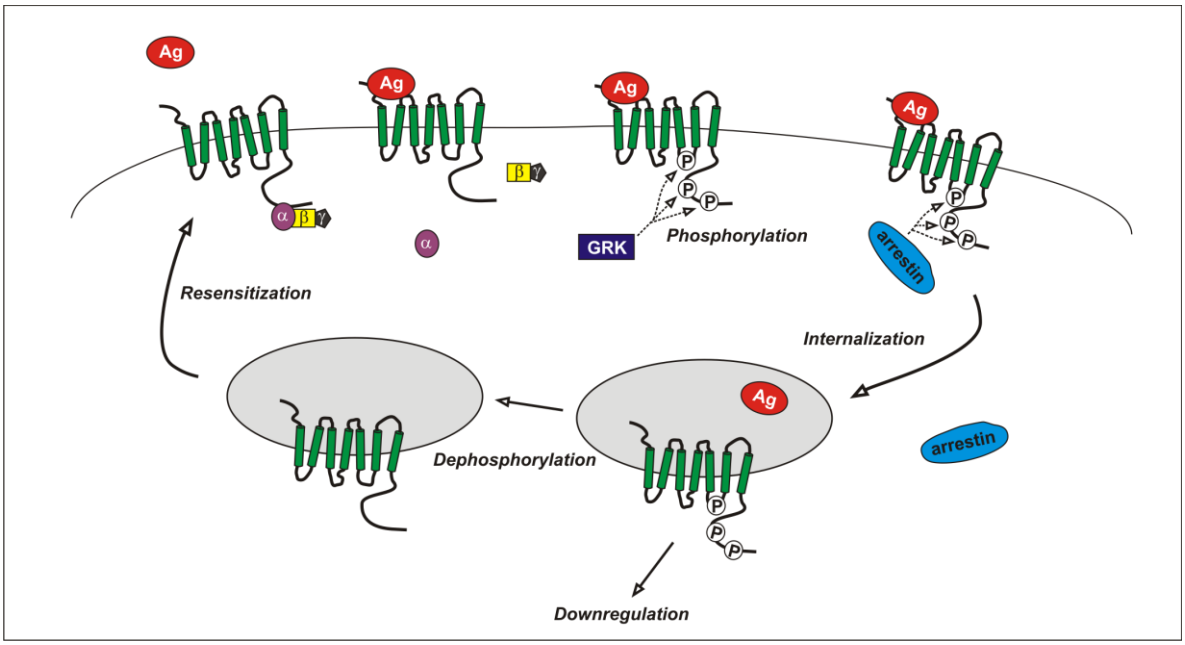


**Figure. 1.6. The classical homologous desensitisation pathway.**
Abbreviations used: Agonist (Ag), phosphorylation sites (P). Adapted from (Kelly *et al.*, 2008).

*GRKS and arrestins*

At present there are seven isoforms of GRKs. GRK2, 3, 5 and 6 are ubiquitously expressed in tissues of mammalian species, while the expression of GRK1, 4 and 7 is somewhat restricted to specific organs e.g. GRK1 and 7 are found in retinal rods and cones (hence sometimes referred to as visual GRKs) while GRK4 is restricted to the testis (Ribas *et al.*, 2007). They all share some homology in their "core structure"; however they are classed into three separate subfamilies on the basis of structural difference at the N and C terminal ends. The core structure is comprised (from N-C terminus) of an RGS domain followed by a catalytic domain. GRK1 and GRK7 are isoprenylated at the C-terminal.

GRK2 and GRK3 contain a pleckstrin homology (PH) domain and phospholipid (PL) and Gβγ binding sites. Additionally GRK2 is distinguished by a PKC and MAPK phosphorylation site. A palmitoylation region at the C-terminus is common to both GRK4 and GRK6; while GRK5 is characterised by the presence of a site for phospholipid binding,

it also has additional sites for autophosphorylation when interacting (auto + and auto -) with membrane bound $PIP_2$ (Figure. 1.7) (Lohse *et al.*, 1996).

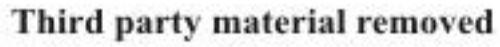


**Figure. 1.7. The gross structure and subfamily of GRKs.**
Adapted from (Lohse *et al.*, 1996).

The arrestins comprise of a four member gene family: arrestin1, arrestin2 (also called β-arrestin1), arrestin3 (also called β-arrestin2) and arrestin4 (cone arrestin). They can be further subdivided into two groups on the basis of the structure and function; namely visual (arrestin1 and arrestin4) or non visual (arrestin2 and arrestin3) (Gurevich *et al.*, 2006).

Arrestins are structurally comprised of two domains (N and C) made of antiparallel β-sheets. In its "inactive" conformation these two domains are held together by a 12 amino acid linker. Also tucked inside within these two domains is a C-terminal tail on which the clathrin and AP2 domains reside. The phosphorylation of a GPCR by GRK serves as a signal for arrestin to convert into an "active" conformation and this results in the release of the C-terminal tail whereby the clathrin and AP2 domains become exposed (Lefkowitz *et al.*, 2006).

GRKs and arrestins work in concert to fulfil the role as mediators of phosphorylation in homologous desensitisation. Together they work on three levels; silencing, trafficking and signalling (Reiter *et al.*, 2006). During silencing the GPCR is uncoupled from G-proteins. Trafficking involves the internalisation of the receptor which can lead to the degradation or

resensitisation and signalling results in the modulation of signalling pathways independent of G-proteins.

### 1.4.2. Heterologous desensitisation

While agonist binding is a pre-requisite in homologous desensitisation this is also the case with heterologous desensitisation, however in this case, the agonist bound receptor is different to the one that is subject to desensitisation. This process occurs through phosphorylation of serine and threonine residues located within the carboxyl terminus of the GPCR. The mediators associated with phosphorylation are second messenger kinases; these include protein kinases A and C (Sibley *et al.*, 1985) (Stadel *et al.*, 1983) however other new kinases (e.g. casein kinases) have also been implicated in desensitisation (Tobin, 2002).

Heterologous desensitisation can occur when a GPCR is activated by a ligand and its activation results in the generation of downstream signalling and generation of second messenger kinases. The second messenger kinases in turn phosphorylated unrelated (agonist unbound) GPCRs in close proximity thereby attenuating their function. While phosphorylation appears to be the primary mechanism of receptor attenuation, there are also other putative non-phosphorylation events that could contribute; such as modification to G-proteins and/or downstream effectors (Hosey, 1999). Additionally phosphorylation can occur both unidirectionally and bidirectionally; the former being observed with $M_3$ muscarinic receptors by bradykinin $B_2$ receptors (Hosey, 1999) and the latter with opioid and chemokine receptors (Rogers *et al.*, 2000) (Figure. 1.8).

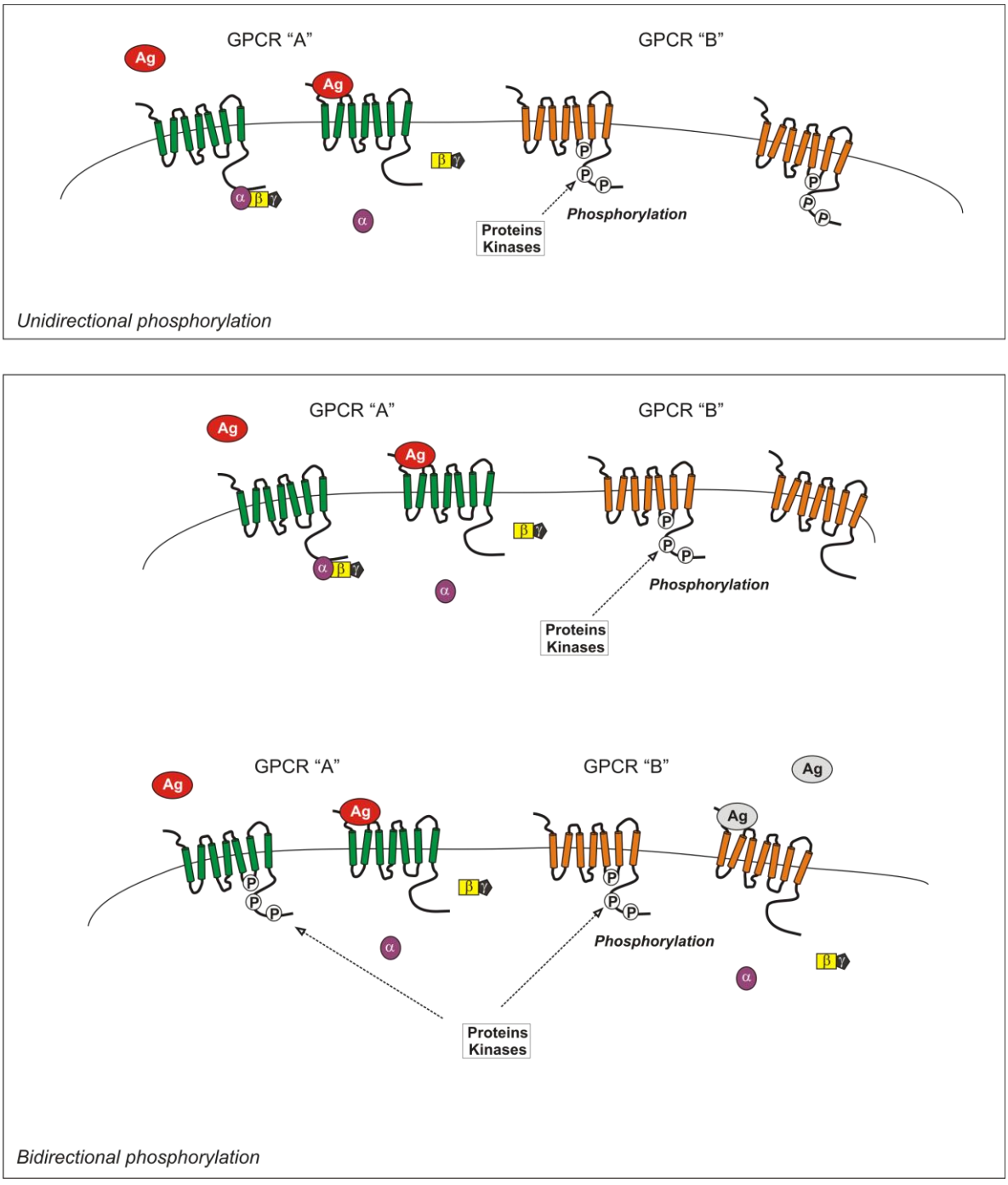


**Figure. 1.8. The pathway of heterologous desensitisation.**
*Top panel:* unidirectional phosphorylation. Stimulation of GPCR "A" by its agonist results in the phosphorylation of GPCR "B" by protein kinases. *Bottom panel:* bidirectional phosphorylation. In this scenario stimulation of GPCR "A" by its agonist results in the phosphorylation of GPCR "B" by protein kinases, additionally stimulation of GPCR "B" can lead to the attenuation of GPCR "A". Abbreviations used: Agonist (Ag), phosphorylation sites (P)

### *1.5. General aims*

The general aims of this thesis are to:

1) Characterise and validate cell line models expressing native and recombinant human UT receptor in order to determine their suitability for desensitisation studies.
2) Characterise the compounds urantide and UFP-803 (both described as antagonists in rat aorta) in recombinant cell lines expressing human UT receptor.
3) Carry out structure activity relationship studies (SARs) with novel U-II(4-11) analogues modified at $Tyr^9$, with the aim of identifying suitable reversible agonists for desensitisation studies.
4) Determine if the native and recombinant human UT receptor is subjected to desensitisation and to probe this at a functional level.
5) To assess if the human UT receptor is subject to genomic desensitisation based on U-II treatments using real time PCR.

Chapter specific aims are described in more detail in subsequent pages.

## 2. Materials and methods

### *2.1. Source of materials*

All suppliers of materials are listed in alphabetical order.

**Alpha Laboratories** (Hampshire, UK): Pipette tips, m-Line pipette series

**Applied Biosystems** (Warrington and Chesire, UK): Reverse transcription kit, qPCR reagents (Gene expression master mix, Taqman probes)

**Fisher Chemicals** (Leicestershire, UK): Sodium chloride, Magnesium sulphate, Sodium hydroxide, Formic acid

**GE Healthcare** (Amersham, UK); myo-[$^{3}$H]Inositol with PT6-271 stabilizer (insoluble pellet) and [$^{125}$I]hU-II.

**Invitrogen** (Scotland): Foetal bovine serum albumin, Fungizone, L-Glutamine, Penicillin/streptomycin, Trypsin EDTA, Geneticin (G418), "OptiPhase Safe" scintillation cocktail, Tissue culture media (RPMI advance 1640, DMEM F12 and MEM), Fluo-4 AM, Pluronic acid, Whatman GF/ B filters.

**Sigma Aldrich** (Poole, Dorset, UK): Tri reagent, Molecular biology grade chloroform, Isopropyl alcohol, Ethanol, Borax, Ammonium formate.

**University of Ferrara Peptide Research** (Ferrara, Italy): U-II and related peptides.

### *2.2. Buffer compositions*

**Assay buffer** (binding studies)

- (mM): Tris-HCl (50), $MgSO_4$(5), 0.5% BSA pH 7.4 KOH

**Buffer A** (Phosphoinositide turnover assay)

- (mM) $NH_4OOCH$ (60) and Borax (5)

**Buffer B** (Phosphoinositide turnover assay)

- (mM) $NH_4OOCH$ (750) and HCOOH (100)

**Dowex regeneration buffer** (Phosphoinositide turnover assay)

- (mM): $NH_4OOCH$ (2000) and HCOOH (100)

**Hank's Balanced Salt Solution** 1x (HBSS) (HTS $Ca^{2+}$ assay)

- (mM): Probenecid (2.5) and HEPES (20). pH 7.4 NaOH

**Harvest buffer** (Harvesting cells for assays)

- (mM): NaCl (154), HEPES (10), EDTA (1.7) pH 7.4 NaOH

**Homogenization buffer** (binding studies)

- (mM): Tris-HCl (50), $MgSO_4$(5) pH 7.4 KOH

**Krebs- HEPES buffer** *(Leicester laboratory)* ($Ca^{2+}$ assay)

- (mM): NaCl (143), glucose (11.7), HEPES (10), KCl (4.7), $KH_2PO_4$ (12), $MgSO_4$ (1.2) and $CaCl_2$ (2.6). pH 7.4 NaOH

**Krebs buffer** *(Rat aorta bioassay physiological salt solution – Ferrara Laboratory)*

(mM): NaCl (118), glucose (10), KCl (4.7), $KH_2PO_4$ (1.2), $MgSO_4$ (1.2) and $CaCl_2$ (1.2), $NaHCO_3$ (25). pH 7.4 NaOH

**Lowry assay reagents** (protein quantification assay)

- BSA (bovine serum albumin fraction V) standards (μg protein/ml): 0, 50, 100, 150, 200 and 250.
- Folin's reagent (1:4 dilution in $dH_2O$)
- Solutions A : 2% $Na_2CO_3$ in 0.1 M NaOH
- Solution B: 1% $CuSO_4$

- Solution C: 2% $Na^+/K^+$ Tartrate.

### *2.3. Cell culture*

Cells (Rhabdomyosarcoma - SJCRH30, Human embryonic kidney- $HEK293_{hUT}$ and Chinese hamster ovary -$CHO_{hUT}$) were maintained at 37°C in an incubator with 5% $CO_2$ humidified air. When confluent, splitting was carried out using trypsin EDTA.

SJCRH30 (purchased from ATCC, LGC Prochem) were cultured in advanced RPMI 1640 supplemented with 10% FBS, 100 IU/ml penicillin and 100 μg/ml streptomycin respectively, 2.5μg/ml fungizone, 2 mM L-glutamine, and 10 mM HEPES.

Experimental flasks of $HEK293_{hUT}$ were maintained in feed media comprising of minimal essential media (MEM) containing 10% FBS, 100 IU/ml each of penicillin and 100 μg/ml streptomycin, 2.5 μg/ml of fungizone and 2 mM L-glutamine. Stock flasks were maintained in selection media with the same composition as above however with the addition of 400μg/ml of geneticin (G418).

Experimental flasks of $CHO_{hUT}$ were maintained in feed media comprising of DMEM/F-12 HAM (1:1 mix) already containing glutamine (146 mg/l). Media was supplemented with 10% FBS, 100 IU/ml each of penicillin and 100 μg/ml streptomycin, 15 mM HEPES and pyridoxine. Stock flasks were maintained in selection media with the same composition as above however with the addition of 800μg/ml of geneticin (G418).

### *2.4. Binding studies: theory*

Binding studies are utilised to evaluate the binding between a ligand and its respective receptor thereby facilitating the calculation of its affinity ($K_d$). Additionally the maximum number of receptors occupied by the ligand ($B_{max}$) can also be calculated. Further additional information can be also obtained on receptor subtypes and the interactions of agonists and antagonists.

When a ligand (L) binds to receptor (R) this results in the formation of a ligand-receptor complex (LR). This process is reversible.

$$L + R \underset{k_{-1}}{\overset{k_{+1}}{\rightleftarrows}} LR$$

The association rate constant between L and R is characterised by $k_{+1}$ while the dissociation rate constant of the LR complex is defined by $k_{-1}$.

The formation of the LR complex is regulated by the Law of Mass Action; which states that the rate of a reaction is proportional to the products of the concentration of reactants.

When the association and dissociation rates are equal the reaction is at a state of equilibrium (where [ ] denotes concentration):

$$[L] \bullet [R] \bullet k_{+1} = [LR] \bullet k_{-1}$$

On re-arranging the above equation:

$$\frac{[L] \bullet [R]}{[LR]} = K_d = \frac{k_{-1}}{k_{+1}}$$

In relation to the equation above, $K_d$ can be defined as the ratio of the dissociation rate and association rate constants.

Three types of binding experiments are utilised to characterise ligands and their cognate receptors; these are kinetic, saturation and displacement experiments. These are described in detail below.

### 2.4.1. Kinetic experiments

Kinetic experiments (alternatively referred to as time course experiments) are utilised in order to determine the time taken for the radiolabel to bind to its receptor and reach equilibrium. This type of experiment gives information pertaining to first-order rate constants for the onset and offset of binding and facilitates the design of saturation and displacement experiments. Additionally by using the above equation and an estimate of $K_{+1}$ and $K_{-1}$ the $K_d$ can be calculated.

### 2.4.2. Saturation experiments

Saturation experiments are employed in order to determine the $K_d$ of a ligand (the [ligand] required to bind to 50% of a receptor population) and the $B_{max}$ of a receptor (a measure of the density of receptors that are occupied by a saturable concentration of a radiolabelled ligand). In this type of experiment fractions of cell membrane expressing the receptor of interest are incubated with an increasing concentration of radio-labelled ligand until the concentration of bound ligand saturates.

Radioligands do not bind only to the receptor under study but also receptor unrelated sites. It is therefore necessary to discriminate between receptor specific and receptor non specific

binding (Figure. 2.1). This is achieved by incubating one set of receptor membrane preparations with radiolabel (tracer) only while simultaneously incubating a second set of tubes with membrane preparation, radiolabel tracer and excess unlabelled ligand. In the tubes (designated set 1), the radiolabelled ligand binds not only to the receptor specifically, but also to the cell membrane non specifically, this is an example of total binding; while in the second set of tubes (set 2) the tracer is unable to bind specifically to the receptor due to the excess unlabelled ligand. Non specific binding (NSB) can be therefore defined as a proportion of radiolabel that binds to the cell membrane and receptor unrelated sites.

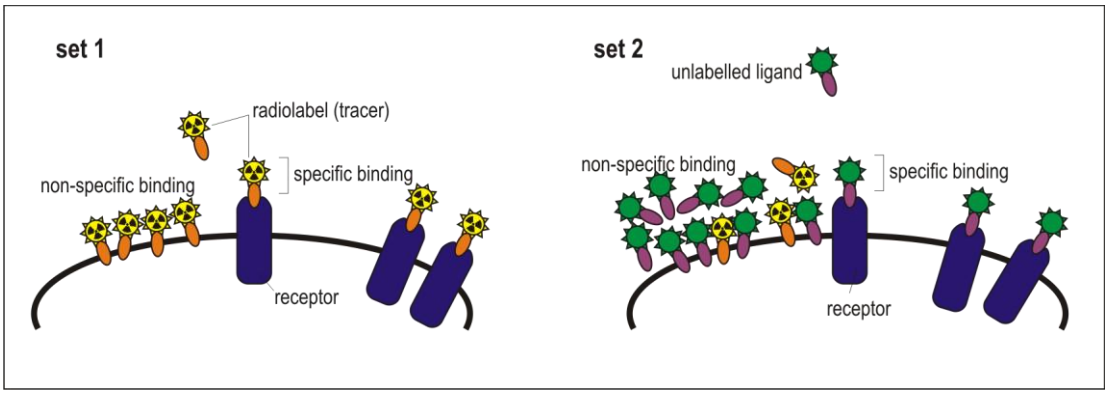


**Figure. 2.1. Discrimination of specific binding from non specific binding (NSB).**
In the first of reaction tubes bound radioactivity is characterised by the tracer binding to specific sites (receptor) as well as non-specific sites of the cell membrane (total binding), while in the second set of tubes bound radioactivity is distinguished by low amount of tracer that is binding to the cell membrane (NSB). Subtracting the NSB from total binding results in obtaining a value for the specific binding.

Specific binding is thus determined by using the following equation:

$$Specific\ binding = Total\ binding - NSB$$

The presence of excess amount of unlabelled ligand does not have an effect on the non-specific binding of the radiolabel. This is because NSB is not saturable within the experiment. The results of a saturation experiment can be plotted by incorporating the Langmuir isotherm (illustrated in Figure. 2.2); where bound ligand is plotted on the *y*-axis against the free radioactive ligand concentration on the *x*-axis.

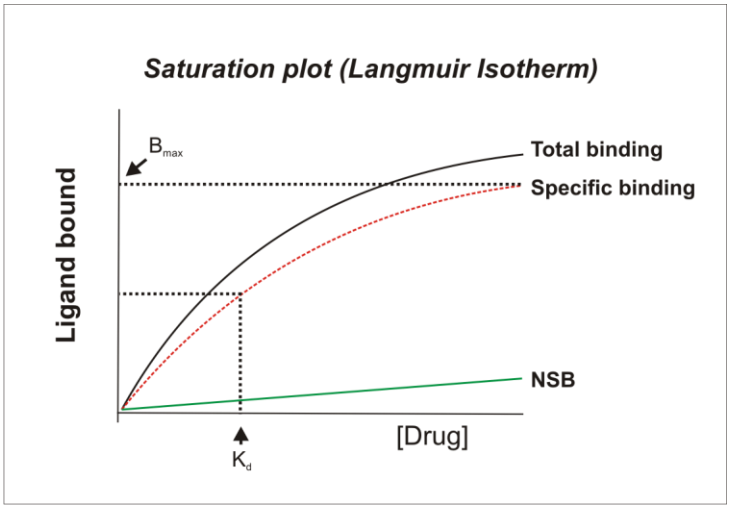


**Figure. 2.2. The Langmuir isotherm.**

As the value on the *x-axis* increases an increase in bound tracer is also observed on the *y-axis*. The amount of bound tracer reaches a point of saturation and this is characterised by the hyperbolic saturation curve. While this hyperbola may result a value for the $B_{max}$ and $K_d$, a more accurate determination of these values is achieved by transforming the data to a Sigmoid plot and for further visual clarity illustrated as a Scatchard plot (Figure. 2.3).

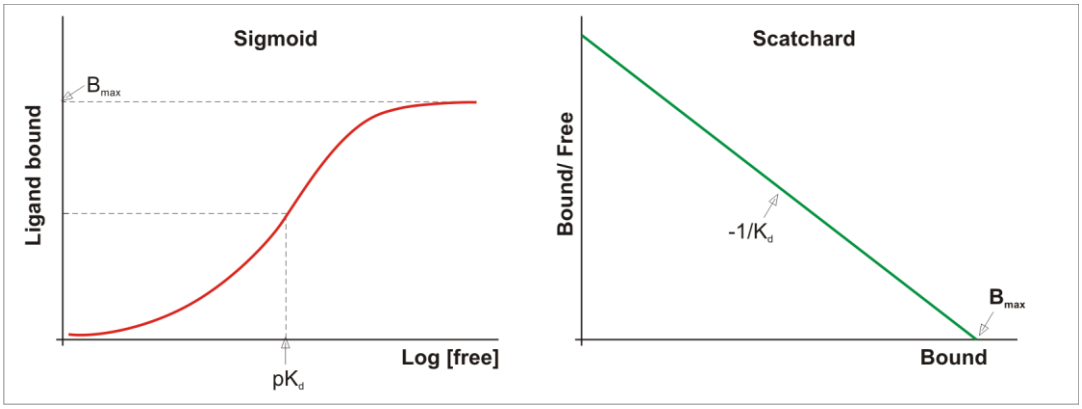


**Figure. 2.3. A representation of Sigmoid and Scatchard plots.**
*Left panel:* Sigmoid plot, *right panel:* Scatchard plot. In the Scatchard plot, $B_{max}$ is the X intercept while $K_d$ is represented by the negative reciprocal of the slope.

Saturation binding experiments can be commonly carried out using two types of radiolabel, these include tritiated [$^{3}$H] and iodinated [$^{125}$I] forms of label. Each type has advantages and disadvantages. For example [$^{3}$H] has a greater half life (~12 years) compared to [$^{125}$I] (~60 days). Additionally tritiated labels are cheaper than iodinated labels. Conversely the advantage of [$^{125}$I] labels is their specific activity (2000 vs. 30-100 Ci/mmol), which makes them very useful in detecting receptors at low density. Furthermore there is no requirement of scintillant with iodinated labels. [$^{3}$H] emits β radiation; with decay energy of ~18 kiloelectron volts (keV). Furthermore its radiation path can be blocked by solid surfaces. [$^{125}$I] on the other hand emits γ radiation with decay energy of ~35 keV. It is therefore capable of penetrating through surfaces. However it can be blocked by lead foil and thick Perspex shielding.

As iodinated radiolabels are expensive, traditional saturation binding experiments are not carried out. In their place isotope dilution experiments are performed. In these studies the radiolabel is kept at a fixed low concentration and "diluted-out" with an increasing concentration of identical non-label. This results in an increasing dilution factor, which is used to infer how much radiolabel would be bound if there were no dilution effects.

### 2.4.3. Displacement experiments

The theory of displacement assays applies to isotope dilution as above. The number of traceable ligands (i.e. radioactive or fluorescent) available to study ligand-receptor relationships is limited. Furthermore it is not necessary to characterise receptors by direct radiolabel binding as this can be very expensive and furthermore technically very

challenging. Displacement assays are used to determine the affinity of a non-radioactive label on the basis of its ability to displace a radiolabel. In this context the non-radioactive ligand is referred to as a displacer or competitor. Data from a typical experiment is plotted as percentage radiolabel bound over log displacer as a decreasing Sigmoid plot which is illustrated in Figure. 2.4 (left panel). If the data was plotted as the percentage of radiolabel displaced vs log displacer this would result in an increasing Sigmoid plot as shown in the figure 2.4. (right panel).

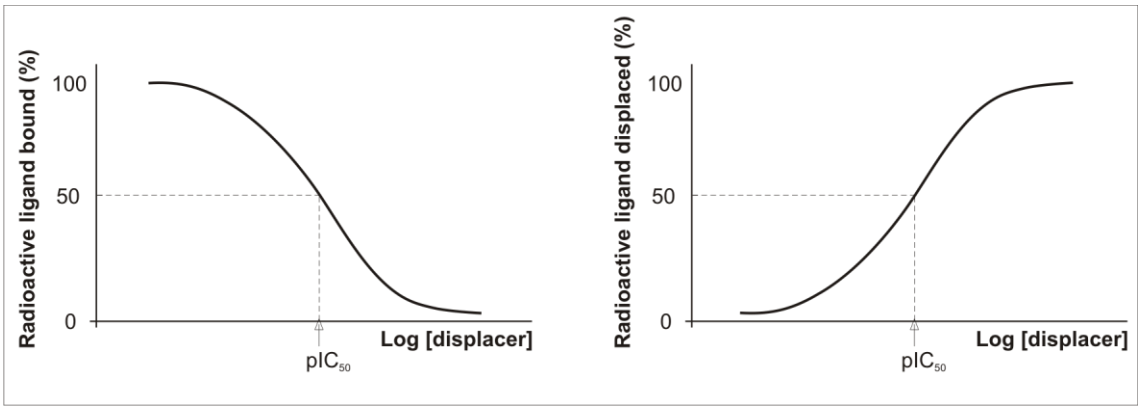


**Figure. 2.4. Sigmoid plots in displacement experiments.**
*Left panel:* percentage ligand bound vs. log displacer concentration. As the concentration of displacer increase, a reduction in the bound radiolabel is observed. *Right panel:* percentage ligand displaced vs. log displacer concentration. Note that as the concentration of displacer increases so does the displacement of the radiolabel. The $pIC_{50}$ can be determined and this can be used to determine the $K_i$ using the Cheng and Prusoff equation.

Displacement binding experiments are used to determine the $IC_{50}$ of a compound. The $IC_{50}$ is the concentration of non-radioactive ligand required to produce half maximal inhibition of the radiolabel binding. Once the $IC_{50}$ is determined, it is also possible to calculate the $K_i$ using the Cheng and Prusoff equation (Cheng *et al.*, 1973):

$$K_i = \frac{IC_{50}}{1 + \left( \frac{[L]}{K_d} \right)}$$

Where $K_i$ is an inhibition constant and the molar concentration of competing ligand that would occupy 50% of receptors in the absence of the radioligand. The $IC_{50}$ is the concentration of non-radioactive ligand required to produce half maximal inhibition of the radiolabel biding. [L] represents a fixed concentration of the radiolabel and the $K_d$ is the dissociation constant for the radiolabel (Bylund, 1990) (Keen, 1997).

### *2.5. Lowry protein assay*

Before carrying out any binding studies with cell membrane preparations, it is necessary to quantify the amount of protein in a membrane preparation. The Lowry assay (Lowry *et al.*, 1951) was used to determine the protein concentration for the membrane fractions. A set of bovine serum albumin (BSA) standards of 0, 50, 100, 150, 200 and 250 μg protein/ ml were prepared in 0.1 M NaOH. 500 μl of standards, incubated for 10 min in a 2.5 ml solution composed of solution A ($NaHCO_3$ in 0.1 M NaOH), solution B (1% $CuSO_4$) and solution C (2% $Na^+$ $K^+$ tartrate) mixed in the ratio of 100:1:1. The standards were then incubated for a further 30 min after the addition of Folin's reagent and their absorbance read at 750nm using a benchtop spectrophotometer. The concentration of protein in the membrane fractions was determined by linear regression of the BSA standard curve as indicated in Figure. 2.5.

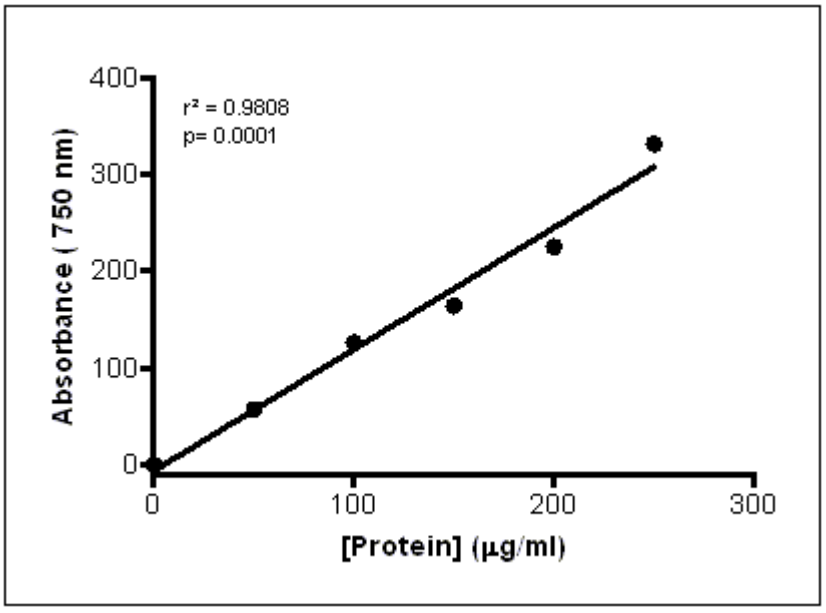


**Figure. 2.5. Example of Lowry protein assay standard curve.**

### *2.6. Binding studies: methodology*

In binding studies the protein concentration of membranes for the three cell lines were 15 μg ($HEK293_{hUT}$ and $CHO_{hUT}$) and 150-300 μg (SJCRH30) cells. The protein concentration was determined by referring to the Lowry assay standard curve. Unless states all assays were carried out at room temperature in 500 μl volumes in the presence of homogenisation buffer and [$^{125}$I]U-II at 10 pM.

Time course experiments were conducted over a duration of 240 min (4 hr) by adding membranes sequentially (longest time point being first and the shortest added last).

The $B_{max}$ and $K_d$ were determined by carrying out isotope dilution studies in the presence of a fixed concentration of [$^{125}$I] (10 pM) while increasing the concentration of unlabelled U-II.

Displacement assays were carried out in the same manner as isotope dilution studies however the unlabelled ligands in this case were urantide and UFP-803. These two compounds are discussed further in this thesis. Non specific binding was determined in the presence of 1 μM U-II. Both isotope dilution and displacement assays were carried out over an incubation period of 4 hr based on the initial time course experiments.

Counting of radiation was carried out as follows; binding reactions were terminated by addition of ice-cold buffer and subsequent vaccuum filtration, using a Brandel harvester, onto Whatman GF/B filters soaked in polyethyleneimine. Radioactivity was measured using a gamma counter (Cobra, Packard).

### *2.7. Phosphoinositide turnover (PIT) assay*

The importance of phosphoinositide metabolism with respect to its role in hormonal signal transduction was first described in 1953 by Hokin and Hokin (Hokin *et al.*, 1953); thereafter a link between phosphoinositide hydrolysis and plasma membrane channel $Ca^{2+}$ entry was suggested by Michell in 1975 (Michell, 1975). There is a variance (between 2-8%) in the amount of inositol-containing phospholipids in cellular membranes and different tissues. Phosphatidylinositols constitute the highest proportion of phospholipids. Phosphoinositols are predominantly located in the inner cell membranes, whilst phosphoinositides (PI) tend to be found in the plasma membrane (Tkachuk, 1998).

#### 2.7.1. Metabolism of inositol phosphates

The phosphoinositide cycle is outlined in Figure. 2.6. Stimulation of $G_q$ coupled G-protein receptors culminates in the activation of phospholipase C beta 1 (PLC β1), which in turn leads to the phosphodiesteric cleavage of phosphotidylinositol 4,5-bisphosphate ($PIP_2$) and the formation of diacylglycerol (DAG) and inositol-1,4,5-trisphosphate (Ins-1,4,5- $P_3$).

Both these molecules are not exclusively generated via the activation of PLCβ1; they are also generated by the stimulation of tyrosine kinase (TK) linked receptors which activate phospholipase C gamma 1 (PLCγ1). Activation of TK –linked receptors activates phosphatidylinositol 3-OH kinase (PI-3K), thereby leading to the activation of the putative phosphatidylinositol 3,4,5-trisphosphate ($PIP_3$) and also the GTPase-activating protein (GAP) which is associated with regulating ras (Berridge, 1993).

Ins-1,4,5-$P_3$ is rapidly dephosphorylated by a 5'-phosphatase enzyme to give Ins-1,4-$P_2$. This is then dephosphorylated by non-specific inositol polyphosphate 1-phosphatase. Ins-4-

P is hydrolysed by inositol monophosphatase. Ins-1,4,5-$P_3$ is also metabolised via a second route to Ins-1,3,4,5-$P_4$ by a 3-kinase enzyme. This is then dephosphorylated presumably by 5-phosphatase to give Ins-1,3,4-$P_3$. This is then dephosphorylated by Inositol polyphosphate 1-phosphatase to give Ins-1,3-$P_2$ and Ins-3,4-$P_2$ respectively. The stereoisomers of Ins-1-P and Ins-3-P are formed when the bisphosphates are metabolised. These are utilised in the re-formation of Inositol. The rate limiting step where the metabolic pathway is sensitive to lithium chloride as indicated in Figure. 2.6. Hence lithium chloride (LiCl) is used as a pharmacological tool when studying inositide turnover.

### *2.8. Phosphoinositide turnover: methodology*

*Adherent cell assay*

Cells ($HEK293_{hUT}$ and $CHO_{hUT}$) were cultured two days prior to the experiment in 6-well trays and allowed to reach a confluent monolayer over 48 hr. The trays were loaded with 1 μCi/ml of [$^3$H]-myoinositol and incubated for 24 hr to allow incorporation of the radiolabel into the PI cycle. On the day of the experiment, excess radiolabel was removed by a gentle wash/aspirate cycle 3 times. After the third wash, the wells were filled with 500 μL KHB containing 10mM LiCl and allowed to equilibrate for 15 mins at 37°C.

Concentration response curves for agonist compounds were generated by adding the drugs into the wells. Reactions were terminated by the addition of 500 μl ice cold trichloroacetic acid (1M) after 15 mins and placing the tubes on ice for 30 mins. The supernatant was then transferred to fresh polypropylene tubes containing EDTA (100 μl at 10 mM).

A mixture of freshly prepared (v/v) tri-n-octylamine and Freon (trichlorotrifluoroethane) were aliquoted into the tubes, capped and vortexed intermittently for 15 min. Afterwards

the tubes were centrifuged at 1300 rpm for 3 mins at room temperature. The supernatant mixture formed two layers; the top phase was transferred into a new polypropylene tube containing 100 μl $NaHCO_3$ (60 mM).

Total [$^3$H]$IP_x$ (comprising of mono and polyphosphorylated inositol species) was extracted using ion exchange Dowex AG 1*8 resin columns. Columns were regenerated by the addition of 10 ml of regeneration buffer to the column and allowed to void. Thereafter columns were washed with 20 ml $dH_2O$.

Samples were pipetted into the columns and the tubes containing the samples washed with 1 ml $dH_2O$ and transferred into the columns to ensure complete removal of samples.

The columns were then washed by the addition of 10 ml $dH_2O$. This step ensures the washing off of any remaining [$^3$H] inositol. 12 ml of buffer A was added to the tubes to void out glycerophosphoinositol. At the end of this step the bottom ends of the columns were dried with a tissue and scintillation vials placed under them using a purpose built rack. Total $IP_x$ was eluted into the vials by the addition of 8 ml of buffer B. 4 ml of this eluate was then transferred into fresh scintillation vials and prepared for counting.

15 ml of scintillation cocktail was aliquoted into the vials, capped and vortexed. The vials were then placed in a Packard Canberra Liquid scintillation β-counter with an 8-hr delay protocol for counting [$^3$H].

The above protocol was used for analyzing $HEK293_{hUT}$ and $CHO_{hUT}$ cells only. After data was acquired from these cells further experiments using this protocol failed, therefore an alternative suspension assay was used to study $HEK29_{rUT}$ (rat UT) cells.

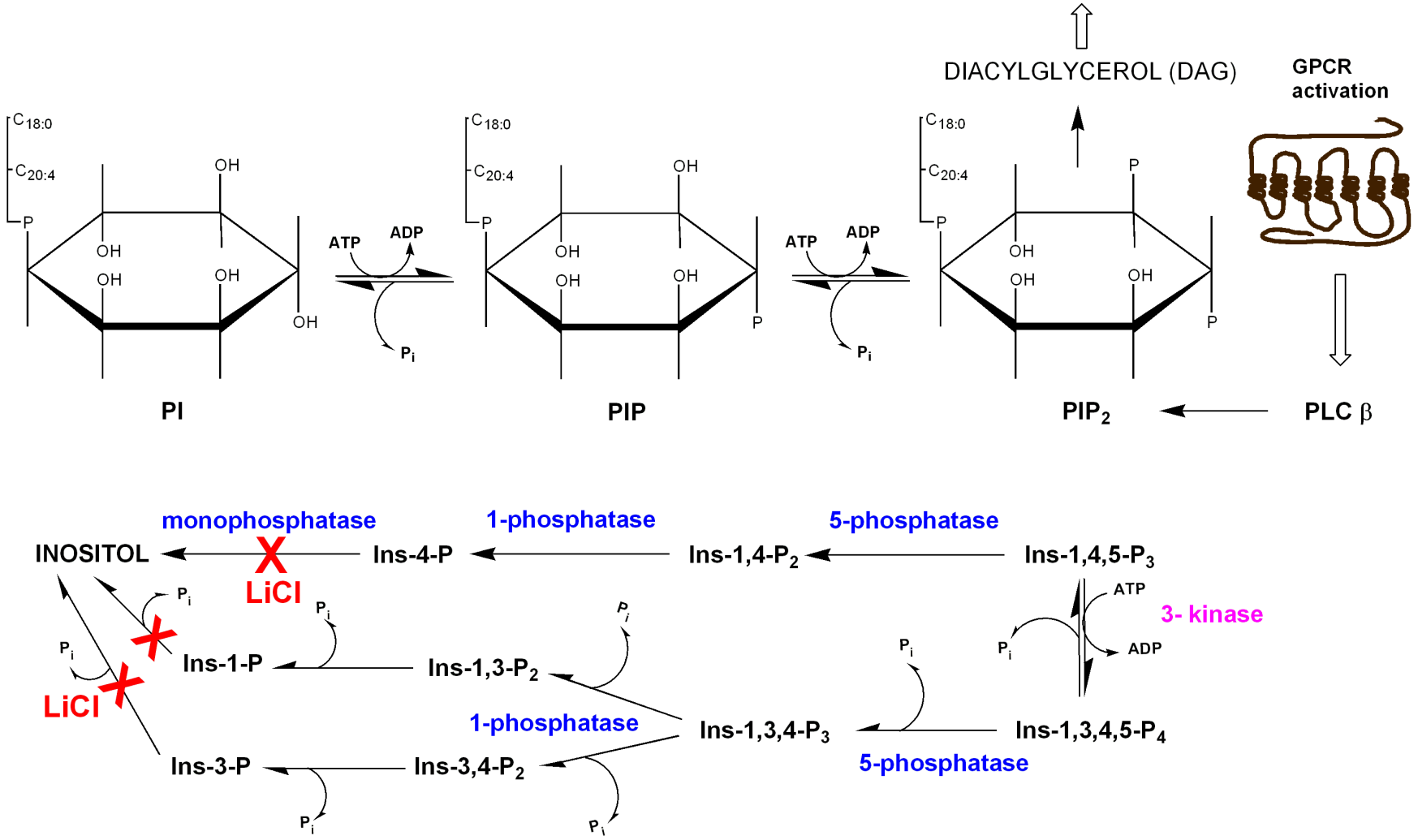


**Figure. 2.6. The metabolic pathway of inositol phosphates.**
The sites where lithium chloride blocks the re-synthesis of inositol are in highlighted by the X. Adapted from (Hughes *et al.*, 1990).

*Cell suspension assays*

$HEK293_{rUT}$ cells were grown in T75 Flasks which were incubated for 48 hr with 1μCi/ml of [$^3$H]-myoinositol with tissue culture media then harvested (into Krebs-HEPES buffer). 400 μl volumes were pre-incubated with 10 mM LiCl for 15 min. Drugs were added at 100 μl volumes to give a final assay volume of 500 μl with a concentration range of $10^{-11}$ M - $10^{-5}$ M. Reactions were terminated by the addition of 500 μl of ice cold TCA (1 M) and left for 30 min on ice and centrifuged (5 min, 3000 rpm). Of the resulting supernatant 800 μl was transferred to polypropylene tubes containing 160 μl EDTA (10 mM). A mixture of freshly prepared (v/v) tri-n-octylamine and Freon (trichlorotrifluoroethane) were aliquoted into these tubes and the samples were vortexed intermittently for 15 min and centrifuged for 5 min at 3000 rpm. 700 μl of the resulting upper phase was transferred to eppendorf tubes containing 175 μl $NaHCO_3$ (60 mM). Total [$^3$H]$IP_x$ fractions were recovered the same way as described in the adherent cell protocol.

### *2.9. Measurement of intracellular $[Ca^{2+}]_i$: theory*

With the discovery and use of the bioluminescent protein aequorin from the Aequorea jellyfish 47 years ago (Shimomura *et al.*, 1962) there has been much advancement in the development of numerous calcium indicators with the aim to improve spatial and temporal resolution of these indicators (Poenie, 1999).

Most of the fluorescent $Ca^{2+}$ dyes available today are modelled on BAPTA - bis(o-aminophenoxy)ethane-N,N,N',N'- tetracetic acid, which share some structural similarities with EGTA (ethylene glycol bis(β-aminoethyl ether)- N,N,N',N'- tetraacetic acid) (Figure. 2.7).

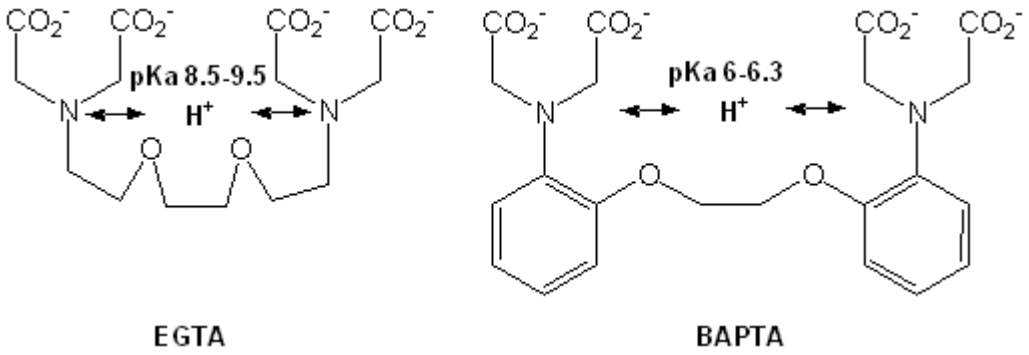


**Figure. 2.7. Structure of EGTA and BAPTA.**

The major difference between these two molecules is attributed to the amino groups; where in EGTA there are two aliphatic amino groups whilst there are two aromatic amino groups in BAPTA.

There are a number of benefits of using BAPTA derived calcium dyes over those based on the structure of EGTA. 1) The range of the acid dissociation constant ($pK_a$) of BAPTA is lower than EGTA (0.35 vs 1.00). Thus under physiological pH these derivatives remain unionized. Furthermore they are insensitive to small fluctuations in pH. 2) BAPTA binds faster to calcium and has a higher selectivity for $Ca^{2+}$ over other divalent cations ($Mg^{2+}$) with a stoichiometry of 1:1; due to 3) amino groups of BAPTA not being protonated at pH 7. In the case of EGTA calcium binding can only occur if there is an $H^+$ to $Ca^{2+}$ ion exchange. BAPTA derived dyes are referred to as high affinity indicators that can be categorised as being either ratiometric or non-ratiometric.

### 2.9.1. Ratiometric $Ca^{2+}$ dyes

Fura-2 AM (acetoxymethyl) is a UV excitable ratiometric dye that is derived from quin-2 AM a first generation single excitation fluorescent indicator. Whilst quin-2 has an excitation at 340nm and on binding to $Ca^{2+}$ has an emission intensity of 505nm, Fura-2 has a broader excitation range between 300-400nm which peaks at 370nm in low $Ca^{2+}$ conditions (Figure. 2.8).

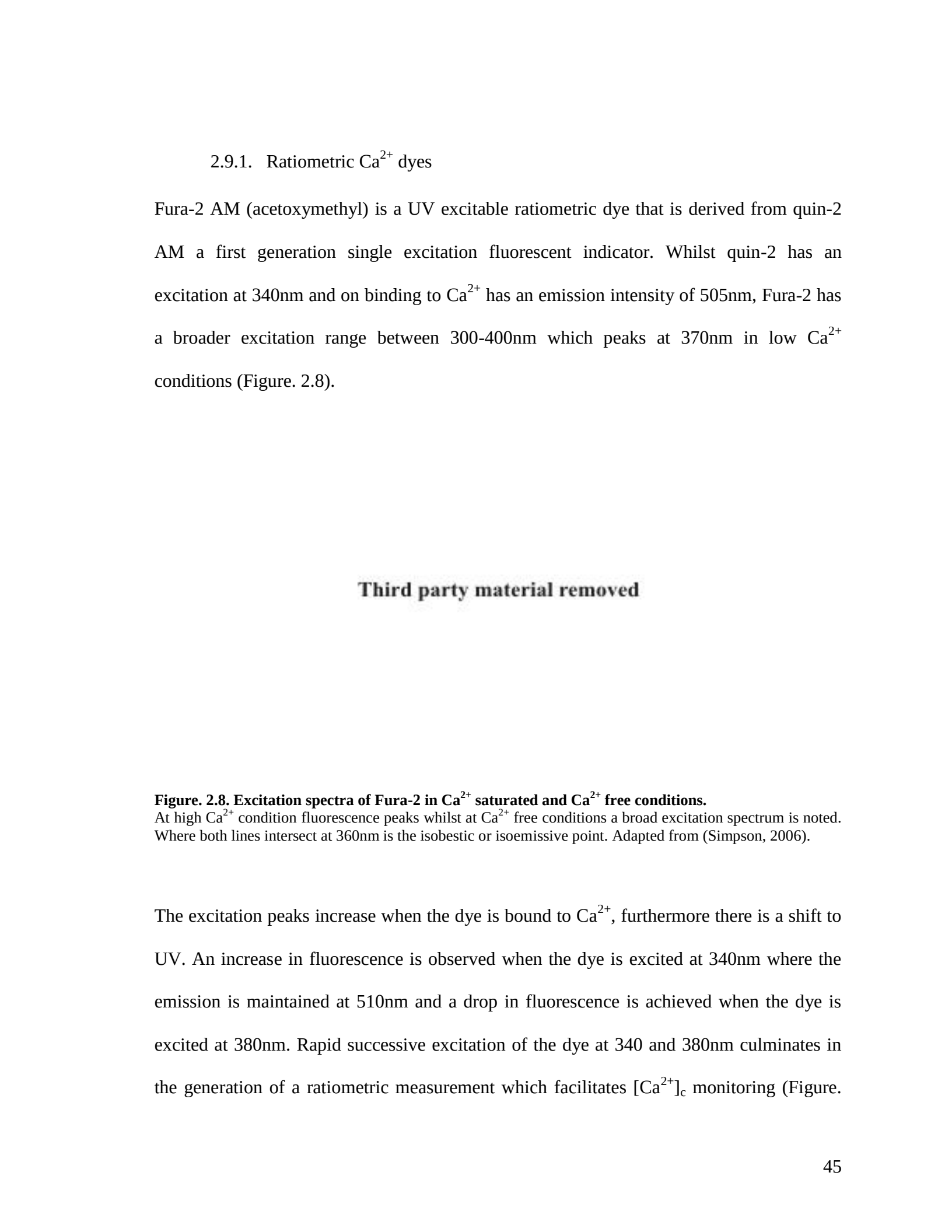


**Figure. 2.8. Excitation spectra of Fura-2 in $Ca^{2+}$ saturated and $Ca^{2+}$ free conditions.**
At high $Ca^{2+}$ condition fluorescence peaks whilst at $Ca^{2+}$ free conditions a broad excitation spectrum is noted. Where both lines intersect at 360nm is the isobestic or isoemissive point. Adapted from (Simpson, 2006).

The excitation peaks increase when the dye is bound to $Ca^{2+}$, furthermore there is a shift to UV. An increase in fluorescence is observed when the dye is excited at 340nm where the emission is maintained at 510nm and a drop in fluorescence is achieved when the dye is excited at 380nm. Rapid successive excitation of the dye at 340 and 380nm culminates in the generation of a ratiometric measurement which facilitates $[Ca^{2+}]_c$ monitoring (Figure.

2.9). The ratiometric signal that is generated is independent of dye concentration, the illumination intensity or path length, the opposite is the case for single excitation fluorescent indicators (Simpson, 2006).

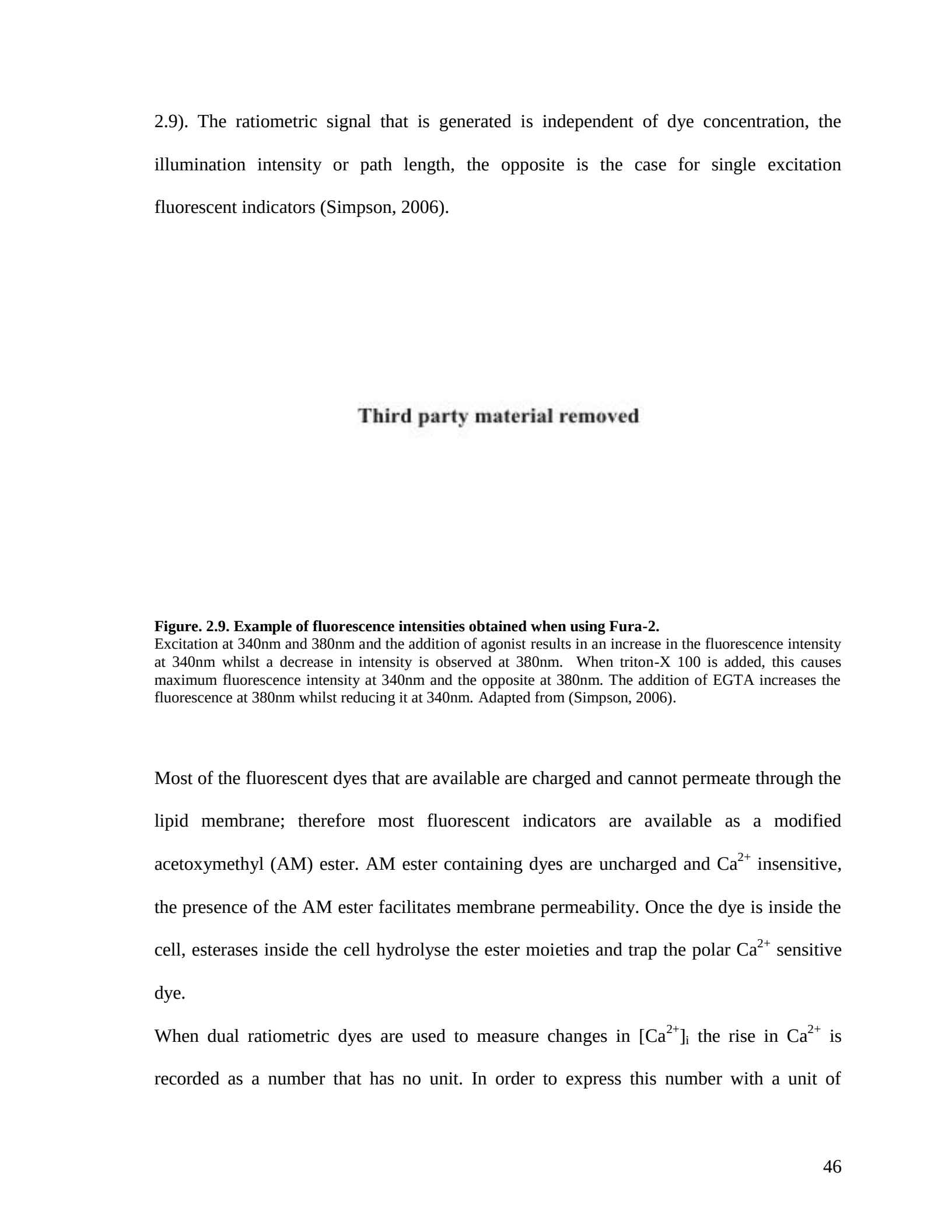


**Figure. 2.9. Example of fluorescence intensities obtained when using Fura-2.**
Excitation at 340nm and 380nm and the addition of agonist results in an increase in the fluorescence intensity at 340nm whilst a decrease in intensity is observed at 380nm. When triton-X 100 is added, this causes maximum fluorescence intensity at 340nm and the opposite at 380nm. The addition of EGTA increases the fluorescence at 380nm whilst reducing it at 340nm. Adapted from (Simpson, 2006).

Most of the fluorescent dyes that are available are charged and cannot permeate through the lipid membrane; therefore most fluorescent indicators are available as a modified acetoxymethyl (AM) ester. AM ester containing dyes are uncharged and $Ca^{2+}$ insensitive, the presence of the AM ester facilitates membrane permeability. Once the dye is inside the cell, esterases inside the cell hydrolyse the ester moieties and trap the polar $Ca^{2+}$ sensitive dye.

When dual ratiometric dyes are used to measure changes in $[Ca^{2+}]_i$ the rise in $Ca^{2+}$ is recorded as a number that has no unit. In order to express this number with a unit of

concentration it is necessary to calibrate the dye. The change in $[Ca^{2+}]_i$ is calculated from the ratio at dual excitation using the Grynkiewicz equation (Grynkiewicz *et al.*, 1985):

$$[Ca^{2+}]_i = K_d \left[ \frac{R - R_{\min}}{R_{\max} - R} \right] \times \left[ \frac{F_{380\,\max}}{F_{380\,\min}} \right]$$

$[Ca^{2+}]_i$ represents the intracellular calcium concentration, $K_d$ is the equilibrium constant of $Ca^{2+}$ for Fura-2 (145/224 nM at 22 and 37°C respectively), $R$ is the fluorescence ratio ($F_{340nm}/F_{380nm}$), $R_{min}$ and $R_{max}$ represents the fluorescence ratio at minimum (EGTA) and maximum (Triton-X) $[Ca^{2+}]$ respectively and $F_{380max}/F_{380min}$ is the fluorescence ratio at minimum saturated $[Ca^{2+}]$.

### 2.9.2. Non-ratiometric $Ca^{2+}$ dyes

Fluo-4 is a visible light excitable non-ratiometric dye that is modeled on fluorescein and BAPTA and is synthesised by the coupling of difluorofluorescein fluorophore to BAPTA. The presence of the halogen fluorine makes this compound insensitive to pH. Furthermore it is brighter than fluo-3 (dichlorofluorescein fluorophore) by approximately 40%, hence this dye is the preferred choice in highthroughput screening of GPCRs associated with $Ca^{2+}$ mobilisation. The excitation peak of fluo-4 is 491nm and the emission is 525nm. Single excitation $Ca^{2+}$ dyes like fluo-4 and fluo-3 are the preferred choice of probe when looking at single cell $Ca^{2+}$ mobilisation utilising confocal microscopy.

### 2.9.3. Single cell microfluorometry

Confocal imaging is defined as the illumination and detection of a single point within a specimen at a resolution close to the theoretical diffraction-limited maximum (Tovey, 2006).

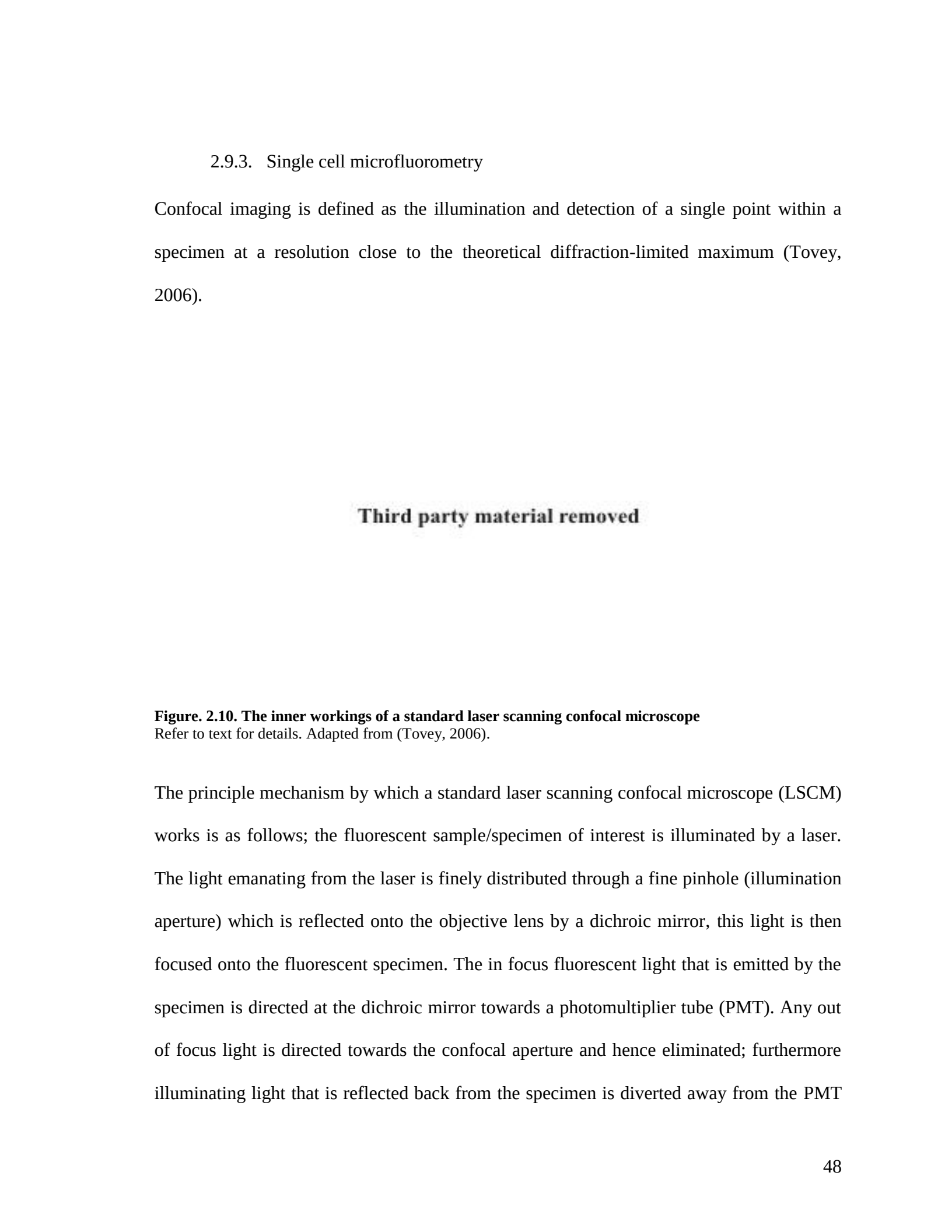


**Figure. 2.10. The inner workings of a standard laser scanning confocal microscope**
Refer to text for details. Adapted from (Tovey, 2006).

The principle mechanism by which a standard laser scanning confocal microscope (LSCM) works is as follows; the fluorescent sample/specimen of interest is illuminated by a laser. The light emanating from the laser is finely distributed through a fine pinhole (illumination aperture) which is reflected onto the objective lens by a dichroic mirror, this light is then focused onto the fluorescent specimen. The in focus fluorescent light that is emitted by the specimen is directed at the dichroic mirror towards a photomultiplier tube (PMT). Any out of focus light is directed towards the confocal aperture and hence eliminated; furthermore illuminating light that is reflected back from the specimen is diverted away from the PMT

by the dichroic mirror. The signal information collected by the PMT exists as an electrical signal; which can be rendered to yield real time images of the specimen under study (Figure. 2.10).

### 2.9.4. Flexstation-II benchtop scanning fluorometer

The Flexstation II (Molecular Devices, Sunnyvale, CA, USA) is used for small scale high throughput screening (HTS) (Figure. 2.11 top panel). It is essentially a plate reader that is capable of measuring $[Ca^{2+}]_i$ by utilising both single and dual wavelength $Ca^{2+}$ indicator dyes.

This instrument is capable of carrying out both bottom and top reading of plates that can be either in 96 or 384 format according to user specification and customisation (Figure. 2.11 bottom panel) at both room temperature and physiological temperature. The excitation (250-850nm) and emission (360-850nm) light is generated by a Xenon flash lamp and monochromators. The high range in both excitation and emission also serves as a means for characterising novel fluorophores. Drugs are transferred from a drug plate to a cell plate during the operation of the instrument by the means of an 8-channel pipettor system coupled to the fluid transfer system. Data acquisition and interpretation is achieved by the SoftMax® Pro software (Molecular Devices, Sunnyvale, CA, USA). Some of the software controlled experimental parameters include; reagent transfer volumes and speed of dispensing, mixing intervals and reagent addition times, data sampling intervals and temperature control (Marshall, 2006).

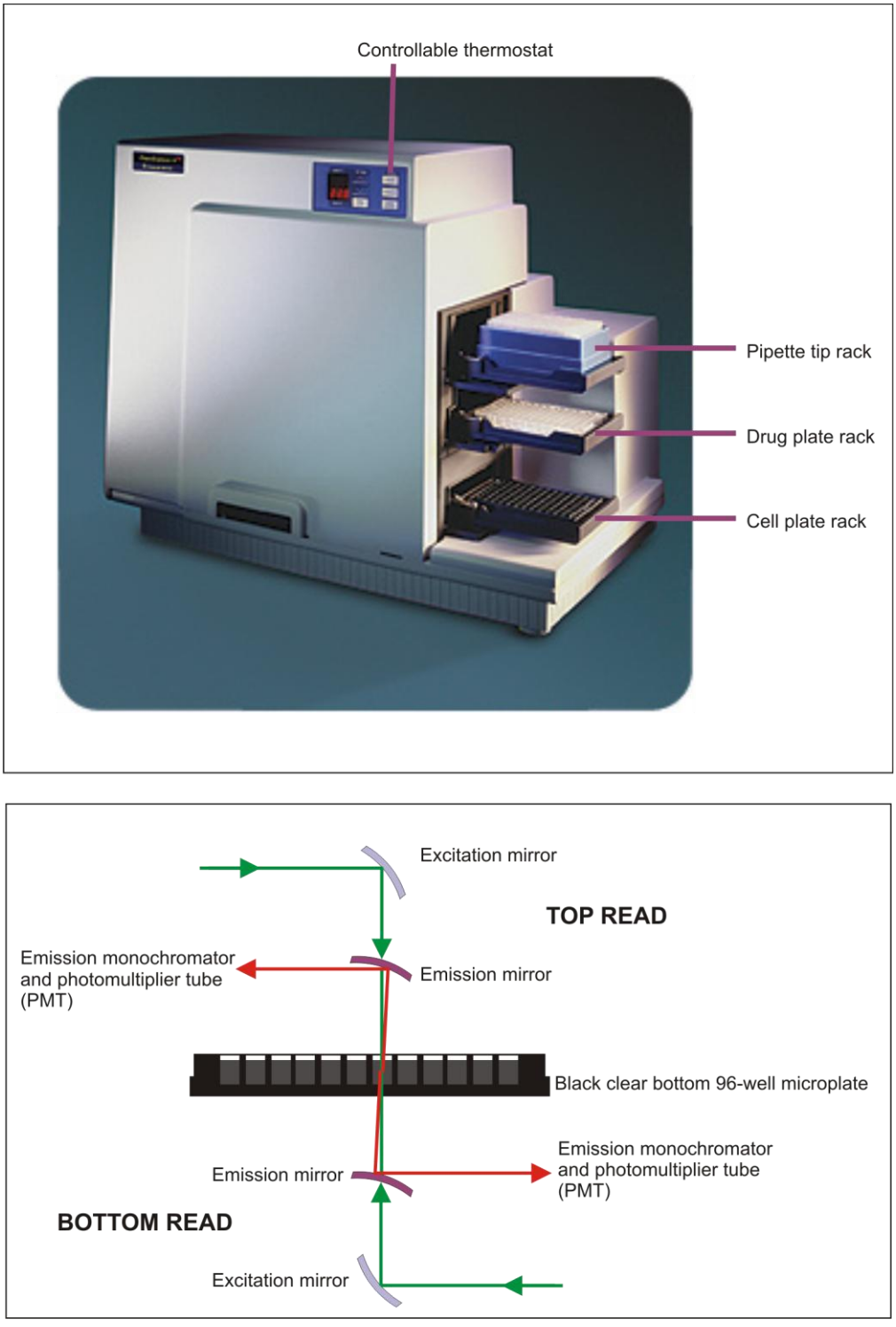


**Figure. 2.11. The Flexstation-II.**
*Top panel*: the instrument and its key components. *Bottom panel*: the optic system by which data acquisition is enabled.

## *2.10. $Ca^{2+}$ mobilisation assays: methodology*

### 2.10.1. Cuvette based $Ca^{2+}$ assay

Cells were detached from two tissue culture flasks (T75 and T175) with 1x harvest buffer, washed twice and suspended in KHB. The cell suspension was loaded with 3-5μM Fura-2 AM for 30 min at 37°C, thereafter the loaded cells were resuspended in KHB to facilitate further de-esterification for 20 min in dark conditions at room temperature.


**Figure. 2.12. The Perkin Elmer LS50-B.**

The assay was carried out in quartz cuvettes on a Perkin-Elmer LS50-B Fluorometer (Figure. 2.12). 2 ml of the cell suspension was aliquoted into a cuvette containing a mini magnetic flea and placed in the instrument. The temperature of the cuvettes was maintained

at 37°C by external silicon tubing connected to a waterbath. Cell suspensions were allowed to equilibrate for 170 seconds prior to the addition of drugs (at 175 seconds). $Ca^{2+}$ mobilisations were generated using a concentration range of $10^{-10}$ -$10^{-5}$M of the agonist (Stock concentration 2 mM). These were prepared by a 10-fold serial dilution. In order to account for the dilution effect when the drug was added to the cell suspension, the top concentration ($10^{-5}$M) was made 40x concentrated. Data collection was carried out using the FLDM program from Perkin Elmer. Calibrations and subsequent determination of $[Ca^{2+}]_i$ were determined using Triton-X (50 μl 1% solution) and EGTA (200 μl 500 mM solution) (to obtain the $R_{max}$ and $R_{min}$ respectively) and the Grynkiewicz equation with a $K_d$ of fura-2 at 22 and 37°C.

### 2.10.2. Single cell $Ca^{2+}$ measurements

Microfluorometric experiments were undertaken to observe and characterise the types of $Ca^{2+}$ mobilisation responses in SJCRH30 rhabdomyosarcoma cells. As these cells express native human UT receptor (Douglas *et al.*, 2004), it would be useful to understand if the response was homogeneous or heterogeneous.

Rhabdomyosarcoma cells were grown in a T25 culture flask to obtain a 90-100% confluent monolayer. Thereafter the cells were split and plated onto 25 mm borosilicate glass coverslips coated with 0.01% poly-D-lysine in a 6-well multidish. Cells were seeded in order to obtain a confluency of 60-70% for experimentation.

On the day of experimentation the cell growth media was aspirated and the coverslips washed with Krebs HEPES buffer at room temperature once. The buffer was aspirated and cells loaded with 2 μM Fluo-3 AM containing 0.02% pluronic acid F-127 made in KHB.

After loading the coverslips were incubated at room temperature for 40 min away from light. The loading media was then removed and the cells were washed once with KHB and incubated in 1 ml KHB to allow de-esterification.

The cells were then mounted into a chamber on the stage of an Olympus IX50 inverted microscope. Physiological temperature (37°C) was maintained using a Peltier thermal heating device and keeping the perfusion buffers in a pre-heated water bath, however the assays were recorded at a temperature ~30°C. This was due to the insulation tubing jacket losing some heat as it traveled from the heating device into the perfusion chamber. The Argon laser in the instrument was used to excite the fluo-3 loaded cells at 488 nm and the emitted fluorescence was collected and processed at wavelengths >505 nm. Image acquisition was carried out through PerkinElmer imagine suite Ultra*VIEW*. Raw data traces were imported into Microsoft Excel and thereafter into Graphpad Prism 3.0 for further viewing and analysis.

### 2.10.3. Flexstation-II $Ca^{2+}$ assays

For $Ca^{2+}$ mobilisation studies, cells were plated in poly-D-Lysine coated 96-well black clear bottom plates (herein referred to as the cell plate) at a density of 50,000 cells/well. After a 24 hr incubation cells were incubated with 100 μL/well of loading solution for a further 30 min at 37°C. The loading solution consisted of medium supplemented with probenecid at 2.5 mM, Fluo-4 AM fluorescent calcium indicator dye (3 μM) and 0.01% pluronic acid. Thereafter the loading solution was aspirated and replaced with 100μL/well of assay buffer comprising of Hank's balanced salt solution (HBSS) supplemented with 2.5 mM probenecid, 20 mM HEPES and 500 μM Brilliant Black.

All U-II analogs and reference peptides; U-II and U-II(4-11) were made up as 1 mM concentrated stocks by dissolving in water. Serial dilutions (10 fold) of all peptides were carried out in HBSS/HEPES (20 mM) supplemented with 0.02% BSA Fraction V (w/v). The concentration of the diluted drugs were 3x concentrated in the drug plate. The cell plate and drug plate were placed in the respective insert of the Flexstation-II and concentration response curves (CRCs) were generated by measuring changes in fluorescence (excitation $\lambda$ = 488nm, emission $\lambda$= 510nm) at ambient room temperature (23° - 25° C). On-line addition of the each drug was in a volume of 50µl/well.

### *2.11. Tissue bioassays: general theory*

Numerous *in vitro* techniques are available to study the pharmacological aspects of drugs however much of the basic understanding of how drugs interact with their respective receptor and their effects (in particular vascular effects) have been facilitated by incorporating studies with crude tissue preparations. This section discusses the basic principles of the tissue organ bath (isometric) preparations.

Prior to the advent of molecular biology and reverse pharmacology strategies the bioassay was the preferred choice of assessing functional aspects of drugs and their receptors. While HTS methods today are considered a valuable tool, *ex-vivo* bioassays are still regarded as being more sensitive due to their amplified end point response and hence are widely utilised (Kenakin, 2009).

The most suitable method for studying large arteries and veins (of more than 1 mm diameter) is the organ bath preparation illustrated in Figure. 2.13. In this method, the tissue

of interest is isolated from the animal and then promptly placed in an oxygenated physiological salt solution (Krebs Solution).

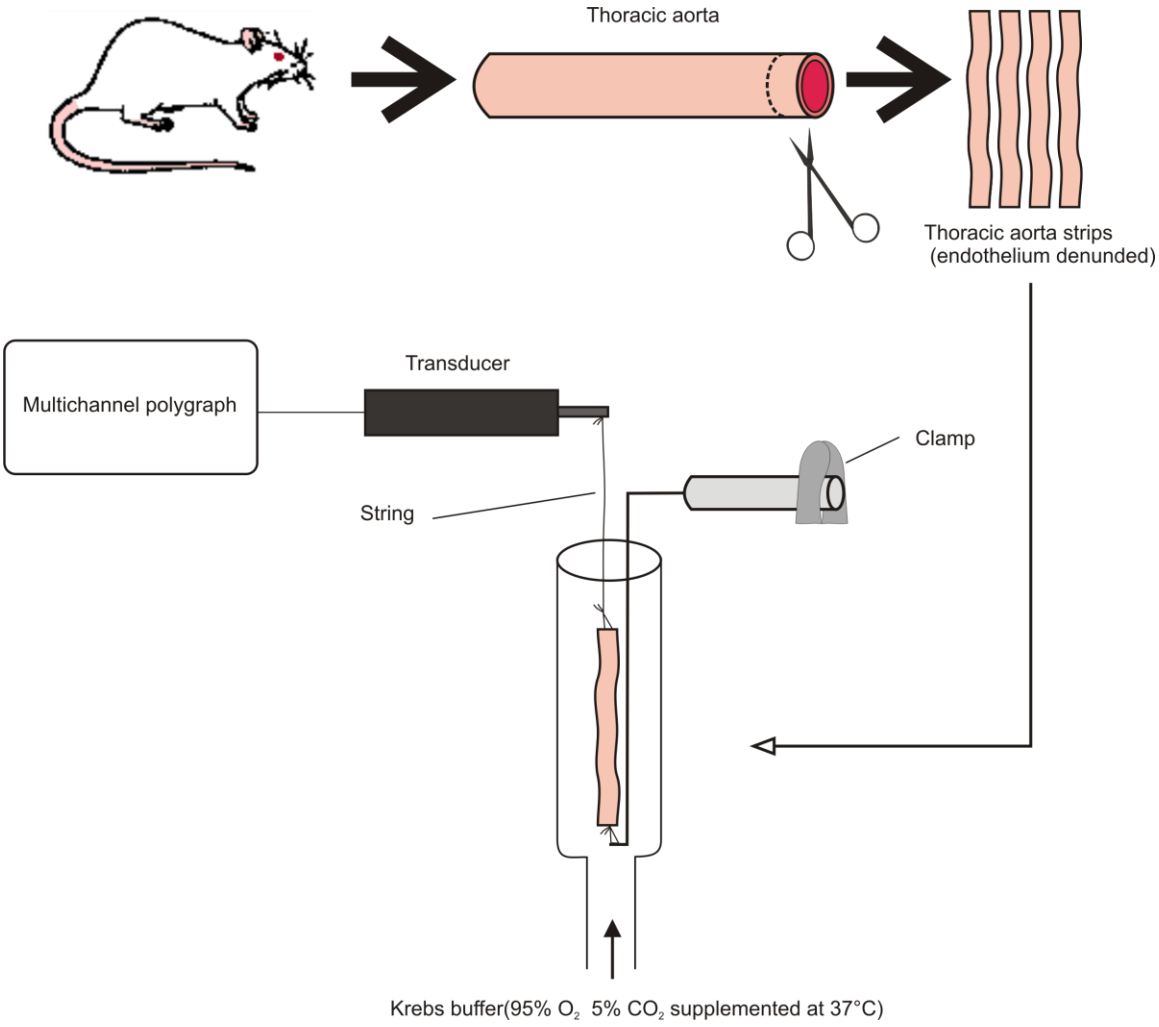


**Figure. 2.13. Schematic outline of rat aorta organ bath preparation.**

This retains the short term viability of the tissue while the tissue is prepared for placing in the organ bath chamber. The tissue is usually cleaned to remove any connective tissue with the aid of a magnifying glass and fine surgical scissors. As part of the preparative criteria depending on the type of tissue that is used (and species) they can be cut into helical strips or rings and then suspended in the chamber using "wires". The method by which the tissue is cut can have a drastic effect on the magnitude of the tissue response to drugs. Therefore it

is very important to understand the geometry of the tissue under investigation. Furthermore in addition to removing connective tissue it is also important to consider the influence of the endothelium on the end point response. The wire (top portion) is usually coupled to an isometric force transducer, which in turn is connected to a multiple channel recorder (Figure. 2.13).

The equilibration process involves calibrating the tissue under study according to a passive force normalisation. Passive force is the force that is exerted upon a tissue without any physiological or chemical stimulus by the elastic elements of muscle; this is achieved by extending resting muscle tissue beyond its normal length at which point a passive force develops. If the investigator is establishing an organ bath preparation for a given tissue for the first time, this would mean raising the passive force by steps while exposing the tissue to an agonist (e.g. $K^+$ or noradrenaline).

For example when the passive force is 0.5g, the contractile response to noradrenaline is 45% however if the passive force was increased to 1g then there would also be an increase of the contractile response (in this case approx 98-100%) any further increases in passive force may or may not result in a lower response. This does not necessarily mean that at 1g tension the response will always be 98-100% (Figure. 2.14). There will be variation in this response and this is dependent on the receptor density, efficiency of stimulus coupling, quality of the tissue and the duration taken in isolating and transfer to an *ex-vivo* environment. Once the optimum passive force is established subsequent challenges with control compounds (i.e. $K^+$ or noradrenaline) serve as a means to clarify the viability of the tissue prior to testing a drug of interest.

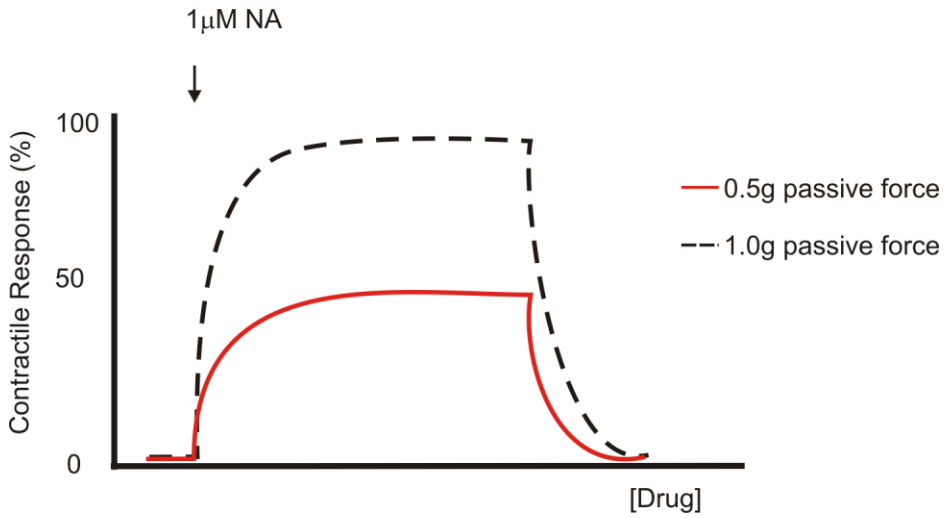


**Figure. 2.14. The effect of force on total contractile response.**

Once the tissue is setup it is left to equilibrate into its new environment of oxygenated Krebs solution at 37°C so that experimentation can proceed (Martin, 1996)(Spiers, 2005) (Angus *et al.*, 2000).

### *2.12. Aorta bioassay: methodology*

Sprague Dawley rats (Morini, Reggio Emilia, Italy) weighing 150-180g were housed at the University of Ferrara under standard conditions (22°C 12 hr light-dark cycle) and were handled in accordance with the European Communities Council Directives.

Following ethoxyethane (ether) asphyxiation and decapitation with a guillotine, thoracic aortae were transferred into glass Petri-dishes containing Krebs-buffer. Thereafter the tissue was cut into helical strips. Prior to this connective tissue surrounding the vessel was trimmed and removed using a pair of fine surgical scissors. The endothelium on the helical strips was removed by gently rubbing the surfaces with a moistened cotton swab.

The tissue strips were suspended in organ baths supplemented with Krebs-buffer at 37°C bubbled with 5% $CO_2$ and 95% $O_2$. A tension of 1 g was applied to the tissue and left to equilibrate for 1 hr. During this time the tissue preparation was washed every 20 min before proceeding with experiments. Recordings were measured using a Grass FT03 force transducer connected to a Linseis 2005 six channel polygraph. Please refer to appendices for calculations and conversions.

### *2.13. Real-time reverse transcriptase polymerase chain reaction*

From a developmental perspective, the origins of nucleic acid detection involved labeling cells with radio labeled deoxythymidine triphosphate (dTTP) and assessing their incorporation in the nucleic acids by precipitation using trichloroacetic acid. While this method was quantitative its major drawback was that investigators could not look at specific changes in gene expression but only gain an insight into global changes (Shipley, 2007). The detection of different genes or transcripts was possible with the development of Northern blotting. While this method also used a radioactive label; it was not quantitative. Hence over time the ribonuclease protection assay was conceived and was considered as being semi-quantitative (Dvorak *et al.*, 2003). A milestone in biotechnical research was the introduction of the polymerase chain reaction (PCR) (Mullis, 1990). The following section gives an overview as to the process of real time reverse transcription PCR; starting from the importance of the starting material to the process involved in detecting mRNA for specific genes and their transcripts.

### 2.13.1. RNA quality and types of reverse transcription

DNA comprises of both introns and exons, while mRNA comprises of transcribed exons (as a consequence of DNA transcription to mRNA). The process of real time reverse transcription (RT) PCR is used to look at RNA and comprises of the following steps: 1) reverse transcription of RNA to give complementary DNA, 2) the amplification of a gene of interest from the complementary DNA by PCR. While the process of RT-PCR is generally very sensitive and reproducible, it requires much attention from a preparative perspective (e.g. quality of the starting materials and reagents, good laboratory practice) (Nolan *et al.*, 2006). Figure. 2.15 summarises of some of the key points in planning a successful real time RT-PCR assay along with a brief overview relating to these points.

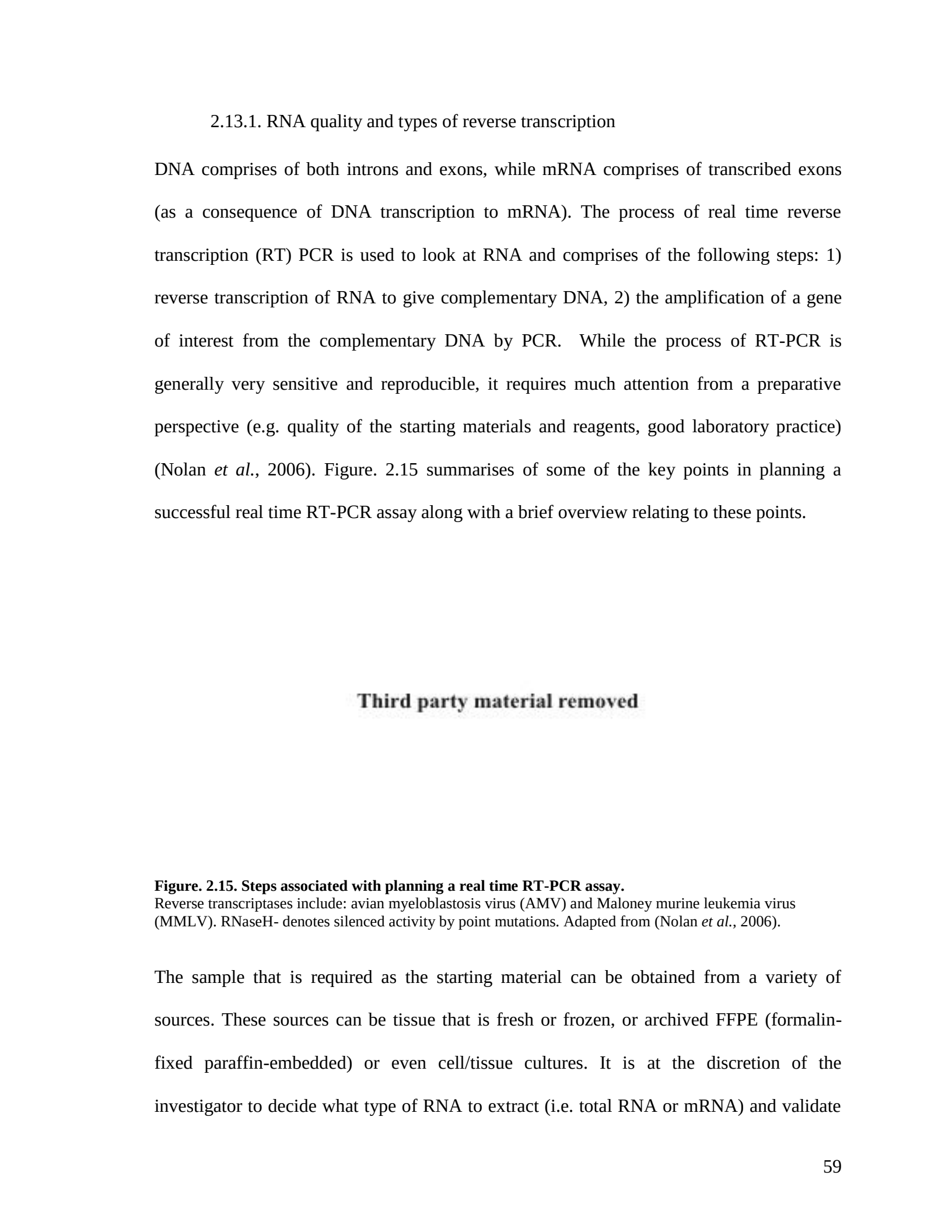


**Figure. 2.15. Steps associated with planning a real time RT-PCR assay.**
Reverse transcriptases include: avian myeloblastosis virus (AMV) and Maloney murine leukemia virus (MMLV). RNaseH- denotes silenced activity by point mutations. Adapted from (Nolan *et al.*, 2006).

The sample that is required as the starting material can be obtained from a variety of sources. These sources can be tissue that is fresh or frozen, or archived FFPE (formalin-fixed paraffin-embedded) or even cell/tissue cultures. It is at the discretion of the investigator to decide what type of RNA to extract (i.e. total RNA or mRNA) and validate

these. The validation process involves looking at the quality and quantity of the starting material by means of traditional spectrophotometry, specialist kits and/or equipment (Ribogreen, Agilent BioAnalyzer 2100).

Total RNA is used as a starting material when the quality is not exceptional (e.g. FFPE). Formalin is a cheap and easy to use fixative which is capable retaining the architecture and ultrastructure of cells within tissue biopsies; however it also has a detrimental effect in that it exacerbates the fragmentation of nucleic acids due to the generation of crosslinks within the tissue (Castiglione *et al.*, 2007).

mRNA is used when the source is of high quality (e.g. fresh tissue or cell/tissue cultures). The type of priming is dependent on the quality of the RNA. There are four methods that are routinely used: (1) specific priming is utilised when amplifying a single gene of interest by one step RT-qPCR and this can be applied to both total RNA and mRNA. (2) Random hexamer priming is used when carrying out a two step RT-qPCR and when RNA samples are degraded (i.e. FFPE). (3) Oligo dT priming is the most suitable priming method when the RNA is structurally intact, as the long T chain within oligo dT binds to the polyA tail. Hence it is more specific than using random primers. However there are problems associated with oligo dT priming; for example mammalian mRNA have many non-translated regions (NTRs) ranging from one to several kilobases. The NTRs tend to be located downstream from a coding region. If one was to amplify a gene that is located towards the 5' end then the option of priming would involve oligo dT. This however will not generate long cDNA transcripts. In this type of scenario, using a random hexamer will very likely generate cDNA that represents the 5' end of the mRNA (Nolan *et al.*, 2006) (O' Connell, 2002).

Recently it has been demonstrated that random hexamers may not be as efficient as pentadecamers (15 nt long). The latter are capable of generating cDNA yields of approx 80% compared to commercially available random hexamers which generate cDNA yields of 40% (O' Connell, 2002).

The quality of the cDNA can also be affected by the type of reverse transcriptase enzyme used. Most of the RT enzymes function by utilising RNA as a template to synthesise a complementary DNA strand under the action of an RNA-dependent DNA polymerase. All naturally occurring enzymes of this type have RNase H activity, which is detrimental to the RNA template as it can degrade RNA by a hydrolytic cleavage mechanism. Thus under all *in-vitro* conditions this is overcome by the usage of an RNase H inhibitor during the process of reverse transcription. However another alternative is to use RT enzymes where the RNase H activity has been blocked by mutating the RNase enzyme in conjunction with an RNase H inhibitor.

### 2.13.2. Real time PCR and conventional PCR

There are 3 distinct phases in the amplification process in a PCR as indicated in Figure. 2.16. These phases are common to both conventional and real time PCR. The difference is the point at which measurements are made.

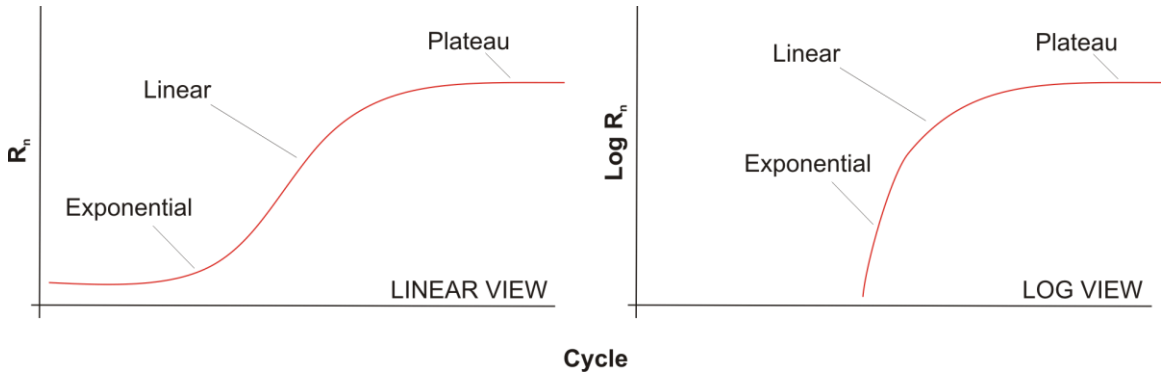


**Figure. 2.16. An illustrative overview of the 3 distinct phases in a polymerase chain reaction.**
*Left panel*: Linear scale depiction of cycles in a PCR reaction. Fluorescence (Rn) units on *y-axis* over Cycle. *Right panel*: Logarithmic scale view is indicated where log fluorescence (denoted by Log Rn) is shown on the *y axis* and the reaction cycle on the *x axis*.

During the early exponential phase there is a doubling of the PCR product (amplicon) for every cycle in the reaction, assuming that the reaction is at 100% efficiency. This is followed by the linear phase. At the linear phase the reaction begins to slow due to the exhaustion of the starting materials (template, dNTPs, primers, Taq polymer enzyme) as they are consumed in the reaction. The third and final phase is the plateau phase where the reaction comes to an end and hence is the end-point (Figure. 2.16).

In the traditional PCR method, the amplicon is detected at the end of the reaction (i.e the end-point) by visual discrimination of the size of the product against a DNA standard ladder. This is a qualitative assessment. It is not possible to discriminate the expression level between 10 copies of a gene versus 20 copies of that same gene in an agarose gel due to following problems associated with end-point detection: poor and low sensitivity and precision, post-PCR processing, staining by EtBr (ethidium bromide) is qualitative, low resolution, size based discrimination.

During a real time PCR experiment the amplification of a gene is measured by fluorescence intensity (relative fluorescence units RFU or $R_n$) (Figure. 2.17) that is emitted each time a PCR product is formed.

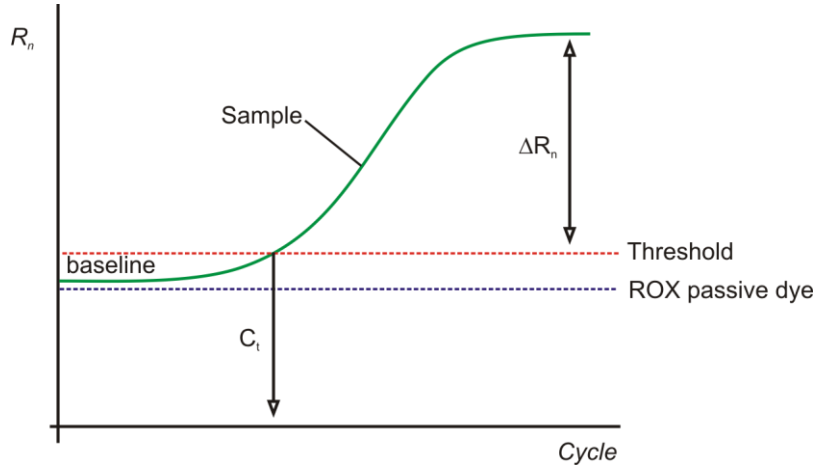


**Figure. 2.17. How Ct and $\Delta R_n$ are determined in a real time reaction.**

The fluorescence that is emitted is normalised against a passive dye referred to as ROX, thereby normalising the original fluorescent signal results in the determination of the change in fluorescence using the formula:

$$\Delta R_n = \frac{RFU_{sample}}{RFU_{ROX}} - \frac{RFU_{sample(initial)}}{RFU_{ROX\,(initial)}}$$

Thereafter $\Delta R_n$ can be plotted against the cycle number thereby facilitating determination of the Ct with reference to the threshold (which is automatically set by the instrument). The Ct is the number at which fluorescence is detected when the reaction cross over the threshold and represents the point where a detectable amount of amplicons have formed.

### 2.13.3. Probe chemistry

There are a numerous probes available for real time qPCR, however a description of all these probes is beyond this thesis. The reader is directed to a very good review by Kubista and co-workers (Kubista *et al.*, 2006). Below is a description of SYBR Green and Taqman probes (Figure. 2.18) two of the most widely used probes in realtime PCR applications.

SYBR Green is a fluorescent probe that shares a common structure with other assymmetric cyanine fluorescent probes such as YOYO®-1 and TOTO®-1 (Singer *et al.*, 1999). Like ethidium bromide SYBR Green binds to dsDNA by means of intercalating between nucleotide base pairs thereby fluorescing. While it is a very effective tool it is incapable of distinguishing dsDNA species; hence while detecting the gene of interest during reactions it can also detect non-specific gene products.

Taqman probes are fluorogenic hydrolysis probes that are dual labeled (comprising of a fluorophore and a quencher tag). These probes work by utilising the 5' exonuclease activity of Taq polymerase (Heid *et al.*, 1996). When the fluorophore and quencher are in close proximity, this prevents the probe from fluorescing; however hydrolysis of the probe during polymerase driven extension of the template results in hydrolysis of the probe and the release of the fluorophore. Unlike SYBR Green, Taqman probes are very specific as they only bind to the target of interest that is been studied, therefore the chances of non-specific products being detected are minimised.

**Figure. 2.18. SYBR Green and Taqman probe chemistry.**
Adapted from (van der Velden *et al.*, 2003).

### 2.13.4. Primer design

An obstacle that is associated with RT-PCR is genomic DNA contaminating RNA during the pre and post PCR stages. Therefore it is necessary to minimise or completely abolish genomic carry over by utilising better primer design strategies.

Genomic DNA carryover can be discriminated from cDNA templates by designing primers that span over introns. If genomic contamination is present this can be distinguished by a larger PCR amplicon compared to when no genomic contamination is present. The alternative strategy to this is to design primers that span the exon-exon junctions. In this scenario genomic DNA cannot be amplified as the intron will be between the primer pairing the template (Figure. 2.19).

The probes used in the present study were pre-validated Taqman probes; therefore primer design was not a necessary step.

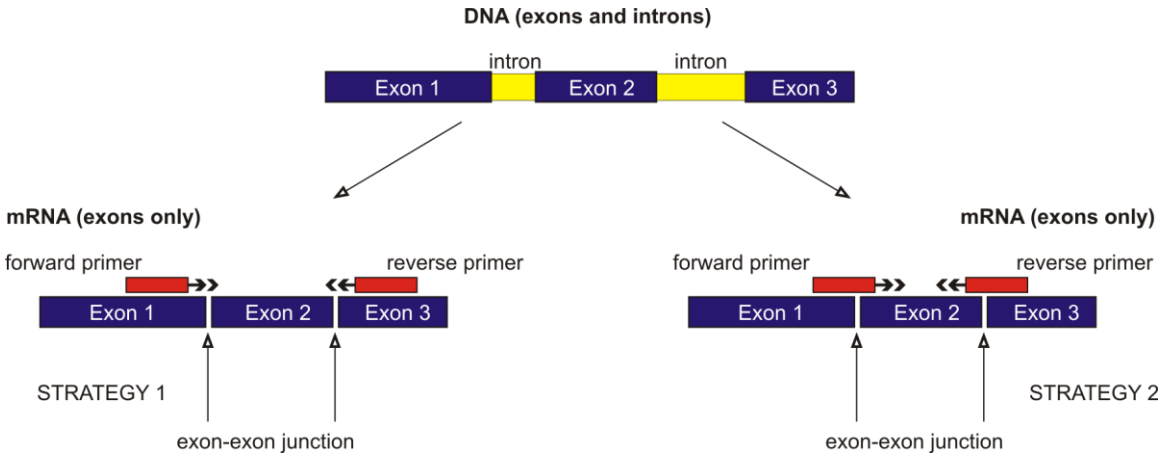


**Figure. 2.19. Strategies for designing primers for RT-PCR.**

### 2.13.5. Gene quantification methods

The amplification of a gene of interest can be quantified using two methods; namely absolute and relative quantitation. In this particular study the latter method has been used. The reader is directed to a good review by (Wong *et al.*, 2005) which summarises both quantification methods. The relative quantification method has been extensively used (Livak *et al.*, 2001). An example of how this method can be used to analyse data is illustrated below with a hypothetical example.

Let us assume that the effects of a new experimental drug were assessed on a cell line. Investigators are interested in assessing the effects of drug treatment on target gene expression. Cells were grown in 6-well plates. Three of the wells were treated with the drug and three remain untreated. The Ct for the treated batches are 25.5, 24.3, 25.2 (gene of interest GOI) and 22.3, 22.7, 22.00 (housekeeper gene HKG). The Ct for the untreated batches are 28.4, 27.8, 28.1 (gene of interest GOI) and 22.2, 22.5, 22.1 (housekeeper gene HKG).

The first step would be to determine the mean Ct of the GOI and HKG.

$$\text{Mean Ct GOI}_{(\text{treated})} = 22.5+24.3+25.2/3 = 25$$
$$\text{Mean Ct HKG}_{(\text{treated})} = 22.3+22.7+22/3 = 22.3$$
$$\text{Mean Ct GOI}_{(\text{untreated})} = 28.4+27.8+28.1/3 = 28.1$$
$$\text{Mean Ct HKG}_{(\text{untreated})} = 22.2+22.5+22.1/3 = 22.27$$

Secondly the ΔCt values in the untreated and treated batches using the formula:

$$\Delta Ct = Ct\ GOI - Ct\ HKG$$
$$\text{mean } \Delta Ct \text{ untreated} = 5.83$$
$$\text{mean } \Delta Ct \text{ treated} = 2.67$$

The second step would be to calculate the ΔΔCt using the formula:

$$\Delta\Delta Ct = \Delta Ct_{(\text{treated})} - \Delta Ct_{(\text{untreated})}$$
$$\text{Therefore } 2.67-5.83 = -3.17$$

The final step would be to determine the fold change of the GOI using the formula

$$\text{Fold change} = 2^{-\Delta\Delta Ct}$$
$$\text{Hence the fold change for the GOI} = 2^{-(-3.17)}$$
$$= 8.9 \text{ fold change}$$

Normal expression of the GOI is expressed as a value of 1.00. Downregulation is indicated if the fold change is <1 and upregulation if >1. In this case the GOI expression is approximately 9 fold greater than the normal expression.

## *2.14. Real time PCR: methodology*

### 2.14.1. Cell culture and RNA extraction

For cell line studies Rhabdomyosarcoma (SJCRH30), $HEK293_{hUT}$ and $CHO_{hUT}$ cells were maintained in T25 flasks until they were 80% confluent. In order to determine if hUT receptor mRNA would be regulated as a consequence of genomic desensitisation, all three

cell lines were treated with 1 μM U-II along with cells treated with vehicle (tissue culture media). The treatment times for SJCRH30 cells were 6, 24 and 48 hr, while the treatment times for $HEK293_{hUT}$ and $CHO_{hUT}$ lines was 6 hr. These time point were used as genomic changes would be expected to occur at longer treatment time as opposed to periods < 6 hr. The treatments were stopped at their respective time points and the cells were harvested with 1x harvest buffer, washed twice with PBS and then centrifuged at 1300x g for 3 min. The resulting cell pellets were then lysed with 1 ml TRI-reagent (Sigma, UK) and transferred into 1.5 ml sterile (DNase/RNase free) eppendorf tubes. Samples were then frozen at -80°C and RNA extracted the following day.

UT expression in PBMC has been demonstrated previously, where mRNA was upregulated upon LPS stimulation (Segain et al 2007). For studies pertaining to peripheral blood mononuclear cells (PBMCs) healthy donor blood was collected from 5 healthy individuals (age range 30-46). PBMCs were isolated using Histopaque 1077 (Sigma, UK). This reagent is solution comprised of polysucrose and sodium diatrizoate adjusted to a density of 1.077 ±0.001 g/ ml. and is suitable for extraction of mononuclear cells from small volumes of blood. PBMCs were isolated by placing 3 ml of histopaque into a sterile 15 ml falcon tube at a 45° angle and gently layering 4 ml of whole blood on top of the histopaque. Two distinct layers are formed the top layer is the whole blood and the bottom layer is the histopaque. This was then subjected to centrifugation for 30 min at 400x g at room temperature. During the centrifugation process, the different cells within the whole blood sample form a density gradient and four new phases are produced consisting of: (1) plasma (2) mononuclear cells (3) histopaque and (4) red cells. Mononuclear cells were isolated by initially removing most of the plasma and then using a fine Pasteur pipette to aspirate the

layer of mononuclear cells into a sterile falcon tube. Thereafter the cells were washed twice with sterile phosphate buffered saline by centrifugation at 250x g for 10 min. The PBMC pellet was then resuspended in 4.5ml of RPMI 1640 media and aliquoted in 1ml volumes into 4 cryovials and treated for 21 hr as outlined:

1) Lipopolysaccharide (LPS) 2μg/ml for 15 hr plus vehicle (RPMI 1640 media) for 6 hr.
2) (LPS) 2μg/ml for 15 hr plus 1μM U-II for 6 hr.
3) Vehicle for 15 hr plus vehicle (RPMI 1640 media) for 6 hr.
4) Vehicle for 15 hr plus 1μM U-II for 6 hr.

Treated PBMCs were maintained at 37°C in an incubator with 5% $CO_2$ and humidified air for the experiment duration. Thereafter the cells were pelletted by centrifugation at 1300x g for 10 min on a benchtop microfuge and resuspended in TRI reagent (a solution used for isolating RNA) and archived at -80°C for later use.

RNA extraction was carried out as outlined by the protocol based on the method developed by Chomcznski and Sacchi (Chomczynski *et al.*, 1987).

In brief the frozen cell/TRI reagent lysates were allowed to defrost to room temperature (22-25°C). This allows for the complete dissociation of nucleoprotein complexes from DNA and RNA species. Afterwards 200 μl of chloroform was added. The tubes were then shaken vigorously and allowed to stand for 5 min and centrifuged at 12,000x g for 15 min at 4°C. During this time three distinct phases were formed in the tube. A top clear phase (containing RNA) followed by a white interphase (containing DNA) and a final dark red/pink organic phase (containing protein). The RNA phase makes up approximately 50%

(500 μl) of the total volume. 450 μl of the clear phase was transferred into another clean eppendorf tube containing 500 μl of TRI reagent and 100 μl of chloroform and shaken and allowed to stand for 2 minutes before centrifuging for 15 min at 12,000x g (4°C). This secondary separation was carried out in order to minimise carryover of any genomic DNA from the interphase. The secondary clear RNA phase (600 μl) was then transferred to another clean eppendorf and mixed with an equivalent volume of isopropanol and allowed to stand for 10 min at room temperature. Thereafter the sample was centrifuged for 10 min at 12,000x g. The isopropanol precipitates the RNA that is in solution into a white pellet. Sometimes this pellet can be opaque in appearance and its visualisation can be enhanced by the addition of 1 μL of glycogen (which is an inert carrier). Once the centrifugation was complete the liquid was eluted and then the RNA pellet was resuspended in 1 ml of 75% ethanol, vortexed and centrifuged at 7500x g for 5 min at 4°C. The ethanol acts as a dehydrating agent and facilitates drying of the RNA pellet further. Afterwards the ethanol was eluted and the RNA pellet was allowed to air dry in the tube until no traces of ethanol were present. The pellet was then dissolved in 70-80 μl 1x TE buffer and either stored at -80°C for later use or quantified, DNase treated and reverse transcribed to form cDNA.

### 2.14.2. RNA quantification and DNase treatment

RNA samples were quantified using a spectrophotometer by recording the absorbance at 260 and 280 nm. RNA quality was assessed by the ratio obtained for 260/280, where samples with good yield had ratios between 1.8-2.0.

3-7 μg (PBMCs or hUT expressing cell lines) of total RNA was treated with DNAfree (Ambion) following the manufacturer's protocol. The RNA stocks were then treated with

DNAase where they were mixed with 5 μl DNAase buffer and 1 μl DNAase enzyme and incubated for 25 min at 37°C in a 200 μl microtube. The DNAase enzyme activity was then stopped by the addition of 5 μl DNAase inactivating agent and pipetting the mixture gently for 2 min and centrifuging the cloudy suspension for 1.5 min at 150x g. The resulting clear phase was then aliquoted to a fresh microtube and either archived at -80°C or transferred onto ice in order to carry out the reverse transcription.

### 2.14.3. Reverse transcription and cDNA synthesis

The synthesis of complementary DNA from the RNA template was carried out using the high capacity reverse transcription kit (Applied Biosystems). 2 μg or equivalent of the RNA template was combined with the following:

| | Volume (μl) |
|---|---|
| RT buffer | 6 |
| dNTP mix | 2.4 |
| Multiscribe® reverse transcriptase enzyme | 3 |
| $H_2O$ (molecular biology grade) | 9.6 |

The samples were mixed gently with a Gilson pipette and then centrifuged and placed in a thermocycler to carry out the cDNA synthesis. For this particular kit the incubation protocol was as follows:

| | | |
|---|---|---|
| STEP 1 | 25°C | 10 min |
| STEP 2 | 37°C | 120 min |
| STEP 3 | 85°C | 5 sec |

2.14.4. Real time PCR with the StepOne thermocycler

Reactions were setup using the gene expression master mix and custom synthesised Taqman™ probes for hUT (urotensin II receptor), hGAPDH (glyceraldyhyde 3-phosphate dehydrogenase) and CHO-GAPDH (Applied Biosystems). The "h" denotes human species while CHO denotes Chinese hamster ovary. The choice of housekeeper gene to use depends on testing a panel of housekeepers in triplicate assays to look at the variation in the Ct values (Dheda *et al.*, 2004). As a rule of thumb, if the variation in Ct value is minimal, and the expression is not altered due to other external factors (e.g. drug treatments) then it is advisable to use the housekeeper with the negligible change. In this instance GAPDH was used in the present study. The probe for gene of interest (GOI) hUT was Taqman coupled to FAM reporter dye while the housekeepers (HSKs) were Taqman coupled to VIC

reporter. This therefore meant that the GOI and HSK could be analysed in the same reaction microtube without any interference to one another (duplex reactions). Reactions were made in triplicate. A typical reaction consisted of the following:

| | Volume (μl) |
|---|---|
| $H_2O$ (molecular biology grade) | 6 |
| Taqman gene expression master mix | 10 |
| Taqman probes (GOI and HKG) | 1 each |
| *Sub-total* | *18* |
| cDNA template | 2 |
| **Total** | **20** |

The reaction mix was mixed gently by pipetting and then vortexed before placing it in the real time PCR instrument, the StepOne (Applied Biosystems).

The Taqman gene expression master mix is an optimised mix that contains all the necessary constituents required for carrying out a PCR, namely: Amplitaq Gold® DNA polymerase UP (ultrapure), uracil-N-glycosylase (UNG), deoxyribonucleotide triphosphates (dNTPs) with deoxyuridine trisphosphate (dUTP) replacing dTTP (deoxythymidine triphosphate), ROX passive reference dye and the other buffer components required for carrying out a reaction.

While carrying out PCRs it is necessary to ensure that no false positive amplification occurs. Uracil-N-glycosylase (UNG) acts on double and single stranded DNA by hydrolysing uracil glycosidic bonds at dU-rich sites on the DNA molecule. This causes the alkali sensitive apyrimidic sites to form in the DNA, thereby by blocking DNA polymerase. UNG is activated at step 1 of the holding stage and thereafter at step 2 its activity is reduced. At this stage the PCR reaction is started by activating the Amplitaq Gold® DNA polymerase UP.

The thermal profile of a typical reaction in the StepOne is shown below:

| | |
|---|---|
| STEP 1 (Holding stage) | 2 min 50°C |
| STEP 2 (Holding stage) | 10 min 95°C |
| STEP 3 (Cycling stage) | 15 sec 95°C |
| | (50 cycles) |
| STEP 4 (Cycling stage) | 1 min 60°C |

### *2.15. Data analysis and statistics*

Unless otherwise stated, all data are presented as mean±SEM.

*Binding studies*

Raw data collected from the respective instruments were processed and analysed using Microsoft Excel. Graphical representations, i.e. saturation curve, Sigmoid binding (variable slope) and Scatchard analysis were carried out using Graphpad Prism v3.0 (San Diego, CA, USA). Furthermore determination of $B_{max}$ and $K_d$ values were obtained using the same software post-graphical representation. $IC_{50}$ values were not corrected for [$^{125}$I]U-II according to Cheng and Prusoff as the [L] was small compared to the $K_d$, thereby making corrections negligible. All $pIC_{50}$ values are therefore simply quoted as $pK_i$.

*PIT assays*

Raw data was processed using Excel. Data was presented after subtracting basal response (unstimulated) from observed (stimulated) responses. Units of data are expressed as DPM (disintegrations per minute) of total [$^3$H] $IP_x$ accumulation over log molar concentration of drug. Concentration response curves (CRCs) have been graphically represented using Sigmoid curves with variable slope in Prism v3.0.

*$Ca^{2+}$ assays*

For the experiments carried out using the LS50-B fluorometer, raw data was imported into Excel. Graphical temporal profiles showing $[Ca^{2+}]_i$ (nM) over log molar [drug] were created by exporting data from Excel to Prism v3.0. CRCs showing change in (Δ) $[Ca^{2+}]_i$ over log molar [drug] were constructed using variable slope Sigmoid curves from which $E_{max}$ and $pEC_{50}$ were determined.

Single cell microfluorometry data was imported into Excel and exported to Prism v3.0. Temporal profiles were graphically presented as fluorescence intensity over time (sec).

Flexstation-II data was acquired through SoftMax Pro (Molecular Devices, Sunnyvale, CA, USA) was exported into Excel and thereafter Graphical representations were carried out using Prism v4.0. Temporal profiles were represented as fluorescence intensity units (FIU) over time (sec). CRCs were created using variable slope Sigmoid plots of FIU (% over the baseline) over log molar [drug].

*Real time PCR*

Data was exported from the Applied Biosystems StepOne software v2.0 (Foster City, CA, USA) into Excel. Gene quantification was carried out using the relative quantification method as described previously. PCR amplification curves were re-drawn by exporting data (ΔRn over cycle number) into Prism v5.0. Fold changes were illustrated using bar charts.

All data in this thesis was analysed using paired student's t-test, analysis of variance (ANOVA), Tukey test, and Dunnett test where applicable.

In antagonist experiments the $pK_B$ was determined by using the Gaddum-Schild equation assuming a Schild slope of unity.

$$pK_B = \left( -\log\left[ \frac{pEC_{50+antagonist}}{pEC_{50-antagonist}} \right] - 1/[Antagonist] \right)$$

## 3. Cell line/model validation

### *3.1. Introduction*

Drugs elicit their biological effects by interacting with target molecules such as enzymes and receptors. This interaction culminates in the generation of cellular and molecular responses at all levels of biological organisation which can range from individual molecules to humans. To this end biological effects of drugs are studied using methods that will facilitate comparison of a given drug against other analogues or to acquire a better understanding of the drug under study. The methods employed in studying ligand interaction with their targets vary from using cell lines expressing native drug targets to recombinant targets (*in vitro* methods) to tissue bioassays (*ex-vivo* methods); with the ultimate objective of using the information derived from these methods as a predictor of a drug's effect *in vivo* and under clinical circumstances (Rang, 2000).

### *3.2. Aims*

The aim of the experiments described in this chapter was to determine whether the three cell lines SJCRH30, $HEK293_{hUT}$ and $CHO_{hUT}$ were suitable as models for studying U-II/UT signalling and further to characterise and compare responses between these cell lines. This was determined by carrying out radioligand binding studies, phosphoinositide turnover assays, and calcium assays.

## *3.3. Results*

### 3.3.1. Binding studies

*Association time courses*

Association time course experiments were carried out in order to determine the association rates of [$^{125}$I]U-II in SJCRH30 and HEK293$_{hUT}$ cells. The association binding of [$^{125}$I]U-II (10 pM) in both membrane preparations was time dependent and reached equilibrium after 240 mins (Figure. 3.1). Association studies were not carried out with CHO$_{hUT}$ cells as this data has been published previously by (Song *et al.*, 2006) with similar results.

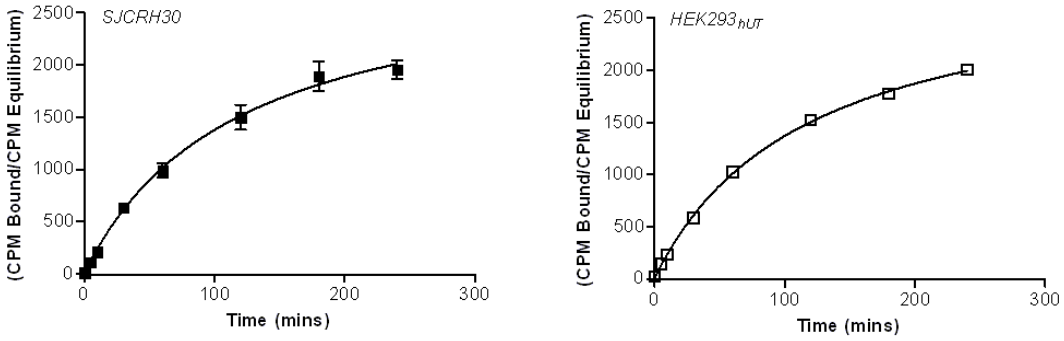


**Figure. 3.1. Association time course.**
[$^{125}$I]urotensin-II (U-II) binding in rhabdomyosarcoma SJCRH30 (left panel) and human embryonic kidney HEK293$_{hUT}$ membranes. Membrane concentrations of protein in these assays were 15μg/ml (HEK293$_{hUT}$) 150-300 μg/ml (SJCRH30). Data present as mean± SEM after 4 hr (240 min) equilibration. ($n \geq 3$).

*Isotope dilution*

Isotope dilution experiments conducted in SJCRH30, HEK293$_{hUT}$ and CHO$_{hUT}$ were used to determine hUT receptor density ($B_{max}$) and $K_d$ (Figure. 3.2). The summary of the $B_{max}$ and $K_d$ values in all three cell lines are indicated in Table. 3.1.

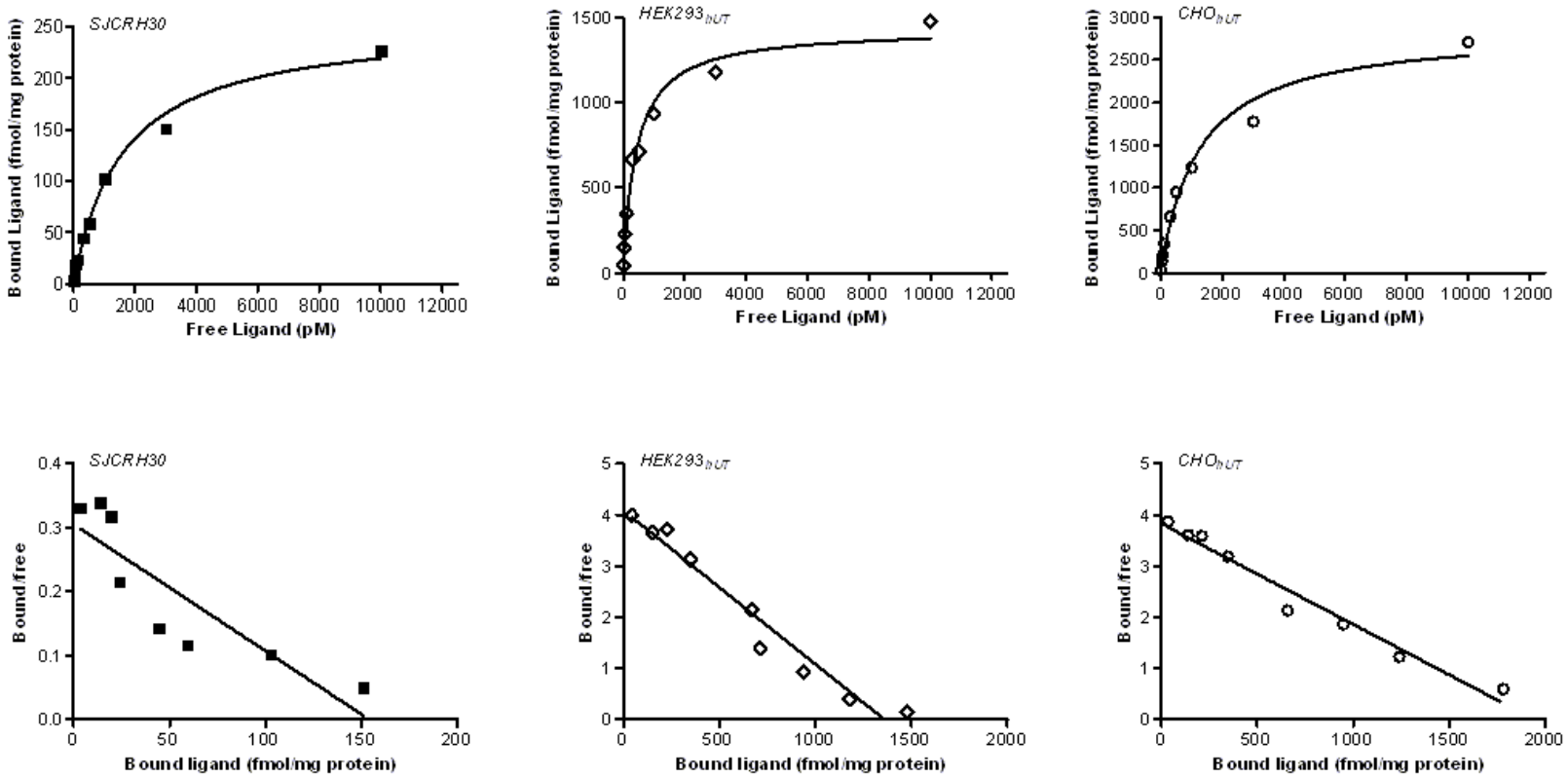


**Figure. 3.2. Representative data for isotope dilution experiments conducted in SJCRH30, HEK293$_{hUT}$ and CHO$_{hUT}$ membrane preparations.**
*Top panels:* hyperbolic curves. *Bottom panels:* Scatchard plots corresponding to top panels. Representative is from n $\geq$ 5.

| Cells | $B_{max}$ (fmol[$^{125}$I]U-II/mg proteins] | $K_d$ (pM) |
|---|---|---|
| SJCRH30 | 107±26 | 613±97 |
| $HEK293_{hUT}$ | 1477±164* | 375±41 |
| $CHO_{hUT}$ | 1770±227* | 557±124 |

**Table. 3.1. $B_{max}$ and $K_d$ values from isotope dilution experiments.**
SJCRH30, $HEK293_{hUT}$ and $CHO_{hUT}$ cell data presented as means± SEM. Statistically significant differences (ANOVA and Tukey test) are indicated by * compared to SJCRH30 where $p < 0.05$ $n \geq 5$.

### 3.3.2. PIT assays

*Native hUT (SJCRH30 cells)*

Experiments in rhabdomyosarcoma cells could not be carried out. Under basal (unstimulated conditions) [$^3$H] inositol DPM values ranged between 200-300. Upon stimulation with U-II (1 μM) an increase was not observable. This may be attributed to low UT receptor expression in these cells.

*Recombinant hUT (HEK293 and CHO cells)*

A concentration dependent increase in the accumulation of total $IP_x$ was observed in $HEK293_{hUT}$ cells when stimulated with U-II (maximal effect 3480± 555 DPM and $pEC_{50}$ of 9.02±0.05). In $CHO_{hUT}$ cells U-II also evoked concentration dependent increases in total $IP_x$ accumulation with a maximal effect of 4393±213 DPM and $pEC_{50}$ of 9.27±0.06 (Figure. 3.3).

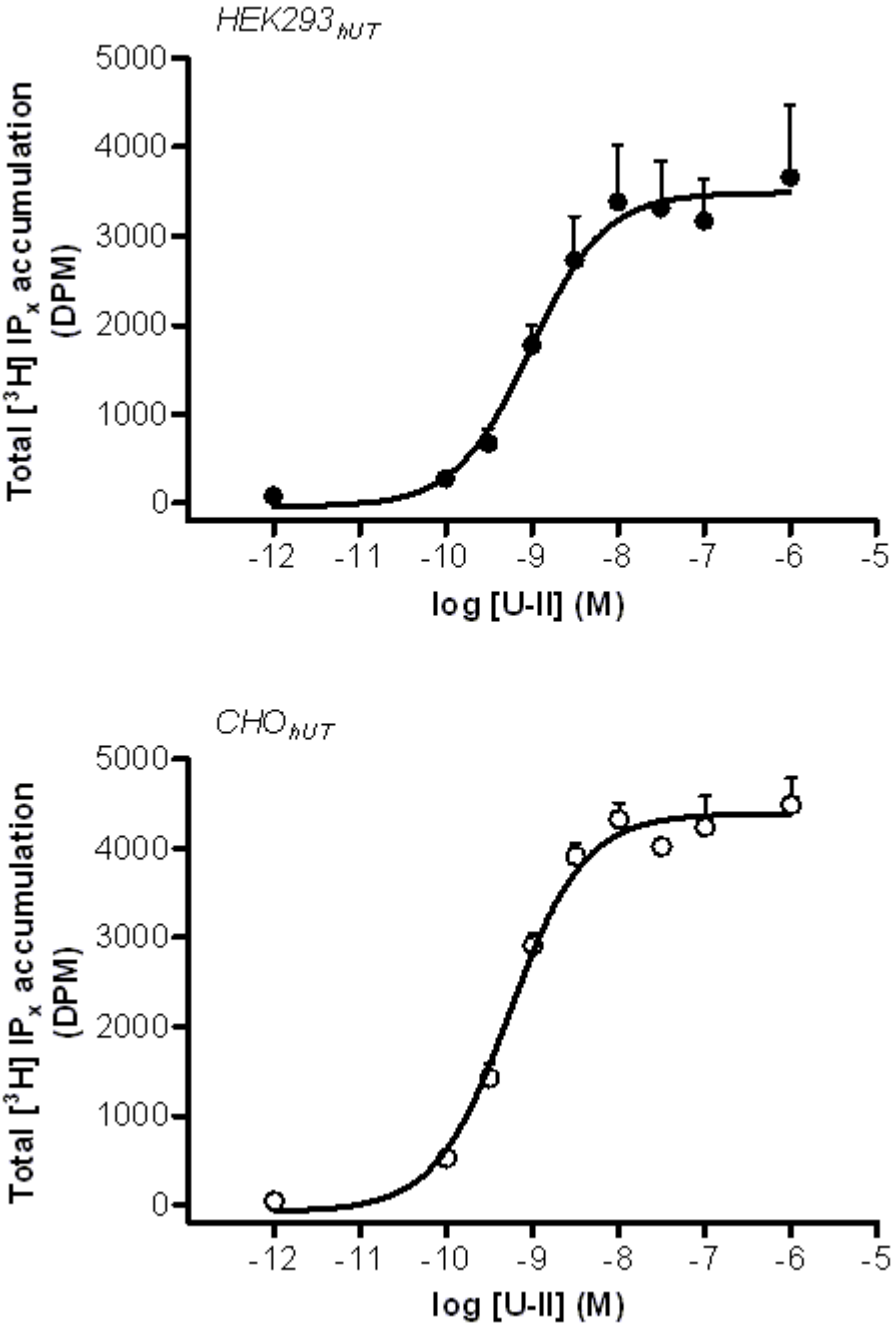


**Figure. 3.3. Phosphoinositide turnover in HEK293$_{hUT}$ and CHO$_{hUT}$ cells.**
Adherent cell assay. Data are presented as mean± SEM n=4 separate experiments.

### 3.3.3. $Ca^{2+}$ mobilisation assays

*Cuvette based assays*

In cuvette based calcium assays conducted at 37°C U-II evoked concentration dependent increases in $Ca^{2+}$ in all three cell lines. In the temporal profiles the responses were biphasic in nature; characterised by an initial peak and followed by a plateau (Figure. 3.4). A summary of the potencies and maximal effects in each cell line are shown in Table. 3.2.

| **Cell line** | **$pEC_{50}$** | **$E_{max}$ (nM)** |
|---|---|---|
| SJCRH30 | 8.22±0.28 | 37±6 |
| $HEK293_{hUT}$ | 8.09±0.24 | 294±34‡ |
| $CHO_{hUT}$ | 8.23±0.28 | 1272±209* |

**Table. 3.2. Summary of $Ca^{2+}$ assay $pEC_{50}$ and $E_{max}$ in SJCRH30, $HEK293_{hUT}$ and $CHO_{hUT}$ cells.**
Data are mean± SEM where n=4 separate experiments. Statistically significant differences are indicated by * and ‡ on the basis of ANOVA and Tukey tests where $p< 0.05$. * denotes comparison between SJCRH30 and $CHO_{hUT}$ while ‡ is a comparison between $HEK293_{hUT}$ and $CHO_{hUT}$.

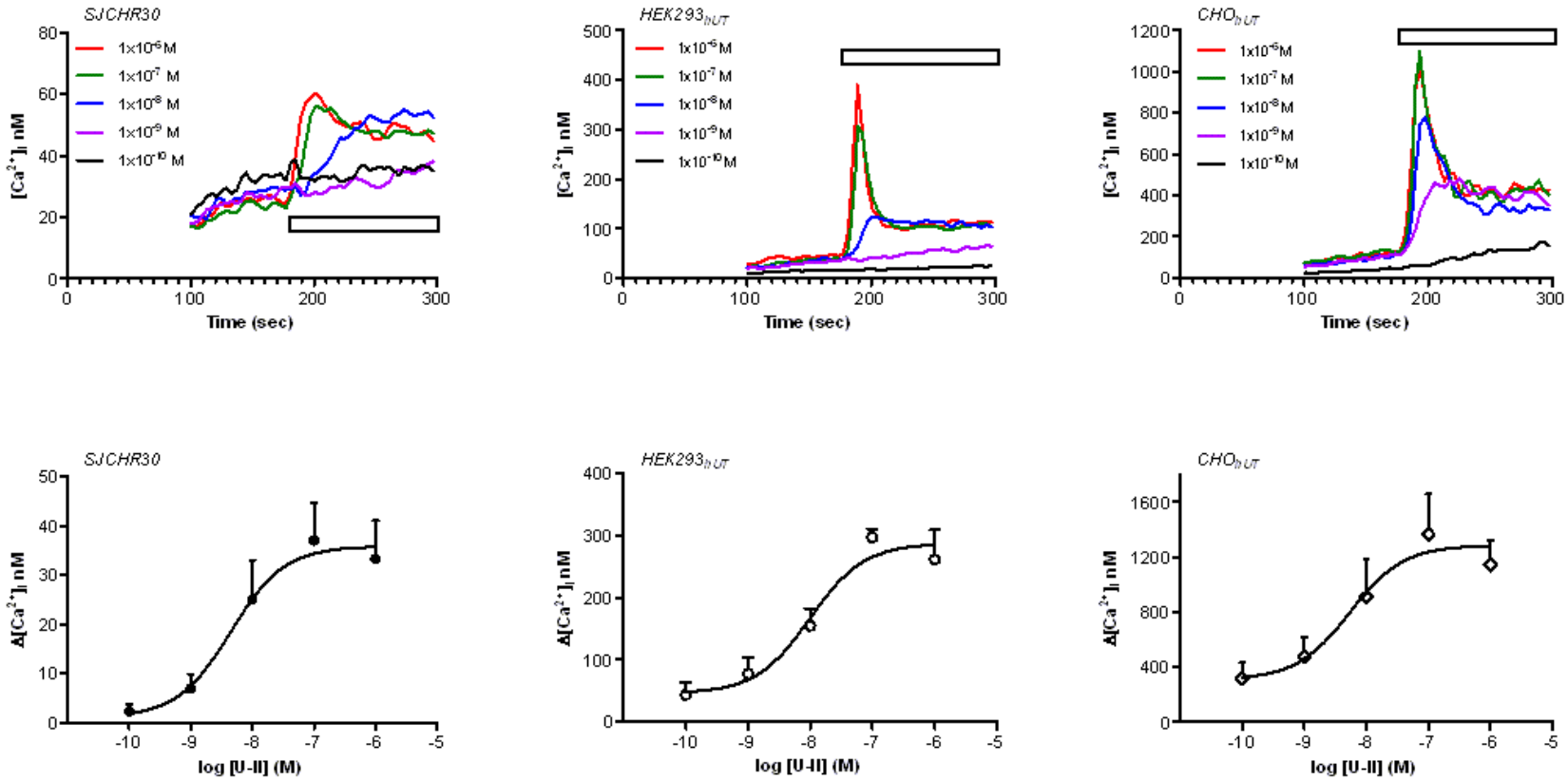


**Figure. 3.4. U-II evoked $Ca^{2+}$ mobilisation in SJCRH30, $HEK293_{hUT}$ and $CHO_{hUT}$ cells.**
*Top panels:* temporal profiles. The duration of U-II stimulation is indicated by the bar. *Bottom panels:* concentration response curves to U-II in the cell lines tested.

*Flexstation II based assays and mechanisms of $Ca^{2+}$ mobilisation in $CHO_{hUT}$ cells*

Further studies were undertaken to delineate the $Ca^{2+}$ mobilisation mechanisms by the U-II/UT system and to corroborate our findings in a recombinant cell line expressing human UT receptor with data published by other groups.

In calcium assays carried out with the Flexstation II at room temperature (between 21-25°C). U-II caused a concentration dependent increase in $Ca^{2+}$ mobilisation in the presence and absence of extracellular calcium in the buffer; however the maximal effect in the absence of extracellular calcium was markedly lower compared to the response observed in the presence of extracellular $Ca^{2+}$, $p<0.05$ (Figure. 3.5). The U-II response was biphasic; an initial increase in $Ca^{2+}$ release followed by a secondary plateau phase, illustrated in Figure. 3.6. In the presence of extracellular calcium, after the initial increase of calcium, the secondary plateau does not diminish toward the basal resting calcium, therefore demonstrating the involvement of $Ca^{2+}$ entry via the components on the plasma membrane. This secondary plateau is abolished in the absence of extracellular calcium. Furthermore it reaches a resting basal state (Figure. 3.6). The initial increase in $[Ca^{2+}]_i$ is attributed to the release of $Ca^{2+}$ from the intracellular stores as demonstrated by the addition of thapsigargin (10μM) a classic inhibitor of the sarco/endoplasmic reticulum (SERCA) $Ca^{2+}$ ATPase pump (Treiman *et al.*, 1998). In the current study, in the absence of extracellular calcium in the buffer, thapsigargin evoked a mean $Ca^{2+}$ release of 146±7 %. After complete store depletion U-II was unable to evoke any $Ca^{2+}$ responses (Figure. 3.7). U-II mediated signalling dependence on PLC was demonstrated by using the PLC inhibitor U-73122 (Bleasdale *et al.*, 1990). Pre-incubation of cells with this compound (10μM) resulted in no $Ca^{2+}$ responses when the cells were challenged with U-II (Figure. 3.7). The potential

contribution of plasmalemmal (PM) $Ca^{2+}$ channels in U-II induced calcium mobilisation was assessed using store operated $Ca^{2+}$ channels (SOCCs) and voltage operated calcium channel blockers (VOCCs). SOCCs are sensitive to Lanthanum and other trivalent cations (Hayat *et al.*, 2003) while L-type VOCCs are sensitive to verapamil (Atlas *et al.*, 1981). Pre-incubation of cells with both of these compounds (10μM) did not affect the U-II maximal response (Figure. 3.8). Further analysis of the effects of lanthanum and verapamil pre-incubations on the plateau phase of the U-II response were not different compared to non-pretreated conditions. A summary of the maximal effects and $pEC_{50}$ are tabulated in Table. 3.3.

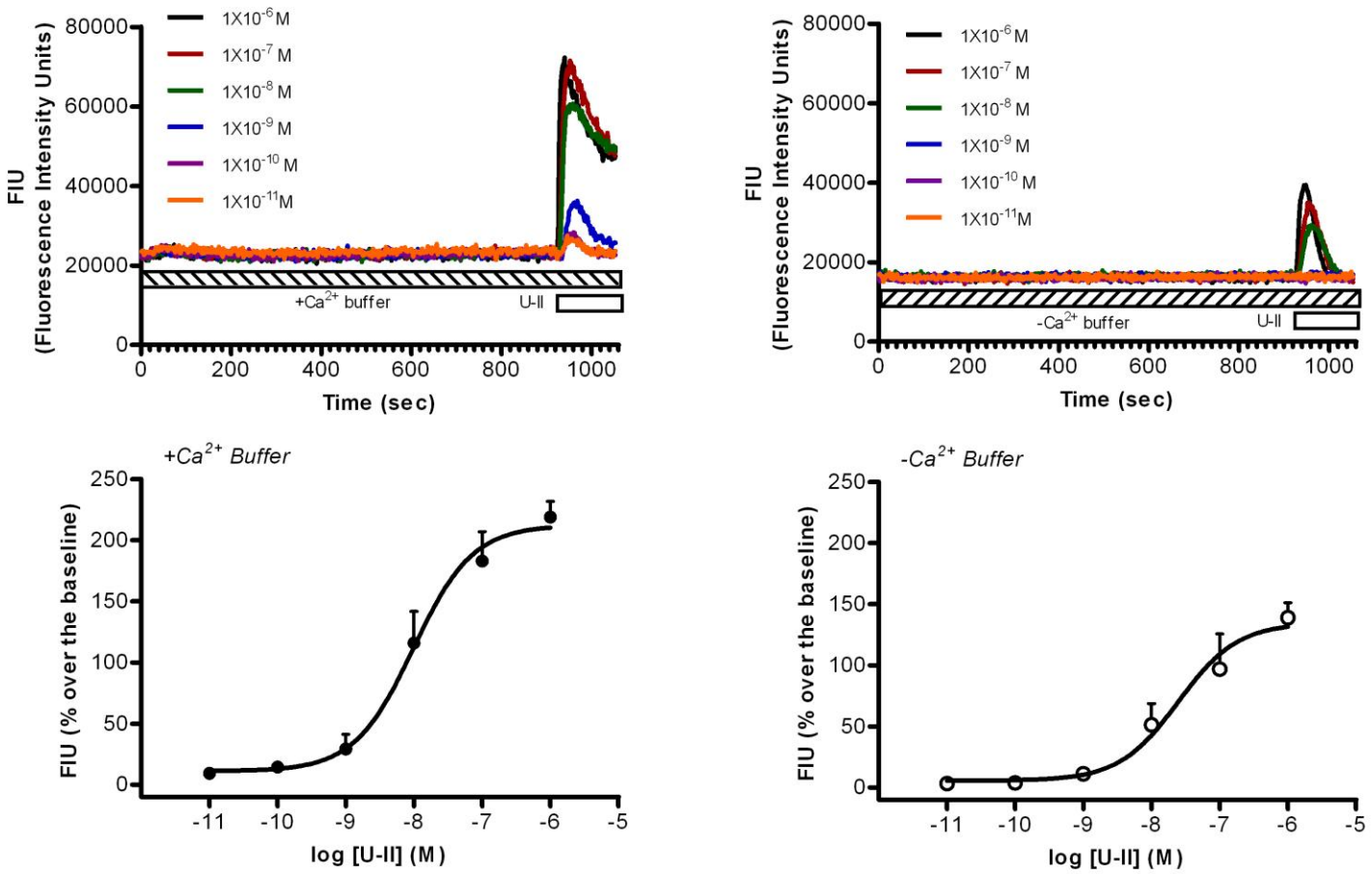


**Figure. 3.5. U-II evoked $Ca^{2+}$ mobilisation in $CHO_{hUT}$ cells in the Flexstation-II.**
*Top panels*: representative temporal profiles of in the presence (left) and absence (right) of extracellular calcium in the buffer. Bottom panels: concentration response curves corresponding to the temporal profiles. Data are mean± SEM (where applicable) n=3 performed in duplicate.

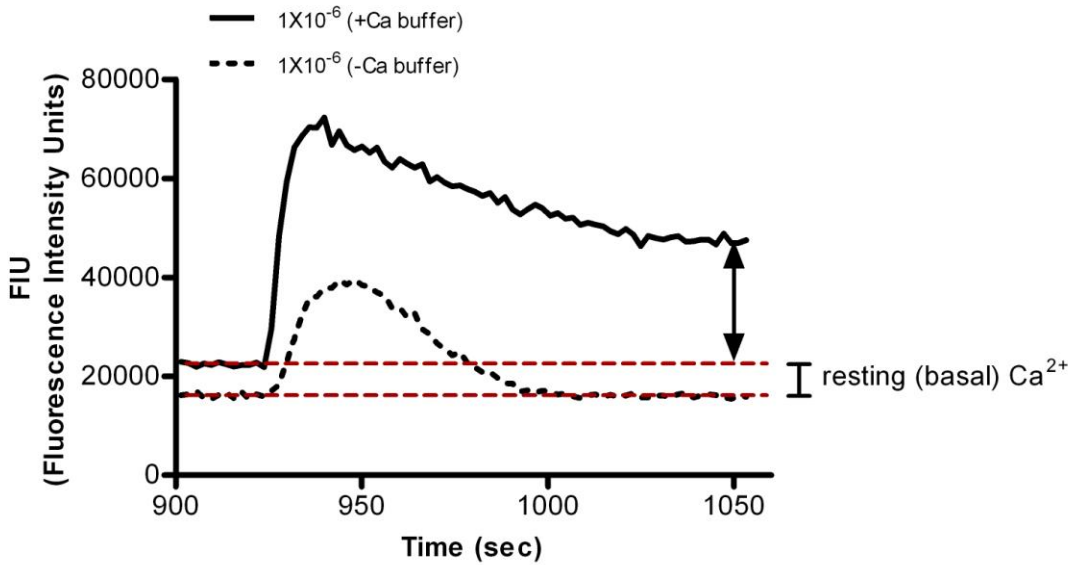


**Figure. 3.6. Representative temporal profile of 1μM U-II evoked $Ca^{2+}$ mobilisation.**
Presence (solid black line) and absence (dashed black line) of extracellular calcium in the buffer. Baseline resting calcium is indicated by the dashed red lines. Representative from n=3 performed in duplicate.

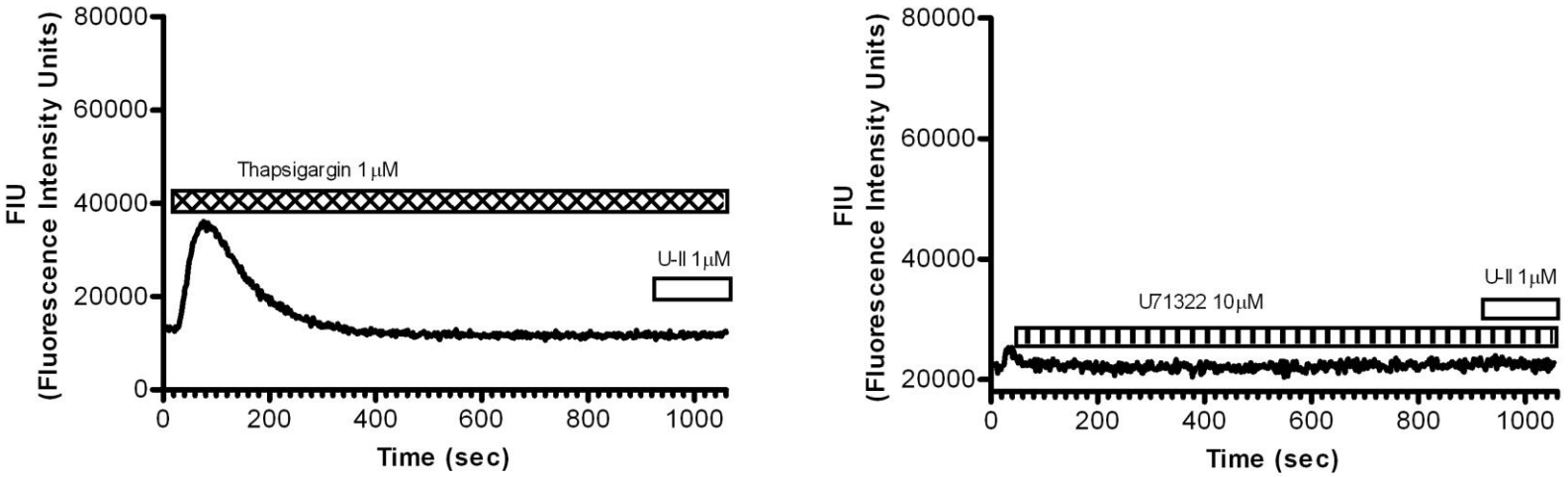


**Figure. 3.7. Representative temporal profile of the effects of thapsigargin and U-73122.**
Thapsgigargin (*left panel*) and U-73122 *(right panel)* pre-incubations on U-II evoked responses in $CHO_{hUT}$. Representative from n=3 performed in duplicate.

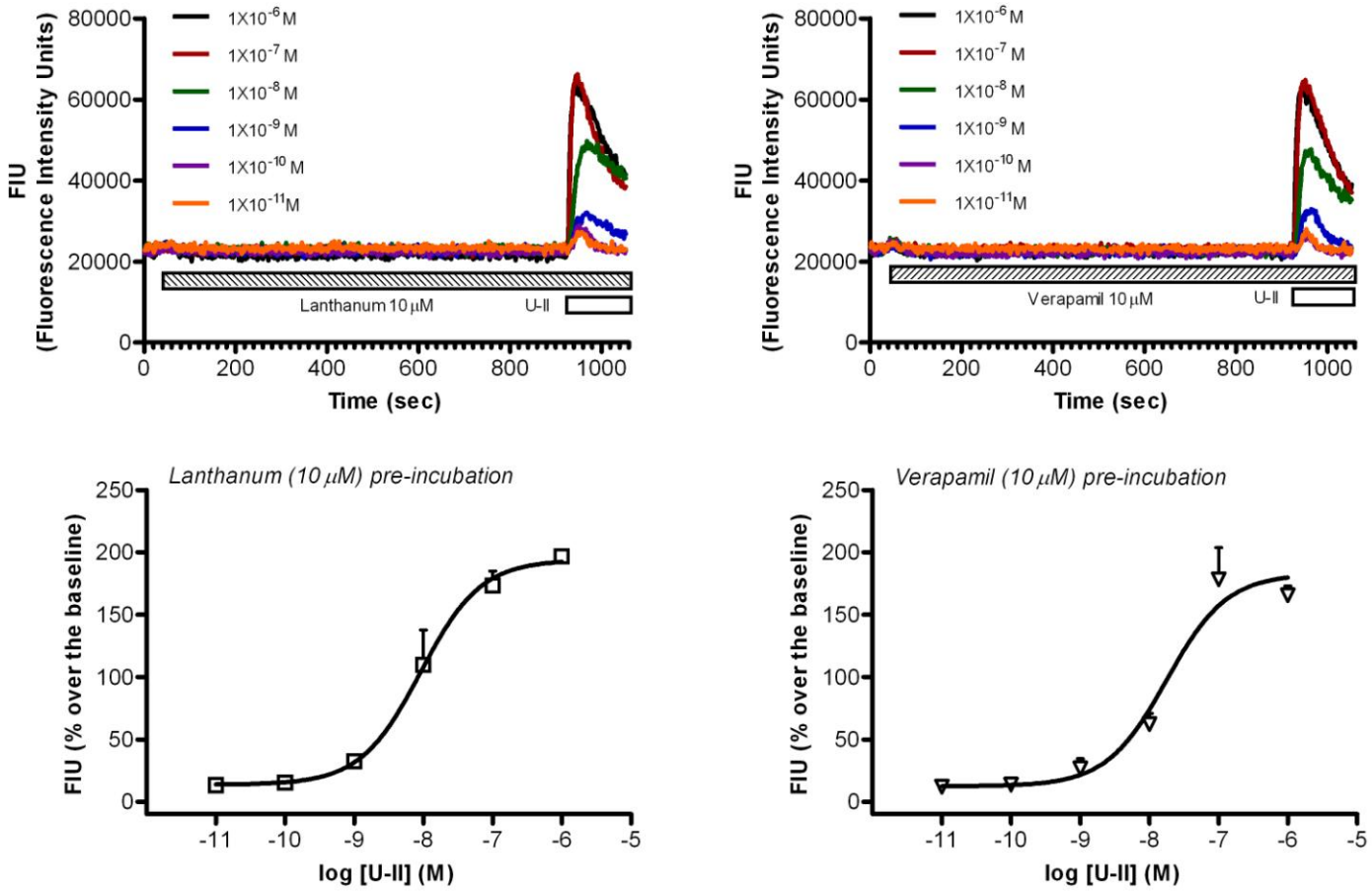


**Figure. 3.8. Lanthanum and verapamil effects on U-II evoked $Ca^{2+}$ mobilisation in $CHO_{hUT}$ cells.**
*Top panels:* representative temporal profiles of cells pre-incubated with lanthanum (left) and verapamil (right) and challenged with U-II. *Bottom panels*: concentration response curves corresponding to the temporal profiles. Data are mean ± SEM n=3 performed in duplicate.

| Treatment type | $pEC_{50}$ | $E_{max}$ (%) |
|---|---|---|
| +Ca buffer | 7.95±0.24 | 217±12 |
| -Ca buffer | 7.42±0.51 | 155±16* |
| Thapsigargin (10μM) (-Ca buffer) | - | - |
| U-73122 (10μM) (+Ca buffer) | - | - |
| Lanthanum (10μM) (+Ca buffer) | 7.98±0.28 | 200±5 |
| Verapamil (10μM) (+Ca buffer) | 7.72±0.13 | 185±6 |

**Table. 3.3. Summary of effects observed in $CHO_{hUT}$ cells with the Flexstation-II.**
U-II $pEC_{50}$ and $E_{max}$ relating to experiments assessing the mechanisms of $Ca^{2+}$ mobilisation. Data are means±SEM (n=3). Statistically significant differences are indicated * where *p<0.05* based on paired student t-tests.

### 3.3.4. Single cell microfluorometry assays

Microfluorometry is a method that is used to look at calcium mobilisation using a microscope. Cells expressing native UT receptor were used in this study. The time span of each experiment varied between 160 and 240 seconds. During the first 40 seconds of the experiment cells were perfused with KHB at 40 seconds time point the perfusion was changed to a supramaximal concentration of U-II (1μM)**.** A total of 61 individual SJCRH30 cells were assessed. Of these approximately 50% of the cells did not exhibit any responses. Four different responses were observed with the remaining 50% of cells; these were biphasic (8.2%), monophasic (11.5%), oscillatory (14.7%), and rapid monophasic oscillatory (18%) in nature (Figure. 3.9). Experiments were carried out at 37°C (however due to the distance between the peltier thermal heating device and the perfusion chamber there was a drop in temperature by approximately 3°C. Therefore the bath temperature was 30°C).

As noted earlier, cuvette based fluorometric experiments (37°C) yielded in a biphasic response when challenged with 1 μM U-II. Interestingly when the individual response from the individual cells were combined, a biphasic response reminiscent to the whole cell population was obtained. (Figure. 3.10).

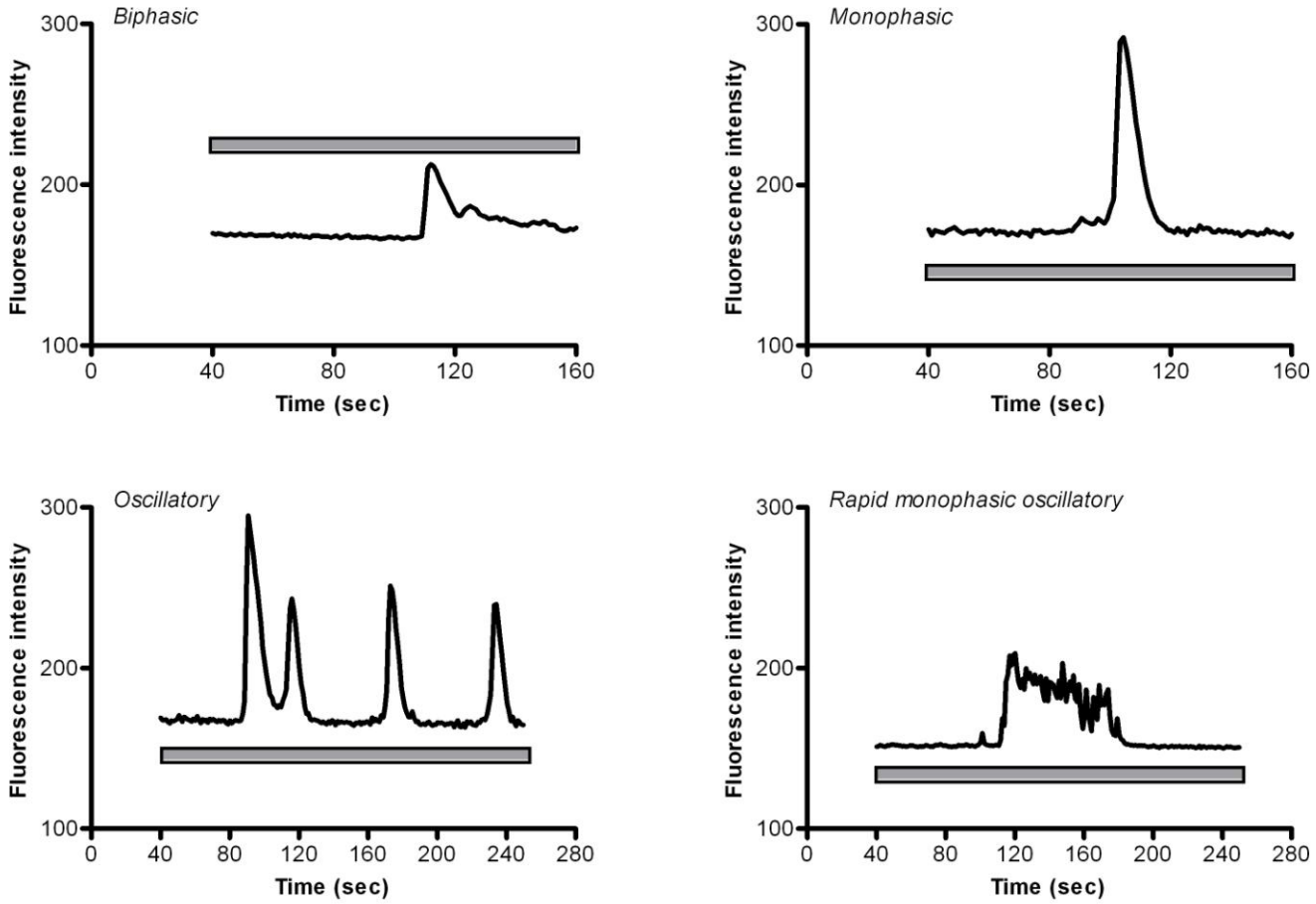


**Figure. 3.9. Four different types of $Ca^{2+}$ responses recorded in SHJCRH30 cells by real time microfluorometry.**
Biphasic, monophasic, oscillatory and rapid monophasic oscillatory responses were recorded. U-II supramaximal (1μM) perfusion is indicated by the bar.

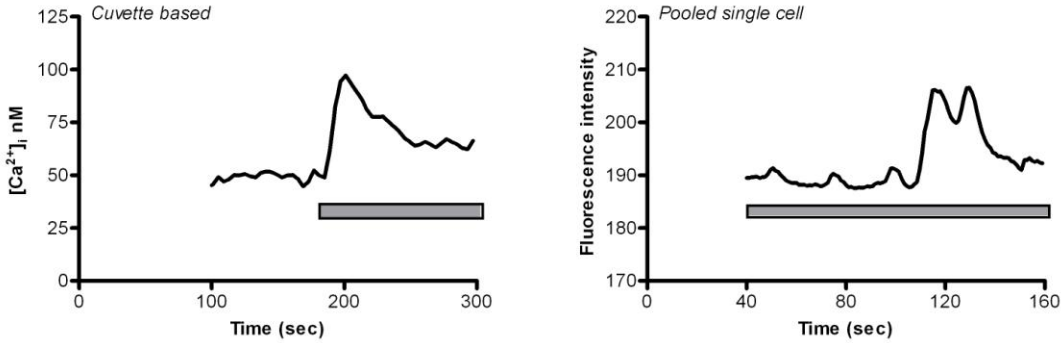


**Figure. 3.10. Similarities in cuvette based and single cell $Ca^{2+}$ assays.**
Time course responses observed in cuvette based fluorometric experiments (*left panel*) and the pooled response of single cell microfluorometry responses (*right panel*). Application U-II (1μM) is indicated by the bar. Note in the single cell assay U-II was added by perfusion.

### *3.4. Discussion*

The association kinetics of [$^{125}$I]U-II binding to native (SJCRH30) and recombinant (HEK293) human UT are slow and in accord with previous studies carried out in $CHO_{hUT}$ cells (Song *et al.*, 2006). Dissociation kinetics by the addition of excess cold U-II was not assessed in the current study. However in studies published by (Song *et al.*, 2006) (Douglas *et al.*, 2004) U-II binding is reported to be irreversible. Isotope dilution experiments demonstrated human UT receptor densities in order of $CHO_{hUT}$>$HEK293_{hUT}$>SJCRH30.

PI turnover assay data obtained in $HEK293_{hUT}$ and $CHO_{hUT}$ demonstrated that U-II is a full agonist with similar $pEC_{50}$ values and maximal effects in both systems. These findings are in general agreement with the data published using rabbit thoracic aorta (Saetrum Opgaard *et al.*, 2000).

In the cuvette based $Ca^{2+}$ assays U-II exhibited full agonist activity with similar $pEC_{50}$ values in the three cell lines tested. Full UT agonism was also observed in $CHO_{hUT}$ with the Flexstation-II $Ca^{2+}$ assays. In the presence of extracellular calcium in the buffer the $E_{max}$ was higher than in the absence of extracellular calcium. This therefore suggest that the increase in maximal effect in the presence of extracellular $Ca^{2+}$ occurs as a consequence of both ER store $Ca^{2+}$ release and plasma membrane $Ca^{2+}$ entry. While a biphasic $Ca^{2+}$ response was observed (primary peak followed by a secondary plateau), the latter component was completely abolished in the absence of $Ca^{2+}$ in the buffer; demonstrating entry via the plasma membrane. This has also been reported by Song and co-workers (Song *et al.*, 2006). The $pEC_{50}$ values in the current study from the Flexstation-II (7.95 and 7.42) were slightly lower compared to those by Song et al, 2006 (8.80 and 8.25 respectively) and cuvette based measurements, this may be due to the assays being carried out at ambient room temperature instead of physiological temperature.

The primary response in the biphasic curve is attributed to ER store $Ca^{2+}$ as demonstrated by blocking SERCA pumps with thapsigargin. SERCA inhibition prevents resequestration of $Ca^{2+}$ into ER stores, however even in the absence of thapsigargin the ER store is subjected to $Ca^{2+}$ leak into the cytosol (Treiman *et al.*, 1998). This leakage is variable in different cell types and in the absence of thapsigargin ER $Ca^{2+}$ pools are in continuous equilibrium with the cytosol. Increased rate of emptying occurs as a consequence of the activation of $IP_3R$ and ryanodine receptors as well as SERCA. After the thapsigargin sensitive extrusion of $Ca^{2+}$ was complete U-II was unable to evoke any $Ca^{2+}$ release, therefore demonstrating that the ER stores are an essential component in U-II mediated signalling via $IP_3$ that binds to $IP_3R$ located on the surface of the ER only. It can be

confidently said that release does not occur via ryanodine receptors as Chinese hamster ovary cells do not express native ryanodine receptors (Bhat *et al.*, 1999).

Lanthanum and verapamil (10 μ M) are used to block plasma membrane entry of $Ca^{2+}$. In the present study pre-incubation of $CHO_{hUT}$ cells with both these drugs did not have an effect on the maximal response induced by 1μM U-II. The inability of verapamil to block entry of $Ca^{2+}$ via the plasma membrane could be due to the absence of L-type $Ca^{2+}$ channels in CHO cells. Previous studies have demonstrated this to be the case (Takekura *et al.*, 1995), therefore suggesting that these cells may not be electrically excitable; however there is also evidence for native CHO (CHO-K1) to be electrically excitable (Skryma *et al.*, 1994). It has to be stressed that the Flexstation-II experiments were conducted at room temperature; therefore it is also likely that this might be a contributing factor in not observing lanthanum and verapamil blocking effects. It would be useful to assess the effect of both these drugs in $CHO_{hUT}$ cells and native human UT expressing SJCRH30 cells at physiological temperature.

In preliminary studies undertaken in SJCRH30 cells with the Flexstation-II U-II evoked $Ca^{2+}$ signalling was not detectable, however single cell microfluorometric measurements demonstrated on increase in fluorescence upon U-II stimulation (data not shown). This therefore suggests a sensitivity issue in the instrument used to detect calcium release in this cell line. So could the discrepancy in the lack of signal detection with SJCRH30 be attributed to receptor density? Or could this be due to the way in which the Flexstation acquires the fluorescence signal?

The U-II evoked $Ca^{2+}$ maximal effect was also insensitive to $La^{3+}$ pre-treatment. Furthermore no changes in the plateau phase were observed within the biphasic response. $La^{3+}$ was used on the assumption that plasma membrane entry may be evoked by a TRP homologous protein (Hayat *et al.*, 2003). Since the Flexstation-II assays were carried at ambient room temperature it is likely that the effects were not observable at this temperature. Alternatively it is also likely that these cells lack $La^{3+}$ sensitive $Ca^{2+}$ entry component. Lanthanides (which include $La^{3+}$, $Gd^{3+}$) have been widely used to study plasma membrane $Ca^{2+}$ entry via the TRP family, along with the compound SKF96365 (Halaszovich *et al.*, 2000). While $La^{3+}$ has been demonstrated to be effective in inhibiting plasma membrane $Ca^{2+}$ entry, this block is dependent on variable concentrations of the trivalent cation. For example a concentration of 1 mM and 150 μM of $La^{3+}$ was capable of inhibiting TRP3 mediated $Ca^{2+}$ entry in COS-M6 and HEK293 cells expressing human TRP3 (Zhu *et al.*, 1998) (Zhu *et al.*, 1996); while an effective concentration of 24 μM and 50 μM was capable of blocking TRP3 in bovine pulmonary endothelial cells (Kamouchi *et al.*, 1999) and porcine aortic endothelial cells respectively (Balzer *et al.*, 1999). This therefore suggests that the effective concentration of $La^{3+}$ required to block $Ca^{2+}$ entry varies in different cell types. In the current studies a concentration of 10 μM was used to attempt to inhibit U-II mediated maximal response and plasma membrane $Ca^{2+}$ entry. A higher concentration might have evoked an inhibitory effect along with compensating for the temperature of the assay.

The identity of SOCC has remained elusive. Initially work conducted in *Drosophila melanogaster* led to the suggestion that mammalian TRP homologs may fulfil the role as

SOCCs (Hardie *et al.*, 1993). However there has been a division in this train of thought; one group accepting the TRP homology story and the other group completely refuting these claims. Numerous groups have independently uncovered the identity of SOCCs, much of the work has been facilitated with the use of RNAi as a technique. Recently two proteins referred to as stromal interacting molecule (STIM) and Orai have been described as the components that make up a functional SOCC (Potier *et al.*, 2008).

In a general context changes in intracellular $Ca^{2+}$ concentrations $[Ca^{2+}]_i$ in a population of cells can be visually characterised by an agonist induced biphasic response, where upon stimulation by the agonist a peak in intracellular calcium can be observed compared to the basal resting $Ca^{2+}$ concentration. While population studies facilitate determination of an agonist's efficacy and potency; these studies do not give detailed insight into the complex pattern of calcium mobilisation that can be observed with single cell $[Ca^{2+}]_i$ measurements (Morgan, 2006).

Four different types of $Ca^{2+}$ responses were observed in SJCRH30 cells expressing native human UT. These included biphasic, monophasic, oscillatory and rapid monophasic oscillatory responses. In a given visual field upon the addition of U-II, not all cells responded to U-II therefore demonstrating heterogeneity in $Ca^{2+}$ response which is indicative of non-uniform distribution of a receptor (Morgan, 2006).

The responses recorded are not exclusive to UT signalling; in fact studies in rat osteoclasts exposed to species specific calcitonin have shown variable $Ca^{2+}$ responses. Asusberic(1-7) Eel calcitonin evoked biphasic $Ca^{2+}$ responses while human calcitonin produced a

monophasic response of varying amplitude (Moonga *et al.*, 1992); this has also been observed with monophasic responses and oscillatory response in SJCRH30 with clear variation in the amplitude of the responses.

Studies in hepatocytes have shown variable cytosolic $Ca^{2+}$ responses to epidermal growth factor challenge; with observable responses such as oscillations which varied from cell to cell. On pooling the individual data into a cell population a biphasic curve was generated. The investigators also found that increasing concentration of EGF increased the frequency of the $Ca^{2+}$ oscillations without any change to the amplitude (Tanaka *et al.*, 1992). It would be interesting to assess how different concentrations of U-II (i.e. lower than 1 μM) affect the spatio-temporal profile of a $Ca^{2+}$ response and also assess the frequency of repetition of the four different responses observed in SJCRH30

.

### *3.5. Conclusion*

In the present study the three cell lines described appear to be suitable for studying U-II/UT signalling on the basis that 1) all three cell lines express appreciable numbers of U-II binding sites and 2) recombinant hUT in HEK293 and CHO cells appear to be functionally coupled to second messenger systems that generate $IP_3$ and $Ca^{2+}$ mobilisation. While in SJCRH30 $Ca^{2+}$ mobilisation can be measured using cuvette and microfluorometric methods, it is not possible to detect $IP_3$ generation in these cells. It is possible that the assay method used in this study is not suited for studying receptors in native environments; therefore it might be necessary to assess $IP_3$ formation using an alternative assay such as a radioreceptor mass assay (Smart, 2006). However there is a need for a system expressing endogenous UT receptors and SJCRH30 is currently the best available.

## 4. Pharmacological characterisation of urantide and UFP-803

### *4.1. Introduction*

With evidence for elevated U-II in cardiovascular diseases, a major focus has been the development of UT antagonists. A problem with U-II is that once bound to UT (in native and recombinant systems) it dissociates very slowly. It is thought that the disulphide bridge between $Cys^5$ and $Cys^{10}$ may contribute to this (Lambert, 2007). Structure activity relationship studies (SARs) have involved modifying the U-II peptide, firstly to understand the significance of the amino acid residues within the pharmacophore for UT activation and secondly to create templates for non-peptide ligands that are reversible.

Urantide and UFP-803 are modeled on U-II(4-11), the shorter biological active form of full length U-II (Figure. 4.1).

Their synthesis has taken place through progressive SARs where initially the introduction of a Pen (penicillamine) residue at $Cys^5$, led to the improvement of agonist potency compared to the natural peptide (Grieco *et al.*, 2002). The first UT receptor partial agonist was synthesised by the replacement of $Lys^8$ with ornithine (Orn) (Camarda *et al.*, 2002a) and thereafter its potency was improved by the incorporation of Pen in place of $Cys^5$. This led to the identification of urantide (Patacchini *et al.*, 2003). Substitution of $Orn^8$ with diaminobutyric acid (Dab) while retaining Pen at $Cys^5$ led to the identification of UFP-803 (Camarda *et al.*, 2006).

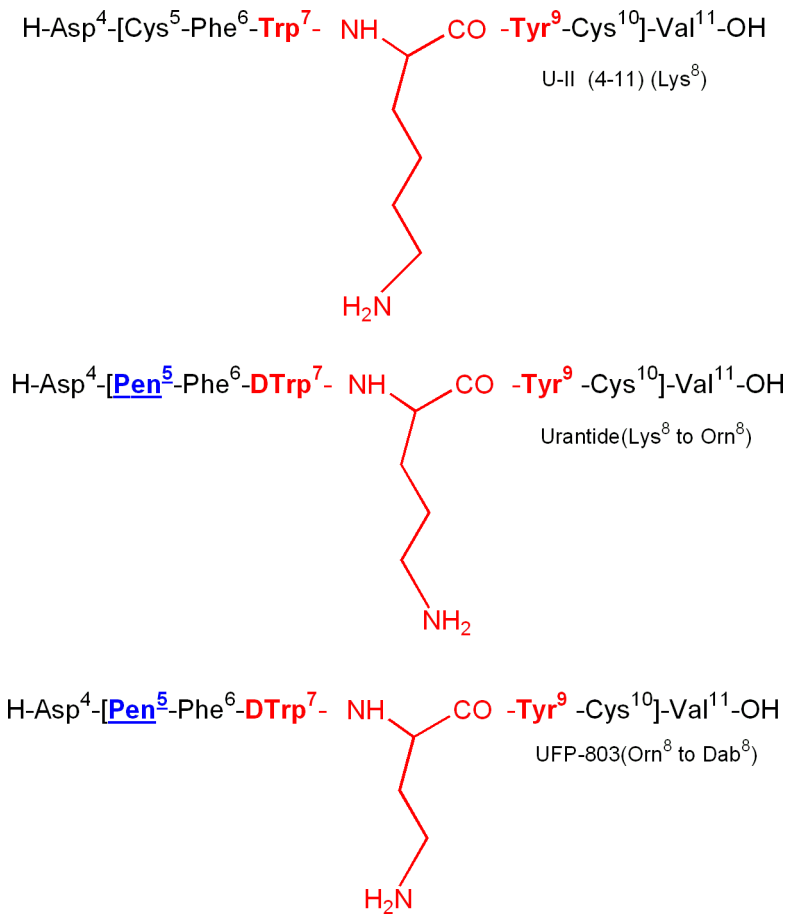


**Figure. 4.1. Structure of U-II(4-11), urantide and UFP-803.**
Amino acid residues that form the pharmacophore are indicated in red bold lettering. Additional amino acid modifications (which increased potency) are indicated in as blue underline. The square brackets [ ] denote cyclisation between residue 5 and residue 10.

### *4.2. Aims*

Urantide and UFP-803 have been described as being pure antagonists at the rat UT expressed in the thoracic aorta. In cuvette based $Ca^{2+}$ assays conducted at 37°C, urantide mimicked U-II like responses with an $\alpha$ value of ~0.80 in a recombinant system where human UT was expressed in CHO cells (Camarda *et al.*, 2004). Additionally UFP-803 appeared as a low efficacy partial agonist ($\alpha$= 0.21) in CHO cells expressing human UT (Camarda *et al.*, 2006). The objective of the set of experiments described below was to

further probe the pharmacological profiles of urantide and UFP-803 in HEK293$_{hUT}$ and CHO$_{hUT}$ cells by carrying out binding studies and phosphoinositide turnover assays in order to further characterise the pharmacological profile of these drugs.

## *4.3. Results*

### 4.3.1. Binding studies

*Competition (Displacement assays)*

Competition binding assays were carried out with urantide and UFP-803 in HEK293$_{hUT}$ cells (Figure. 4.2). Both these compounds displaced [I$^{125}$]U-II in a concentration dependent manner with pK$_i$ values of 8.41±0.04 and 8.20±0.11 respectively. This compares with the U-II pK$_d$ values of 9.43 (table 3.1 HEK293$_{hUT}$ K$_d$).

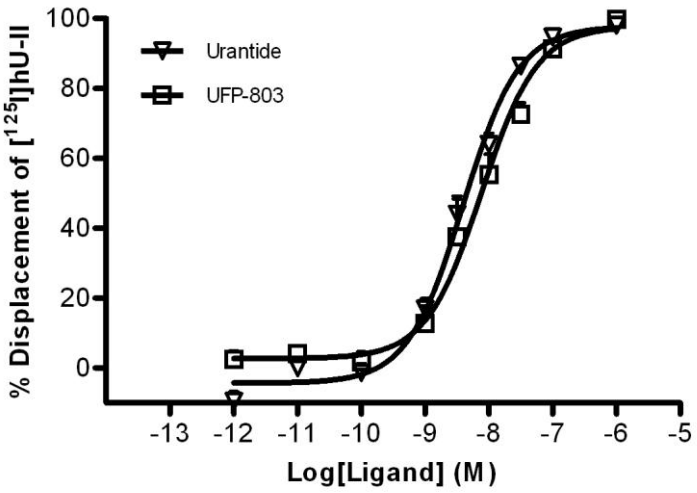


**Figure. 4.2. Displacement binding curves for urantide and UFP-803 in HEK293$_{hUT}$ cells.**
Data are mean ±SEM. Where n≥5.

### 4.3.2. PIT assays

In phosphoinositide turnover assays carried out in $HEK293_{hUT}$ and $CHO_{hUT}$ cells urantide and UFP-803 mimicked U-II like responses. However their maximal effects were lower than U-II (Figure. 4.3 and 4.4). The potencies and maximal effects of both drugs are summarised in Table. 4.1.

| Compound | $pEC_{50}$ | | $E_{max}$ (DPM) | | Relative intrinsic activity ($\alpha$) | |
|---|---|---|---|---|---|---|
| | *$HEK_{293hUT}$* | *$CHO_{hUT}$* | *$HEK_{293hUT}$* | *$CHO_{hUT}$* | *$HEK_{293hUT}$* | *$CHO_{hUT}$* |
| U-II | 9.02±0.05 | 9.27± 0.06 | 3549± 609 | 4393± 213 | 1.00 | 1.00 |
| Urantide | 8.71±0.20 | 8.75±0.04* | 675±79* | 1438±47* | 0.19 | 0.33 |
| *UFP-803* | 8.15±0.29* | 8.15±0.10*‡ | 322±48* | 954±32* | 0.09 | 0.22 |

**Table. 4.1. Effects of U-II, urantide and UFP-803 in $HEK293_{hUT}$ and $CHO_{hUT}$ cells.**
Summary of effects of U-II, urantide and UFP-803 in $HEK_{293hUT}$ and $CHO_{hUT}$ cells. Data are mean±SEM. Statistically significant differences are indicated by * (compared to U-II) and ‡ (compared to urantide) with $p< 0.05$ based on one way ANOVA and Tukey test.

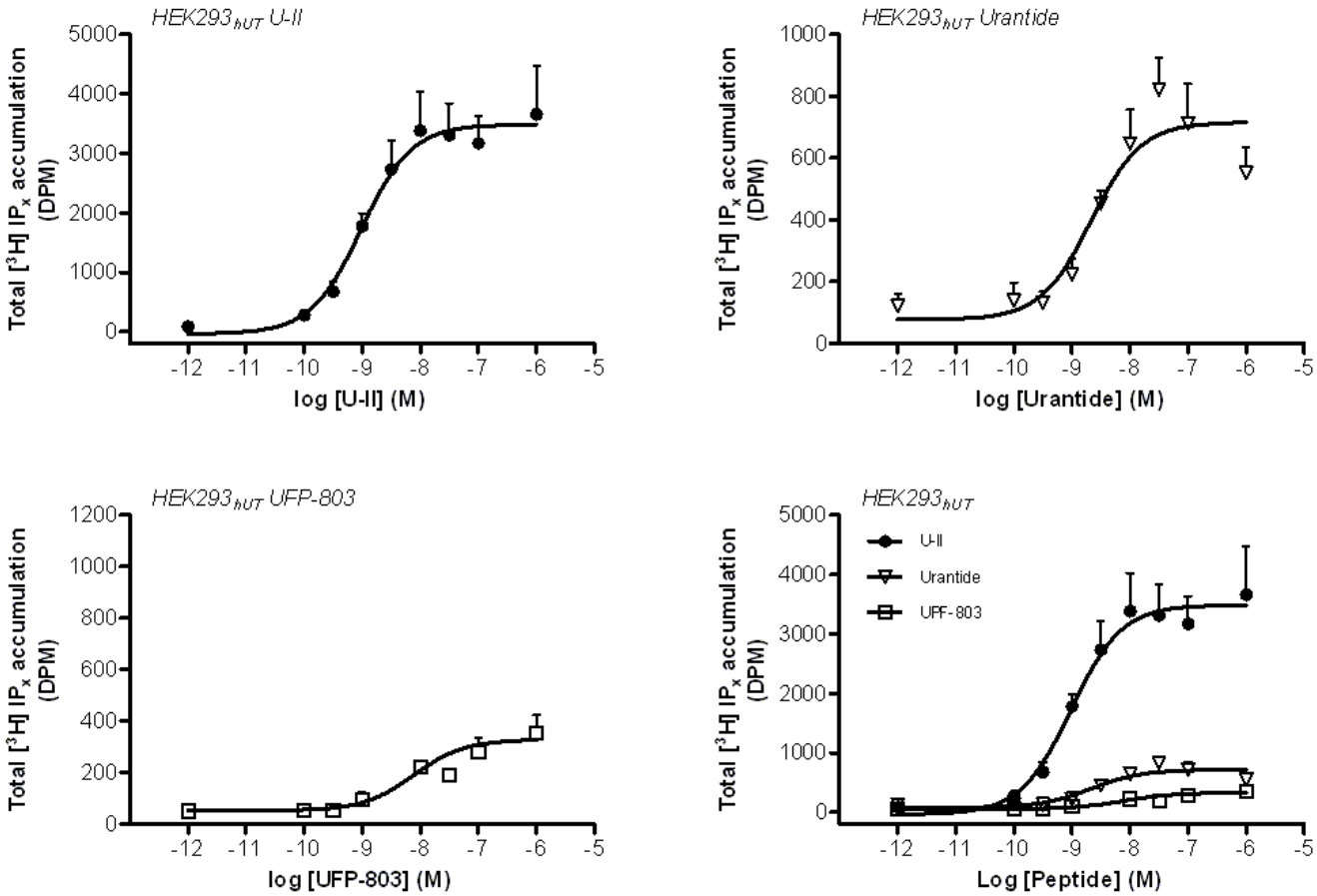


**Figure. 4.3. The effects of U-II, urantide and UFP-803 in PI turnover in HEK293$_{hUT}$ cells.**
Adherent cell assay. *Top panels*: effects of U-II and urantide. *Bottom panels*: effects of UFP-803 and a summary of the three drugs. Data are mean± SEM where n = 4 of separate experiments.

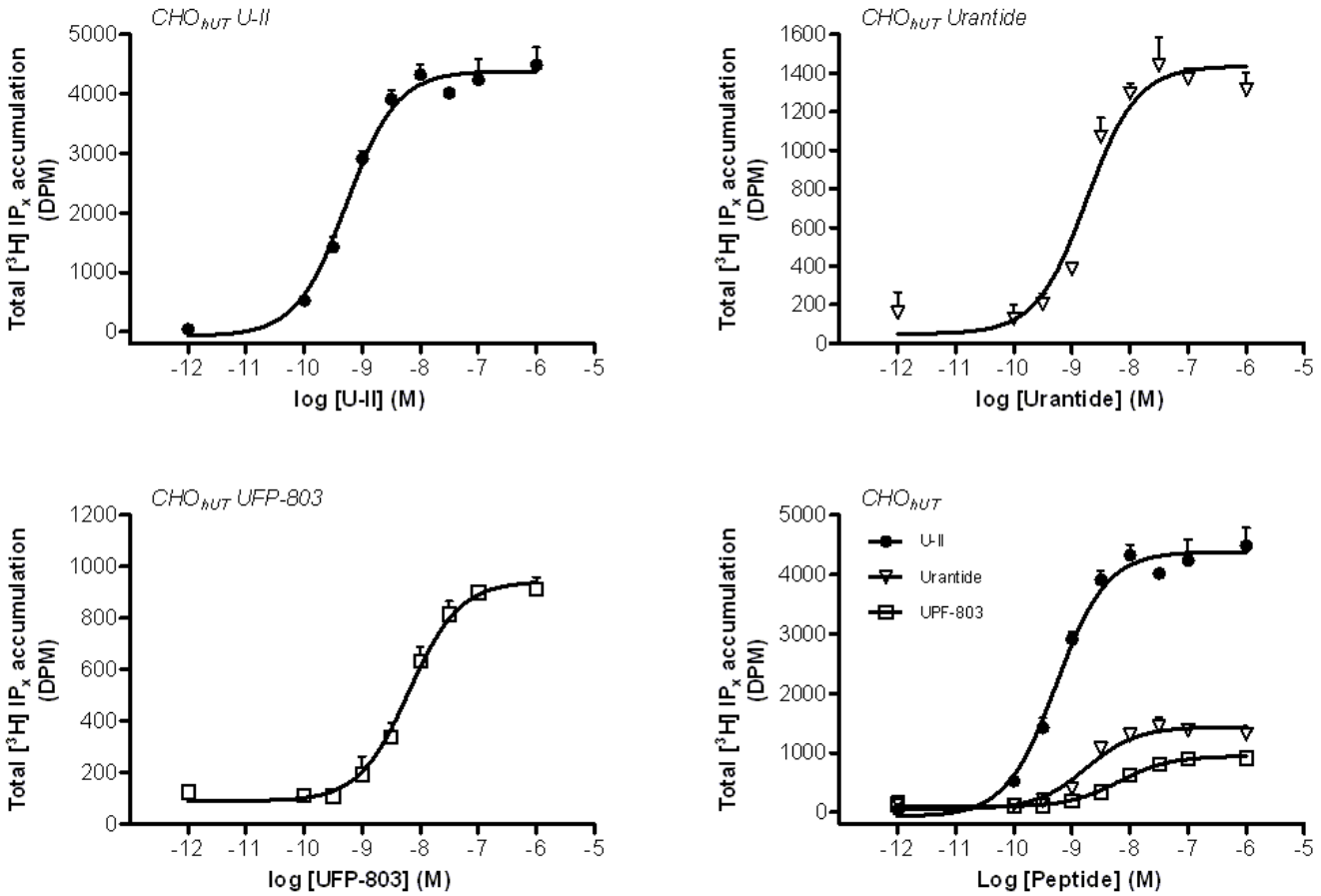


**Figure. 4.4. The effects of U-II, urantide and UFP-803 in PI turnover in $CHO_{hUT}$ cells.**
Adherent cell assay. *Top panels*: effects of U-II and urantide. *Bottom panels*: effects of UFP-803 and a summary of the three drugs. Data are mean± SEM where n = 4 of separate experiments.

UFP-803 appeared as a low efficacy partial agonist therefore antagonism experiments were performed in $HEK293_{hUT}$ and $CHO_{hUT}$ cells. U-II evoked a concentration dependent increase in $IP_x$ accumulation with $pEC_{50}$ of 8.98±0.16 and 8.96±0.05 respectively. UFP-803 at 0.1 μM caused a rightward shift of the U-II control curve, with negligible reduction in the maximal effect (Figure. 4.5). The $pK_B$ values were 7.64 and 8.27 for UFP-803 in $HEK_{293hUT}$ and $CHO_{hUT}$ cells respectively. UFP-803 appeared to possess some intrinsic activity in $CHO_{hUT}$ cells, however this was not evident in $HEK293_{hUT}$ cells.

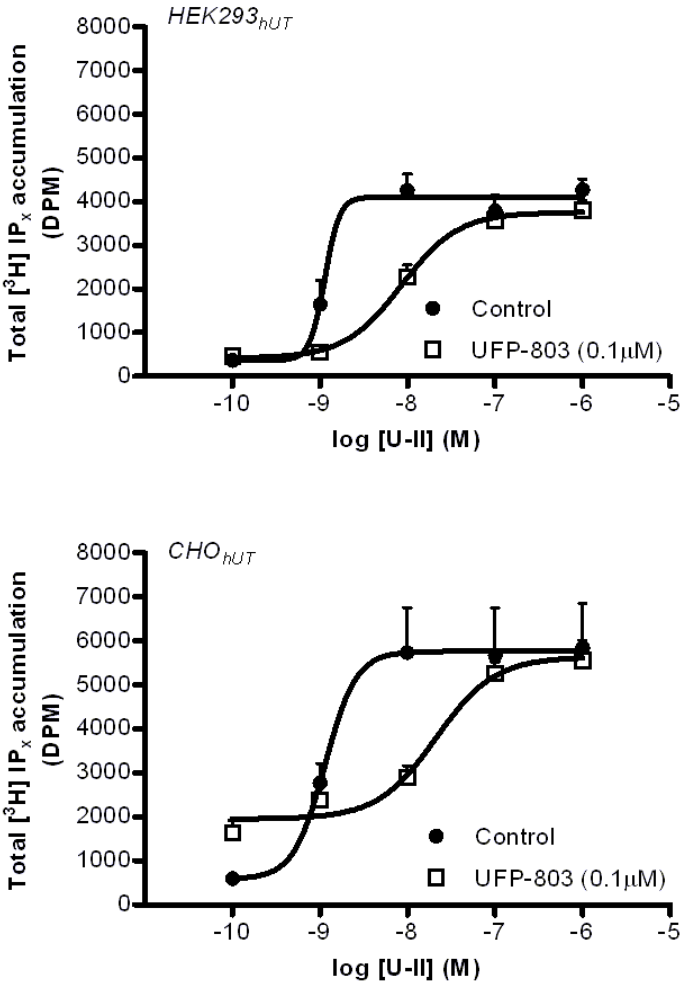


**Figure. 4.5. Antagonism of U-II by UFP-803 in $HEK293_{hUT}$ and $CHO_{hUT}$ cells.**
Adherent cell assay. Data presented as mean± SEM where $n \geq 4$ of separate experiments.

Similar experiments with urantide were conducted independently by J. McDonald in our laboratory using $CHO_{hUT}$ cells. Like UFP-803, urantide also demonstrated a rightward shift from the U-II control curve with a $pK_B$ of 7.45. No changes to the maximal effect were observed. Urantide is yet to be assessed in $HEK293_{hUT}$ cells by antagonism assays.

### *4.4. Discussion*

The $pK_i$ value obtained in the displacement binding studies for urantide was 8.41 while for UFP-803 this was 8.20. The $pK_d$ of U-II was 9.43. Studies by Patacchini and co-workers (2003) have also confirmed this; the $pK_i$ for U-II and U-II(4-11) was found to be 9.1 and 9.6 respectively, while the $pK_i$ for urantide was 8.3 which was also superimposable with its $pK_B$ value from rat aorta bioassays. Previous studies by (Camarda *et al.*, 2006) have described a $pK_B$ of 8.45 in $HEK293_{hUT}$ cells for UFP-803 based on $Ca^{2+}$ assays.

Urantide is modeled on U-II(4-11) as shown in Figure. 4.1. The synthesis of this peptide was initiated by SARs studies at $Cys^5$. The introduction of a Penicillamine moiety in place of Cys led to the identification of a superagonist (P5U) with greater potency than the template control. The usage of Pen has been described in other studies with developing antagonists specifically; this is indeed true with the case of oxytocin and hCGRP antagonists (Hruby *et al.*, 1979); (Saha *et al.*, 1998). In the case of urantide, the introduction of a Pen at position $Cys^5$ caused a conformational constraint; which improved its affinity for the UT receptor. The rationale for replacing $Trp^7$ with D-Trp was on the basis that this modification was also used in the generation of the antagonists BIM-23127 and SB 710411 (Patacchini *et al.*, 2003). Inversion of a single amino acid residue can change its pharmacological property from an agonist to an antagonist; such is the case with

endothelin antagonists (Kinney *et al.*, 2002). On the other hand the introduction of ornithine in place of $Lys^8$, was based on the fact that this residue can cause a reduction in peptide efficacy (Camarda *et al.*, 2002a).

While urantide displayed antagonist activity at rat aorta, studies in recombinant systems demonstrated residual agonist activity (Camarda *et al.*, 2004). As a consequence UFP-803 was developed by modeling it on urantide in order to eliminate residual agonism. The key difference in UFP-803 is the Dab residue a position 8 in place of ornithine. The rationale for incorporating this amino acid residue was based on previous studies where Dab substitution in [$Orn^8$]U-II yielded a peptide that had reduced potency and efficacy (Guerrini *et al.*, 2005).

These data demonstrate urantide and UFP-803 are low efficacy partial agonists at hUT receptor expressed in HEK293 and CHO cells at the level of $IP_x$ formation; with a rank order of potency and efficacy of U-II> urantide> UFP-803. This rank order of potency can be corroborated with previously published work by (Camarda *et al.*, 2006) in $CHO_{hUT}$ cells at 22 and 37°C in a more downstream $Ca^{2+}$ assay. The reduction in potency and efficacy of the tested compounds has been achieved by altering the distance of the primary alphatic amine of the amino acid at position 8 from the U-II backbone, as demonstrated in rat aorta bioassay (Guerrini *et al.*, 2005).

In antagonist assays conducted in $HEK293_{hUT}$ and $CHO_{hUT}$ cells, UFP-803 (at 0.1 μM) shifted the U-II curve to the right from that of the control, with no detriment on the maximal response. The apparent $pK_B$ values obtained here (7.64) for UFP-803 in

$HEK293_{hUT}$ cells is different from that published by Camarda and co-workers (2006) (8.55). However in relation to $pA_2$ values obtained from aorta, our values are very similar.

UPF-803 was developed with the aim of reducing residual agonist activity that was observed with urantide. The lack of residual agonist activity of UFP-803 is affected by the temperature as demonstrated with $CHO_{hUT}$ cell $Ca^{2+}$ assays. At room temperature UFP-803 lacks any activity. However at 37°C some residual agonist activity is detectable (Camarda *et al.*, 2006). In the PI assays conducted at physiological temperature, this is evident for both urantide and UFP-803. The latter compound should be classed as a very low efficacy partial agonist on the basis that it exhibits some residual agonist activity in PI turnover assays at physiological temperature.

## 5. SAR studies of U-II(4-11) analogues modified at Tyr$^{9}$

### *5.1. Introduction*

Urotensin-II(4-11) or U-II(4-11) is the truncated form of full length U-II. While it differs in length from the N-terminal end of the peptide the shorter form still retains the cyclic hexapeptide that is required for full biologically activity. The Trp-Lys-Tyr motif is highly conserved throughout mammalian, amphibian and piscean species (Douglas *et al.*, 2000a). Furthermore its importance is highlighted by its existence within the sequence of U-II related peptide (URP) which codes for a peptide that binds to UT with high potency and has been cloned in rat, mouse and human (Sugo *et al.*, 2003) (Figure. 5.1).


**Figure. 5.1. Structure of full length U-II, its truncated form (4-11) and urotensin related peptide (URP).** The amino acids that confer biological activity are highlighted in red.

An important reduction in peptide efficacy has been obtained by substituting Lys$^{8}$ with ornithine (Camarda *et al.*, 2002a) or diaminobutyric acid (Guerrini *et al.*, 2005) while an increase in affinity for the UT receptor has been achieved by replacing Cys$^{5}$ with Pen (Grieco *et al.*, 2002). A similar increase in affinity has also been obtained by substituting Trp$^{7}$ with its enantiomers, however this only applies for the antagonist templates urantide (Patacchini *et al.*, 2003) and UFP-803 (Camarda *et al.*, 2006).

Previous SAR studies of position 9 have indicated that the phenol moiety of $Tyr^9$ can be replaced with different aromatic moieties without any loss of affinity (Guerrini *et al.*, 2005) (Kinney *et al.*, 2002). Position 9 is also important with respect to increasing the bioactivity as reported with [2-Nal] substituted peptides, where a 3-fold increase in potency was reported (Kinney *et al.*, 2002).

According to molecular modeling studies the side chain of $Tyr^9$ interacts with the large hydrophobic pocket of the UT receptor in which the receptor residues His208 (ELII), Leu212 (TMV), Trp277 (TMVI), Ala281 (TMVI), Gln285 (ELIII) and Val296 (ELIII) are involved (Kinney *et al.*, 2002); (Lavecchia *et al.*, 2005). Binding experiments using surface plasmon resonance technology revealed U-II binding to the ELII and ELIII of the UT receptor (Boivin *et al.*, 2006).

The objective of this study was to enhance the binding of U-II analogues to UT by replacing $Tyr^9$ with non natural analogues characterised by the presence of the phenol ring potentially able to interact via hydrogen bonding with the U-II receptor residues. As part of the strategy i) the OH group in $Tyr^9$ was shifted from para to ortho and meta positions, ii) the $Tyr^9$ was replaced with (3,5-diiodo)Tyr, (N-$CH_3$)Tyr and the shorter analogue (4OH)Phg, iii) $Tyr^9$ was substituted with a series of conformationally constrained analogues by cyclisation of the side chain on the nitrogen or the C-alpha chiral carbon. This SAR study was performed by using U-II(4-11) as a template as this has been used previously and lead to the identification of the UT ligands; namely the agonist P5U ([$Pen^5$]U-II(4-11) (Grieco *et al.*, 2002), and the antagonists urantide [($Pen^5$-$DTrp^7$-Orn8)]U-II(4-11) (Patacchini *et al.*, 2003) and UFP-803 [($Pen^5$-$DTrp^7$-$Dab^8$)]U-II(4-11) (Camarda *et al.*, 2006) (see chapter 4).

All peptides in this study were synthesised by solid phase peptide synthesis. The synthesis methodology consisted of a series of selective acylation and deprotection reactions summarised as follows: (1) amino acid linkage to a polymeric support. (2) selective deprotection of the alpha amino acid group of the amino acid previously linked to the support (3) coupling of another protected amino acid. Thereafter steps (2) and (3) were repeated until the primary sequence of the peptide was complete. (4) Peptide cleavage and release. Amino acids characterised by a reactive side chain were selectively protected by acid labile protecting groups which can be removed, at the end of the synthesis, in the same experimental conditions required for the cleavage of the peptide from the solid support (Benoiton, 2005). For illustrative purposes the synthesis of U-II is shown in Figure. 5.2. For a more detailed scheme and description of the synthesis of the individual Tyr analogs the reader is referred to the appendix.

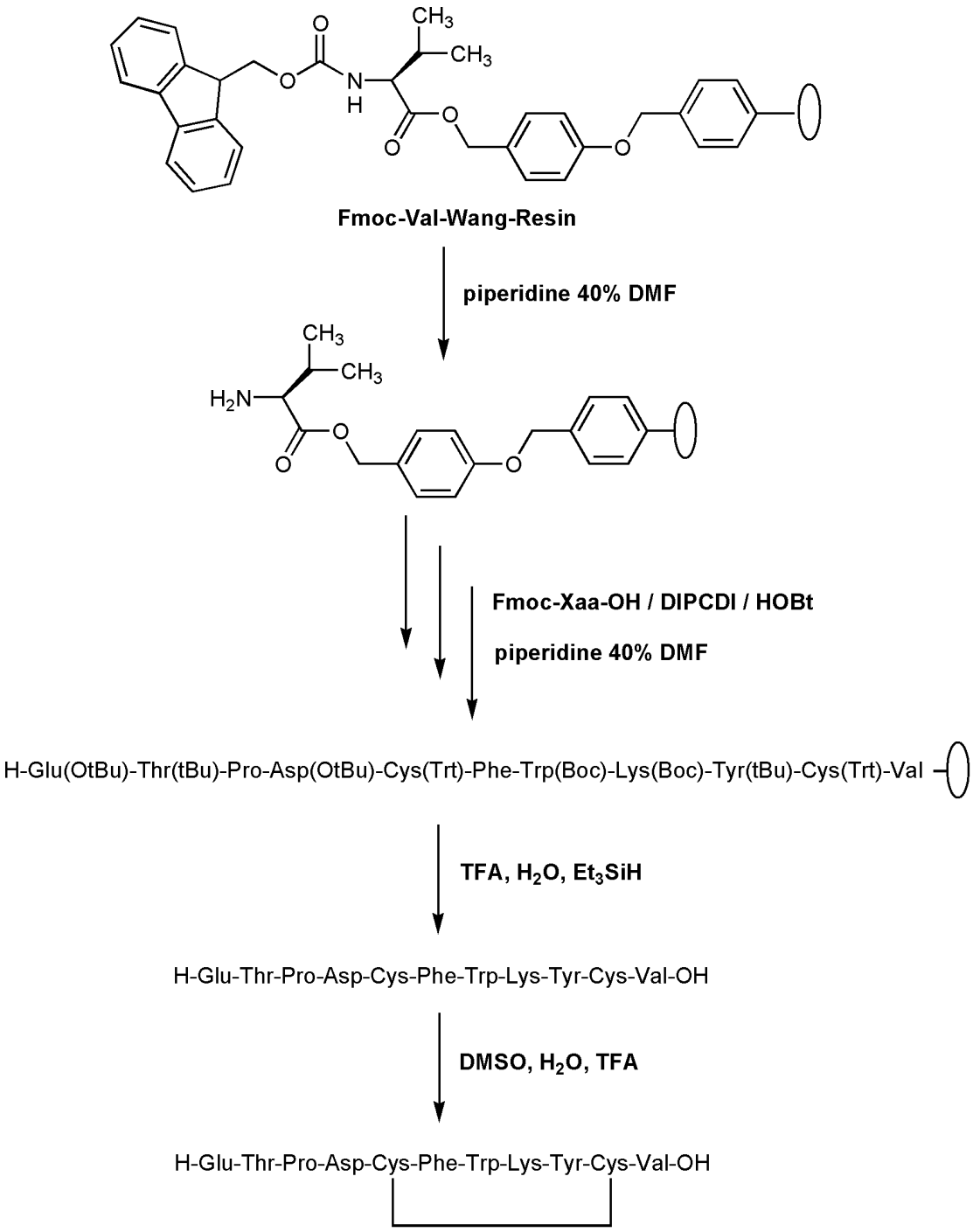


**Figure. 5.2. The synthesis of full length U-II by solid phase peptide synthesis.**

The polystyrene-Wang support loaded with N-alpha Fmoc (9-fluorenylmethoxycarbonyl) valine was treated with a solution of 40% piperidine made in dimethyl formamide to remove the Fmoc group. Thereafter the coupling of another protected amino acid was initiated in the presence of diisopropylcarbodiimide (DIPCDI) and l-hydroxybenzotriazole (HOBt). Both these reagents facilitated the coupling of the amino acid to the Valine Wang resin. This was followed by deprotection with 40% piperidine. The coupling and deprotection process was repeated until a peptide chain was generated. Once the peptide synthesis finished it was cleaved by trifluoroacetic acid (TFA) water and triethylsilane ($Et_3SiH$). The linear peptide was then cyclised in the presence of dimethylsulphoxide (DMSO), water and TFA and lyophilised. Since some amino acids (o-Tyr; m-Tyr; (5-OH)-Aic and Hat) were used as a racemic mixture, the corresponding diastereomeric U-II analogues were separated by preparative HPLC. The chemical formulae of the Tyr analogs employed in the current study are shown in Figure. 5.3 followed by the structures of the peptides in Figure. 5.4.

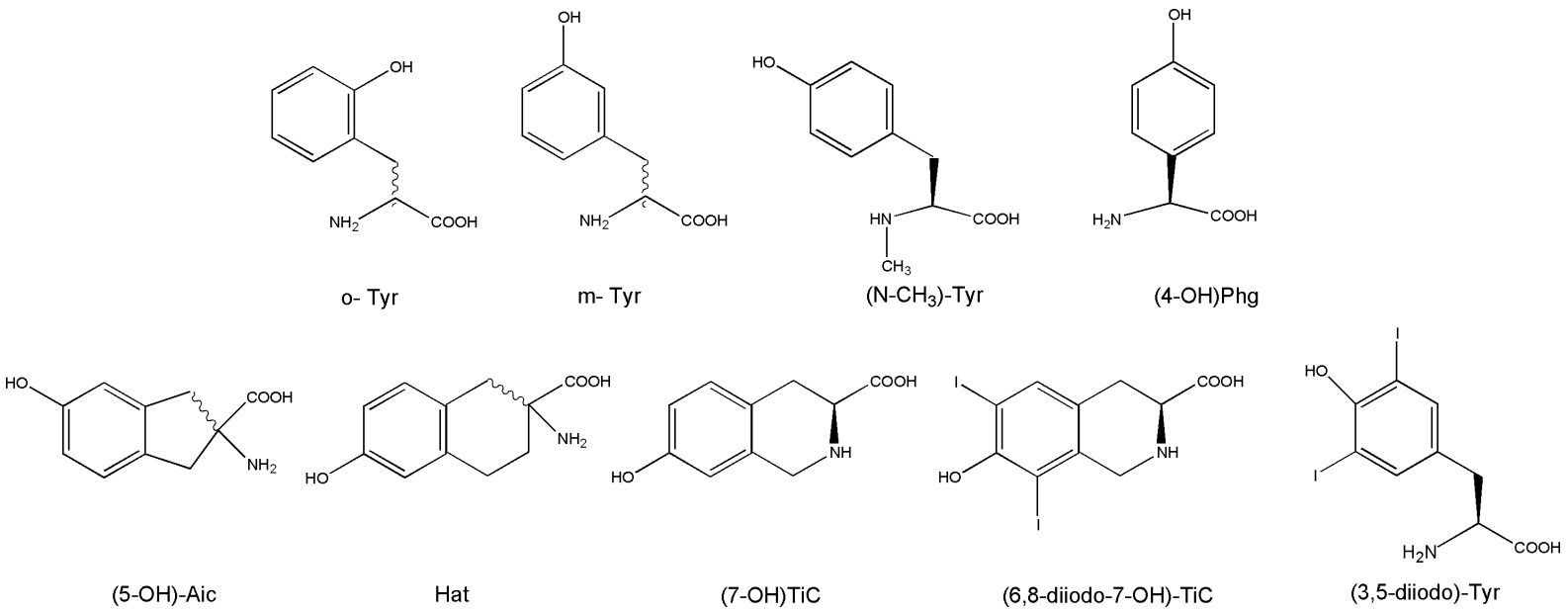


**Figure. 5.3. Chemical formulae of the Tyr analogues.**

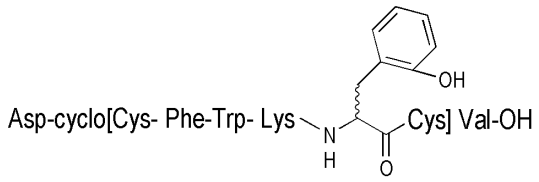


[*o*-Tyr$^{9}$]hU-II(4-11)

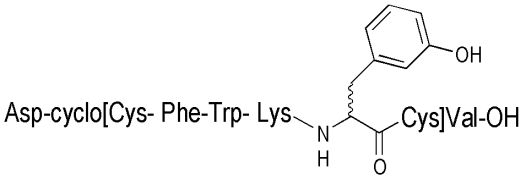


[*m*-Tyr$^{9}$]hU-II(4-11)

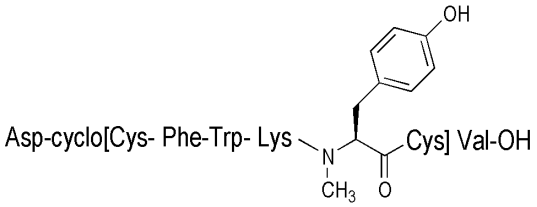


[(N-CH$_3$)-Tyr$^{9}$]hU-II(4-11)

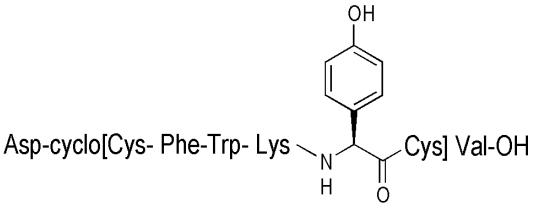


[(4-OH)-Phg$^{9}$]hU-II(4-11)

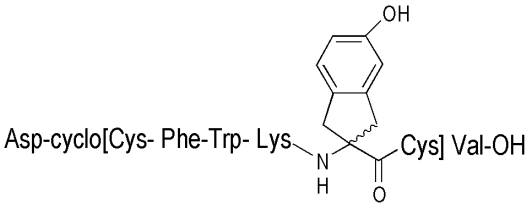


[(5-OH)-Aic$^{9}$]hU-II(4-11)

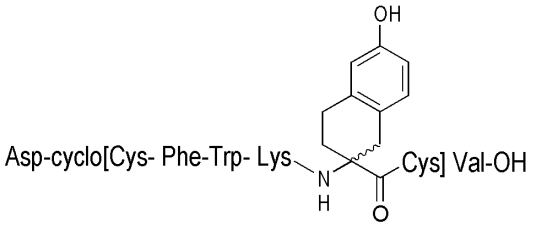


[Hat$^{9}$]hU-II(4-11)

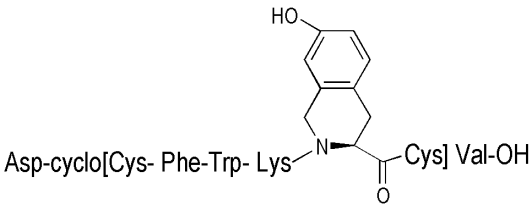


[(7-OH)-Tic$^{9}$]hU-II(4-11)

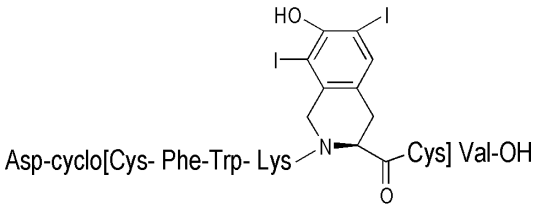


[(6,8-diiodo-7-OH)-Tic$^{9}$]hU-II(4-11)

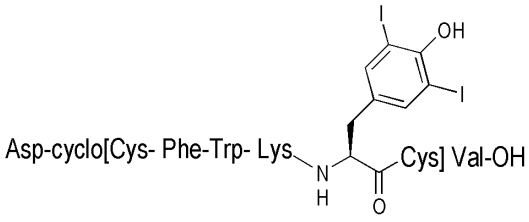


[(3,5-diiodo)-Tyr$^{9}$]hU-II(4-11)

**Figure. 5.4. Structure of Tyr analogue peptides of U-II(4-11).**

### *5.2. Aims*

The purpose of the current study was to characterise nine analogs of U-II(4-11) modified at $Tyr^9$ by Flexstation-II screening $Ca^{2+}$ assays in $HEK293_{rUT}$ cells. On this basis thereafter further aims were to characterise any potential lead compounds by other secondary assays; namely (1) phosphoinositide turnover assays with $HEK293_{rUT}$ cells, (2) cuvette based $Ca^{2+}$ mobilisation assays with SJCRH30 and $HEK293_{hUT}$ cells and (3) rat thoracic aorta bioassays.

### *5.3. Results*

#### 5.3.1. Flexstation-II compound screening

In calcium mobilisation assays carried out on $HEK293_{rUT}$ cells with the Flexstation-II both U-II and U-II(4-11) elicited a concentration dependent stimulation with similar potencies ($pEC_{50}$ 7.60 and 7.52) and maximal effects of (372±14% and 435±% over the baseline). The $pEC_{50}$ for U-II in $HEK293_{rUT}$ cells is similar to the value obtained with assay conducted in $CHO_{hUT}$ cells (Chapter 3, Table 3.3). Representative temporal profiles and average concentration response curves to U-II and U-II(4-11) are displayed in Figure. 5.5.

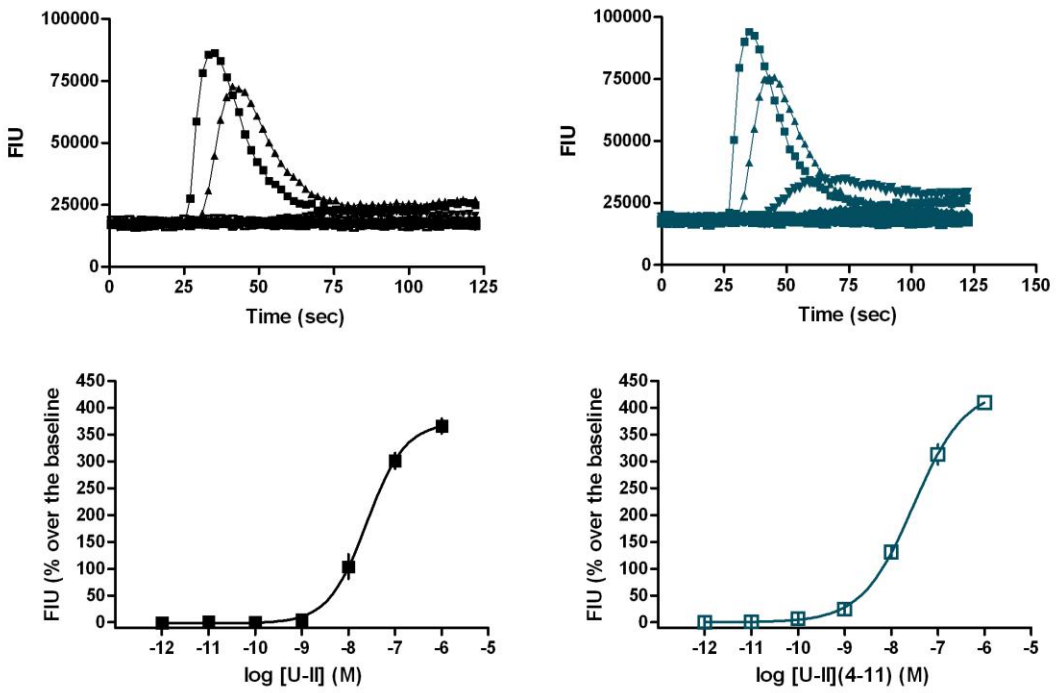


**Figure. 5.5. Flexstation-II temporal curves and concentration response curves.**
U-II (left panels) and U-II(4-11) (right panels) in HEK293$_{rUT}$ cells in the Flexstation-II [$Ca^{2+}$] mobilisation assay. *Top panels:* raw data from a single representative experiment (concentration range $10^{-12}$M – $10^{-6}$ M). *Bottom panels:* average concentration response curves obtained from 5 separate experiments performed in duplicate. Changes in intracellular calcium were expressed as % increase of fluorescence intensity units (FIU) over the baseline. Data are mean± SEM).

The effects of all the peptides synthesised are summarised in Table. 5.1. Since all the compounds were modeled on U-II(4-11), the relative intrinsic activity of all the compounds were determined with reference to the U-II(4-11) template.

| # | Compound | $pEC_{50}$ (CL95%) | $E_{max}$ ± SEM | $\alpha^a$ |
|---|---|---|---|---|
| | hU-II | 7.60 (7.34-7.87) | 372 ± 14% | 1.00 |
| | hU-II (4-11) | 7.52 (7.26-7.79) | 435 ± 12% | 1.00 |
| 1a | L-[ortho-Tyr$^9$]hU-II (4-11) | 7.49 (6.89-8.09) | 438 ± 11% | 1.01 |
| 1b | D-[ortho-Tyr$^9$]hU-II (4-11) | *Incomplete CRC. 10$\mu$M = 166 ± 51%* | | - |
| 2a | L-[meta-Tyr$^9$]hU-II (4-11) | 7.70 (7.24-8.16) | 357 ± 29% | 0.82 |
| 2b | D-[meta-Tyr$^9$]hU-II (4-11) | *Incomplete CRC. 10$\mu$M = 260 ± 42%* | | - |
| 3 | [(N-methyl)Tyr$^9$]hU-II (4-11) | *Incomplete CRC. 10$\mu$M = 140 ± 35%* | | - |
| 4 | [(4-OH)Phg$^9$]hU-II (4-11) | *Incomplete CRC. 10$\mu$M = 200 ± 26%* | | - |
| 5a | L-[(5-OH)Aic$^9$]hU-II (4-11) | *Inactive at 10 $\mu$M* | | - |
| 5b | D-[(5-OH)Aic$^9$]hU-II (4-11) | *Inactive at 10 $\mu$M* | | - |
| 6a | L-[(6-OH)Atc$^9$]hU-II (4-11) | *Incomplete CRC. 10$\mu$M = 27 ± 12%* | | - |
| 6b | D-[(6-OH)Atc$^9$]hU-II (4-11) | *Inactive at 10 $\mu$M* | | - |
| 7 | [(7-OH)Tic9]hU-II (4-11) | *Incomplete CRC. 10$\mu$M = 284 ± 15%* | | - |
| 8 | [(6,8-diiodo-7-OH)Tic$^9$]hU-II (4-11) | *Incomplete CRC. 10$\mu$M = 305 ± 51%* | | - |
| *9* | [(3,5-diiodo)Tyr$^9$]hU-II (4-11) | 7.74 (7.19-8.29) | 240 ± 24% | 0.55 |

**Table. 5.1. Effects of U-II, U-II(4-11) and its analogues in the Flexstation-II calcium mobilisation assay.**
CRC - concentration response curve. a- $\alpha$ value is calculated with reference to U-II(4-11).
Mean $pEC_{50}$ with confidence level (CL95%) $E_{max}$ data are mean ± SEM of at least 5 separate experiments performed in duplicate.*: significantly different from the $E_{max}$ of U-II(4-11) according to ANOVA followed by the Dunnett test.

Compounds **1a** and **2a** (both L conformation) in which the OH moiety have been shifted in ortho and meta position of the phenyl ring behaved as UT receptor full agonists with potencies comparable to that of the reference template. On the contrary the corresponding diastereomers (Compounds **1b** and **2b**) displayed a profound loss of potency (> 100 fold).

N-methylation of Tyr$^9$ (Compound **3**) produced a dramatic reduction of peptide potency. The shortening of the Tyr$^9$ side chain (Compound **4**) generated an inactive compound. The side chain cyclisation on the C-alpha chiral carbon with one (Compounds **5a-b**) or two (Compounds **6a-b**) carbon atoms consistently generated inactive analogues. Similar results were obtained by cyclisation of the side chain on the nitrogen atom (Compound **7** and **8**). The 3,5-diiodination of the phenol moiety (Compound 9) did not modify peptide potency but produced a statistically significant reduction of ligand efficacy ($\alpha$ = 0.55) thus generating a potent partial agonist.

The lead compound identified (compound 9 - [(3,5-diiodo)Tyr$^9$]U-II(4-11)) was thereafter characterised further in phosphoinositide turnover, calcium assays and rat aorta bioassays.

### 5.3.2. PIT assay

In phosphoinositide turnover assays carried out in HEK293$_{rUT}$ cells U-II(4-11) evoked a concentration dependent increase in total $IP_x$ formation with a $pEC_{50}$ 8.23 and a maximal effect of 3172±332 DPM. The lead compound [(3,5-diiodo)Tyr$^9$]U-II(4-11) mimicked similar maximal effect (3073±510 DPM) as the control however with lower $pEC_{50}$ of 7.57 (Figure. 5.6).

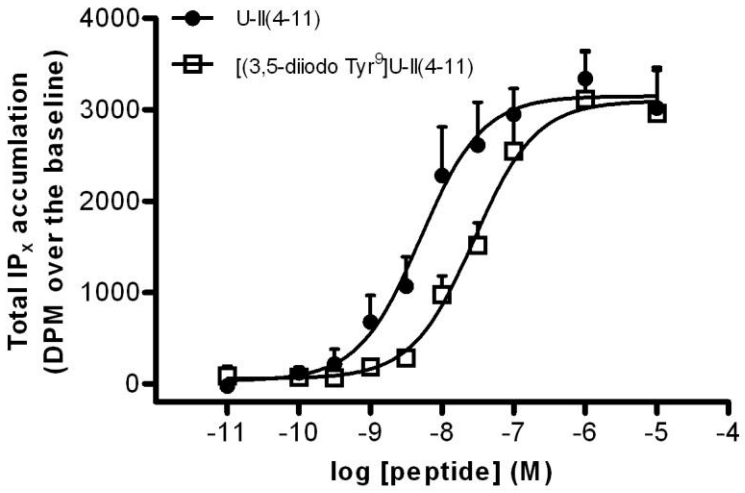


**Figure. 5.6. Total $IP_x$ accumulation in HEK293$_{rUT}$ cells.**
Suspension cell assay. Concentration response curve of U-II(4-11) and [(3,5-diiodo)Tyr$^9$]U-II(4-11). Data are means± SEM of n= 3 separate experiments.

### 5.3.3. Cuvette based $Ca^{2+}$ assay

After assessing the effect of this new compound on rat UT receptor, further studies were carried out in relation to human UT receptors. The effects of U-II(4-11) and [(3,5-diiodo)$Tyr^{9}$]U-II(4-11) were assessed in cuvette based calcium mobilisation assays in cells expressing the native (SJCRH30) and recombinant ($HEK293_{hUT}$) human UT.

In SJCRH30 U-II(4-11) evoked a concentration dependent increase in $Ca^{2+}$ mobilisation with a $pEC_{50}$ of 7.87 while exhibiting maximal effects of 26±5 nM. [(3,5-diiodo)$Tyr^{9}$]U-II(4-11) exhibited a similar profile to its template with a lower potency of 7.32 and maximal effect of 29±5 nM.

A concentration dependent increase in $Ca^{2+}$ mobilisation was also observed with U-II(4-11) in $HEK293_{hUT}$ cells with a $pEC_{50}$ of 7.57 and maximal effect of 245±34 nM while [(3,5-diiodo)$Tyr^{9}$]U-II(4-11) displayed a $pEC_{50}$ of 7.73 and maximal effect of 290±21 nM. It is noteworthy to mention that these assays were conducted at 37°C while the initial Flexstation-II screen was carried out room temperature (Figure. 5.7).

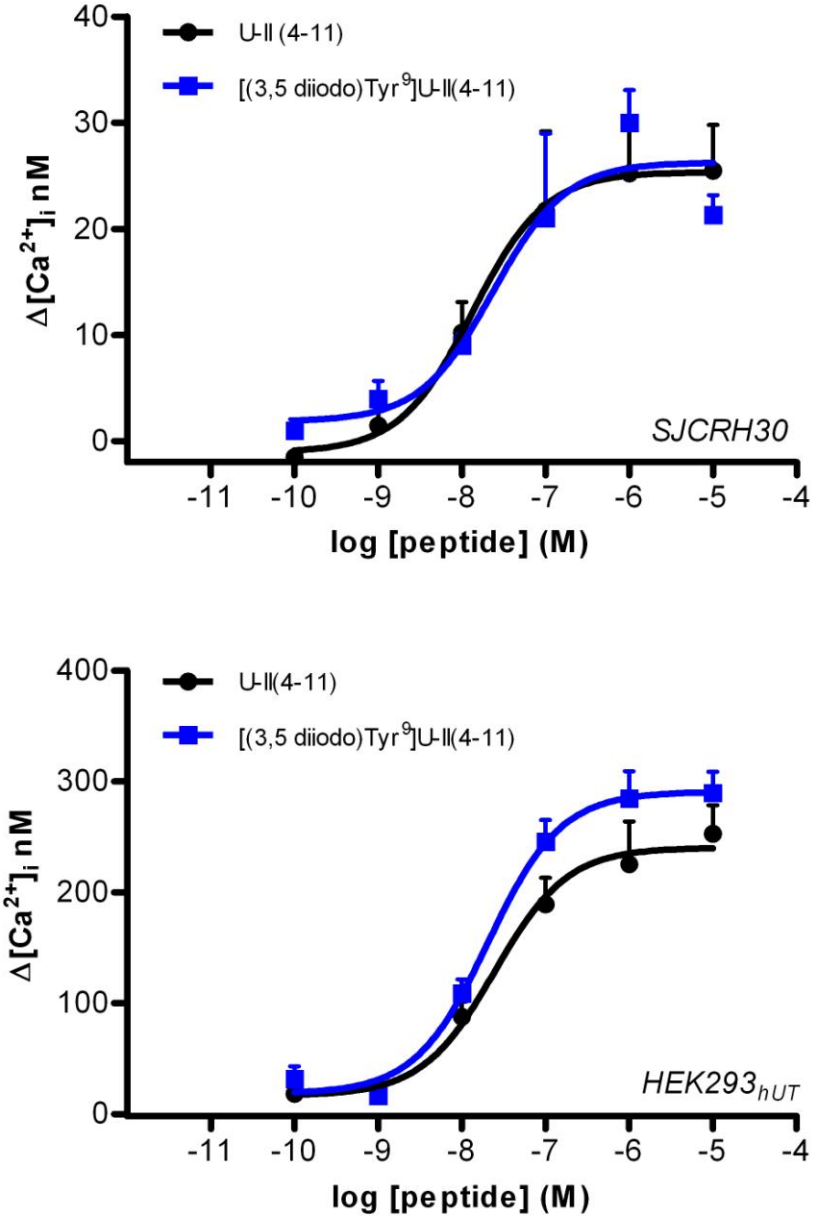


**Figure. 5.7. Effects of U-II(4-11) and [(3,5-diiodo)Tyr$^{9}$]U-II(4-11).**
*Top panel:* SJCRH30 cells expressing native receptor. *Bottom panel:* HEK293 cells expressing recombinant human UT receptor. Data are mean± SEM of n=4 separate experiments.

### 5.3.4. Rat aorta bioassay

To further characterise the pharmacological properties of [(3,5-diiodo)Tyr$^{9}$]U-II(4-11) a separate series of experiments were performed using the rat thoracic aorta bioassay where the effects evoked by this compound were compared to those of U-II and those of UFP-803, which appears as a pure antagonist in the rat thoracic aorta (Camarda *et al.*, 2006). U-II produced a concentration dependent contraction with high potency ($pEC_{50}$ 8.53) with maximal effects corresponding to 55% of that induced by 1 μM noradrenaline (NA). In parallel experiments UFP-803 was inactive up to micromolar concentrations while [(3,5-diiodo)Tyr$^{9}$]U-II(4-11) mimicked the contractile effects of U-II with lower potency ($pEC_{50}$ 7.70) and maximal effects ($\alpha$=0.58) (Figure. 5.8 top panel). In antagonist type experiments (bottom panel Figure. 5.8) both UFP-803 and [(3,5-diiodo)Tyr$^{9}$]U-II(4-11) tested at 1 μM produced a parallel rightward shift in the concentration response curve to U-II approximately by two log units. $pK_B$ values of 7.59 and 7.75 were derived for these experiments for UFP-803 and [(3,5-diiodo)Tyr$^{9}$]U-II(4-11) respectively.

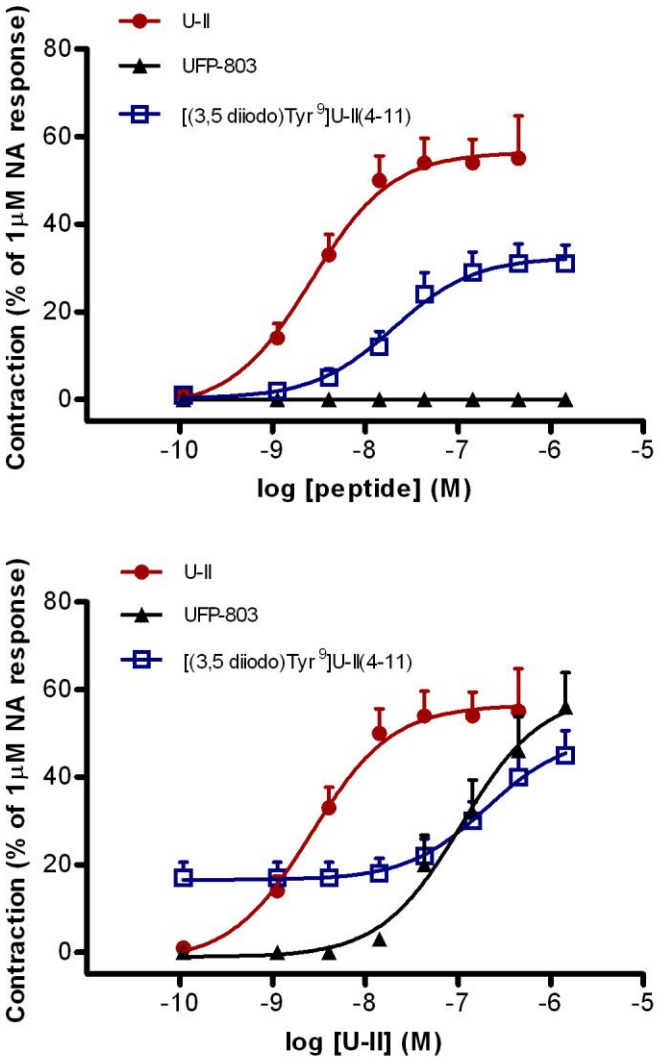


**Figure. 5.8. Summary of the effects observed in rat thoracic aorta.**
*Top panel*: concentration response curves to U-II, [(3,5-diiodo)Tyr$^9$]U-II(4-11) and UFP-803 in the rat aorta bioassay. *Bottom panel*: concentration response curves to U-II in the absence (control) and in the presence of 1 μM [(3,5 diiodo)Tyr$^9$]U-II(4-11) or UFP-803. Data are mean± SEM of n= 5 separate experiments.

## *5.4. Discussion*

### 5.4.1. Flexstation-II screening

The current SAR study in relation to compound **1a** and **2a** demonstrates that shifting the OH group has no detrimental effect on the biologically activity, further suggesting that its position in the phenyl ring is not a critical component in UT receptor binding. In contrast the inversion of position 9 chirality from L to D relative configuration had a detrimental effect on biological activity. Several groups have independently confirmed that [D-$Tyr^9$]U-II does not bind to the UT receptor (Flohr *et al.*, 2002) (Guerrini *et al.*, 2005); (Labarrere *et al.*, 2003). Hence the current results confirm the importance of chirality with reference to position 9.

N-methylation of $Tyr^9$ (Compound **3**) produced a dramatic reduction of peptide potency. Molecular modeling studies (Chatenet *et al.*, 2004) and NMR investigations (Lescot *et al.*, 2007) suggested that the NH of $Tyr^9$ may be involved in hydrogen bonding with the CO of $Trp^7$ stabilising a turn centred on the $Trp^7$-$Cys^{10}$ sequence which can be important for U-II bioactivity. Methylation of $Tyr^9$ prevents the possibility of the formation of such hydrogen bond and this is probably the reason for the inactivity of this U-II analog. However, it cannot be excluded that the introduction of a methyl group on $Tyr^9$ could produce steric hindrance that prevents UT receptor binding.

A consequence of shortening the $Tyr^9$ side chain (compound **4**) is highlighted by the importance of the distance of the phenol moiety from the peptide backbone. This resulted in the generation of a compound not retaining any biological activity.

Conformational restriction of side chains (compounds **5a**, **5b**, **6a**, **6b**, **8** and **7**) is not tolerated and generated inactive analogues. This therefore demonstrates the importance of the flexibility of the $Tyr^9$ side chain as an important requirement for UT receptor interaction.

The 3,5-diiodination of the phenol moiety (Compound **9**) increases both lipophilicity and steric hindrance of the side chain and at the same time limited the side chain flexibility. The relative importance of these factors in the reduction of efficacy of Compound 9 is at present unknown. Interestingly, two iodine atoms on the Tyr phenol moiety seem to be required for reducing efficacy since [3-iodo$Tyr^9$]U-II(4-11) was reported to behave as a UT receptor full agonist (Labarrere *et al.*, 2003).

### 5.4.2. PIT assay and cuvette $Ca^{2+}$ assay

In these set of experiments conducted at 37°C [(3,5-diiodo)$Tyr^9$]U-II(4-11) displayed full agonist activity like U-II. This contrasts to its partial agonist profile in the initial screen which was conducted at room temperature.

The rank order of efficacy in $HEK293_{rUT}$ cells at room temperature was U-II(4-11)> [(3,5-diiodo)$Tyr^9$]U-II(4-11) while in the PI assay in the same cells at physiological temperature was U-II(4-11)=[(3,5-diiodo)$Tyr^9$]U-II(4-11). This was also the case in cuvette based calcium assays conducted at physiological temperature in SJCRH30 and HEK293 cells expressing native and recombinant human receptor. Hence the results in these studies emphasise the importance of temperature with regard to estimating ligand efficacy as

previously demonstrated with urantide and UFP-803 (Camarda *et al.*, 2006). While the rank order of potency differed in $HEK293_{rUT}$ and $HEK293_{hUT}$ both U-II and [(3,5-diiodo)$Tyr^9$]U-II(4-11) clearly exhibited almost super-imposable potencies 7.52 vs 7.57 for U-II(4-11) and 7.74 vs 7.73 for [(3,5-diiodo)$Tyr^9$]U-II(4-11).

### 5.4.3. Rat aorta bioassay

[(3,5-diiodo)$Tyr^9$]U-II(4-11) displays a partial agonist profile not only in the rat aorta bioassay but also in $HEK293_{rUT}$ cells (Flexstation-II assay). Furthermore the potencies are very similar (7.70 and 7.74 respective).

The $pK_B$ value of 7.75 should be interpreted with caution since it is clearly biased by the residual agonist activity of [(3,5-diiodo)$Tyr^9$]U-II(4-11). Despite this, in line with theoretical predictions there is an excellent match between the potency displayed by Compound 9 in agonist ($pEC_{50}$ 7.70) and antagonist ($pK_B$ 7.75) type experiments. Therefore, these results confirm and extend to the native UT receptor, expressed in the rat aorta, the pharmacological behavior of Compound 9 as a potent partial agonist.

## *5.5. Conclusion*

Collectively the results of the present SAR study on position 9 of U-II(4-11) demonstrated that i) the position of the OH group of the Tyr side chain is not important for biological activity, ii) the distance of the phenol moiety from the peptide backbone and its conformational freedom are crucial for UT receptor recognition, iii) this position is important not only for receptor binding but also for its activation since the (3,5-diiodo)-

$Tyr^9$ chemical modification generated a potent low efficacy agonist which behaved as a partial agonist both at recombinant and native rat UT receptors. This latter chemical modification can be combined in future studies with those already described in the literature which were used for generating useful UT receptor ligands such as P5U (Grieco *et al.*, 2002), urantide (Patacchini *et al.*, 2003), and UFP-803 (Camarda *et al.*, 2006) with the aim of identifying novel interesting pharmacological tools to be used in U-II/ UT receptor system studies. One drawback of designing U-II related ligands is likely to be irreversibility of binding.

## 6. Functional desensitisation of UT signalling

### *6.1. Introduction*

GPCRs are affected by the process referred to as desensitisation- a process in which an agonist causes attenuation of receptor responsiveness. The phenomenon of pharmacological desensitisation occurs as a consequence of a combination of mechanisms; such as the uncoupling of the receptor from G-proteins due to receptor phosphorylation, internalisation of cell surface receptors to intracellular membranous compartments and downregulation of receptor as a consequence of a reduction in receptor mRNA (see chapter 7) and protein synthesis. Desensitisation is a process with distinct time courses in the order of seconds, minutes, hours or days of receptor activation (Ferguson *et al.*, 1998) (Ferguson, 2001).

There is some evidence demonstrating that the UT receptor is susceptible to desensitisation. In studies on rat aorta, a primary challenge of U-II (increasing concentration gradient) resulted in increased tonic contraction. When the same tissue was challenged with a secondary U-II stimulus, after 5 hr the contractile effects had diminished (Camarda *et al.*, 2002b). In a recent study conducted in human aortic endothelial cells, a primary addition of 100 nM of U-II evoked a 100% in calcium mobilisation, while a second administration of U-II caused a ~46% reduction in the $Ca^{2+}$ response (Brailoiu *et al.*, 2008). It is important, however, to remember that U-II binding is essentially irreversible and this will confound any interpretation.

### *6.2. Aims*

As noted U-II binding is essentially irreversible. In this set of experiments human UT signalling was assessed in three cell lines expressing native (SJCRH30) or recombinant human UT receptor ($HEK293_{hUT}$ and $CHO_{hUT}$). The following experimental paradigm was utilised:

1). As a control cells were initially stimulated with a primary addition of vehicle (Krebs HEPES buffer) followed by a secondary addition of agonist (U-II, Cch or ATP). The change in intracellular calcium $[\Delta Ca^{2+}]_i$ was determined by subtracting the basal from the maximum response (Figure 6.1).

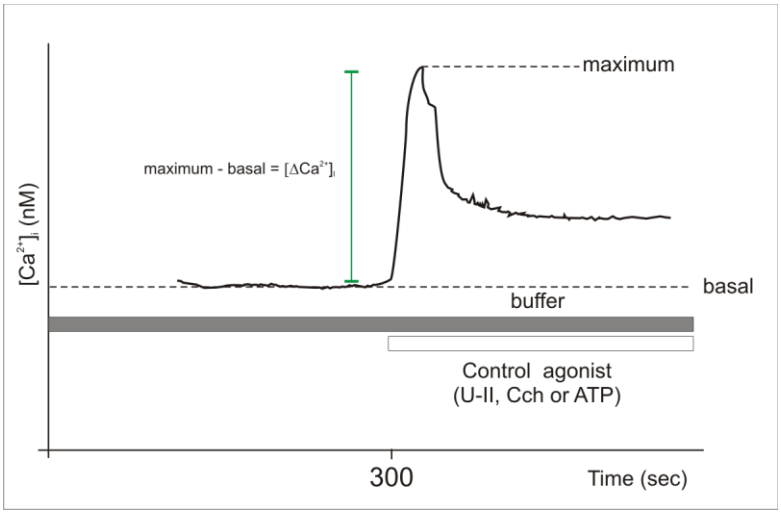


**Figure. 6.1. An example of control agonist challenge.**
Agonist responses to U-II, Cch and ATP were conducted in the three cell lines. Additions were carried out at 300 sec. Figure is not to scale.

2). Cells were challenged with a primary addition with agonist (carbachol –for SJCRH30 and $HEK293_{hUT}$ cells) or ATP (for $CHO_{hUT}$ cells). This was then followed by the secondary addition of U-II and vice versa. (Figure. 6.2).

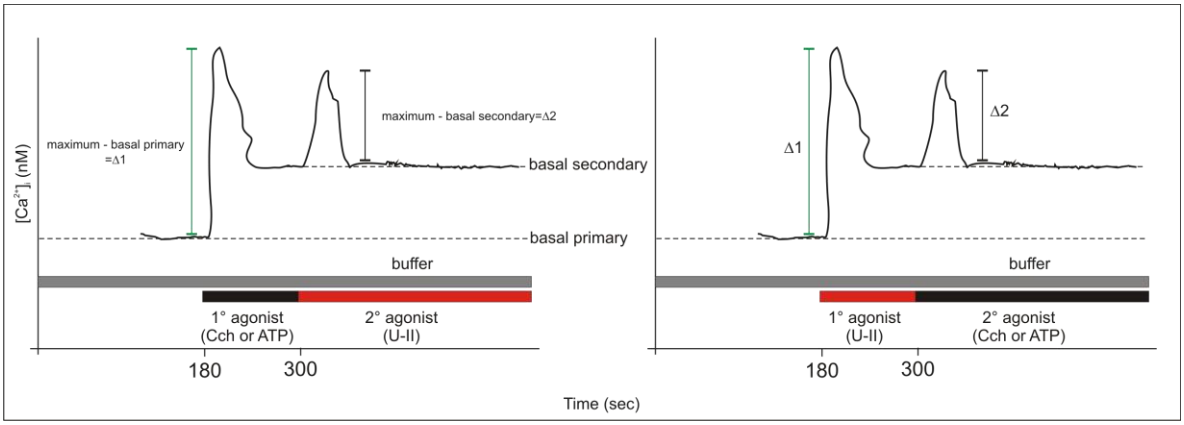


**Figure. 6.2. An example of the double addition protocol.**
Δ1 denotes the change in $[Ca^{2+}]_i$ of the primary (1˚) agonist determined as shown with the formula (left panel). Δ2 denotes the change in $[Ca^{2+}]_i$ of the secondary (2°) agonist. Figure is not to scale.

Carbachol (Cch) was used in SJCRH30 and $HEK293_{hUT}$ cells as both these cells are sensitive to muscarinic stimulation (Douglas *et al.*, 2004); (Ancellin *et al.*, 1999), while adenosine trisphosphate (ATP) was used in CHO cells as these cells express $P_2Y$ receptors (Iredale *et al.*, 1993).

The objective of this experiment was to (1) observe if the application primary agonist had an effect on the secondary agonist response and to (2) compare the secondary agonist response with the control agonist response in order to assess changes to the secondary agonist response.

## *6.3. Results*

### 6.3.1. Basal $Ca^{2+}$ levels

In SJCRH30, $HEK293_{hUT}$ and $CHO_{hUT}$ cells (25 and 37°C) the mean basal $[Ca^{2+}]_i$ measured at 173 sec (prior to the addition of agonist at 175 sec) is summarised in Table. 6.1. Basal values were temperature dependent.

| **Cell Line** | **25°C (nM)** | **37°C (nM)** |
|---|---|---|
| *SJCRH30* | 14±1 | 40±2 * |
| *$HEK293_{hUT}$* | 21±1 | 26±1 * |
| $CHO_{hUT}$ | 37±4 | 85±9 * |

**Table. 6.1. Summary of basal $Ca^{2+}$ level in the three cell lines tested at 25 and 37°C.**
Statistical differences between the two temperatures (based on paired t-tests) are indicated by * ($p<0.05$). Data are mean± SEM, n=20.

### 6.3.2. Double additions

The effects of the double addition protocols are summarised with representative temporal profiles for SJCRH30, $HEK293_{hUT}$ and $CHO_{hUT}$ at 25°C and 37°C respectively.

*Effects in SJCRH30 cells*

At room temperature buffer application did not evoke any responses. However subsequent U-II (1 μM) and Cch (250 μM) addition resulted in $\Delta[Ca^{2+}]_i$ of 20±3 nM and 19±2 nM respectively. The $Ca^{2+}$ release was characterised by a biphasic curve in the case of both agonists (Figure. 6.3 i and iii).

In the double addition experiments primary challenges of Cch and U-II resulted in biphasic responses with $\Delta[Ca^{2+}]_i$ of 20±1 and 22±1 nM respectively. Secondary application of U-II and Cch caused a $\Delta[Ca^{2+}]_i$ of 26±4 and 25±2 nM. (Figure 6.3. iv and iv).

Under physiological temperature, no responses were observed with the addition of buffer however $\Delta[Ca^{2+}]_i$ of 146±16 nM and 30±7 nM were observed in subsequent U-II and Cch challenges (Figure 6.4. i and iii).

A $\Delta[Ca^{2+}]_i$ of 25±4 and 132±11 nM in the double addition experiments upon primary challenges of Cch and U-II, while the secondary additions of U-II and Cch culminated in a $\Delta[Ca^{2+}]_i$ of 171±21 and 29±6 nM respectively. The shapes of these responses were biphasic.

A summary of all the responses observed in SJCRH30 is shown in Table. 6.2. The primary responses evoked by Cch and U-II did not have a detrimental effect on the secondary U-II and Cch responses respectively at either temperature. Statistically significant differences were observed for the U-II control response as well as the U-II secondary response in relation to temperature.

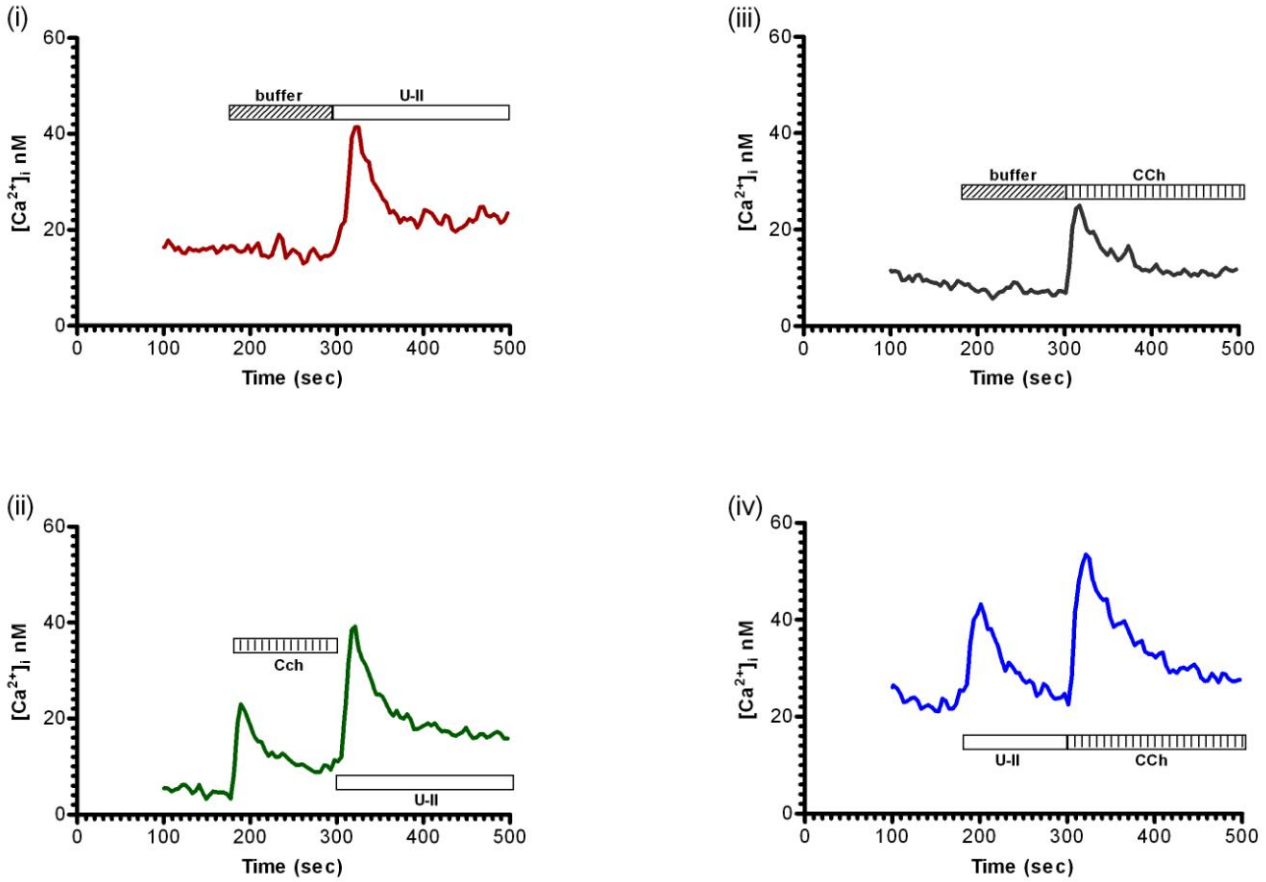


**Figure. 6.3. Representative graphs of effects elicited by double addition protocols in SJCRH30 cells at 25°C.**
*Top panels*: U-II (left) and Carbachol- Cch (right) responses (controls) after a vehicle challenge. *Bottom panels*: Secondary $Ca^{2+}$ response of U-II (left) and Cch (right) after a primary challenge of Cch and U-II respectively. The duration of exposure to buffer, U-II and Cch are indicated by the bars (n=4 of separate experiments).

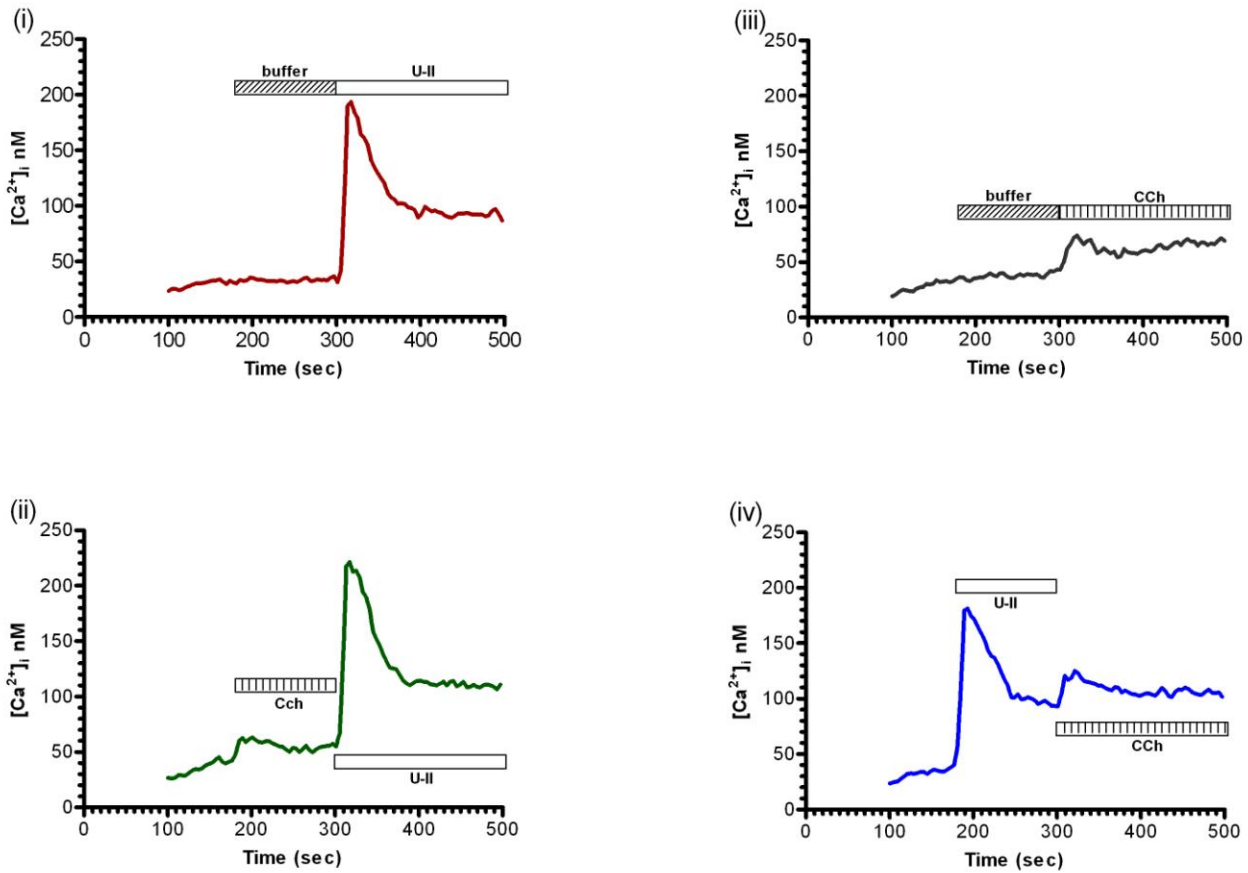


**Figure. 6.4. Representative graphs of effects elicited by double addition protocols in SJCRH30 cells at 37°C.**
*Top panels*: U-II (left) and Carbachol- Cch (right) responses (controls) after a vehicle challenge. *Bottom panels*: Secondary $Ca^{2+}$ response of U-II (left) and Cch (right) after a primary challenge of Cch and U-II respectively. The duration of exposure to buffer, U-II and Cch are indicated by the bars (n=4 of separate experiments).

| Temperature (°C) | U-II (control) response (nM) | Cch (control) response (nM) | Primary (Cch) response (nM) | Secondary (U-II) response (nM) | Primary (U-II) response (nM) | Secondary (Cch) response (nM) |
|---|---|---|---|---|---|---|
| 25 | 20±3 | 19±2 | 20±1 | 26±4 | 22±1 | 25±2 |
| 37 | 146±16* | 30±7 | 25±4 | 171±21* | 132±11 | 29±6 |

**Table. 6.2. Summary of the $Ca^{2+}$ response in SJCRH30 cells at 25 and 37°C.**
Statistically significant difference are indicated as * where *p<0.05* (25°C vs 37°C). n=4 of separate experiments.

*Effects in HEK293$_{hUT}$ cells*

At room temperature following buffer additions U-II and Cch (1 μM and 250 μM respectively) addition caused a $\Delta[Ca^{2+}]_i$ of 46±23 and 172±31 nM (Figure 6.5 i and iii). In the double addition protocol primary challenge of Cch and U-II resulted in $\Delta[Ca^{2+}]_i$ of 156±15 and 38±15 nM respectively. This was followed by U-II and Cch responses of were 5±1 and 157±6 nM due to secondary additions respectively (Figure 6.5. ii and iv).

In the same set up experiments conducted at 37°C the U-II and Cch controls were 142±27 and 191±41 nM respectively (Figure. 6.6 i and iii). In the double addition experiments the following occurred: primary challenge of Cch and U-II resulted in $\Delta[Ca^{2+}]_i$ of were 146±26 and 113±25 nM while the secondary challenge of U-II and Cch was characterised by a $\Delta[Ca^{2+}]_i$ of 23±3 and 45±7 nM (Figure 6.6. ii and iv).

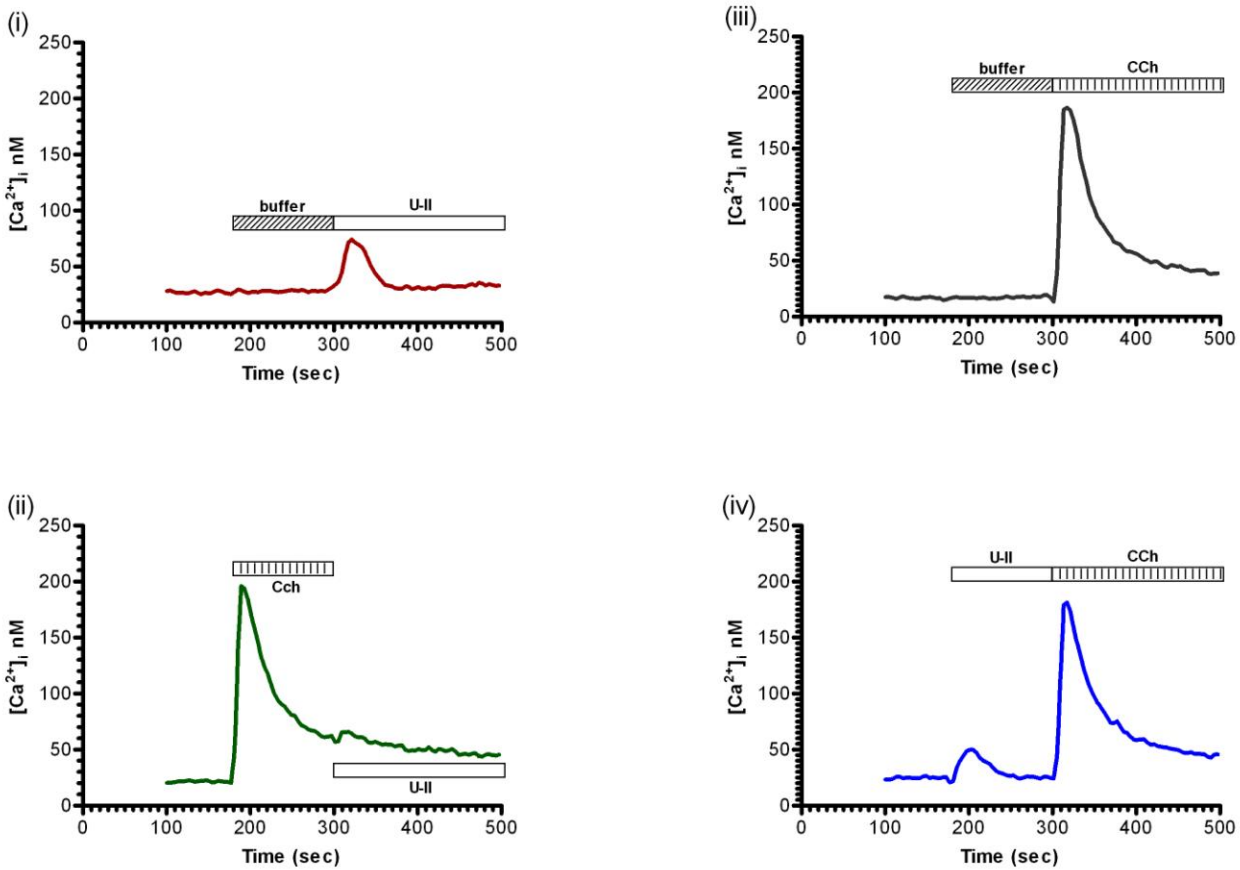


**Figure. 6.5. Representative graphs of effects elicited by double addition protocols in HEK293$_{hUT}$ cells at 25°C.**
*Top panels*: U-II (left) and Carbachol- Cch (right) responses (controls) after a vehicle challenge. *Bottom panels*: Secondary $Ca^{2+}$ response of U-II (left) and Cch (right) after a primary challenge of Cch and U-II respectively. The duration of exposure to buffer, U-II and Cch are indicated by the bars (n=4 of separate experiments).

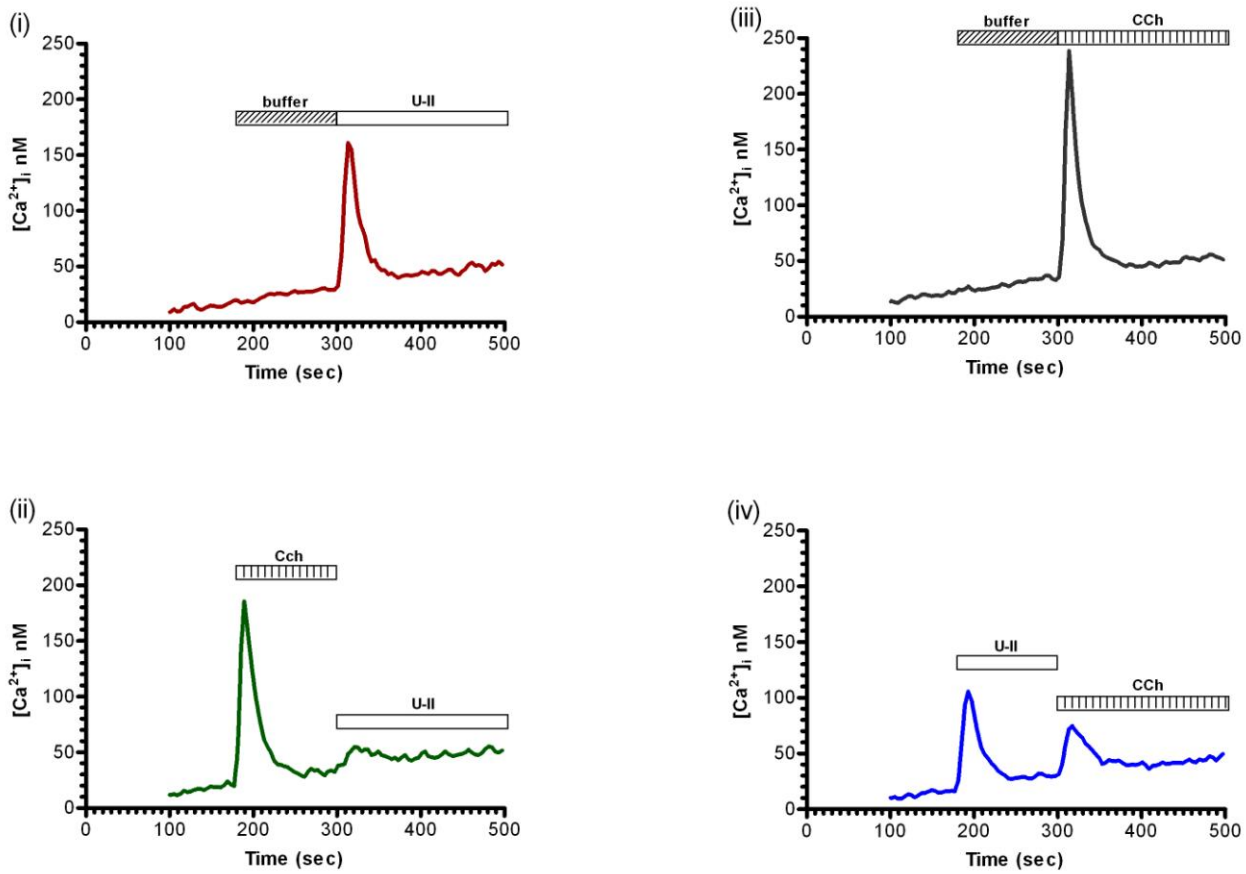


**Figure. 6.6. Representative graphs of effects elicited by double addition protocols in HEK293$_{hUT}$ cells at 37°C.**
*Top panels*: U-II (left) and Carbachol- Cch (right) responses (controls) after a vehicle challenge. *Bottom panels*: Secondary $Ca^{2+}$ response of U-II (left) and Cch (right) after a primary challenge of Cch and U-II respectively. The duration of exposure to buffer, U-II and Cch are indicated by the bars (n=4 of separate experiments).

| Temperature (°C) | U-II (control) response (nM) | Cch (control) response (nM) | Primary (Cch) response (nM) | Secondary (U-II) response (nM) | Primary (U-II) response (nM) | Secondary (Cch) response (nM) |
|---|---|---|---|---|---|---|
| 25 | 46±23 | 172±31 | 156±15 | 5±1 | 38±15 | 157±6 |
| 37 | 142±27* | 191±41 | 146±26 | 23±3*‡ | 113±25 | 45±7*‡ |

**Table. 6.3. Summary of the $Ca^{2+}$ response in $HEK293_{hUT}$ cells at 25 and 37°C.**
Statistically significant differences are indicated as * (25°C vs 37°C) and ‡ (control vs secondary response) where $p<0.05$. n=4 of separate experiments.

At 25°C the U-II evoked secondary response was attenuated by the primary Cch response. This secondary response was also lower than the U-II control. However based on student's t-tests this was not significant. The secondary muscarinic response was greater than the primary U-II response but was not different from its respective Cch control (Table. 6.3).

Under physiological (37°C) temperature the U-II secondary response was attenuated by the primary Cch response; furthermore this was lower than its respective U-II control. A reduction in the secondary Cch response was also observed after the primary U-II response. Statistically significant (temperature) differences were observed for the U-II controls, primary U-II and Cch responses (Table. 6.3).

*Effects in $CHO_{hUT}$ cells*

Under room temperature conditions following buffer additions U-II (1 μM) and ATP (10 μM) evoked $\Delta[Ca^{2+}]_i$ values of 302±60 and 58±31 nM (Figure 6.7 i and iii). In the double addition experiments a $\Delta[Ca^{2+}]_i$ of 86±32 and 423±88 was observed when ATP and U-II were applied as a primary challenge. On application of U-II and ATP as a secondary challenge the $\Delta[Ca^{2+}]_i$ were 473±134 and 36±9 nM respectively (Figure 6.7 ii and iv).

At 37°C after buffer applications U-II and ATP stimulation resulted in a $Ca^{2+}$ response of 966±108 nM and 356±39 nM respectively (Figure. 6.8 i and iii). During the double addition protocol ATP and U-II caused primary responses of 215±26 and 492±70 nM. The secondary response was characterised by $\Delta[Ca^{2+}]_i$ of 472±55 nM upon the addition of U-II however ATP failed to evoke a response.

At room temperature secondary response evoked by the U-II challenge was greater than the primary ATP challenge; however this was not statistically significant from the U-II control response. A reduction in the secondary ATP response was observed after the primary U-II exposure however it was not different from its control.

Under physiological temperatures the secondary response evoked by U-II application was elevated in comparison to the primary response evoked by ATP, furthermore the secondary U-II response was lower than its respective control. A substantial amount of Fura-2 leakage (increase in baseline) was observed at 37°C with respect to $CHO_{hUT}$ cells.

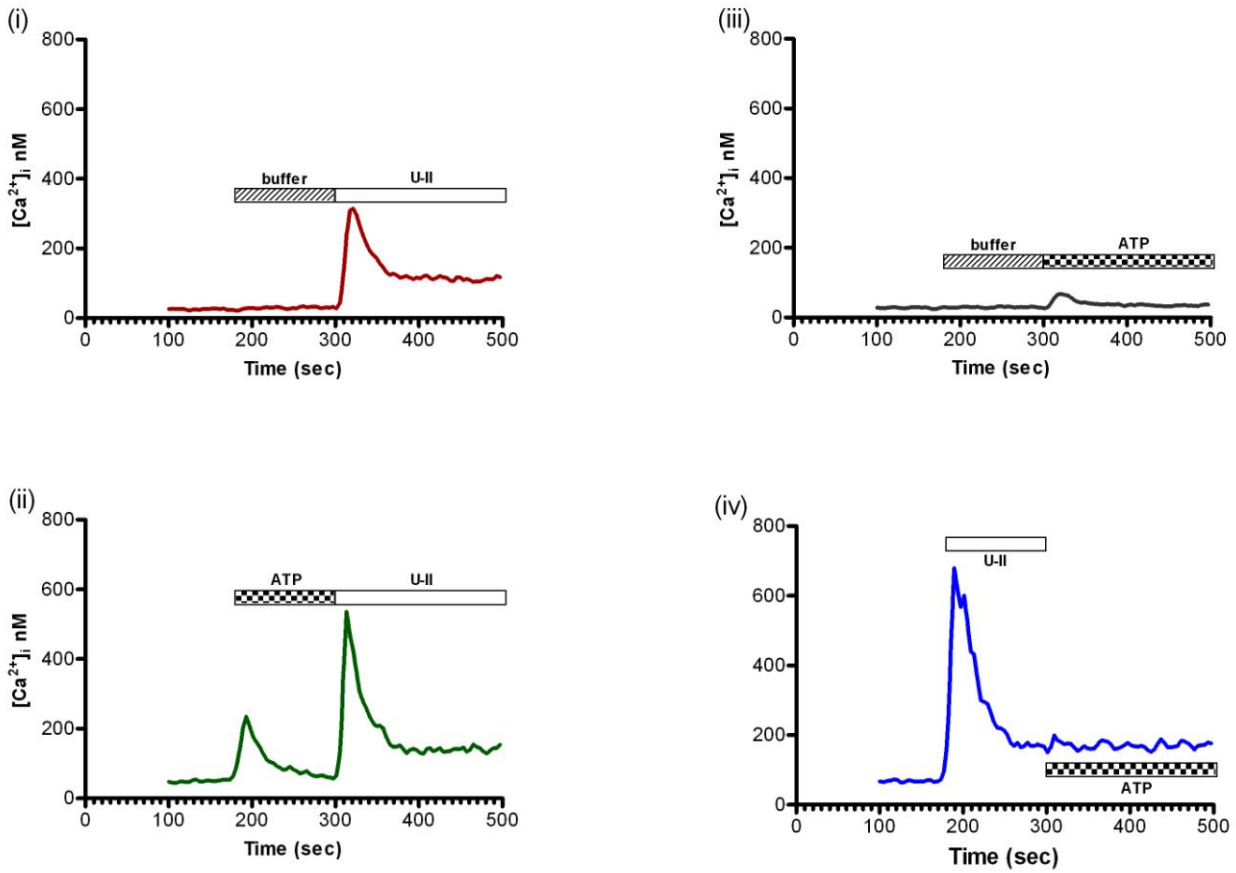


**Figure. 6.7. Representative graphs of effects elicited by double addition protocols in $CHO_{hUT}$ cells at 25°C.**
*Top panels*: U-II (left) and ATP (right) responses (controls) after a vehicle challenge. *Bottom panels*: Secondary $Ca^{2+}$ response of U-II (left) and ATP (right) after a primary challenge of ATP and U-II respectively. The duration of exposure to buffer, U-II and ATP are indicated by the bars (n=4 of separate experiments).

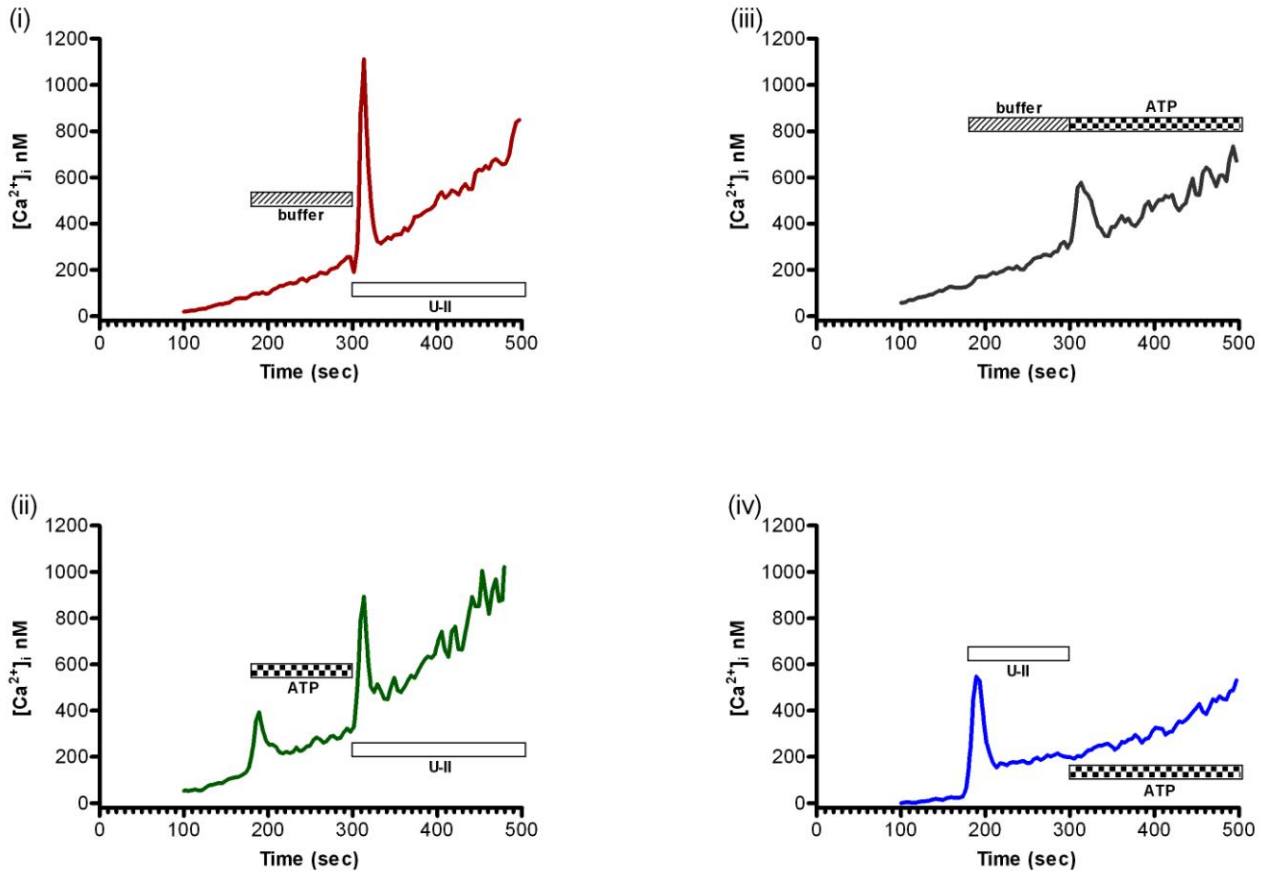


**Figure. 6.8. Representative graphs of effects elicited by double addition protocols in $CHO_{hUT}$ cells at 37°C.**
*Top panels*: U-II (left) and ATP (right) responses (controls) after a vehicle challenge. *Bottom panels*: Secondary $Ca^{2+}$ response of U-II (left) and ATP (right) after a primary challenge of ATP and U-II respectively. The duration of exposure to buffer, U-II and ATP are indicated by the bars (n=4 of separate experiments).

| Temperature (°C) | U-II (control) response (nM) | ATP (control) response (nM) | 1° (ATP) response (nM) | 2° (U-II) response (nM) | 1° (U-II) response (nM) | 2° (ATP) response (nM) |
|---|---|---|---|---|---|---|
| 25 | 302±60 | 58±31 | 86±32 | 473±134 | 423±88 | 36±9 |
| 37 | 966±108* | 356±39* | 215±26 | 472±55‡ | 492±70 | 0*‡ |

**Table. 6.4. Summary of the $Ca^{2+}$ response in $CHO_{hUT}$ cells at 25 and 37°C.**
Statistically significant differences are indicated as * (25°C vs 37°C) and ‡ (control vs secondary response) where *p<0.05*. n=4 of separate experiments.

The U-II (control) induced $\Delta[Ca^{2+}]_i$ at 37°C was significantly different to the corresponding value at 25°C (302 vs 966 nM), this was also the case for the ATP control (58 vs 356 nM). No changes were observed for the U-II 2◦ response at either temperature (473 vs 472 nM); however this was not the case for ATP – where at 37°C no response was observed compared to 25°C (0 vs 36 nM). At physiological temperature the secondary U-II response diminished by approximately 49% compared to its control while the secondary ATP response was absent and non-existent compared to its control (Table. 6.4).

### *6.4. Discussion*

In the present study conducted in cells expressing native human UT receptor (SJCRH30 cells) at room temperature (25°C) and physiological temperature (37°C) acute muscarinic stimulation does not appear to affect the U-II induced $Ca^{2+}$ response; furthermore acute urotensin stimulation does not appear to affect the secondary muscarinic response.

This also appears to be the case with respect to $HEK293_{hUT}$ cells at room temperature; however at physiological temperature the initial acute muscarinic stimulation has a detrimental effect on the U-II evoked response and U-II appears also to diminish Cch-inducible response. The phenomenon observed in $HEK293_{hUT}$ cells is suggestive of heterologous desensitisation by means of bidirectional control/cross talk.

At room temperature acute (primary) ATP stimulation does not attenuate the secondary U-II $Ca^{2+}$ response in $CHO_{hUT}$ cells; however a primary stimulus of U-II reduces the secondary ATP $Ca^{2+}$ response, this response is not significantly different to its corresponding control. Interestingly at physiological temperature, in $CHO_{hUT}$ cells acute ATP stimulation does not cause a reduction in the secondary U-II evoked response; however acute U-II stimulation does have a detrimental effect on the ATP $Ca^{2+}$ response which is indicated by complete absence of the secondary ATP evoked $Ca^{2+}$ response. The latter observation is indicative of heterologous desensitisation potentially via a unidirectional control pathway.

### 6.4.1. Bidirectional regulatory mechanisms

The assumption for a bidirectional control/cross-talk pathway existing in $HEK293_{hUT}$ cells is based on observations made in previous studies carried out by other groups. One such example is the Vasopressin receptor 1a expressed in HEK293 cells (Ancellin *et al.*, 1999). Here the authors assessed if there was a form of cross talk occurring between $M_3R$ and V1aR. Carbachol at 100 μM stimulated muscarinic acetylcholine receptors and was capable of reducing vasopressin (0.1 μM) evoked $Ca^{2+}$ responses by 46%. Furthermore vasopressin was capable of reducing the Cch induced muscarinic signalling by 77%. The investigators delineated the mechanism by which this desensitisation might be taking place. Initially measurements of cyclic AMP were made; as vasopressin could potentially stimulate V2 receptors coupled to adenylyl cyclase. Vasopressin had no effect on cAMP levels, therefore demonstrating the absence of V2a receptors. Forskolin however had a stimulatory effect on adenylyl cyclase to generate cAMP; the cAMP elevation had no effect on the vasopressin

induced $Ca^{2+}$ response compared to the control. This therefore meant that the desensitisation phenomenon observed with Cch is independent of cAMP activity. Test with 1 μM PMA (phorbol-12-myristate-13-acetate) – a PKC stimulant, resulted in a 55% reduction of the vasopressin induced $Ca^{2+}$ response compared to the control. This reduction was comparable to that observed after muscarinic stimulation; therefore demonstrating the potential involvement of PKC in the heterologous desensitisation of V1aR.

Bidirectional receptor control has also been demonstrated for the kappa (κ) opioid receptor (KOR) using two different functional assays; namely chemotactic assays and calcium assays in Jurkat cells and murine B-cells (Finley *et al.*, 2008).

In Jurkat cells overexpressing KOR (J-KOR cells) a concentration dependent increase in chemotaxis can be observed which peaks at 10 nM but is reduced at 100 nM with the agonist U50,488H; similarly the cells also responded to the CXCR4 receptor agonist CXCL12, where the peak was observed at 1 nM but was reduced at 10 nM. Pre-treatment of J-KOR cells with CXCL12 resulted in complete abrogation of the U50,488H induced chemotactic response. This could be reversed in the presence of the CXCR4 antagonist AMD3100. Conversely U50,488H pre-treatments also significantly reduced the ability of CXCR4 to evoke responses upon stimulation. Desensitisation in terms of the $Ca^{2+}$ response was also demonstrated in recombinant 300.19 murine B-cells expressing KOR and CXCR4 receptors. CXCL12 failed to evoke $Ca^{2+}$ response after acute pre-stimulation with the KOR agonist. U50,488H was tested at three different concentrations; 1000, 100 and 10 nM respectively. On this basis the KOR response decreased. At the high concentrations (1000 and 100 nM) CXCR4 was not active however when 10 nM U50,488H was used this

resulted in a CXCL12 evoked response. In this series of experiments the overall CXCL12 evoked response was significantly reduced in comparison to the control (minus KOR pre-stimulation). Acute stimulation with CXCL12 (100 ng/ml) did not affect the U50,488H (1000 and 100 nM respectively) response. However a reduction was observed upon 10 nM U50,488H stimulation. The reason for this response was apparently attributed to 10 nM representing a physiological relevant concentration according to the authors.

### 6.4.2. Unidirectional regulatory mechanisms

The existence of unidirectional cross talk mechanisms have been described in relation to receptors that include platelet activating factor receptor (PAFR), acetylcholine muscarinic receptors type 3 ($M_3R$) to name a couple of examples (Hosey, 1999).

Studies have shown PAFR is prone to heterologous desensitisation when chemoattractant receptors are stimulated by their respective ligands as characterised by reduced coupling of PAFR to G-proteins, cross-phosphorylation of PAFR and reduced $Ca^{2+}$ responses upon PAF stimulation. The phosphorylation of PAFR could be blocked with staurosporine (an inhibitor of PKC), therefore implicating a role for PKC in mediating phosphorylation. Mutants lacking the C-terminal tail were not phosphorylated. The C-terminal tail of GPCRs contains Ser and Thr residues which act as targets for PKC. While PAFR was desensitised by the activation of chemoattractant receptors, PAFR activation did not phosphorylate or desensitise the chemoattractant receptors, thus demonstrating a form of unidirectional control (Richardson *et al.*, 1996).

In a separate study (Willars *et al.*, 1999) have demonstrated activation of the bradykinin $B_2$ receptor ($B_2R$) leads to heterologous phosphorylation of muscarinic $M_3$ receptor ($M_3R$) but no functional desensitisation of the receptor. Stimulation of $M_3R$ receptors caused a reduction in phosphoinositide and $Ca^{2+}$ signalling of $B_2R$, but the $B_2R$ was not subject to heterologous phosphorylation. This therefore suggests receptor phosphorylation does not determine if a receptor should be desensitised and that control of receptor function could occur through alternate mechanisms.

This therefore presents the following questions: does the absence of purinergic signalling in $CHO_{hUT}$ after U-II pre-stimulation occur as a consequence of receptor phosphorylation or as a consequence of an alternative mechanism (e.g. depletion of intracellular stores)? The reason for suggesting the latter is due to observations made in SH-SY5Y cells; where pre-stimulation of cells with three increasing concentrations of carbachol results in a reduction in the $Ca^{2+}$ response to bradykinin (Willars *et al.*, 1995). This latter mechanism is also supported by the fact that at room temperature a small but noticeable purinergic signal (36 nM) is detected after a 423 nM response with U-II. So could the absence of a secondary ATP response be due to the initial release of $Ca^{2+}$ as a consequence of the supramaximal concentration of U-II?

Why would the hUT receptor not be prone to desensitisation in the face of purinergic stimulation? Is it possible that the concentration of ATP (10 μM) was insufficient to cause heterologous phosphorylation of hUT? Or is there an alternative explanation potentially involving intracellular $Ca^{2+}$ pools? What is interesting in relation to hUT signalling in CHO cells is that although purinergic $Ca^{2+}$ signal (215 nM) does not diminish the U-II driven $Ca^{2+}$ signal (472 nM), the latter is significantly reduced compared to the U-II control

(966 nM), this could be attributed to the fact that both UT and $P_2Y$ receptors share a common intracellular pool of $Ca^{2+}$. Therefore the secondary U-II stimulation although not affected by $P_2Y$ receptor activation is significantly lower than the U-II control.

The present study has attempted to demonstrate human UT receptor desensitisation mechanisms in native and recombinant models; to an extent this has been successful in that heterologous (bidirectional) desensitisation of both hUT and $M_3R$ has been demonstrated in $HEK293_{hUT}$ cells. On the other hand while hUT does not appear to desensitise after purinergic stimulation, $P_2Y$ receptors appear to be desensitised by the stimulation of hUT. Therefore a unidirectional mode of GPCR control has been observed.

One of the shortcomings of this experiment was the usage of a single dose to study desensitisation. This approach has only enabled the demonstration of an "effect". If one were to carry out a concentration response experiment then it would be possible to assess changes in efficacy and potency as a consequence of desensitisation.

Another important point to take into consideration is that in some cases the analysis of desensitisation should be studied in relation to the vantage point of the signalling cascade. For example desensitisation (in terms of $E_{max}$) may not be detectable in a downstream second messenger assays, however an upstream assay such as GTPγ[$^{35}$S] may demonstrate a better profile of desensitisation. This has been demonstrated with regard to the human NOP receptor which undergoes desensitisation when preatreated with the agonist N/OFQ. In cAMP inhibition assays no changes in $E_{max}$ were observed in the control vs treated groups; however differences were noted in potency. The results from the upstream GTPγ[$^{35}$S] demonstrated a reduction in $E_{max}$ as well as potency (Barnes *et al.*, 2007).

A suitable starting point would be to determine assessing phosphorylation status of hUT (homologously and heterologously); this should be accompanied by PI turnover assays as a well as $Ca^{2+}$ assays to correlate if the hUT receptor is subject to desensitisation. A reversible agonist is essential.

## 7. Genomic desensitisation

### *7.1. Introduction*

While desensitisation can cause loss of receptor function, as demonstrated in the previous chapter, receptor expression can also be modulated genomically, i.e. at the messenger RNA (mRNA) level. Messenger RNA is subjected to regular turnover – the rate of which varies in cells. Furthermore mRNA levels in cells can be regulated on the basis of 1) stability of mRNA and 2) rate of mRNA synthesis or gene transcription (Iredale, 1997) 3) miRNA (Moss, 2002).

While it is generally perceived that mRNA is unstable, this is not completely correct. Eukaryotic mRNA is relatively stable; though highly labile compared to DNA. Its stable conformation is conferred by the terminal structure; m7GpppN cap and poly(A) tail located at the 5' and 3' ends respectively which protect the mRNA from exonuclease attack (Meyer *et al.*, 2004). Control of gene expression by miRNA has been a relatively recent discovery; initial work carried out in *C.elegans* led to the identification of the first non-mammalian miRNA by two independent groups (Chalfie *et al.*, 1981) (Reinhart *et al.*, 2000). This seminal research has since paved the way for the discovery of many mammalian miRNAs over the last two decades. For further information on miRNA the reader is directed to the review by (Boyd, 2008).

### *7.2. Aims*

Studies have shown that treatment of cells with an agonist can result in reduction of receptor mRNA. For example treatment of human breast cancer MCF-7 cells with morphine, endormorphine-1 and 2 treatment results in a reduction mu opioid receptor mRNA (Gach *et al.*, 2008). With this in mind the effects of U-II treatments on SJCRH30 rhabdomyosarcoma cells expressing native human UT and donor peripheral blood mononuclear cells (PBMCs) were assessed. PBMCs are comprised of four types of cells; monocytes, NK cells, T and B lymphocytes. The latter (B lymphocytes) were used in previous studies where functional hUT expression has been demonstrated, furthermore mRNA was elevated upon stimulation with lipopolysaccharide (Segain *et al.*, 2007). In addition to using native systems to study human UT expression, the effects of U-II treatment on hUT expression in recombinant systems ($HEK293_{hUT}$ and $CHO_{hUT}$) was also assessed in the present study.

### *7.3. Results*

#### 7.3.1. U-II treatments in SJCRH30 cells

Treatment (1μM U-II) studies were conducted at three separate time intervals; namely 6, 24 and 48 hr. These treatments were paired with vehicle treatments which served as the control group. As shown in Figure. 7.1, under control conditions, with basal U-II expression set to 1.00, a reduction in UT expression was observed after 6 hr treatments (0.87±0.02) which was significantly different compared to the control. Treatments at 24 hr and 48 hr had no

effect on UT expression compared to the control where relative expression was 1.07±0.07 and 1.08±0.05 respectively.

### 7.3.2. U-II treatments in HEK293 and CHO cells

The relative expression of human UT in the recombinant cell lines $HEK293_{hUT}$ and $CHO_{hUT}$ were increased after U-II treatments compared to the vehicle control (1.50±0.07 and 1.63±0.02 respectively) as shown in Figures. 7.2 and 7.3. Six hr treatments were carried out with these cells on the basis of the initial findings in SJCRH30.

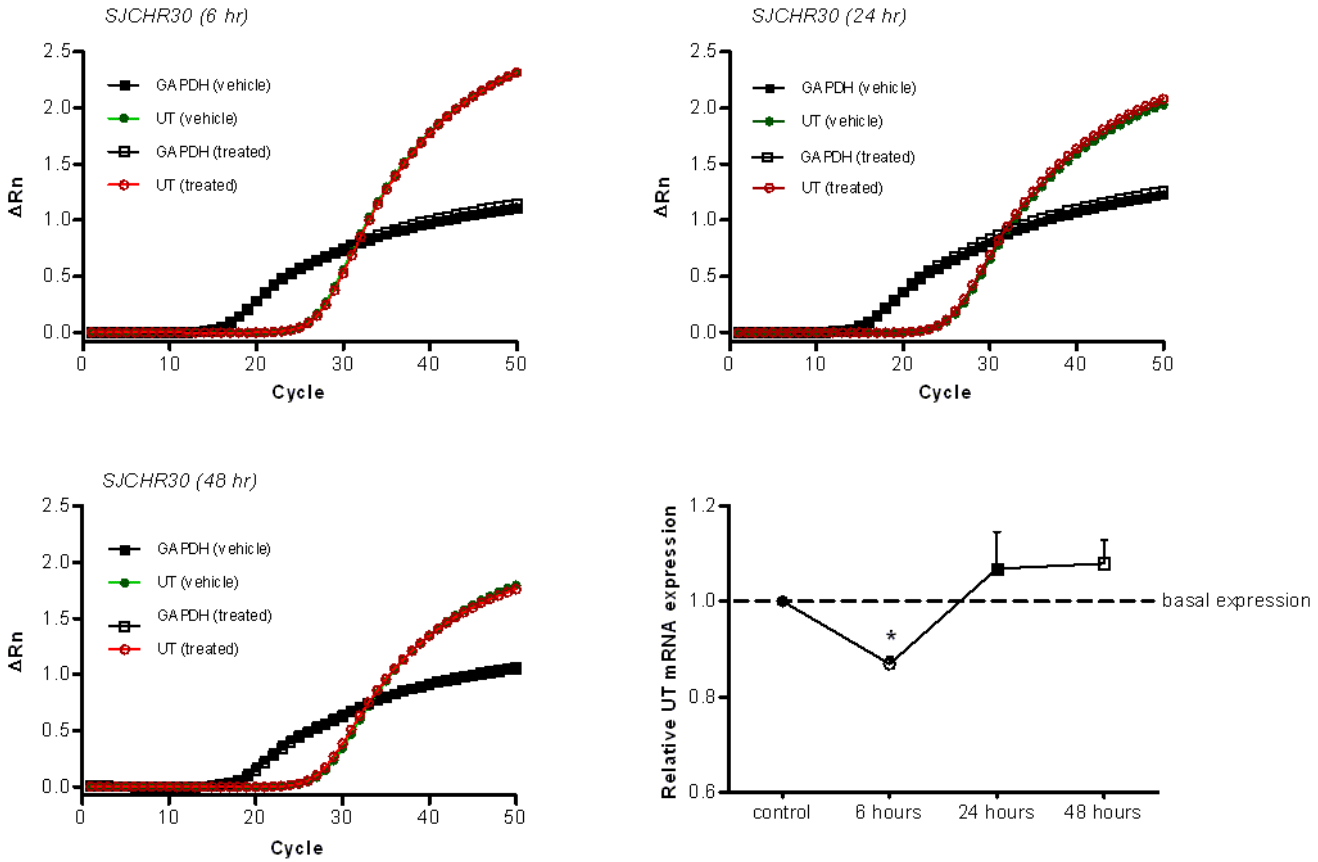


**Figure. 7.1. Human UT receptor expression in SJCRH30 cells.**
Representative amplification plots are illustrated in relation to the three different time-courses studied. An increase in UT mRNA is indicative of a shift of the treated (1 μM U-II) amplification curve to the left of the vehicle group (hence lower cycle number), while a decrease in mRNA is noted by a shift of the treated (1 μM U-II) group to the right of the vehicle group (higher cycle number). Relative expression of UT receptor are illustrated, where basal UT expression is indicated by the dashed line. Relative UT mRNA expression was calculated by the $2^{-\Delta\Delta Ct}$ method. Data are the mean± SEM where $n \geq 3$ performed in triplicate. Statistically significant differences are indicated by * $p < 0.05$ based on student's t-test.

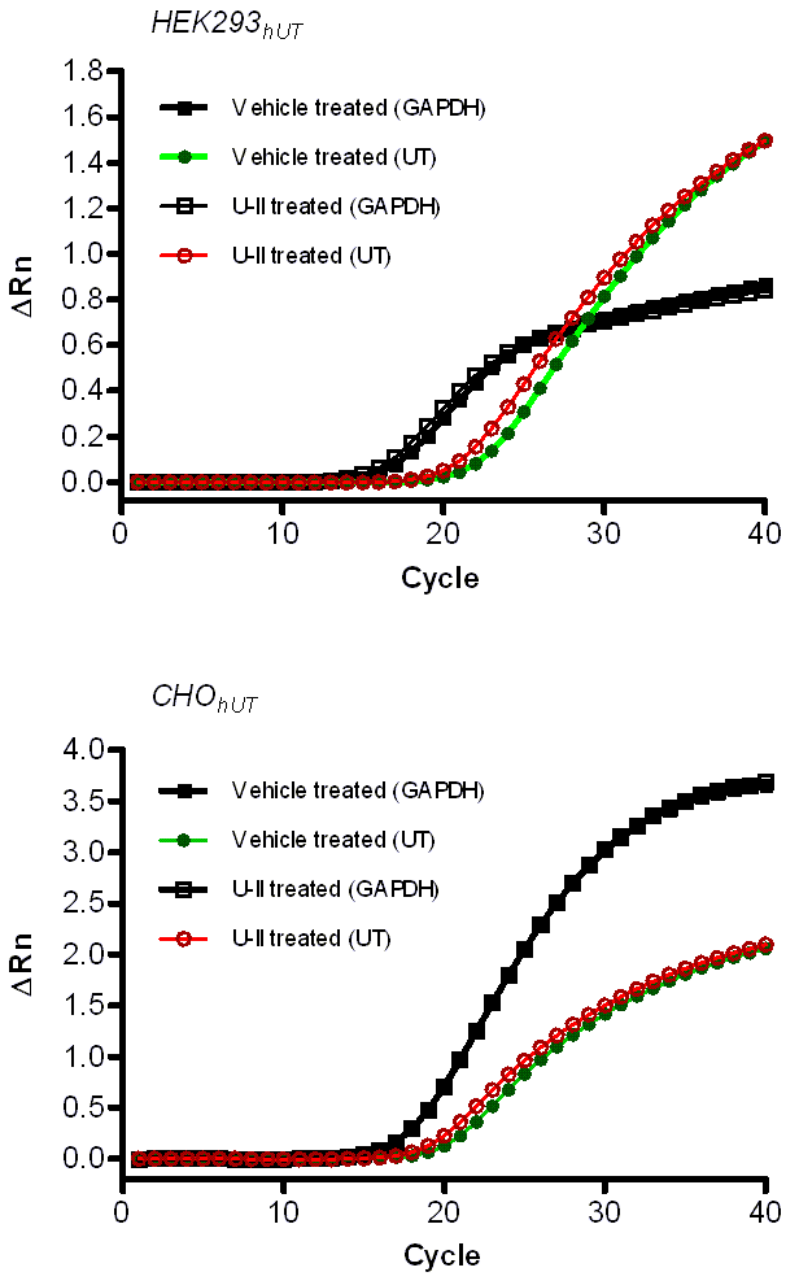


**Figure. 7.2. Representative qPCR amplification plot for HEK293$_{hUT}$ cells and CHO$_{hUT}$ cells.**
After 6 hr U-II (1 μM) treatment. An increase in UT mRNA is indicated by a shift of the treated amplification curve to the left of the control group (hence lower cycle number). Representatives of n≥3 performed in triplicate.

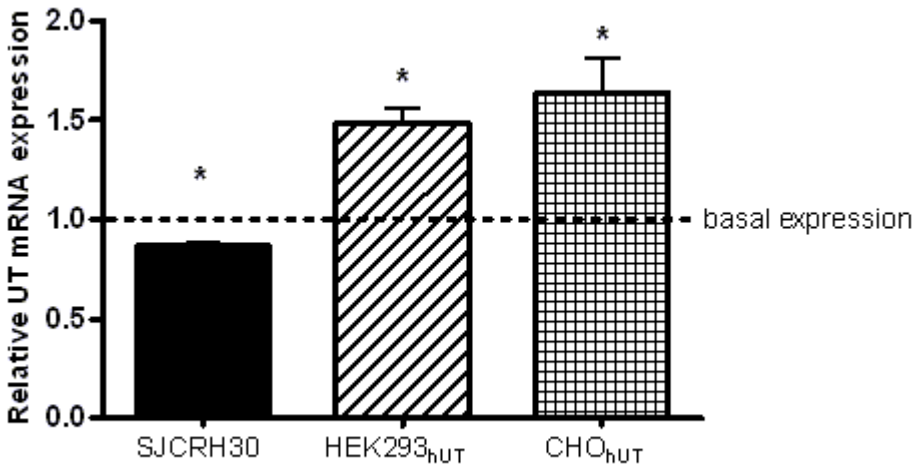


**Figure. 7.3. Relative UT mRNA expression in SJCRH30, HEK293$_{hUT}$ and CHO$_{hUT}$ after 6 hr U-II (1 μM) treatment.**
Relative UT mRNA expression was calculated by the $2^{-\Delta\Delta Ct}$ method. Data are the mean± SEM where n≥3 performed in triplicate. Statistically significant differences compared to basal UT expression are indicated by * *p<0.05* based on student's t-tests of raw data.

### 7.3.3. Effects of U-II and LPS on human UT receptor expression

The overall treatment time for the studies conducted with donor PBMCs was 21 hr. This time period was used as 18 hr LPS treatments were capable of upregulating hUT expression in donor monocytes (Segain *et al.*, 2007).

In studies assessing U-II treatments on UT mRNA, donor PBMCs were split into two batches. They were initially treated with vehicle for 15 hrs. Thereafter one batch was treated with further vehicle for 6 hrs while the other was treated with U-II (1 μM) for 6 hrs. The relative UT mRNA expression compared to the control (1.00) was 1.15± 0.13 and was not significantly different (Figure. 7.4 top left and right panel). LPS treatment (2 μg/ml) for 21 hrs caused a significant increase in UT mRNA relative to the control; where relative UT expression was 4.00±0.86 (Figure. 7.4 middle left and right panel). Thereafter the effects of 1 μM U-II treatment on 2 μg/ml LPS stimulated PBMCs was assessed. In this experimental

paradigm PBMCs were split into two batches. One batch was treated with only LPS (21 hrs) and served as a control whilst the other was initially treated with LPS for 15 hrs and then exposed to U-II (1 μM) (6 hrs) on top of the initial LPS challenge. LPS treatment was consistent between both groups. U-II caused a reduction in the UT mRNA levels (1.33±0.33) compared to the LPS control, and this reduction was statistically significant (Figure. 7.4 bottom left and right panel).

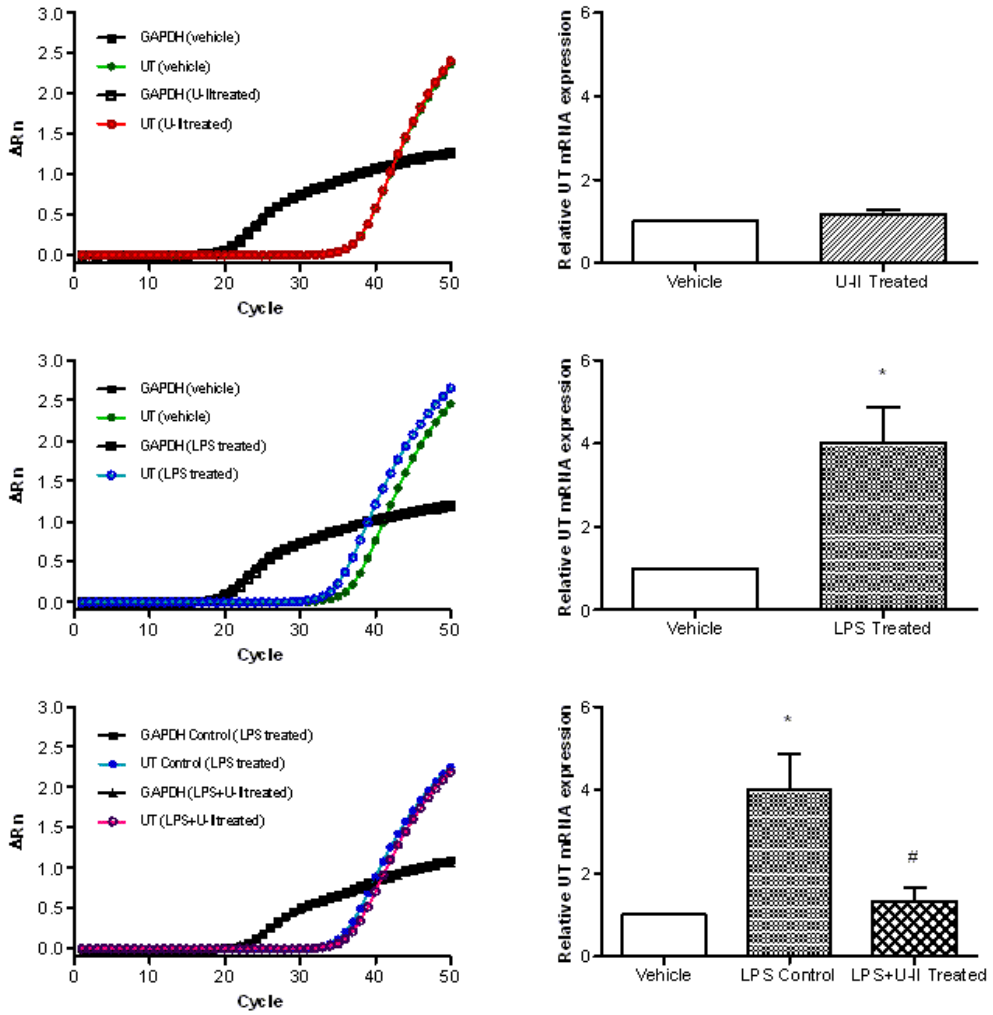


**Figure. 7.4. Effects of U-II (1 μM) and LPS (2 μg/μl) treatments on PBMCs.**
Left panels are representative amplification plots. Right panels are summary of effects after different treatment conditions as indicated in the figure. Data are mean± SEM where n=5 performed in triplicate. Statistically significant data are indicated by * (vehicle vs LPS treated/control) and # (LPS control vs LPS+U-II treated). $p<0.05$ based on the student's t-tests, one way ANOVA and Tukey tests.

### *7.4. Discussion*

GPCRs expressed within the cardiovascular system are subject to desensitisation upon stimulation by physiological or pharmacological stimuli or both. Desensitisation serves as a process that can precisely regulate cell function by termination of signal transduction pathways. This phenomenon is not restricted to one biological system but pervades through all biological systems (Bunemann *et al.*, 1999).

In the current study native human UT mRNA in SJCRH30 was reduced after short-term stimulation with U-II for 6 hr and demonstrated homologous genomic desensitisation. This process was not observed after 24 and 48 hr U-II treatments, where UT mRNA expression recovered back to a basal state.

Studies in intact C6 glioma and WEHI 7 cells have demonstrated a reduction in plasma membrane beta-adrenergic (β-AR) receptor density by approximately 40% upon stimulation with isoproterenol and assaying with a radiolabelled ligand. This reduction was dependent on the assay being carried out at non physiological temperatures <37°C. At normal physiological temperature no reduction in plasma membrane receptor was observed. The onset of 40% receptor reduction occurred within 15 and 3 min of agonist exposure in the respective cell lines which could be recovered upon washing the cells (Staehelin *et al.*, 1982).

According to the classical model of GPCR regulation by GRKs and arrestins; upon agonist stimulation of the target receptor, heterotrimeric G proteins separate and this leads to downstream signalling activation. Thereafter the agonist occupied GPCR is phosphorylated

by GRK thus facilitating its interaction with arrestins and causing desensitisation. The desensitised receptor then is internalised through endocytosis into clathrin coated pits and transferred to endosomal vesicles where the phosphorylated agonist receptor undergoes dephosphorylation; a process that involves endosome associated phosphatases. Once this has taken place the dephosphorylated receptor is recycled to the plasma membrane in its resensitised form to be stimulated by agonist again (von Zastrow, 2003) (Kelly *et al.*, 2008). The fate of the agonist bound receptor is determined by the subtype of β-arrestin. Class A GPCRs include the β2-AR, mu (μ) opioid receptor (MOP) and endothelin (ET) A receptor. These receptors bind transiently to β-arrestin 2 with higher affinity than β -arrestin 1. Both these arrestins are non-visual and therefore are associated with non-visual GPCRs. Conversely class B GPCRs (e.g. neurokinin NK1 receptor, vasopressin 2 receptor and angiotensin AT1a receptor) bind to visual arrestins as well as non-visual arrestins with equal affinity. Class A GPCRs undergo rapid resensitisation as is the case with β2-AR while slow resensitisation (vasopressin 2 receptor) or even degradation is observed with class B receptors (i.e. AT1a receptor) (Luttrell *et al.*, 2002).

Unlike isoproterenol which can be washed off the β-AR, U-II binds irreversibly to UT therefore hampering binding studies to determine receptor densities in intact cells. At present the complement of GRKs and arrestins in SJCRH30 are not known. Human UT contains several conserved amino acid residues and motifs that are found in class A GPCRs (Proulx *et al.*, 2008); therefore it is reasonable to suggest that the homologous genomic desensitisation and resensitisation observed could be related to what is observed with β2-AR. Apart from GRKs, there is also another potential candidate that may fullfil a role

similar to GRKs. Originally referred to as muscarinic receptor kinase due to its actions on $M_3$ receptors, this kinase has been identified as casein kinase 1$\alpha$ (CK1$\alpha$). It is capable of phosphorylating agonist occupied $M_3$ receptors as well as Rhodopsin (Tobin *et al.*, 1997).

The recycling and resensitisation observed post 6 hr U-II treatments could be assessed further by using monensin (a monocarboxylic acid cation ionophore) or cycloheximide; both these drugs have shown to be effective in preventing GPCR recycling and de-novo protein synthesis (Benya *et al.*, 1994).

### 7.4.1. The putative role of hCMV promoter in hUT transcriptional control

An upregulation of recombinant hUT mRNA was observed in HEK293 and CHO cells after a 6 hr U-II treatment. Both $HEK293_{hUT}$ and $CHO_{hUT}$ cells were established by insertion of hUT DNA into a vector driven by the human cytomegalovirus (hCMV) promoter (Ames *et al.*, 1999); (Brkovic *et al.*, 2003). It is important to note the presence of response elements in native receptor systems. These components are associated with regulating receptor gene expression. The addition of drugs into native systems therefore can result in positive and negative effects on the functional aspects of response elements. In recombinant systems such as HEK293 and CHO there is an absence of response elements hence it is likely that receptor gene expression is modulated by alternative mechanisms.

Activation of the hCMV promoter and hCMV replication is dependent on the immediate/early (IE) genes p72 and p86 – both transcription factors which form sequence specific DNA binding and activator domains. This hCMV-IE promoter is under further regulation by an enhancer which is required for RNA polymerase-II directed transcription

(Fortunato *et al.*, 1999). The IE hCMV promoter/enhancer complex contains binding sites for CREB/ATF, AP-1 and also NF-κB/rel (Sun *et al.*, 2001) (Sambucetti *et al.*, 1989).

The CMV promoter is routinely used in expression studies of transgenes. In studies with NIH 3T3 cells the CMV promoter activity was demonstrated to be sensitive to external environmental stress, which in turn increased activity of the promoter. Exposure of these cells to a sublethal (50 μM) dose of sodium arsenite induced increased levels of heat/shock proteins HSP27 and HSP70. Lower concentrations of arsenite failed to induce any protein expression. The elevation of mitogen-activated protein kinase kinase 1 (MEKK1) due to arsenite exposure was also demonstrated using β-galactosidase assays. Furthermore MEKK1 activity was dependent on downstream activation of MAPK pathways, as demonstrated by elevated JNK in Northern blots. The authors suggested that MAPK was responsible for elevating CMV promoter activity and an increase in transgene expression and advised caution when using such a promoter (Bruening *et al.*, 1998).

In separate studies conducted by Sun and co-workers (Sun *et al.*, 2001) IE-hCMV promoter activity based on luciferase reporter assays was elevated as a consequence of over-expression of MEKK1. Over expression of other kinases was achieved by mutating the WT DNA into constitutively active mutants and expressing these in CHO-K1 and HEK293 cells.

Over expression of constitutively active MEKK1-TRU in CHO-K1 and HEK293 cells has caused elevated IE-hCMV promoter activity by approximately 9 fold (based on luciferase assays), while a 6 fold increase in activity was observed with constitutively active MEK1. Other kinases assessed which included MEK3, MEK4 and MEK7 did not induce any effects. In a separate set of experiments where MEKK1-TRU was co-expressed with JNK1, Erk2 or p38 repression of promoter activity was observed, therefore contradicting the previous findings of (Bruening *et al.*, 1998). This is no surprise; especially since sodium arsenite acts as an activator of JNK and p38 (Suzuki *et al.*, 2006).

Previous studies have shown MEKK1 to activate NF-κB and IKK (Schlesinger *et al.*, 1998). Details pertaining to NF-κB and its activation and signalling are discussed later on in this chapter. Over-expression of IκBα results in a 65-75% reduction in IE-hCMV promoter activity stimulated by MEKK1-TRU. Furthermore deletion of the NF-κB/rel sites had a detrimental effect on the promoter activity therefore highlighting the importance of NFκ-B/rel in modulating CMV promoter activity (Sun *et al.*, 2001).

Studies conducted in isolated VSMCs from rat aorta have shown increase in cell proliferation as a consequence of synergistic activity between U-II and mildly oxidising LDL (moxLDL). This synergistic effect was reduced in the presence of the MAP kinase inhibitor PD098059, therefore demonstrating a role for MAP kinase maintaining cell proliferation (Watanabe *et al.*, 2001b). U-II is capable of causing increased hypertrophy of neonatal rat cardiomyocytes as a consequence of MAP kinase signalling activation; in particular Erk1/2 and p38 but not JNK (Onan *et al.*, 2004b). U-II additionally causes proliferation of rat adventitial fibroblasts as demonstrated in [$^{3}$H]-thymidine incorporation

experiments. The proliferative effects of U-II were inhibited by PD098059 (Zhang *et al.*, 2008).

Based on the information discussed so far; elevated UT expression in the recombinant cells lines HEK293 and CHO could result as a consequence of activation of MAP Kinase signalling pathways or in combination with the NFκ-B/rel pathway; which in turn have a positive effect on the CMV promoter that drives transcription of UT. The latter pathway could be activated through a combination of MAP kinase activity and reactive oxygen oxygen species (ROS); especially since U-II is capable of generating ROS through the activation of NADPH oxidase (p22phox/NOX4). U-II dependent activation of the phosphorylation of MAP kinase members (erk1/2, p38, JNK) is also dependent on NADPH oxidase activity. This can be inhibited by the flavin inhibitor DPI and also knocking out NADPH oxidase. U-II also increases expression of PAI-1 a component of the extracellular matrix which can be blocked by inhibiting MAP Kinase members (Djordjevic *et al.*, 2005). U-II induced elevation in ROS has been demonstrated in rat cardiac fibroblasts (Chen *et al.*, 2008). Furthermore NFκ-B can be stimulated by oxidative stress as well as a plethora of other insults (Pahl, 1999).

If indeed MAP kinases are involved in CMV promoter driven UT upregulation in the cell lines tested, the involvement of NFκ-B could be assessed by stimulating the system with hydrogen peroxides (which generates ROS).

What is the mechanism for enhanced CMV promoter activity? Could U-II initiate ROS/MAPK generation and this in turn act on the CMV promoter activity? Could ROS be acting on NFκ-B? Further studies would be warranted to assess which MAP Kinase signalling members are present. Furthermore inhibition studies could also be carried out using drugs such as PD098059 in the presence of U-II. It would also be necessary to determine the UT mRNA status after 24 and 48 hr incubation as this is at present unknown. As UT mRNA is upregulated in CHO and HEK cells as a consequence of U-II exposure could this mRNA upregulation be reversed by a UT antagonist? A hypothetical mechanism for recombinant cell lines is illustrated in Figure. 7.5 based on what has been discussed above.

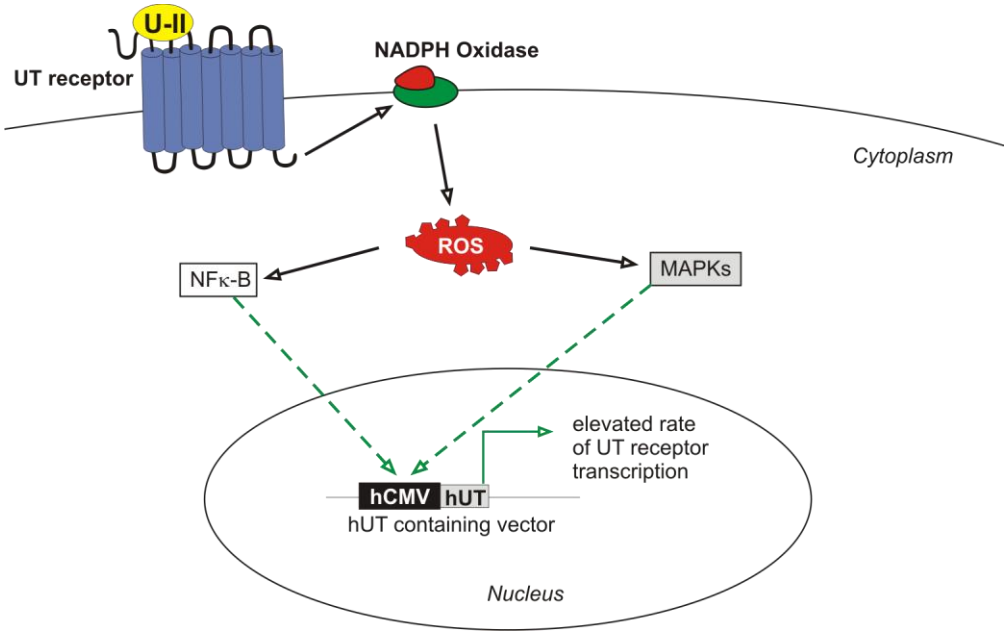


**Figure. 7.5. Hypothetical pathway for UT mRNA elevation in recombinant cell lines (HEK293$_{hUT}$ and CHO$_{hUT}$).**
UT stimulation by U-II results in the activation of NADPH oxidase, leading to the generation of reactive oxygen species (ROS) and the activation of mitogen activation protein kinases (MAPKs) pathway and/or NFκ-B signalling. These two components in turn may act upon the hCMV promoter thereby elevating hUT mRNA transcription rate.

### 7.4.2. The NFκ-B pathway in hUT receptor transcription

The paucity of cell lines expressing native human UT poses a problem when studying U-II/UT signalling. At present SJCRH30 cells appear to be the only well characterised native human receptor cell line. Recently studies carried out in PBMCs from human donors have demonstrated UT mRNA expression along with functional UT. UT receptor mRNA was upregulated when stimulated with a number of inflammatory stimulators (Segain *et al.*, 2007). With this in mind, a set of experiments were undertaken to study the expression of UT mRNA in relation to U-II treatments before and after exposure to LPS.

U-II applications over a 6 hr time period did not have an effect on UT mRNA expression, however LPS alone induced a 4 fold increase in UT expression which was reduced when stimulated with U-II therefore demonstrating genomic homologous desensitisation in this model and this reduction is in general agreement with data in SJCRH30 cells.

The actions of LPS are induced through Toll like receptors (TLRs), in particular TLR-4. These receptors are key players associated with immune defence mechanisms and therefore have an important role in establishing adaptive immune responses against numerous infectious pathogens. Their role has been highlighted in relation to conditions such as atherosclerosis, autoimmune disorders and sepsis. All TLR dependent immune responses rely on NF-κB activation (Carmody *et al.*, 2007).

The NFκ-B family of transcription factors comprises of NFκ-B1 (p50 and p105 its precursor), NFκ-B2 (p52 and its precursor p100), RelA (p65), RelB and c-Rel. The

TLR/NFκ-B signalling pathway is illustrated in Figure. 7.6. Under unstimulated (inactive) conditions, NFκ-B exists as homo- and heterodimers within the cytoplasm of the cell. The inactive state is conferred by the inhibitory IκB proteins which form a complex. TLR stimulation culminates in recruitment of the adapter complex TIR-containing adapter protein/myeloid differentiation primary response gene (TIRAP/MyD88), which in turn recruits Interleukin-1 receptor associated kinases (IRAKs). IRAKs interact with Tissue necrosis factor receptor associated factor (TRAF6), which undergoes ubiqutination and recruits Transforming growth factor β- activated kinase 1 (TAK1). Activation of TAK1 is the rate limiting step for the activation of the IKK/NEMO complex which is required for activating the NFκ-B/IκB complex as well as the MAPK signalling pathway. Activated NFκ-B and MAPK signalling members are then able to participate in nuclear processes (Kawai *et al.*, 2007).

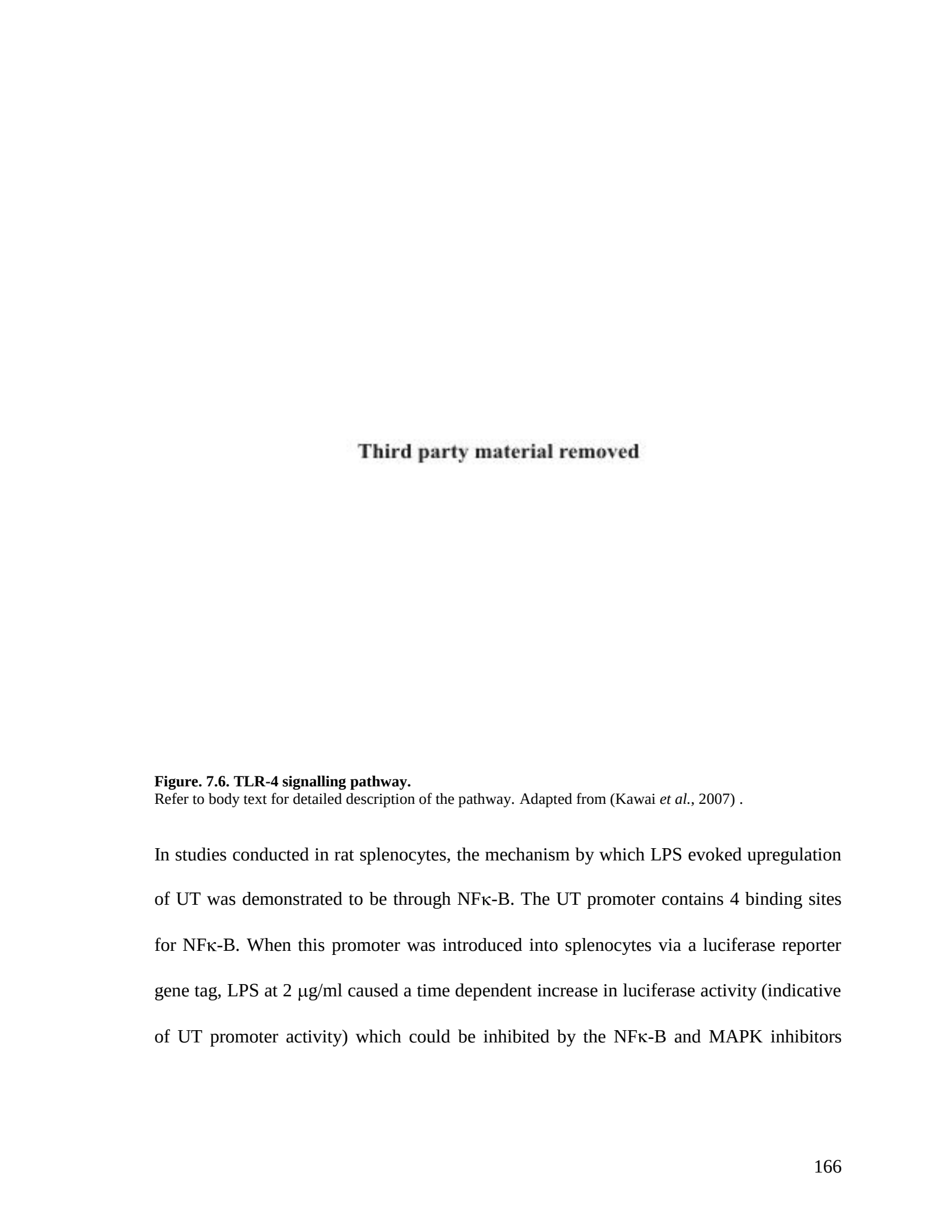


**Figure. 7.6. TLR-4 signalling pathway.**
Refer to body text for detailed description of the pathway. Adapted from (Kawai *et al.*, 2007) .

In studies conducted in rat splenocytes, the mechanism by which LPS evoked upregulation of UT was demonstrated to be through NFκ-B. The UT promoter contains 4 binding sites for NFκ-B. When this promoter was introduced into splenocytes via a luciferase reporter gene tag, LPS at 2 μg/ml caused a time dependent increase in luciferase activity (indicative of UT promoter activity) which could be inhibited by the NFκ-B and MAPK inhibitors

CAPE and U0126. In another set of experiments, mutations of the four NFκ-B binding sites led to the identification of the crucial binding site required for UT promoter activity.

The UT promoter also contains additional binding sites for AP-1, 2 and 4, CRE, Egr, Elk1, GATA and RasREBP1 (Segain *et al.*, 2007). The importance of these sites in relation to U-II/UT signalling is at present unknown. It would be very interesting to assess their functions within the UT promoter.

The control of gene expression can occur at seven different regulatory levels; these are 1) chromatin structure 2) transcription initiation 3) transcription processing 4) mRNA translocation 5) transcript stability 6) translation initiation and 7) post translational modification. Over the last 20 years with the discovery of micro RNA (miRNA) this means now that there is an additional mechanism known to modulate gene expression (Catalucci *et al.*, 2008). These regulatory molecules are widely expressed in every cell of an organism; however their expression can also be tissue specific. For example one particular miRNA may be found in one cell abundantly; but maybe absent in another cell type. In rat hearts abundant expression of mIR-1, let-7,miR-23, miR26a, miR30c, miR126 and miR130 can be observed. Conversely in rat artery these miRNAs are poorly expressed or absent (Zhang, 2008).

miRNAs play an important role in health and disease. In the cardiovascular system miR-1 is required for cardiomyocyte differentiation (Zhang, 2008). Conversely over expression of miR-23a, miR-23b, miR-24, miR-195 or miR-214 causes hypertrophic growth of cultured cardiomyocytes whilst over-expression of miR-199a causes pronounced morphological

changes to cultured cells (van Rooij *et al.*, 2006). The machinery required to translocate miRNA from the nucleus to the cytoplasms is also important, e.g. mice lacking the endoribonuclease Dicer are incapable of forming blood vessels (Yang *et al.*, 2005) therefore demonstrating the importance of miRNA in angiogenesis. Northern blot analysis has shown aberrant over-expression of miRNAs in end-stage heart failure compared to control hearts (van Rooij *et al.*, 2006). Given that miRNA have a role to play in health and disease; it is very likely that the UT receptor expression (and molecules associated with its expression) may also be modulated by a set of miRNAs; though the identity of these remains elusive at present.

### *7.5. Conclusion*

In summary the present set of experiments demonstrate:

1) Genomic desensitisation of native hUT mRNA during 6 hr U-II treatments and recovery of UT mRNA post 6 hr treatment.

2) Increased UT mRNA expression during 6 hr U-II treatment in recombinant systems could be attributed to increased CMV promoter activity which could be increased by U-II driven signalling via ROS, MAP kinase/NFκ-B/rel cross talk.

3) LPS inducible UT mRNA upregulation was reduced by the addition of U-II, therefore demonstrating homologous genomic desensitisation similar to SJCRH30 cells.

One major drawback in these studies was that only the message of RNA was measured. Further studies on active receptors are required. Irreversibility of binding of the desensitizing stimulus precludes determination of changes in receptor density to corroborate changes in mRNA.

# 8. General Discussion

## *8.1. Summary of findings*

### 8.1.1. Model validation and characterisation of urantide and UFP-803

The HEK293 and CHO cell lines expressing recombinant human UT may be used as models for studying U-II/UT signalling on the basis that both the cells lines express appreciable numbers of receptors that are functionally coupled to appropriate second messenger signalling pathways ($IP_3$ and $Ca^{2+}$). The SJCRH30 cell line expressing native human UT expresses easily measurable receptor numbers; however there is no measurable coupling to PI turnover. However a robust population $Ca^{2+}$ mobilisation response can be measured that varies from cell to cell. The likely reason for not detecting PI with these cells may be due to low sensitivity of the PI assay as a consequence of low receptor density in the cells.

The two compounds urantide and UFP-803 (previously reported to be antagonist within rat aorta) exhibited some agonist activity with a potency and efficacy profile in the order of U-II> urantide> UFP-803 in $HEK293_{hUT}$ and $CHO_{hUT}$ cells based on PIT assays. As both these compounds demonstrate agonist activity in one or more assay type (PI turnover and $Ca^{2+}$) their pharmacological profile as partial agonists should be re-considered.

### 8.1.2. SARs with novel U-II analogues

Although the initial hope was to obtain a reversible U-II agonist, this was not realised. However in the SAR studies conducted in our collaborators' laboratories in Italy, we have identified and characterised a novel partial agonist modified at $Tyr^9$ of the U-II(4-11) template. Based on the assays conducted, this compound appears to be a partial agonist at the rat UT receptor; however on the human receptor it appears to have a full agonist profile. This could be due to the receptor density of UT in $HEK293_{hUT}$ being greater than $HEK293_{rUT}$ cells, and also as it is in a human host cell background instead of a rodent host cell.

### 8.1.3. Functional desensitisation

By utilising previously published methodologies functional desensitisation of human UT receptor has been demonstrated in the present study via calcium mobilisation assays. This is the first study showing functional desensitisation of hUT receptor in HEK293 and CHO cells with this assay. The process appears to be dependent on temperature; where the process can be observed only when the assays were conducted at physiological temperature but not at ambient room temperature. Functional desensitisation was not demonstrated in SJCRH30. Why this might be the case in the native hUT cell line is unclear at present. Based on the experimental protocol used, the type of desensitisation observed in the present study is of a heterologous nature; i.e. in $HEK293_{hUT}$ cells acute muscarinic stimulation dimished U-II inducible $Ca^{2+}$ signalling and vice versa, while in $CHO_{hUT}$ cells acute urotensin stimulation had a negative effect on ATP evoked $Ca^{2+}$ mobilisation and ATP stimulation had no detrimental effect on urotensin induced $Ca^{2+}$ release.

This is an example of bidirectional regulation. On the contrary hUT was not desensitised in the presence of purinergic receptor activity. However purinergic $Ca^{2+}$ release was reduced due to hUT activation, suggestive of a unidirectional regulatory mechanism. It should be stressed that further investigations are required to deduce the complete path of desensitisation in both these cell lines.

#### 8.1.4. Genomic desensitisation

The current study is the first to assess UT receptor mRNA levels pre and post U-II treatment. Native human UT receptor mRNA was reduced when stimulated with the agonist for 6 hr. However time periods >6 hr (i.e. 24 and 48 hr) UT mRNA expression recovered to basal conditions. In the recombinant cell lines HEK293 and CHO expressing hUT, U-II treatments at 6 hr appeared to upregulate UT mRNA expression significantly above basal.

## *8.2. Discussion*

#### 8.2.1. Factors affecting ligand efficacy

The ability of an agonist to evoke a biological response comprises of two key events; firstly the ability of an agonist to act as a stimulus on its target (receptor) and secondly the ability of the receptor to translate this information into a response. A pharmacological response cannot be defined by a singular end point response due to the existence of different levels of responses within a signal transduction pathway, i.e. signal cascades. Therefore the determination of efficacy does not rely on a singular response but on the net accumulation of responses observed downstream of receptor activation. Downstream events after initial

receptor activation include the generation of second messengers (e.g. cAMP, $IP_3$, $Ca^{2+}$) or even more distal processes such as alteration of gene expression (Galandrin *et al.*, 2007) (Kenakin, 2009).

An aspect of signal cascades is that they are capable of being amplified (Figure 8.1); therefore this can have an impact on how efficacy is defined for a given ligand. Furtheremore the efficacy can vary in accord with the following factors:

a) Receptor density.

b) Cellular background of receptor under study.

c) Coupling efficiency of receptor in a given system.

d) Type of assay used (upstream and downstream amplification).

e) Temperature of the assay.



**Figure. 8.1. The amplification process that occurs at different points along a stimulus-response pathway.**
The rank order of efficacy is ***c*** > ***b*** > ***a***, however potency is in the order of ***b*** > ***a*** > ***c***. Low levels of amplification are evident closer towards the vantage point where agonist-receptor interaction takes place. As the cascade progress from this point, amplification is observed. Adapted from (Kenakin, 2009).

The above (Figure. 8.1.) illustrates the pharmacological profile of three hypothetical agonists with reference to different vantage points along a stimulus-response pathway. Upon agonist interaction it can be seen that drugs ***a*** and ***b*** are partial agonists while drug ***c*** is a full agonist (graph on left panel). Therefore the rank order of efficacy and potency is ***c*** > ***b*** > ***a*** and ***b*** > ***a*** > ***c*** respectively. As the cascade progress to the point of second messenger generation/detection (graph middle panel) the rank order of potency is unaltered. However now agonist ***a*** is a partial agonist and agonists ***b*** and ***c*** cannot be distinguished from one another as they both have similar efficacies. At the end organ response all three compounds appear as full agonists with similar rank order of potency. This example demonstrates the importance of not relying on a single vantage point in a signalling cascade in determining the profile of a ligand; especially since downstream amplification can cause a masking of changes that occur upstream in a cascade (Kenakin, 2009).

The influence of increasing receptor density on maximal $Ca^{2+}$ responses can be demonstrated with respect to the three cells lines expressing human UT (Figure. 8.2). While U-II remains an agonist throughout these three systems; it can be seen that the maximal response to U-II increases as the receptor density increases in the three cell lines. However it should be appreciated with some caution; as the background at which maximal response is recorded varies i.e. that is to say that there are three different cell lines with different cellular background which influence the manner by which the maximal response occurs. Ideally if one were to assess the relationship between increasing $B_{max}$ and $E_{max}$ it would be important to maintain the same background while altering one variable. Hence for example using a recombinant cell line where receptor densities can be regulated.

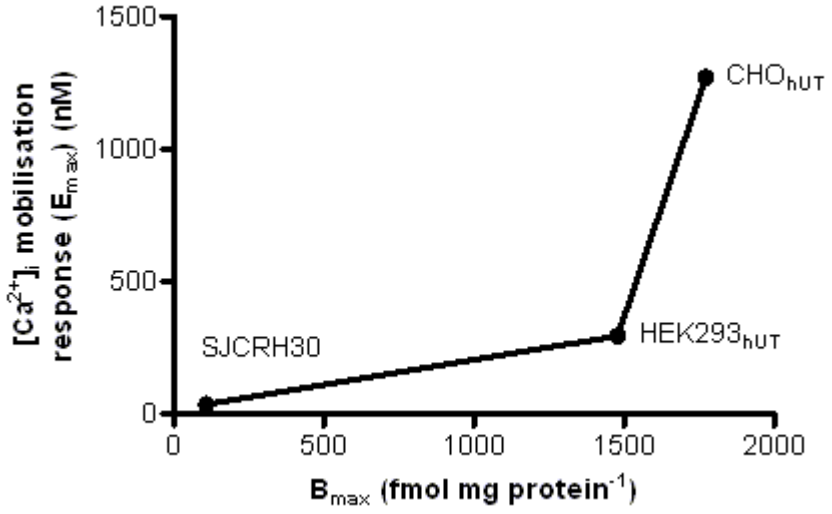


**Figure. 8.2. The relationship between human UT receptor density ($B_{max}$) and maximal U-II induced response ($E_{max}$).**
The increase in $E_{max}$ in with respect to the three cell lines used in the study is shown.

This type of relationship has also been demonstrated by (Behm *et al.*, 2006), for U-II and urantide; implicating that alternations in receptor density can influence pharmacological profile of drugs that are considered to be antagonists in end-point assays (tissue bioassays). On a similar vein in previous studies assessing [Orn$^8$]U-II, (Camarda *et al.*, 2002a) this modification of U-II appears as an antagonist in aorta bioassays, but exhibits full agonist activity in $Ca^{2+}$ assays in $HEK293_{rUT}$ cells. Further, whilst urantide and UFP-803 have been classed as antagonists (Patacchini *et al.*, 2003) (Camarda *et al.*, 2006), at the tissue level their profiles change in recombinant systems.

In the present study the ligands U-II, urantide, UFP-803 and [(3,5diiodo)Tyr$^9$]U-II(4-11) were assessed in four different pharmacological test systems; where UT receptor is expressed in native environments (rat thoracic aorta and SJCRH30 cell) and recombinant environments ($HEK293_{hUT}$ and $CHO_{hUT}$ cells). A summary of their pharmacological profiles are indicated in Table. 8.1.

While U-II demonstrates full agonism from aorta to recombinant systems; both urantide and UFP-803 profiles vary. Note that as the receptor density increases the pharmacological profiles of both these drugs are indifferent with respect to rUT, however in recombinant systems where hUT is expressed, the pharmacological profile differs with respect to the signalling cascade. For example in $HEK293_{hUT}$ cells, urantide and UFP-803 behave as low efficacy partial agonists in $IP_3$ assays; however in $Ca^{2+}$ assays they exhibit antagonist behaviour. The latter observation results from the temperature under which the assay was carried out. At physiological temperature these compounds are partial agonists, whilst at room temperature are antagonists.

In $CHO_{hUT}$ cells urantide appears to be a partial agonist throughout the signal transduction cascade, however at physiological temperature (in $Ca^{2+}$ assays) is as an agonist. UFP-803 exhibits antagonist properties at room temperature, but appears as a low efficacy partial agonist at 37°C.

The new U-II(4-11) analogue [(3,5diiodo)$Tyr^9$]U-II(4-11) has been demonstrated as being a partial agonist in the rat aorta bioassay (37°C) and $Ca^{2+}$ assay (25°C) in HEK293 expressing rat UT receptor; however in the $IP_3$ assay (upstream of $Ca^{2+}$) it exhibited full agonism (37°C). This compound also exhibits full agonist activity (at 37°C) in SJCRH30 $Ca^{2+}$ assays and in $HEK293_{hUT}$ whether it be upstream ($IP_3$) or downstream ($Ca^{2+}$) signalling, irrespective of increasing receptor densities.

| Model | $B_{max}$ (fmol mg $^{-1}$) and reference (where applicable) | Assay type | Compound | | | | References (where applicable) |
|---|---|---|---|---|---|---|---|
| | | | *U-II* | *Urantide* | *UFP-803* | *[(3,5diiodo)Tyr$^{9}$]U-II(4-11)* | |
| Rat aorta | 2-20 (Ames *et al.*, 1999) | Bioassay | Agonist$^{\#}$ | Antagonist$^{\#}$ | Antagonist$^{\#}$ | Partial agonist$^{\#}$ | (Patacchini *et al.*, 2003); (Camarda *et al.*, 2006) |
| SJCRH30 | 107 (This study) | $IP_3$ | ND | ND | ND | ND | - |
| | | $Ca^{2+}$ | Agonist$^{\#}$ | ND | ND | Agonist$^{\#}$ | This study |
| $HEK293_{rUT}$ | 325 (Douglas *et al.*, 2005) | $IP_3$ | Agonist$^{\#}$ | ND | ND | Agonist$^{\#}$ | This study |
| | | $Ca^{2+}$ | Agonist$^{\#}$ | Antagonist | Antagonist | Partial agonist | (Camarda *et al.*, 2006) |
| $HEK293_{hUT}$ | 1477 (This study) | $IP_3$ | Agonist$^{\#}$ | Partial agonist$^{*\#}$ | Partial agonist$^{*\#}$ | Agonist$^{\#}$ | This study |
| | | $Ca^{2+}$ | Agonist | Antagonist | Antagonist | Agonist$^{\#}$ | (Camarda *et al.*, 2006) |
| $CHO_{hUT}$ | 1770 (This study) | GTPγ[$^{35}$S] | Agonist$^{\#}$ | Partial agonist | ND | ND | (Song *et al.*, 2006) |
| | | $IP_3$ | Agonist$^{\#}$ | Partial agonist$^{*\#}$ | Partial agonist$^{*\#}$ | ND | This study |
| | | $Ca^{2+}$ | Agonist$^{\#}$ | Partial agonist/ Agonist$^{\#}$ | Antagonist/ Partial agonist$^{*\#}$ | ND | (Camarda *et al.*, 2004); (Camarda *et al.*, 2006) |

**Table. 8.1. Summary of effects demonstrated by U-II, urantide and UFP-803 in the cell lines $CHO_{hUT}$, $HEK293_{hUT}$, SJCRH30 and rat aorta.**
denotes low efficacy, $^{\#}$ effect observed at 37°C, ND: no data

### 8.2.2. Desensitisation of the human UT receptor

Most of the work carried out to date to delineate the exact mechanism of UT receptor desensitisation at the molecular level have involved using rat UT receptor expressed in recombinant cell lines such as COS (Proulx *et al.,* 2005) and HEK293 (Giebing *et al.,* 2005). Many efforts to date have focussed on the downstream process of receptor internalisation as opposed to receptor phosphorylation. Desensitisation experiments with the UT receptor are hampered by the lack of commercially available reversible agonists. This therefore means that alternative experimental paradigms are required in order to elucidate mechanisms. To this end the present study has demonstrated bidirectional cross-talk mechanism between muscarinic and human UT receptors in $HEK293_{hUT}$ cells. Desensitisation of the human UT receptor does not occur in $CHO_{hUT}$ cells; however native $P_2Y$ receptors are subjected to functional attenuation upon stimulation of the urotensin system. Hence there appears to be a heterologous unidirectional regulation of these receptors in this cell line. While it is impossible to give a definite mechanism it is likely that there are other events apart from phosphorylation that may contribute towards desensitisation e.g. involvement of intracellular $Ca^{2+}$ stores. The data provided for functional desensitisation herein should serve as a means to design further investigations.

A hypothetical mechanism (in the context of human UT) by which protein kinase C (PKC) and possible casein kinase 1 (CK1) may contribute towards heterologous desensitisation is outlined (see Figure. 8.3).

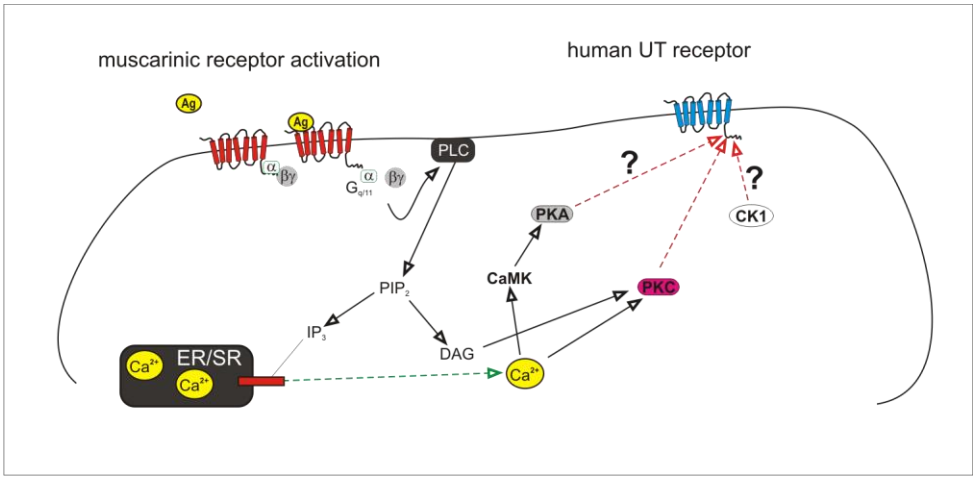


**Figure. 8.3. Putative mechanisms of desensitisation of the human UT receptor.**
Abbreviations used: Agonist (Ag), phospholipase C (PLC), (PIP2), (IP3), diacylglycerol (DAG), protein kinase C (PKC), calmodulin kinase (CaMK), protein kinase A (PKA), casein kinase 1 (CK1).

Upon muscarinic stimulation, G proteins uncouple and this in turn results in the activation of the enzyme phospholipase C which in turn is associated with the hydrolysis of $PIP_2$ to form DAG and $IP_3$. The release of $Ca^{2+}$ ensues as $IP_3$ binds to $IP_3R$ located on the ER. The cytosolic rise in $Ca^{2+}$ together with DAG activates PKC. This activated PKC then is capable of phosphorylating free human UT receptor. Additionally CaM kinase could stimulate PKA. PKA therefore may also be involved in phosphorylation as the human UT receptor contains a putative site for PKA interaction. It is also likely that casein kinase (CK1) might also phosphorylate hUT as a putative phosphorylation site for this kinase can be found on the receptor (Onan *et al.*, 2004a). The extent of involvement of CK1 is not known; however this kinase has been demonstrated to phosphorylate (agonist bound) $G_q$ coupled $M_3$ receptors and rhodopsin (Tobin *et al.*, 1997). This therefore suggests that it may have a role to play similar to GRKs. Perhaps the presence of a CK1 site on hUT receptors may serve to compensate in the absence of GRK expression/activity. Perhaps

CK1 would phosphorylate agonist bound UT receptor if GRK is not expressed in that particular cell line; however this is only a matter of speculation.

The involvement of these second messenger kinases (e.g. PKC) could be studied by pharmacological means using inhibitors and activators of these molecules e.g. PKC activators such as PMA (Phorbol 12-myristate 13-acetate) and then conducting phosphorylation assays of UT receptor and muscarinic receptors. PKC activity could also be blocked using Myristoylated Protein Kinase C Peptide Inhibitor and staurosporine thereby assessing UT phosphorylation.

The process of desensitisation of GPCR is an important physiological function that enables fine control of receptor activity in response to repeated or prolonged stimuli. This physiological phenomenom takes place in 4 key stages; (1) phosphorylation upon agonist binding to receptor, (2) receptor uncoupling from G- protein and (3) internalisation and (4) downregulation. During the last stage the desensitised receptor may be resequestered back to the plasma membrane to form functional receptor or alternately be degraded. The data for this thesis can be summarised in the form of a desensitisation time course consisting of second, minutes and hours (Figure. 8.4.).

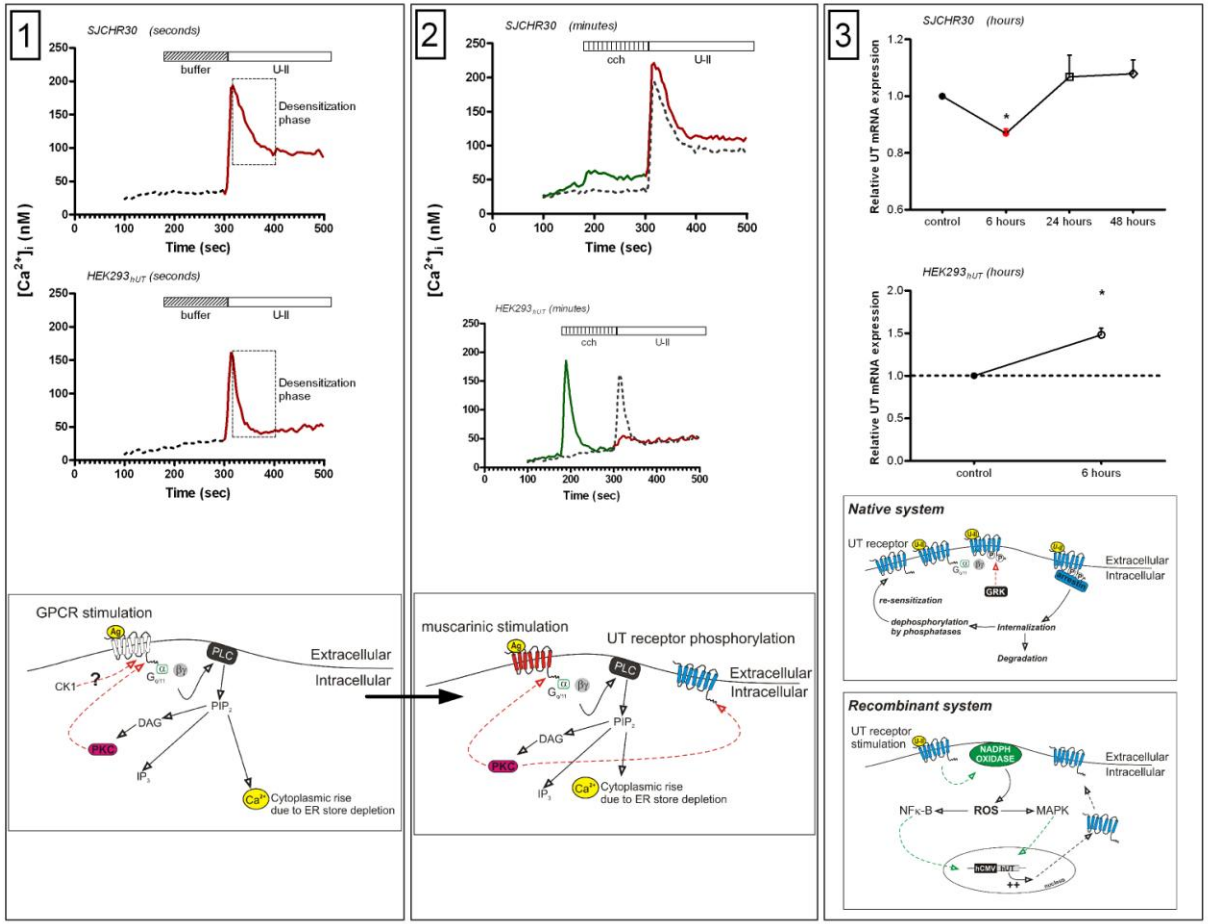


**Figure. 8.4. The seconds, minutes, hours "snapshot" profile of hUT desensitisation from this thesis.**
*Panel 1*: Functional desensitisation is indicated as a time course comprising of seconds. The region that indicated by the dashed box is the phase at with desensitisation is occurring. *Panel 2*: Functional desensitisation of hUT occurring in the time course of minutes. The respective controls are underlayed in order to illustrate desensitisation (dashed). *Panel 3*: Genomic desensitisation/resensitisation occurring in the time frame of hours. In All three panels the bottom illustrations depict putative mechanisms by which desensitisation may take place.

In *Panel 1* ("seconds" profile), in SJCRH30 and HEK293 cells hUT stimulation by U-II causes an initial rise in $Ca^{2+}$ as indicated in the temporal profiles. This is followed by a rapid drop to the plateau. The peak is characteristic of intracellular $Ca^{2+}$ store release. The rapid drop (indicated by the dashed boxed) may be due to PKC activity hence homologous desensitisation. There is also likelihood that CK1 might be associated with phosphorylating agonist bound receptor, however in the context of hUT there is no data available at present.

The "minutes" profile of desensitisation (*Panel 2*) consists of the following: the previous seconds profile precedes the minutes profile and feeds into the latter. Here upon muscarinic stimulation a $Ca^{2+}$ response is observed along with the generation of PKC. The PKC in turn heterologously phosphorylates free hUT. Hence when hUT is stimulated with U-II a reduction in the $Ca^{2+}$ response is noted compared to the control (dashed line). This is indeed the case in $HEK293_{hUT}$ cells, however there does not appear to be any $Ca^{2+}$ desensitisation in SJCRH30 cells. It is also possible for the existence of a negative PKC feedback mechanism where PKC generated due to muscarinic stimulation attenuates muscarinic receptor activation.

Genomic desensitisation (hours) is illustrated in *Panel 3*. In the native system there is a reduction in hUT mRNA after 6 hr U-II treatments, however this reaches basal post 6 hr. Native systems contain response elements (REs) upstream of target genes. Conversely in recombinant system there is a lack of REs. It is possible that these REs are controlled by upstream G protein activation. Hence as a consequence of RE regulation target gene expression is also affected. While this is speculative, there is no proof of whether this is applicable for hUT however $G_q$ coupled receptor activation increases $[Ca^{2+}]_i$ and this is known to induce gene transcription (Mellstrom *et al.*, 2008). In the recombinant system U-II stimulation results in activation of hUT and over a 6 hr period may lead to elevated levels

of reactive oxygen species as a consequence of NADPH activation. ROS stimulates MAPKs and these in turn act on the hCMV/UT promoter in the nucleus thereby upregulating UT transcription. It is also likely that the hCMV/UT promoter is stimulated by NFκ-B. This is on the basis that deletion of NFκ-B/rel site upstream of the CMV promoter can have a detrimental effect on CMV promoter activity (Sun *et al.*, 2001). Further experimentation is required.

### *8.3. Conclusion*

This thesis has contributed to the field of U-II/UT research significantly in that:

1). A new partial agonist has been indentified whose modification may be incorporated in the currently available U-II ligands.

2). To the best of my knowledge this is the first demonstration where functional heterologous desensitisation of the human UT receptor has been assessed by using a GPCR "cross talk" protocol. This work has demonstrated a "work-around" the obstacle of the absence of commercially available reversible agonists.

3). This is the first time to my knowledge that

a) Homologous desensitisation of the human UT receptor mRNA on the genomic level has been described for a native system.

b) UT mRNA upregulation in recombinant systems has been described. While the mechanisms proposed are putative, further studies are required to dissect the genomic mechanisms of desensitisation.

# 9. Appendices

## *9.1. Amino acids and their abbreviations*

A = Ala, alanine

C = Cys, cysteine

D = Asp, aspartate

E = Glu, glutamate

F = Phe, phenylalanine

G = Gly, glycine

H = Hist, histidine

I = Ile, isoleucine

K = Lys, lysine

L = Leu, leucine

M = Met, methionine

N = Asn, asparagine

P = Pro, proline

Q = Gln, glutamine

R = Arg, arginine

S = Ser, serine

T = Thr, threonine

V = Val, valine

W = Trp, tryptophan

Y = Tyr, tyrosine

### *9.2. Analytical properties of U-II, U-II (4-11) and its [Xaa$^9$] analogues*

| N° | Abbreviated names | $^a t_r$ | | $^b MH^+$ | |
|---|---|---|---|---|---|
| | | I | II | calculated | found |
| | U-II | 10.42 | 13.28 | 1389.6 | 1389.9 |
| | U-II (4-11) | 10.25 | 9.73 | 1062.3 | 1062.4 |
| 1a | [*o*-Tyr$^9$]U-II (4-11) | 9.41 | 12.07 | 1062.3 | 1062.0 |
| 1b | [*o*-Tyr$^9$]U-II (4-11) | 9.52 | 12.85 | 1062.3 | 1062.3 |
| 2b | [*m*-Tyr$^9$]U-II (4-11) | 10.23 | 12.78 | 1062.3 | 1062.0 |
| 2b | [*m*-Tyr$^9$]U-II (4-11) | 10.30 | 13.13 | 1062.3 | 1061.9 |
| 3 | [(N-$CH_3$)-Tyr$^9$]U-II (4-11) | 10.79 | 13.16 | 1076.3 | 1076.2 |
| 4 | [(4-OH)-Phg$^9$]U-II (4-11) | 10.59 | 13.35 | 1048.2 | 1048.1 |
| 5a | [(5-OH)-Aic$^9$]U-II (4-11) | 11.44 | 14.42 | 1074.3 | 1074.0 |
| 5b | [(5-OH)-Aic$^9$]U-II (4-11) | 11.62 | 15.78 | 1074.3 | 1074.3 |
| 6a | [Hat$^9$]U-II (4-11) | 9.29 | 12.91 | 1088.3 | 1088.4 |
| 6b | [Hat$^9$]U-II (4-11) | 9.46 | 13.03 | 1088.3 | 1088.3 |
| 7 | [(7-OH)-Tic$^9$]U-II (4-11) | 10.70 | 15.80 | 1074.3 | 1074.3 |
| 8 | [(6,8-diiodo-7-OH)-Tic$^9$]U-II (4-11) | 10.41 | 12.77 | 1326.1 | 1326.3 |
| 9 | [(3,5-diiodo)-Tyr$^9$]U-II (4-11) | 11.94 | 14.45 | 1313.1 | 1313.6 |

**Table. 9.1. The analytical properties of U-II and related analogues modified at Tyr$^9$.**
$^a t_r$ is the retention time determined by analytical HPLC.
$^b$The mass ion ($MH^+$) was obtained by electro spray mass spectrometry.

### *9.3. Procedures for the synthesis of racemic ortho tyrosine*

*Acetic acid 2- iodo phenyl ester*

To a solution of 2-iodophenol (1 g, 4.54 mmol) in pyridine (3 ml), was added 695 mg (6.82 mmol) of acetic anhydride and the solution heated at 50 °C for 30 min. After this time, the reaction mixture was cooled and ethyl acetate (20 ml) was added. The organic layer was washed three time with a solution of hydrochloric acid (1 N), separated and concentrated in vacuo to obtain 1.07 g (4.08 mmol) of the desired product. Yield 90%. Rf= 0.9 (AcOEt/EtPt, 1/9); $^{1}$H NMR ($CDCl_3$) δ: 7.61 (m, 1H), 7.22 (m, 1H), 6.80 (m, 2H), 2.12 (s, 3H). $[M+H]^+$ Calc. 263.04; found 263.3. (Figure. 9.1 **[10]**).

*3-(2-Acetoxy-phenyl)-2-acetylamino-acrylic acid methyl ester*

To a stirred solution of compound **[10]** (871 mg, 3.33 mmol) in acetonitrile (15 ml) were added methyl 2-acetamido acrylate (500 mg (3.49 mmol), tri-*o*-tolyl phosphine (53 mg, 0.17 mmol), triethylamine (0.92 ml, 6.6 mmol) and palladium acetate (13.8 mg, 0.06 mmol). The reaction was stirred at reflux for 24 hr. The solution was cooled at room temperature, filtered over celite pad and evaporated in vacuo. The crude material was dissolved in 20 ml of ethyl acetate and the organic layer was washed with 20 ml of water. To the organic phase was added vegetable black and the corresponding solution was stirred for 3 hr. After this time the solution was filtered and evaporated in vacuo to obtain a brown oil that was crystallized using a solution of ethyl acetate/pentane 1/1. Yield= 75%; Rf. 0.9 (EtOAc/EtPt, 0.2/9.8); $^{1}$H NMR ($CDCl_3$) δ: 7.27 (m, 1H), 7.11 (m, 1H), 6.98 (m, 2H), 6.79,

(s, 1H), 3.82, (s, 3H), 2.14, (s, 3H), 2.01 (s, 3H). $[M+H]^+$ Calc. 278.28; found 278.4; m.p. 170-175 °C. (Figure. 9.1 **[11]**).

*3-(2-Acetoxy-phenyl)-2-acetylamino-propionic acid methyl ester*

Compound **[11]** (160 mg, 0.57 mmol) was dissolved in 10 ml of ethanol and hydrogenated in a Parr apparatus at 65 psi for 6 hr in the presence of Pd/C 10% (0.1 g). Filtration of the catalyst through Celite pad and solvent evaporation gave [**12]** (150 mg, 0.53 mmol) as a colorless oil. Yield= 94%; Rf. 0.9 (EtOAc/EtPt, 0.2/9.8); $^1$H NMR ($CDCl_3$) δ: 7.12-7.02 (m, 4H), 4.82 (dd, J= 7.6 Hz, J= 3.9 Hz, 1H), 3.70, (s, 3H), 3.14-3.10 (m, 2H), 2.12, (s, 3H), 2.05, (s, 3H). $[M+H]^+$ Calc. 280.30; found 280.5 (Figure. 9.1. **[12]**).

*2-Amino-3-(2-hydroxy-phenyl)-propionic acid*

Compound **12** (150 mg, 0.53 mmol) was dissolved in 10 ml of ultra pure concentrated hydrochloric acid and stirred at reflux for 6 hr. The solvent was removed under reduced pressure.

Yield= 90%; $^1$H NMR (DMSO) δ: 12.8, (bs, 1H), 6.95-6.68, (m, 4H), 4.96, (bs, 1H), 3.96, (m, 1H), 2.99, (m, 2H). $[M+H]^+$ Calc. 182.2; found 182.4. (Figure. 9.1. **[13]**).

*2-(9H-Fluoren-9-ylmethoxycarbonylamino)-3-(2-hydroxy-phenyl)-propionic acid*

To a stirred solution of **13** (172 mg, 0.79 mmol) in water/dioxane 1:1 (10 ml) were added sodium carbonate (212 mg, 2 mmol) and, drop by drop, a dioxane solution of Fmoc-Cl (155mg, 0.6mmol). The reaction is maintained at room temperature under stirring for 4 h and after this time 50 ml of 1N hydrochloric acid was added. The aqueous solution was

extracted twice with ethyl acetate (50 ml each), dried and evaporated under vacuum. The residue was crystallized from ethyl ether/light petroleum 1/1. Yield= 63%; $^1$H NMR ($CDCl_3$) δ: 7.76-7.03, (m, 12H), 5.03, (bs, 1H), 4.57-4.54 (d, J= 6.6 Hz, 1H), 4.76, (m, 2H), 4.41-4.30, (m, 1H), 3.16, (bs, 2H). $[M+H]^+$ Calc. 404.44; found 404.3; M.p.= 95-97°C. (Figure. 9.1. **[14]**).

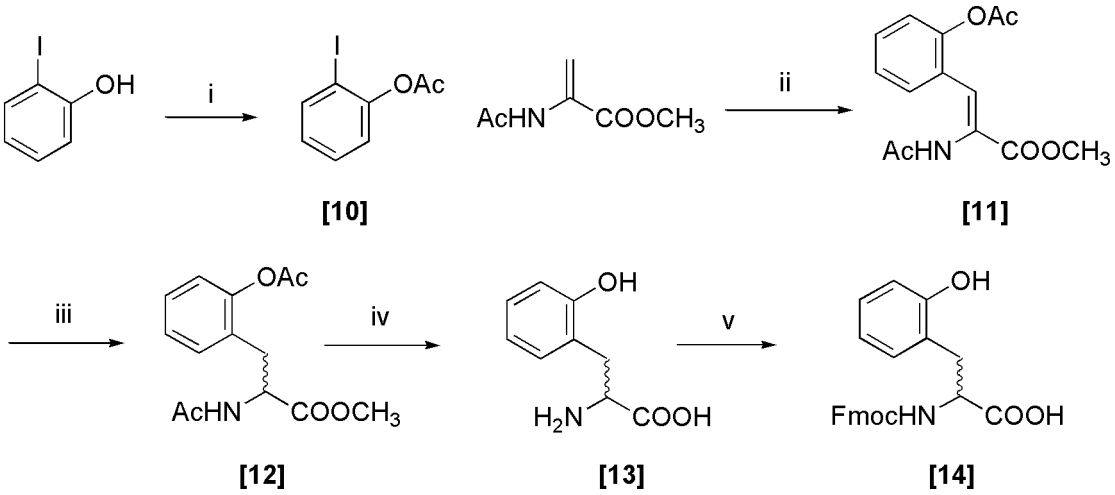


**Figure. 9.1. Scheme for Synthesis of racemic ortho tyrosine.**
Reagents and conditions: (i) $Ac_2O$, Py, 50°C, 30'; (ii) $Pd(OAc)_2$, $CH_3CN$, $Et_3N$, o-$(CH_3C_6H_4)_3P$, reflux 24 hr; (iii) $H_2$, C/Pd 10%, EtOH, 6 hr, (iv) HCl conc reflux, 6 hr; (v) Fmoc-Cl, $Na_2CO_3$, $H_2O$/Dioxane, room temperature, 24 hr.

### *9.4. Data conversions: rat aorta bioassay*

Data acquisition in the Linseis polygraph occurs through the force transducer which detects minute contractile changes in the tissue upon agonist stimulation. The response that is generated by the tissue is transferred via the force transducer to the polygraph. The data that is collected is then amplified and produced as a response on paper.

Different amplification settings result in different response peaks when a 1g load is applied to the force transducer as indicated below (Table. 9.2).

| Amplification | Pre-load (g) | Movement response (cm) |
|---|---|---|
| 1 | 1 | 10 |
| 2 | 1 | 5 |
| 5 | 1 | 2 |
| 10 | 1 | 1 |

**Table. 9.2. Amplification settings and the effects of 1g pre-load on response.**

All experimental data is collected when the amplification is set to 2. The response to drug stimulation are measured in centimetres, however require conversion into a value in grams.

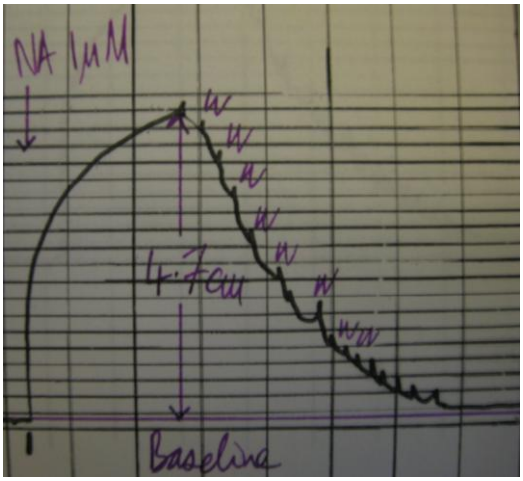


**Figure. 9.2. Illustration of a typical trace response to 1 μM noradrenaline (NA).**
Peak response is measure from the baseline. W denotes washing of the tissue until all drug was washed off and the tissue returned back to baseline.

A typical trace is illustrated in Figure. 9.2. If a contractile response of 4.7 cm was observed when a tissue was challenged with 1 μM noradrenaline then the response in grams would be calculated using the following formula:

$$\text{Contractile response (g)} = \frac{\text{contractile response observed (cm)}}{5 \text{ cm}}$$

$$4.7/5 = \mathbf{0.94 \text{ g contractile response}}$$

### *9.5. Publications arisen from this thesis*

#### *Research papers*

**Batuwangala MS,** Calo' G, Guerrini R, Ng LL, McDonald J and Lambert DG. Desensitization of native and recombinant human urotensin II receptors. (Submitted to ***Naunyn Schmiedebergs Arch Pharmacol.***)

**Batuwangala M**, Camarda V, McDonald J, Marzola E, Lambert DG, Ng LL, Calo' G, Regoli D, Trapella C, Guerrini R and Salvadori S. Structure-activity relationship study on $Tyr^9$ of urotensin-II(4-11): identification of a partial agonist of the UT receptor. ***Peptides.*** 2009. 30(6): 1130-1136.doi:10.1016/j.peptides.2009.02.003.

Marzola E, Camarda V, **Batuwangala M**, Lambert DG, Calo' G, Guerrini R, Trapella C, Regoli D, Tomatis R and Salvadori S. Structure activity relationship study on position 4 in the urotensin-II receptor ligand U-II(4-11). ***Peptides.*** 2008. 29(5): 674-679. doi:10.1016/j.peptides.2007.07.025.

#### *Reviews*

McDonald J, **Batuwangala M** and Lambert DG. Role of urotensin-II and its receptor in health and diseases. ***J. Anesth.*** 2007. 21(3):378-389. doi:10.1007/s00540-007-0524-z.

#### *Abstracts*

**Batuwangala M**, Camarda V, Marzola E, McDonald J, Lambert DG, Ng LL, Guerrini R, Salvadori S, Regoli D and Calo' G. Pharmacological characterisation of the Urotensin-II receptor ligands urantide and UFP-803 in $CHO_{hUT}$ cells. ***33° Congresso Nazionale della Societa' Italiana di Farmacologia***. 6-9 June 2007.

**Batuwangala M**, McDonald J, Calo' G, Ng LL, Lambert DG. Characterisation of native urotensin II receptors expressed in SJCRH30 rhabdomyosarcoma cells. ***Brit. J. Anaes. (Proc. Anaes. Res. Soc. Meet)***. **97**(3):431-42P. DOI: 10.1 093/bja/ael146.

## 10. References


Ames, RS, Sarau, HM, Chambers, JK, Willette, RN, Aiyar, NV, Romanic, AM, Louden, CS, Foley, JJ, Sauermelch, CF, Coatney, RW, Ao, Z, Disa, J, Holmes, SD, Stadel, JM, Martin, JD, Liu, WS, Glover, GI, Wilson, S, McNulty, DE, Ellis, CE, Elshourbagy, NA, Shabon, U, Trill, JJ, Hay, DW, Ohlstein, EH, Bergsma, DJ, Douglas, SA (1999). Human urotensin-II is a potent vasoconstrictor and agonist for the orphan receptor GPR14. *Nature* **401:** 282-6.

Ancellin, N, Preisser, L, Le Maout, S, Barbado, M, Creminon, C, Corman, B, Morel, A (1999). Homologous and heterologous phosphorylation of the vasopressin V1a receptor. *Cell Signal* **11:** 743-51.

Angus, JA, Wright, CE (2000). Techniques to study the pharmacodynamics of isolated large and small blood vessels. *J Pharmacol Toxicol Methods* **44:** 395-407.

Ashton, N (2006). Renal and vascular actions of urotensin II. *Kidney Int* **70:** 624-9.

Atlas, D, Adler, M (1981). alpha-adrenergic antagonists as possible calcium channel inhibitors. *Proc Natl Acad Sci U S A* **78:** 1237-41.

Balzer, M, Lintschinger, B, Groschner, K (1999). Evidence for a role of Trp proteins in the oxidative stress-induced membrane conductances of porcine aortic endothelial cells. *Cardiovasc Res* **42:** 543-9.

Barnes, TA, McDonald, J, Rowbotham, DJ, Duarte, TL, Lambert, DG (2007). Effects of receptor density on Nociceptin/OrphaninFQ peptide receptor desensitisation: studies using the ecdysone inducible expression system. *Naunyn Schmiedebergs Arch Pharmacol* **376:** 217-25.

Behm, DJ, Harrison, SM, Ao, Z, Maniscalco, K, Pickering, SJ, Grau, EV, Woods, TN, Coatney, RW, Doe, CP, Willette, RN, Johns, DG, Douglas, SA (2003). Deletion of the UT receptor gene results in the selective loss of urotensin-II contractile activity in aortae isolated from UT receptor knockout mice. *Br J Pharmacol* **139:** 464-72.

Behm, DJ, McAtee, JJ, Dodson, JW, Neeb, MJ, Fries, HE, Evans, CA, Hernandez, RR, Hoffman, KD, Harrison, SM, Lai, JM, Wu, C, Aiyar, NV, Ohlstein, EH, Douglas, SA (2008). Palosuran inhibits binding to primate UT receptors in cell membranes but demonstrates differential activity in intact cells and vascular tissues. *Br J Pharmacol* **155:** 374-86.

Behm, DJ, Stankus, G, Doe, CP, Willette, RN, Sarau, HM, Foley, JJ, Schmidt, DB, Nuthulaganti, P, Fornwald, JA, Ames, RS, Lambert, DG, Calo, G, Camarda, V, Aiyar, NV, Douglas, SA (2006). The peptidic urotensin-II receptor ligand GSK248451 possesses less intrinsic activity than the low-efficacy partial agonists SB-710411 and urantide in native mammalian tissues and recombinant cell systems. *Br J Pharmacol* **148:** 173-90.

Benovic, JL, Pike, LJ, Cerione, RA, Staniszewski, C, Yoshimasa, T, Codina, J, Caron, MG, Lefkowitz, RJ (1985). Phosphorylation of the mammalian beta-adrenergic receptor by cyclic AMP-dependent protein kinase. Regulation of the rate of receptor phosphorylation and dephosphorylation by agonist occupancy and effects on coupling of the receptor to the stimulatory guanine nucleotide regulatory protein. *J Biol Chem* **260:** 7094-101.

Benovic, JL, Strasser, RH, Caron, MG, Lefkowitz, RJ (1986). Beta-adrenergic receptor kinase: identification of a novel protein kinase that phosphorylates the agonist-occupied form of the receptor. *Proc Natl Acad Sci U S A* **83:** 2797-801.

Benya, RV, Kusui, T, Shikado, F, Battey, JF, Jensen, RT (1994). Desensitization of neuromedin B receptors (NMB-R) on native and NMB-R-transfected cells involves down-regulation and internalization. *J Biol Chem* **269:** 11721-8.

Berridge, MJ (1993). Inositol trisphosphate and calcium signaling. *Nature* **361:** 315-25.

Bhat, MB, Hayek, SM, Zhao, J, Zang, W, Takeshima, H, Wier, WG, Ma, J (1999). Expression and functional characterization of the cardiac muscle ryanodine receptor Ca(2+) release channel in Chinese hamster ovary cells. *Biophys J* **77:** 808-16.

Bleasdale, JE, Thakur, NR, Gremban, RS, Bundy, GL, Fitzpatrick, FA, Smith, RJ, Bunting, S (1990). Selective inhibition of receptor-coupled phospholipase C-dependent processes in human platelets and polymorphonuclear neutrophils. *J Pharmacol Exp Ther* **255:** 756-68.

Boivin, S, Guilhaudis, L, Milazzo, I, Oulyadi, H, Davoust, D, Fournier, A (2006). Characterization of urotensin-II receptor structural domains involved in the recognition of U-II, URP, and urantide. *Biochemistry* **45:** 5993-6002.

Bottrill, FE, Douglas, SA, Hiley, CR, White, R (2000). Human urotensin-II is an endothelium-dependent vasodilator in rat small arteries. *Br J Pharmacol* **130:** 1865-70.

Boyd, SD (2008). Everything you wanted to know about small RNA but were afraid to ask. *Lab Invest* **88:** 569-78.

Brailoiu, E, Jiang, X, Brailoiu, GC, Yang, J, Chang, JK, Wang, H, Dun, NJ (2008). State-dependent calcium mobilization by urotensin-II in cultured human endothelial cells. *Peptides* **29:** 721-6.

Brkovic, A, Hattenberger, A, Kostenis, E, Klabunde, T, Flohr, S, Kurz, M, Bourgault, S, Fournier, A (2003). Functional and binding characterizations of urotensin II-related peptides in human and rat urotensin II-receptor assay. *J Pharmacol Exp Ther* **306:** 1200-9.

Bruening, W, Giasson, B, Mushynski, W, Durham, HD (1998). Activation of stress-activated MAP protein kinases up-regulates expression of transgenes driven by the cytomegalovirus immediate/early promoter. *Nucleic Acids Res* **26:** 486-9.

Bunemann, M, Lee, KB, Pals-Rylaarsdam, R, Roseberry, AG, Hosey, MM (1999). Desensitization of G-protein-coupled receptors in the cardiovascular system. *Annu Rev Physiol* **61:** 169-92.

Bylund, DB, Yamamura, H.I. (1990). *Methods for receptor binding*. Raven Press.

Camarda, V, Guerrini, R, Kostenis, E, Rizzi, A, Calo, G, Hattenberger, A, Zucchini, M, Salvadori, S, Regoli, D (2002a). A new ligand for the urotensin II receptor. *Br J Pharmacol* **137:** 311-4.

Camarda, V, Rizzi, A, Calo, G, Gendron, G, Perron, SI, Kostenis, E, Zamboni, P, Mascoli, F, Regoli, D (2002b). Effects of human urotensin II in isolated vessels of various species; comparison with other vasoactive agents. *Naunyn Schmiedebergs Arch Pharmacol* **365:** 141-9.

Camarda, V, Song, W, Marzola, E, Spagnol, M, Guerrini, R, Salvadori, S, Regoli, D, Thompson, JP, Rowbotham, DJ, Behm, DJ, Douglas, SA, Calo, G, Lambert, DG (2004). Urantide mimics urotensin-II induced calcium release in cells expressing recombinant UT receptors. *Eur J Pharmacol* **498:** 83-6.

Camarda, V, Spagnol, M, Song, W, Vergura, R, Roth, AL, Thompson, JP, Rowbotham, DJ, Guerrini, R, Marzola, E, Salvadori, S, Cavanni, P, Regoli, D, Douglas, SA, Lambert, DG, Calo, G (2006). In vitro and in vivo pharmacological characterization of the novel UT receptor ligand [Pen5,DTrp7,Dab8]urotensin II(4-11) (UFP-803). *Br J Pharmacol* **147:** 92-100.

Carmody, RJ, Chen, YH (2007). Nuclear factor-kappaB: activation and regulation during toll-like receptor signaling. *Cell Mol Immunol* **4:** 31-41.

Castiglione, F, Degl'Innocenti, DR, Taddei, A, Garbini, F, Buccoliero, AM, Raspollini, MR, Pepi, M, Paglierani, M, Asirelli, G, Freschi, G, Bechi, P, Taddei, GL (2007). Real-time PCR analysis of RNA extracted from formalin-fixed and paraffin-embeded tissues: effects of the fixation on outcome reliability. *Appl Immunohistochem Mol Morphol* **15:** 338-42.

Catalucci, D, Latronico, MV, Condorelli, G (2008). MicroRNAs control gene expression: importance for cardiac development and pathophysiology. *Ann N Y Acad Sci* **1123:** 20-9.

Chalfie, M, Horvitz, HR, Sulston, JE (1981). Mutations that lead to reiterations in the cell lineages of C. elegans. *Cell* **24:** 59-69.

Chatenet, D, Dubessy, C, Leprince, J, Boularan, C, Carlier, L, Segalas-Milazzo, I, Guilhaudis, L, Oulyadi, H, Davoust, D, Scalbert, E, Pfeiffer, B, Renard, P, Tonon, MC, Lihrmann, I, Pacaud, P, Vaudry, H (2004). Structure-activity relationships and structural conformation of a novel urotensin II-related peptide. *Peptides* **25:** 1819-30.

Chen, YL, Liu, JC, Loh, SH, Chen, CH, Hong, CY, Chen, JJ, Cheng, TH (2008). Involvement of reactive oxygen species in urotensin II-induced proliferation of cardiac fibroblasts. *Eur J Pharmacol* **593:** 24-9.

Cheng, Y, Prusoff, WH (1973). Relationship between the inhibition constant (K1) and the concentration of inhibitor which causes 50 per cent inhibition (I50) of an enzymatic reaction. *Biochem Pharmacol* **22:** 3099-108.

Chomczynski, P, Sacchi, N (1987). Single-step method of RNA isolation by acid guanidinium thiocyanate-phenol-chloroform extraction. *Anal Biochem* **162:** 156-9.

Clozel, M, Hess, P, Qiu, C, Ding, SS, Rey, M (2006). The urotensin-II receptor antagonist palosuran improves pancreatic and renal function in diabetic rats. *J Pharmacol Exp Ther* **316:** 1115-21.

Coulouarn, Y, Jegou, S, Tostivint, H, Vaudry, H, Lihrmann, I (1999). Cloning, sequence analysis and tissue distribution of the mouse and rat urotensin II precursors. *FEBS Lett* **457:** 28-32.

Coulouarn, Y, Lihrmann, I, Jegou, S, Anouar, Y, Tostivint, H, Beauvillain, JC, Conlon, JM, Bern, HA, Vaudry, H (1998). Cloning of the cDNA encoding the urotensin II precursor in frog and human reveals intense expression of the urotensin II gene in motoneurons of the spinal cord. *Proc Natl Acad Sci U S A* **95:** 15803-8.

de Lecea, L, Bourgin, P (2008). Neuropeptide interactions and REM sleep: a role for Urotensin II? *Peptides* **29:** 845-51.

Dheda, K, Huggett, JF, Bustin, SA, Johnson, MA, Rook, G, Zumla, A (2004). Validation of housekeeping genes for normalizing RNA expression in real-time PCR. *Biotechniques* **37:** 112-4, 116, 118-9.

Djordjevic, T, BelAiba, RS, Bonello, S, Pfeilschifter, J, Hess, J, Gorlach, A (2005). Human urotensin II is a novel activator of NADPH oxidase in human pulmonary artery smooth muscle cells. *Arterioscler Thromb Vasc Biol* **25:** 519-25.

Do-Rego, JC, Chatenet, D, Orta, MH, Naudin, B, Le Cudennec, C, Leprince, J, Scalbert, E, Vaudry, H, Costentin, J (2005). Behavioral effects of urotensin-II centrally administered in mice. *Psychopharmacology (Berl)* **183:** 103-17.

Douglas, SA, Behm, DJ, Aiyar, NV, Naselsky, D, Disa, J, Brooks, DP, Ohlstein, EH, Gleason, JG, Sarau, HM, Foley, JJ, Buckley, PT, Schmidt, DB, Wixted, WE, Widdowson, K, Riley, G, Jin, J, Gallagher, TF, Schmidt, SJ, Ridgers, L, Christmann, LT, Keenan, RM, Knight, SD, Dhanak, D (2005). Nonpeptidic urotensin-II receptor antagonists I: in vitro pharmacological characterization of SB-706375. *Br J Pharmacol* **145:** 620-35.

Douglas, SA, Naselsky, D, Ao, Z, Disa, J, Herold, CL, Lynch, F, Aiyar, NV (2004). Identification and pharmacological characterization of native, functional human urotensin-II receptors in rhabdomyosarcoma cell lines. *Br J Pharmacol* **142:** 921-32.

Douglas, SA, Ohlstein, EH (2000a). Human urotensin-II, the most potent mammalian vasoconstrictor identified to date, as a therapeutic target for the management of cardiovascular disease. *Trends Cardiovasc Med* **10:** 229-37.

Douglas, SA, Sulpizio, AC, Piercy, V, Sarau, HM, Ames, RS, Aiyar, NV, Ohlstein, EH, Willette, RN (2000b). Differential vasoconstrictor activity of human urotensin-II in vascular tissue isolated from the rat, mouse, dog, pig, marmoset and cynomolgus monkey. *Br J Pharmacol* **131:** 1262-74.

Douglas, SA, Tayara, L, Ohlstein, EH, Halawa, N, Giaid, A (2002). Congestive heart failure and expression of myocardial urotensin II. *Lancet* **359:** 1990-7.

Dschietzig, T, Bartsch, C, Pregla, R, Zurbrugg, HR, Armbruster, FP, Richter, C, Laule, M, Romeyke, E, Neubert, C, Voelter, W, Baumann, G, Stangl, K (2002). Plasma levels and cardiovascular gene expression of urotensin-II in human heart failure. *Regul Pept* **110:** 33-8.

Dvorak, Z, Pascussi, JM, Modriansky, M (2003). Approaches to messenger RNA detection - comparison of methods. *Biomed Pap Med Fac Univ Palacky Olomouc Czech Repub* **147:** 131-5.

Ferguson, SS (2001). Evolving concepts in G protein-coupled receptor endocytosis: the role in receptor desensitization and signaling. *Pharmacol Rev* **53:** 1-24.

Ferguson, SS, Caron, MG (1998). G protein-coupled receptor adaptation mechanisms. *Semin Cell Dev Biol* **9:** 119-27.

Finley, MJ, Chen, X, Bardi, G, Davey, P, Geller, EB, Zhang, L, Adler, MW, Rogers, TJ (2008). Bi-directional heterologous desensitization between the major HIV-1 co-receptor CXCR4 and the kappa-opioid receptor. *J Neuroimmunol* **197:** 114-23.

Flohr, S, Kurz, M, Kostenis, E, Brkovich, A, Fournier, A, Klabunde, T (2002). Identification of nonpeptidic urotensin II receptor antagonists by virtual screening based on a pharmacophore model derived from structure-activity relationships and nuclear magnetic resonance studies on urotensin II. *J Med Chem* **45:** 1799-805.

Fortunato, EA, Spector, DH (1999). Regulation of human cytomegalovirus gene expression. *Adv Virus Res* **54:** 61-128.

Gach, K, Piestrzeniewicz, M, Fichna, J, Stefanska, B, Szemraj, J, Janecka, A (2008). Opioid-induced regulation of mu-opioid receptor gene expression in the MCF-7 breast cancer cell line. *Biochem Cell Biol* **86:** 217-26.

Galandrin, S, Oligny-Longpre, G, Bouvier, M (2007). The evasive nature of drug efficacy: implications for drug discovery. *Trends Pharmacol Sci* **28:** 423-30.

Gartlon, J, Parker, F, Harrison, DC, Douglas, SA, Ashmeade, TE, Riley, GJ, Hughes, ZA, Taylor, SG, Munton, RP, Hagan, JJ, Hunter, JA, Jones, DN (2001). Central effects of urotensin-II following ICV administration in rats. *Psychopharmacology (Berl)* **155:** 426-33.

Giebing, G, Tolle, M, Jurgensen, J, Eichhorst, J, Furkert, J, Beyermann, M, Neuschafer-Rube, F, Rosenthal, W, Zidek, W, van der Giet, M, Oksche, A (2005). Arrestin-independent internalization and recycling of the urotensin receptor contribute to long-lasting urotensin II-mediated vasoconstriction. *Circ Res* **97:** 707-15.

Grieco, P, Carotenuto, A, Campiglia, P, Zampelli, E, Patacchini, R, Maggi, CA, Novellino, E, Rovero, P (2002). A new, potent urotensin II receptor peptide agonist containing a Pen residue at the disulfide bridge. *J Med Chem* **45:** 4391-4.

Gruson, D, Rousseau, MF, Ahn, SA, van Linden, F, Ketelslegers, JM (2006). Circulating urotensin II levels in moderate to severe congestive heart failure: its relations with myocardial function and well established neurohormonal markers. *Peptides* **27:** 1527-31.

Grynkiewicz, G, Poenie, M, Tsien, RY (1985). A new generation of Ca2+ indicators with greatly improved fluorescence properties. *J Biol Chem* **260:** 3440-50.

Guerrini, R, Camarda, V, Marzola, E, Arduin, M, Calo, G, Spagnol, M, Rizzi, A, Salvadori, S, Regoli, D (2005). Structure-activity relationship study on human urotensin II. *J Pept Sci* **11:** 85-90.

Gurevich, EV, Gurevich, VV (2006). Arrestins: ubiquitous regulators of cellular signaling pathways. *Genome Biol* **7:** 236.

Halaszovich, CR, Zitt, C, Jungling, E, Luckhoff, A (2000). Inhibition of TRP3 channels by lanthanides. Block from the cytosolic side of the plasma membrane. *J Biol Chem* **275:** 37423-8.

Hardie, RC, Peretz, A, Pollock, JA, Minke, B (1993). Ca2+ limits the development of the light response in Drosophila photoreceptors. *Proc Biol Sci* **252:** 223-9.

Hayat, S, Wigley, CB, Robbins, J (2003). Intracellular calcium handling in rat olfactory ensheathing cells and its role in axonal regeneration. *Mol Cell Neurosci* **22:** 259-70.

Heid, CA, Stevens, J, Livak, KJ, Williams, PM (1996). Real time quantitative PCR. *Genome Res* **6:** 986-94.

Heringlake, M, Kox, T, Uzun, O, Will, B, Bahlmann, L, Klaus, S, Eleftheriadis, S, Armbruster, FP, Franz, N, Kraatz, E (2004). The relationship between urotensin II plasma immunoreactivity and left ventricular filling pressures in coronary artery disease. *Regul Pept* **121:** 129-36.

Herold, CL, Behm, DJ, Buckley, PT, Foley, JJ, Wixted, WE, Sarau, HM, Douglas, SA (2003). The neuromedin B receptor antagonist, BIM-23127, is a potent antagonist at human and rat urotensin-II receptors. *Br J Pharmacol* **139:** 203-7.

Hokin, MR, Hokin, LE (1953). Enzyme secretion and the incorporation of P32 into phospholipides of pancreas slices. *J Biol Chem* **203:** 967-77.

Hosey, MM (1999). What molecular events underlie heterologous desensitization? Focus on "receptor phosphorylation does not mediate cross talk between muscarinic M(3) and bradykinin B(2) receptors". *Am J Physiol* **277:** C856-8.

Hruby, VJ, Deb, KK, Yamamoto, DM, Hadley, ME, Chan, WY (1979). [1-Penicillamine,2-leucine]oxytocin. Synthesis and pharmacological and conformational studies of a potent peptide hormone inhibitor. *J Med Chem* **22:** 7-12.

Hughes, AR, Putney, JW, Jr. (1990). Inositol phosphate formation and its relationship to calcium signaling. *Environ Health Perspect* **84:** 141-7.

Iredale, P, Charlton, ME, Alvaro, JD, Duman RS (1997). Regulation of Receptor Expression: Analysis of Receptor mRNA and Gene Transcription. In: Challiss, R (ed). *Receptor Signal Transduction Protocols*, Vol. 83. Humana Press. pp 251-272.

Iredale, PA, Hill, SJ (1993). Increases in intracellular calcium via activation of an endogenous P2-purinoceptor in cultured CHO-K1 cells. *Br J Pharmacol* **110:** 1305-10.

Joyal, D, Huynh, T, Aiyar, N, Guida, B, Douglas, S, Giaid, A (2006). Urotensin-II levels in acute coronary syndromes. *Int J Cardiol* **108:** 31-5.

Kamouchi, M, Philipp, S, Flockerzi, V, Wissenbach, U, Mamin, A, Raeymaekers, L, Eggermont, J, Droogmans, G, Nilius, B (1999). Properties of heterologously expressed hTRP3 channels in bovine pulmonary artery endothelial cells. *J Physiol* **518 Pt 2:** 345-58.

Kawai, T, Akira, S (2007). Signaling to NF-kappaB by Toll-like receptors. *Trends Mol Med* **13:** 460-9.

Keen, M (1997). Radioligand binding methods for membrane preparations and intact cells. In: Challiss, R (ed). *Receptor Signal Transduction Protocols*, Vol. 83. Humana Press. pp 1-25.

Kelly, E, Bailey, CP, Henderson, G (2008). Agonist-selective mechanisms of GPCR desensitization. *Br J Pharmacol* **153 Suppl 1:** S379-88.

Kenakin, T (2009). *A Pharmacology Primer: Theory, Application and Methods*. Third edn. Academic Press.

Khan, SQ, Bhandari, SS, Quinn, P, Davies, JE, Ng, LL (2007). Urotensin II is raised in acute myocardial infarction and low levels predict risk of adverse clinical outcome in humans. *Int J Cardiol* **117:** 323-8.

Kinney, WA, Almond Jr, HR, Qi, J, Smith, CE, Santulli, RJ, de Garavilla, L, Andrade-Gordon, P, Cho, DS, Everson, AM, Feinstein, MA, Leung, PA, Maryanoff, BE (2002). Structure-function analysis of urotensin II and its use in the construction of a ligand-receptor working model. *Angew Chem Int Ed Engl* **41:** 2940-4.

Kruger, S, Graf, J, Kunz, D, Stickel, T, Merx, MW, Hanrath, P, Janssens, U (2005). Urotensin II in patients with chronic heart failure. *Eur J Heart Fail* **7:** 475-8.

Kubista, M, Andrade, JM, Bengtsson, M, Forootan, A, Jonak, J, Lind, K, Sindelka, R, Sjoback, R, Sjogreen, B, Strombom, L, Stahlberg, A, Zoric, N (2006). The real-time polymerase chain reaction. *Mol Aspects Med* **27:** 95-125.

Labarrere, P, Chatenet, D, Leprince, J, Marionneau, C, Loirand, G, Tonon, MC, Dubessy, C, Scalbert, E, Pfeiffer, B, Renard, P, Calas, B, Pacaud, P, Vaudry, H (2003). Structure-activity relationships of human urotensin II and related analogues on rat aortic ring contraction. *J Enzyme Inhib Med Chem* **18:** 77-88.

Lambert, DG (2007). Urotensin II: from osmoregulation in fish to cardiovascular regulation in man. *Br J Anaesth* **98:** 557-9.

Lancien, F, Leprince, J, Mimassi, N, Mabin, D, Vaudry, H, Le Mevel, JC (2004). Central effects of native urotensin II on motor activity, ventilatory movements, and heart rate in the trout Oncorhynchus mykiss. *Brain Res* **1023:** 167-74.

Lapp, H, Boerrigter, G, Costello-Boerrigter, LC, Jaekel, K, Scheffold, T, Krakau, I, Schramm, M, Guelker, H, Stasch, JP (2004). Elevated plasma human urotensin-II-like immunoreactivity in ischemic cardiomyopathy. *Int J Cardiol* **94:** 93-7.

Lavecchia, A, Cosconati, S, Novellino, E (2005). Architecture of the human urotensin II receptor: comparison of the binding domains of peptide and non-peptide urotensin II agonists. *J Med Chem* **48:** 2480-92.

Lefkowitz, RJ, Rajagopal, K, Whalen, EJ (2006). New roles for beta-arrestins in cell signaling: not just for seven-transmembrane receptors. *Mol Cell* **24:** 643-52.

Lescot, E, Sopkova-de Oliveira Santos, J, Dubessy, C, Oulyadi, H, Lesnard, A, Vaudry, H, Bureau, R, Rault, S (2007). Definition of new pharmacophores for nonpeptide antagonists of human urotensin-II. Comparison with the 3D-structure of human urotensin-II and URP. *J Chem Inf Model* **47:** 602-12.

Lim, M, Honisett, S, Sparkes, CD, Komesaroff, P, Kompa, A, Krum, H (2004). Differential effect of urotensin II on vascular tone in normal subjects and patients with chronic heart failure. *Circulation* **109:** 1212-4.

Lin, Y, Tsuchihashi, T, Matsumura, K, Fukuhara, M, Ohya, Y, Fujii, K, Iida, M (2003). Central cardiovascular action of urotensin II in spontaneously hypertensive rats. *Hypertens Res* **26:** 839-45.

Liu, Q, Pong, SS, Zeng, Z, Zhang, Q, Howard, AD, Williams, DL, Jr., Davidoff, M, Wang, R, Austin, CP, McDonald, TP, Bai, C, George, SR, Evans, JF, Caskey, CT (1999). Identification of urotensin II as the endogenous ligand for the orphan G-protein-coupled receptor GPR14. *Biochem Biophys Res Commun* **266:** 174-8.

Livak, KJ, Schmittgen, TD (2001). Analysis of relative gene expression data using real-time quantitative PCR and the 2(-Delta Delta C(T)) Method. *Methods* **25:** 402-8.

Lohse, MJ, Benovic, JL, Codina, J, Caron, MG, Lefkowitz, RJ (1990). beta-Arrestin: a protein that regulates beta-adrenergic receptor function. *Science* **248:** 1547-50.

Lohse, MJ, Krasel, C, Winstel, R, Mayor, F, Jr. (1996). G-protein-coupled receptor kinases. *Kidney Int* **49:** 1047-52.

Lowry, OH, Rosebrough, NJ, Farr, AL, Randall, RJ (1951). Protein measurement with the Folin phenol reagent. *J Biol Chem* **193:** 265-75.

Luttrell, LM, Lefkowitz, RJ (2002). The role of beta-arrestins in the termination and transduction of G-protein-coupled receptor signals. *J Cell Sci* **115:** 455-65.

Marchese, A, Heiber, M, Nguyen, T, Heng, HH, Saldivia, VR, Cheng, R, Murphy, PM, Tsui, LC, Shi, X, Gregor, P, et al. (1995). Cloning and chromosomal mapping of three novel genes, GPR9, GPR10, and GPR14, encoding receptors related to interleukin 8, neuropeptide Y, and somatostatin receptors. *Genomics* **29:** 335-44.

Marshall, ICB, Boyfield, I, McNulty, S. (2006). Ratiometric Ca2+ measurements using the Flexstation Scanning Fluorometer. In: Lambert, DG (ed). *Calcium Signaling Protocols*. Humana Press. pp 199-124.

Martin, G, Giles, H (1996). Pharmacological principles for analysing responses of vascular smooth muscle. In: Garland CJ, A, JA (ed). *Pharmacology of vascular smooth muscle*. 1 edn. Oxford University Press. pp 1-24.

McDonald, J, Batuwangala, M, Lambert, DG (2007). Role of urotensin II and its receptor in health and disease. *J Anesth* **21:** 378-89.

Mellstrom, B, Savignac, M, Gomez-Villafuertes, R, Naranjo, JR (2008). Ca2+-operated transcriptional networks: molecular mechanisms and in vivo models. *Physiol Rev* **88:** 421-49.

Meyer, S, Temme, C, Wahle, E (2004). Messenger RNA turnover in eukaryotes: pathways and enzymes. *Crit Rev Biochem Mol Biol* **39:** 197-216.

Michell, RH (1975). Inositol phospholipids and cell surface receptor function. *Biochim Biophys Acta* **415:** 81-47.

Moonga, BS, Alam, AS, Bevis, PJ, Avaldi, F, Soncini, R, Huang, CL, Zaidi, M (1992). Regulation of cytosolic free calcium in isolated rat osteoclasts by calcitonin. *J Endocrinol* **132:** 241-9.

Morgan, A, Thomas, AP (2006). Single cell and subcellular measurement of intracellular Ca2+ concentration In: Lamber, D (ed). *Calcium signaling protocols*. 2nd edn. Humana Press. pp 87-117.

Mori, M, Sugo, T, Abe, M, Shimomura, Y, Kurihara, M, Kitada, C, Kikuchi, K, Shintani, Y, Kurokawa, T, Onda, H, Nishimura, O, Fujino, M (1999). Urotensin II is the endogenous ligand of a G-protein-coupled orphan receptor, SENR (GPR14). *Biochem Biophys Res Commun* **265:** 123-9.

Moss, EG (2002). MicroRNAs: hidden in the genome. *Curr Biol* **12:** R138-40.

Mullis, KB (1990). Target amplification for DNA analysis by the polymerase chain reaction. *Ann Biol Clin (Paris)* **48:** 579-82.

Ng, LL, Loke, I, O'Brien, RJ, Squire, IB, Davies, JE (2002). Plasma urotensin in human systolic heart failure. *Circulation* **106:** 2877-80.

Nolan, T, Hands, RE, Bustin, SA (2006). Quantification of mRNA using real-time RT-PCR. *Nat Protoc* **1:** 1559-82.

Nothacker, HP, Wang, Z, McNeill, AM, Saito, Y, Merten, S, O'Dowd, B, Duckles, SP, Civelli, O (1999). Identification of the natural ligand of an orphan G-protein-coupled receptor involved in the regulation of vasoconstriction. *Nat Cell Biol* **1:** 383-5.

O' Connell, J (2002). The Basics of RT-PCR. In: O' Connell, J (ed). *RT-PCR Protocols*, Vol. 193. Humana Press. pp 19-29.

Onan, D, Hannan, RD, Thomas, WG (2004a). Urotensin II: the old kid in town. *Trends Endocrinol Metab* **15:** 175-82.

Onan, D, Pipolo, L, Yang, E, Hannan, RD, Thomas, WG (2004b). Urotensin II promotes hypertrophy of cardiac myocytes via mitogen-activated protein kinases. *Mol Endocrinol* **18:** 2344-54.

Ong, KL, Lam, KS, Cheung, BM (2005). Urotensin II: its function in health and its role in disease. *Cardiovasc Drugs Ther* **19:** 65-75.

Ovcharenko, E, Abassi, Z, Rubinstein, I, Kaballa, A, Hoffman, A, Winaver, J (2006). Renal effects of human urotensin-II in rats with experimental congestive heart failure. *Nephrol Dial Transplant* **21:** 1205-11.

Pahl, HL (1999). Activators and target genes of Rel/NF-kappaB transcription factors. *Oncogene* **18:** 6853-66.

Patacchini, R, Santicioli, P, Giuliani, S, Grieco, P, Novellino, E, Rovero, P, Maggi, CA (2003). Urantide: an ultrapotent urotensin II antagonist peptide in the rat aorta. *Br J Pharmacol* **140:** 1155-8.

Pearson, D, Shively, JE, Clark, BR, Geschwind, II, Barkley, M, Nishioka, RS, Bern, HA (1980). Urotensin II: a somatostatin-like peptide in the caudal neurosecretory system of fishes. *Proc Natl Acad Sci U S A* **77:** 5021-4.

Pitcher, J, Lohse, MJ, Codina, J, Caron, MG, Lefkowitz, RJ (1992). Desensitization of the isolated beta 2-adrenergic receptor by beta-adrenergic receptor kinase, cAMP-dependent protein kinase, and protein kinase C occurs via distinct molecular mechanisms. *Biochemistry* **31:** 3193-7.

Poenie, M (1999). Fluorescent calcium indicators based on BAPTA. In: Putney Jr, J (ed). *Calcium Signaling*. CRC Press. pp 1-47.

Potier, M, Trebak, M (2008). New developments in the signaling mechanisms of the store-operated calcium entry pathway. *Pflugers Arch* **457:** 405-15.

Proulx, CD, Holleran, BJ, Lavigne, P, Escher, E, Guillemette, G, Leduc, R (2008). Biological properties and functional determinants of the urotensin II receptor. *Peptides* **29:** 691-9.

Proulx, CD, Simaan, M, Escher, E, Laporte, SA, Guillemette, G, Leduc, R (2005). Involvement of a cytoplasmic-tail serine cluster in urotensin II receptor internalization. *Biochem J* **385:** 115-23.

Rang, H, Dale, MM, Ritter JM (2000). Methods and measurement in pharmacology. *Pharmacology*. 4th edn. Harcourt Publishers. pp 47-60.

Reinhart, BJ, Slack, FJ, Basson, M, Pasquinelli, AE, Bettinger, JC, Rougvie, AE, Horvitz, HR, Ruvkun, G (2000). The 21-nucleotide let-7 RNA regulates developmental timing in Caenorhabditis elegans. *Nature* **403:** 901-6.

Reiter, E, Lefkowitz, RJ (2006). GRKs and beta-arrestins: roles in receptor silencing, trafficking and signaling. *Trends Endocrinol Metab* **17:** 159-65.

Ribas, C, Penela, P, Murga, C, Salcedo, A, Garcia-Hoz, C, Jurado-Pueyo, M, Aymerich, I, Mayor, F, Jr. (2007). The G protein-coupled receptor kinase (GRK) interactome: role of GRKs in GPCR regulation and signaling. *Biochim Biophys Acta* **1768:** 913-22.

Richards, AM, Nicholls, MG, Lainchbury, JG, Fisher, S, Yandle, TG (2002). Plasma urotensin II in heart failure. *Lancet* **360:** 545-6.

Richardson, RM, Haribabu, B, Ali, H, Snyderman, R (1996). Cross-desensitization among receptors for platelet activating factor and peptide chemoattractants. Evidence for independent regulatory pathways. *J Biol Chem* **271:** 28717-24.

Rogers, TJ, Steele, AD, Howard, OM, Oppenheim, JJ (2000). Bidirectional heterologous desensitization of opioid and chemokine receptors. *Ann N Y Acad Sci* **917:** 19-28.

Russell, FD (2004). Emerging roles of urotensin-II in cardiovascular disease. *Pharmacol Ther* **103:** 223-43.

Russell, FD, Meyers, D, Galbraith, AJ, Bett, N, Toth, I, Kearns, P, Molenaar, P (2003). Elevated plasma levels of human urotensin-II immunoreactivity in congestive heart failure. *Am J Physiol Heart Circ Physiol* **285:** H1576-81.

Russell, FD, Molenaar, P, O'Brien, DM (2001). Cardiostimulant effects of urotensin-II in human heart in vitro. *Br J Pharmacol* **132:** 5-9.

Saetrum Opgaard, O, Nothacker, H, Ehlert, FJ, Krause, DN (2000). Human urotensin II mediates vasoconstriction via an increase in inositol phosphates. *Eur J Pharmacol* **406:** 265-71.

Saha, S, Waugh, DJ, Zhao, P, Abel, PW, Smith, DD (1998). Role of conformational constraints of position 7 of the disulphide bridge of h-alpha-CGRP derivatives in their agonist versus antagonist properties. *J Pept Res* **52:** 112-20.

Sambucetti, LC, Cherrington, JM, Wilkinson, GW, Mocarski, ES (1989). NF-kappa B activation of the cytomegalovirus enhancer is mediated by a viral transactivator and by T cell stimulation. *Embo J* **8:** 4251-8.

Schlesinger, TK, Fanger, GR, Yujiri, T, Johnson, GL (1998). The TAO of MEKK. *Front Biosci* **3:** D1181-6.

Segain, JP, Rolli-Derkinderen, M, Gervois, N, Raingeard de la Bletiere, D, Loirand, G, Pacaud, P (2007). Urotensin II is a new chemotactic factor for UT receptor-expressing monocytes. *J Immunol* **179:** 901-9.

Shimomura, O, Johnson, FH, Saiga, Y (1962). Extraction, purification and properties of aequorin, a bioluminescent protein from the luminous hydromedusan, Aequorea. *J Cell Comp Physiol* **59:** 223-39.

Shipley, G (2007). An Introduction to real-time PCR. In: Dorak, MT (ed). *Real-time PCR (Advanced Methods)* Taylor & Francis Ltd. pp 1-37.

Shiraishi, Y, Watanabe, T, Suguro, T, Nagashima, M, Kato, R, Hongo, S, Itabe, H, Miyazaki, A, Hirano, T, Adachi, M (2008). Chronic urotensin II infusion enhances macrophage foam cell formation and atherosclerosis in apolipoprotein E-knockout mice. *J Hypertens* **26:** 1955-65.

Sibley, DR, Lefkowitz, RJ (1985). Molecular mechanisms of receptor desensitization using the beta-adrenergic receptor-coupled adenylate cyclase system as a model. *Nature* **317:** 124-9.

Sidharta, PN, Wagner, FD, Bohnemeier, H, Jungnik, A, Halabi, A, Krahenbuhl, S, Chadha-Boreham, H, Dingemanse, J (2006). Pharmacodynamics and pharmacokinetics of the urotensin II receptor antagonist palosuran in macroalbuminuric, diabetic patients. *Clin Pharmacol Ther* **80:** 246-56.

Simpson, A (2006). Fluorescent measurement of [Ca2+]c: basic pratical considerations. In: Lambert, D (ed). *Calcium Signaling Protocols*. 2 edn, Vol. 312. Humana Press. pp 3-37.

Singer, VL, Lawlor, TE, Yue, S (1999). Comparison of SYBR Green I nucleic acid gel stain mutagenicity and ethidium bromide mutagenicity in the Salmonella/mammalian microsome reverse mutation assay (Ames test). *Mutat Res* **439:** 37-47.

Skryma, R, Prevarskaya, N, Vacher, P, Dufy, B (1994). Voltage-dependent ionic conductances in Chinese hamster ovary cells. *Am J Physiol* **267:** C544-53.

Smart, D (2006). Measurement of inositol(1,4,5)triphosphate using a stereospecific radioreceptor mass assay. In: Lambert, D (ed). *Calcium Signaling Protocols*, Vol. 312. Humana Press. pp 195-204.

Sondermeijer, B, Kompa, A, Komesaroff, P, Krum, H (2005). Effect of exogenous urotensin-II on vascular tone in skin microcirculation of patients with essential hypertension. *Am J Hypertens* **18:** 1195-9.

Song, W, McDonald, J, Camarda, V, Calo, G, Guerrini, R, Marzola, E, Thompson, JP, Rowbotham, DJ, Lambert, DG (2006). Cell and tissue responses of a range of Urotensin II analogs at cloned and native urotensin II receptors. Evidence for coupling promiscuity. *Naunyn Schmiedebergs Arch Pharmacol* **373:** 148-57.

Spiers, A, Padmanabhan, N (2005). A Guide to wire myography. In: Fennell, J, Baker, AH (ed). *Hypertension: Methods and Protocols*. Humana Press. pp 91-104.

Stadel, JM, Nambi, P, Shorr, RG, Sawyer, DF, Caron, MG, Lefkowitz, RJ (1983). Catecholamine-induced desensitization of turkey erythrocyte adenylate cyclase is associated with phosphorylation of the beta-adrenergic receptor. *Proc Natl Acad Sci U S A* **80:** 3173-7.

Staehelin, M, Simons, P (1982). Rapid and reversible disappearance of beta-adrenergic cell surface receptors. *Embo J* **1:** 187-90.

Sugo, T, Murakami, Y, Shimomura, Y, Harada, M, Abe, M, Ishibashi, Y, Kitada, C, Miyajima, N, Suzuki, N, Mori, M, Fujino, M (2003). Identification of urotensin II-related peptide as the urotensin II-immunoreactive molecule in the rat brain. *Biochem Biophys Res Commun* **310:** 860-8.

Suguro, T, Watanabe, T, Ban, Y, Kodate, S, Misaki, A, Hirano, T, Miyazaki, A, Adachi, M (2007). Increased human urotensin II levels are correlated with carotid atherosclerosis in essential hypertension. *Am J Hypertens* **20:** 211-7.

Suguro, T, Watanabe, T, Kodate, S, Xu, G, Hirano, T, Adachi, M, Miyazaki, A (2008). Increased plasma urotensin-II levels are associated with diabetic retinopathy and carotid atherosclerosis in Type 2 diabetes. *Clin Sci (Lond)* **115:** 327-34.

Sun, B, Harrowe, G, Reinhard, C, Yoshihara, C, Chu, K, Zhuo, S (2001). Modulation of human cytomegalovirus immediate-early gene enhancer by mitogen-activated protein kinase kinase kinase-1. *J Cell Biochem* **83:** 563-73.

Suzuki, T, Tsukamoto, I (2006). Arsenite induces apoptosis in hepatocytes through an enhancement of the activation of Jun N-terminal kinase and p38 mitogen-activated protein kinase caused by partial hepatectomy. *Toxicol Lett* **165:** 257-64.

Takekura, H, Takeshima, H, Nishimura, S, Takahashi, M, Tanabe, T, Flockerzi, V, Hofmann, F, Franzini-Armstrong, C (1995). Co-expression in CHO cells of two muscle proteins involved in excitation-contraction coupling. *J Muscle Res Cell Motil* **16:** 465-80.

Tanaka, Y, Hayashi, N, Kaneko, A, Ito, T, Miyoshi, E, Sasaki, Y, Fusamoto, H, Kamada, T (1992). Epidermal growth factor induces dose-dependent calcium oscillations in single fura-2-loaded hepatocytes. *Hepatology* **16:** 479-86.

Tasaki, K, Hori, M, Ozaki, H, Karaki, H, Wakabayashi, I (2004). Mechanism of human urotensin II-induced contraction in rat aorta. *J Pharmacol Sci* **94:** 376-83.

Thanassoulis, G, Huyhn, T, Giaid, A (2004). Urotensin II and cardiovascular diseases. *Peptides* **25:** 1789-94.

Tian, L, Li, C, Qi, J, Fu, P, Yu, X, Li, X, Cai, L (2008). Diabetes-induced upregulation of urotensin II and its receptor plays an important role in TGF-beta1-mediated renal fibrosis and dysfunction. *Am J Physiol Endocrinol Metab* **295:** E1234-42.

Tkachuk, VA (1998). Phosphoinositide metabolism and Ca2+ oscillation. *Biochemistry (Mosc)* **63:** 38-46.

Tobin, AB (2002). Are we beta-ARKing up the wrong tree? Casein kinase 1 alpha provides an additional pathway for GPCR phosphorylation. *Trends Pharmacol Sci* **23:** 337-43.

Tobin, AB, Totty, NF, Sterlin, AE, Nahorski, SR (1997). Stimulus-dependent phosphorylation of G-protein-coupled receptors by casein kinase 1alpha. *J Biol Chem* **272:** 20844-9.

Totsune, K, Takahashi, K, Arihara, Z, Sone, M, Ito, S, Murakami, O (2003). Increased plasma urotensin II levels in patients with diabetes mellitus. *Clin Sci (Lond)* **104:** 1-5.

Totsune, K, Takahashi, K, Arihara, Z, Sone, M, Satoh, F, Ito, S, Kimura, Y, Sasano, H, Murakami, O (2001). Role of urotensin II in patients on dialysis. *Lancet* **358:** 810-1.

Tovey, S, Brighton, PJ, Willars GB (2006). Confocal microscopy: theory and applications for cellular signaling In: Lambert, D (ed). *Calcium Signaling Protocols*. 2 edn, Vol. 312. Humana Press. pp 57-87.

Treiman, M, Caspersen, C, Christensen, SB (1998). A tool coming of age: thapsigargin as an inhibitor of sarco-endoplasmic reticulum Ca(2+)-ATPases. *Trends Pharmacol Sci* **19:** 131-5.

van der Velden, VH, Hochhaus, A, Cazzaniga, G, Szczepanski, T, Gabert, J, van Dongen, JJ (2003). Detection of minimal residual disease in hematologic malignancies by real-time quantitative PCR: principles, approaches, and laboratory aspects. *Leukemia* **17:** 1013-34.

van Rooij, E, Sutherland, LB, Liu, N, Williams, AH, McAnally, J, Gerard, RD, Richardson, JA, Olson, EN (2006). A signature pattern of stress-responsive microRNAs that can evoke cardiac hypertrophy and heart failure. *Proc Natl Acad Sci U S A* **103:** 18255-60.

von Zastrow, M (2003). Mechanisms regulating membrane trafficking of G protein-coupled receptors in the endocytic pathway. *Life Sci* **74:** 217-24.

Wang, ZJ, Shi, LB, Xiong, ZW, Zhang, LF, Meng, L, Bu, DF, Tang, CS, Ding, WH (2006). Alteration of vascular urotensin II receptor in mice with apolipoprotein E gene knockout. *Peptides* **27:** 858-63.

Watanabe, T, Pakala, R, Katagiri, T, Benedict, CR (2001a). Synergistic effect of urotensin II with mildly oxidized LDL on DNA synthesis in vascular smooth muscle cells. *Circulation* **104:** 16-8.

Watanabe, T, Pakala, R, Katagiri, T, Benedict, CR (2001b). Synergistic effect of urotensin II with serotonin on vascular smooth muscle cell proliferation. *J Hypertens* **19:** 2191-6.

Watson, AM, May, CN (2004). Urotensin II, a novel peptide in central and peripheral cardiovascular control. *Peptides* **25:** 1759-66.

Wenyi, Z, Suzuki, S, Hirai, M, Hinokio, Y, Tanizawa, Y, Matsutani, A, Satoh, J, Oka, Y (2003). Role of urotensin II gene in genetic susceptibility to Type 2 diabetes mellitus in Japanese subjects. *Diabetologia* **46:** 972-6.

Willars, GB, Muller-Esterl, W, Nahorski, SR (1999). Receptor phosphorylation does not mediate cross talk between muscarinic M(3) and bradykinin B(2) receptors. *Am J Physiol* **277:** C859-69.

Willars, GB, Nahorski, SR (1995). Heterologous desensitization of both phosphoinositide and Ca2+ signaling in SH-SY5Y neuroblastoma cells: a role for intracellular Ca2+ store depletion? *Mol Pharmacol* **47:** 509-16.

Wong, ML, Medrano, JF (2005). Real-time PCR for mRNA quantitation. *Biotechniques* **39:** 75-85.

Yang, WJ, Yang, DD, Na, S, Sandusky, GE, Zhang, Q, Zhao, G (2005). Dicer is required for embryonic angiogenesis during mouse development. *J Biol Chem* **280:** 9330-5.

Yoshimoto, T, Matsushita, M, Hirata, Y (2004). Role of urotensin II in peripheral tissue as an autocrine/paracrine growth factor. *Peptides* **25:** 1775-81.

Zhang, C (2008). MicroRNAs: role in cardiovascular biology and disease. *Clin Sci (Lond)* **114:** 699-706.

Zhang, Y, Li, Y, Wei, R, Wang, Z, Bu, D, Zhao, J, Pang, Y, Tang, C (2008). Urotensin II is an autocrine/paracrine growth factor for aortic adventitia of rat. *Regul Pept* **151:** 88-94.

Zhu, X, Jiang, M, Birnbaumer, L (1998). Receptor-activated Ca2+ influx via human Trp3 stably expressed in human embryonic kidney (HEK)293 cells. Evidence for a non-capacitative Ca2+ entry. *J Biol Chem* **273:** 133-42.

Zhu, X, Jiang, M, Peyton, M, Boulay, G, Hurst, R, Stefani, E, Birnbaumer, L (1996). trp, a novel mammalian gene family essential for agonist-activated capacitative Ca2+ entry. *Cell* **85:** 661-71.

Zhu, YC, Zhu, YZ, Moore, PK (2006). The role of urotensin II in cardiovascular and renal physiology and diseases. *Br J Pharmacol* **148:** 884-901.